

Dissertation

Establishing fast-growing Cyanobacteria as Platform for Whole- cell Catalysis

ausgeführt zum Zwecke der Erlangung des akademischen Grades eines Doktors der
Naturwissenschaften unter der Leitung von

Associate Prof. Dipl.-Ing. Dr. techn. Florian Rudroff

Institut für Bioorganische Synthesechemie, E163

Eingereicht an der **Technischen Universität Wien**

Fakultät für Technische Chemie

von

Thomas Rohr

Matrikelnummer 11944418

Wien, am 03.10.2024

T. Rohr

With magic, you can turn a frog into a prince. With science, you can turn a frog into a Ph.D. and you still have the frog you started with.

Terry Pratchett, The Science of Discworld

Die Neugier ist die mächtigste Antriebskraft im Universum, weil sie die beiden größten Bremskräfte im Universum überwinden kann: die Vernunft und die Angst.

Walter Moers, Die Stadt der Träumenden Bücher

AFFIDAVIT

I declare in lieu of oath, that I wrote this thesis and carried out the associated research myself, using only the literature cited in this volume. If text passages from sources are used literally, they are marked as such.

I confirm that this work is original and has not been submitted for examination elsewhere, nor is it currently under consideration for a thesis elsewhere.

I acknowledge that the submitted work will be checked electronically-technically using suitable and state-of-the-art means (plagiarism detection software). On the one hand, this ensures that the submitted work was prepared according to the high-quality standards within the applicable rules to ensure good scientific practice "Code of Conduct" at the TU Wien. On the other hand, a comparison with other student theses avoids violations of my personal copyright.

06.10.2024

Place and Date

T. Rohr

Signature

ACKNOWLEDGMENTS

Here is the part, where I say thank you. Thank you, to all and everyone. The amount of people I want to thank approximates infinity, but I must start somewhere. And I will have to end somewhere, which, in conclusion, means, I will not be able to thank everyone. If you have met me and we laughed, cried, or shared a special moment together: Thank you!

But now, it gets personal.

I want to thank my supervisor, Florian Rudroff, who allowed me to pursue any direction I wanted if I could argue it well enough. Your direct form of criticism let me see clearly in times when my vision was fogged. You showed me around the Colosseum of Science and guided me in becoming my own gladiator and fight. Thank you

Thanks to Christian Stanetty, Michael Schnürch, and Marko Mihovilovic, for their support and open ears, under any circumstances. Your mentorship stretches to every student, and this can be felt. Thank you

My gratitude goes out to all members of the PhD program at TU Wien Bioactive. Thank you all for your support, the fun times, the open ears in dark times, and the overall great attitude and lovable moments. Thanks to Nadine, Sebastian, Caro, Gabriel, Irene, Katie, Richie and Ricarda.

Great thanks to my former supervisors, Ilka Axmann and Meike Siebers. Both people I admire for who they are and how they treat the people around them. You showed me, what it means to be a scientist and supported and encouraged me in pursuing this career. Without both of you, I would never be able to see myself as a scientist.

I am grateful, that I had the opportunity to work with amazing people for the last 5 years. I mean, of course, everyone in the bioorganic synthesis group. Although most of you, jokingly, never let me forget, that I am from Germany, you greeted me with open arms and a smile. A thank you to everyone I had the pleasure to be there when they finished their PhD-journeys, David, Resi, Drasi, Clemens, Hamid, Michi, Blanca, Heci, Kathi, Johanna and very recently Eleni and Viktor, and every else, I might have forgotten. I am incredibly lucky to have more wonderful people around me when I finish my journey myself. Christoph Standfest, Björn (another German engaged by Austria), Stefan, Verena, and a special thanks to Christoph Suster. No computer problem, you could not fix, always knowing, who to ask and how to reach them, and ever working in the background to ensure a livable and loveable atmosphere in the group, Thank you! Next, we have Dominik, Pierre Simon, Markus, and Max, a room full of people, full of support, and full of laughter. Followed by Ashadi, Mario, Astrid, Nanditha, Rahele, Nina and Jorge. A lovely bunch, all of them. Finally, there are Lydia, Freddy, Richie, and Farooq, thank you for everything. These mentions are in no particular order, I love you all in your ways and I feel unbelievably fortunate to call you my friends!

A thank you to the *map*ADO people, Astrid, Margit, and Lukas. This enzyme is an amazing discovery, and I am grateful to be part of this.

A quick thanks to the cooking group, where I could live out my love for preparing a tasty dish for my friends, where I learned a lot and enjoyed every moment. I miss that a lot!

A BIG thanks go out to all the Cyantists in our group, first and foremost: Julia! Cyanobacteria are a tricky, fascinating, confusing, hate-inducing, awe-inspiring bunch of bastards and together we could navigate those murky waters. You are a wonderful person, please never change! When mentioning cyanobacteria, I must not forget Christian Waltl, the dry-humored and nihilistic Voralberger. It was and is a joy to be around you.

And also thanks to the group around Brūno Bühler in Leipzig. It was a great pleasure to meet you at all the conferences and share our thoughts and ideas.

A special thanks to all those who shared the boulder gym with me Hubs, Jakob, Kathi, Heci, the other Kathi, Richie, Max, Christoph, Verena, and Stefan. I was the one 'who danced with the wall' and I danced for you!

I have to thank Hubs again, for introducing me to DnD and the nice people in our, Mina, Gitte, and Julia. We may be more of a ADHDnD group, but I enjoy every moment of this!

I also want to thank everyone at Alpenrausch by Alpenverein for showing the beauty and wonder of alpine sport one can do without skis! Thank you Lovrence, Azra, Sahra, and everyone else!

The next part is in German, just to make sure, my family understands, how much they mean to me.

Ich kann meinen Eltern gar nicht genug danken. Ihr habt mich zu dem gemacht, wer ich heute bin (Ha! Selber schuld!) und ich bin euch unendlich dankbar dafür. Man kann sich keine liebevolleren und verständnisvolleren Eltern wünschen und nur dank eurer Unterstützung in allem, was ich tue, kann ich sicher und glücklich durch das Leben gehen. Danke!

Ich kann in zuversichtlich in die Zukunft blicken, denn ich weiß, meine Schwester und ihr Mann haben die Welt mit den 4 tollsten Kindern bereichert, die ich kenne. Vielen lieben Dank für die tollen Stunden Tillmann, Thies, Class und Constantin und ich freue mich auf viele weitere! Ich habe das große Glück Fiona als Schwester zu haben, auch wenn wir nicht in allem übereinstimmen 😊 Danke für Alles, Schwesterherz! Und Jörg, keine Sorge, wir gehen bald wieder Wandern, ganz sicher!

I would love to write the next part in Hungarian, but I am not there yet.

This is of course for Judit. Thank you. You are my motivation, my inspiration, my safe space, and my freak-out spot. Around you, I feel complete and like myself. You were always there for me when I needed you, you gave me a swift kick in the butt when I needed it, and no matter how I felt, you were the light at the end of the tunnel. Thank you for being there, in all ups and downs. Thank you. For everything.

In the end, there are all the scientists to thank, who came before us. The pioneers and ever-curious, driven by the search for knowledge. Science can only flourish when people work together. We are truly dwarves on the shoulders of giants.

CONTENTS

Affidavit	V
Acknowledgments.....	VII
Contents	X
List of abbreviations	XIII
Abstract.....	XV
Kurzzusammenfassung	XVII
1 Introduction	1
1.1 Cyanobacteria – Making the world go around.....	1
1.1.1 In general.....	1
1.2 Cyanobacteria in Biotechnology	6
1.2.1 Potential Compounds for cyanobacterial-based Manufacturing	7
1.2.2 Limits and disadvantages of cyanobacteria in biotechnology	9
1.2.3 Cyanobacterial stains used in biotechnology.....	14
1.3 Biocatalysis	21
1.3.1 Biotransformation and fermentation	21
1.3.2 Whole-cell catalysis	22
1.4 Whole-cell catalysis in cyanobacteria.....	28
1.4.1 <i>In situ</i> oxygen production in cyanobacteria	28
1.4.2 Draining reduction equivalents from photosynthesis.....	28
1.4.3 CO ₂ limitations in Whole-cell Catalysis and its role in cyanobacterial metabolism	29
1.4.4 Examples	30
1.5 Aim of this work	34
2 Results.....	36
2.1 Growth and Physiology	37
2.1.1 <i>Synechococcus</i> sp. UTEX9273.....	37
2.1.2 <i>Synechococcus</i> sp. PCC11901	38
2.2 Carboxylic Acid Reductase in <i>Synechococcus</i> sp. UTEX2973	42
2.2.1 Genome-scale Models and Flux Balance Analysis.....	42
2.2.2 Inducible Protein Expression	45
2.2.3 Cloning	46
2.3 <i>Synechococcus</i> sp. PCC11901 and the enzymatic conversion of ferulic acid into vanillin	52
	X

2.3.1	The two-step cascade in <i>E. coli</i> BL21	53
2.3.2	Genomic integration and protein expression in <i>S. sp.</i> PCC11901	60
2.3.3	Optimizing 4-vinyl guaiacol production from ferulic acid by <i>S. sp.</i> PCC11901 <i>fadA::pad</i>	64
2.3.4	Mixed species whole-cell catalysis	71
3	Discussion	73
3.1	Carboxylic Acid Reductase in <i>S. sp.</i> UTEX2973	74
3.2	<i>S. sp.</i> PCC11901 and the enzymatic conversion of Ferulic acid into Vanillin .	77
3.2.1	The highly efficient aromatic dioxygenase <i>mapADO</i>	77
3.2.2	Unprecedented yields for whole-cell catalysis in cyanobacteria with a phenolic acid decarboxylase in <i>S. sp.</i> PCC11901	78
3.2.3	The hardships of genomic integration in cyanobacteria	79
3.2.4	A mixed-species approach to increased enzymatic vanillin production .	79
4	Conclusion and Outlook.....	81
5	Methods and Materials.....	84
5.1	Cultivation and strain handling	84
5.1.1	Cyanobacteria.....	84
5.1.2	<i>E. coli</i>	86
5.2	Whole-cell catalysis	88
5.2.1	Phenolic acid decarboxylase in <i>S. sp.</i> PCC11901 <i>fadA::pad</i>	88
5.2.2	Aromatic dioxygenase in <i>E. coli</i> BL21	89
5.2.3	PAD and <i>mapADO</i> in mixed species reaction	89
5.3	Analytics.....	89
5.3.1	HPLC	89
5.3.2	Gas-Chromatography	89
5.3.3	NMR spectroscopy	90
5.3.4	Absorbance, optical density, and fluorescence	90
5.3.5	SDS-PAGE for protein analysis.....	90
5.3.6	Dissolved oxygen.....	90
5.3.7	Nano Differential Scanning fluorimetry for the determination of the melting point of <i>mapADO</i>	91
5.4	Molecular genetics	92
5.4.1	NEBuilder HiFi DNA Assembly	92
5.4.2	Golden Gate Cloning	92

5.4.3	Construction of pPMQAK1-T-Y25F	93
6	Appendix.....	94
6.1	Media used for bacterial cultivation	95
6.2	Enzymes	96
6.2.1	Carboxylic acid reducaters	96
6.2.2	Aromatic Dioxygenases.....	99
6.2.3	Phenolic Acid Decarboxylase	100
6.3	Plasmids.....	101
6.4	Primer.....	102
6.5	Python script for flux balance analysis	109
7	Contributions to this Thesis	117
8	Publications resulting from this thesis	118
8.1	Poster Presentations	119
9	Curriculum Vitae.....	121
10	References	124

LIST OF ABBREVIATIONS

2,4-diacetyl phloroglucinol	DAPG
4-Vinyl guaiacol	4VG
Adenosine triphosphate	ATP
anhydrous Tetracycline	aTc
Bayer-Villinger-monooxygenase	BVMO
Bicistronic Device	BCD
Calvin-Benson-Bassham-Cycle	CBB-cycle
Carbon concentrating mechanism	CCM
Carboxylic acid	CA
Carboxylic acid reductase	CAR
Chlorophyll <i>a</i>	Chl <i>a</i>
Cyclopentyl methyl ester	CPME
<i>Escherichia coli</i>	<i>E. coli</i>
ferredoxin-NADP ⁺ reductase	FNR
Ferulic acid	FA
Flux balance analysis	FBA
Gas-chromatography	GC
Gene of interest	GOI
Genetically Modified Organisms	GMO
Genome-scale model	GSM
High-performance liquid chromatography	HPLC
Inorganic carbon	<i>Ci</i>
Isopropyl myristate	IPM
Isopropyl β-D-1-thiogalactopyranoside	IPTG
Isopropyl β-D-1-thiogalactopyranoside	IPTG
Kanamycin resistance Cassette	Km ^R
Light harvesting complex	LHC
Methyl tert-butyl ether	MTBE
Nano Differential Scanning Fluorimetry	NanoDSF
Nicotinamide adenine Dinucleotide Phosphate	NADP
Open Raceway Pond	ORP
Optical Density	OD
Phosphate Buffer Saline	PBS
Phosphopantetheinyl-Transferase	PPTase
Photobioreactor	PBR
Photosystem I	PS I
Photosystem II	PS II
Poly-Hydroxy Butyrate	PHB
Polymerase chain reaction	PCR
Radical Oxygen Species	ROS
Revolution per minute	rpm
Ribosome Binding Site	RBS
Ribosome binding site	RBS
Ribulose-1,5-bisphosphate carboxylase/oxygenase	RubisCO
SDS polyacrylamide gel electrophoresis	SDS-PAGE
Single nucleotide polymorphism	SNP

Space-Time-Yield
Synechococcus sp. PCC11901
Synechococcus sp. UTEX2973
Wild type
Yellow fluorescent protein

STY
PCC11901
UTEX2973
WT
YFP

ABSTRACT

Climate change represents the most significant challenge humanity has ever faced, driven largely by anthropogenic greenhouse gas emissions and environmental degradation. Rapid decarbonization and minimizing industrial waste streams are critical for mitigating its impact. Cyanobacteria offer a promising avenue to transform biotechnology into a carbon-neutral or even carbon-negative industry.

Cyanobacteria are ancient prokaryotes capable of oxygenic photosynthesis. Their photoautotrophic metabolism enables them to harness light as an energy source and atmospheric CO₂ as a carbon source, requiring only water and salts. These characteristics make them highly suitable for biotechnological applications, allowing the conversion of CO₂ into valuable products, as demonstrated by several proof-of-concept studies and limited industrial-scale applications, such as in the production of nutraceuticals and pigments. Furthermore, cyanobacteria possess advantageous traits for whole-cell catalysis.

Whole-cell catalysis is a subset of biocatalysis and instead of isolating an enzyme to catalyze the reaction of interest, the cell is intact and thus provides a reaction vessel for the reaction and so stabilizes the enzyme(s), regulates pH and osmotic pressure, and can even provide a recycling system for required co-factors, such as ATP or NADPH. However, traditional whole-cell systems often require sacrificial compounds like glucose for cofactor recycling, which adds cost and environmental burden. Cyanobacteria can overcome this limitation by converting light energy into biologically available energy through photosynthesis. Moreover, the *in situ* production of oxygen can mitigate limitations associated with oxygen transfer in whole-cell catalysis.

Despite these advantages, the application of cyanobacteria in industrial-scale processes is hindered by their slow growth and low biomass accumulation compared to conventional bacteria such as *E. coli*, making them less economically viable. However, recent discoveries of fast-growing cyanobacterial strains, such as *Synechococcus sp.* UTEX2973 and *Synechococcus sp.* PCC11901, with doubling times comparable to yeast species like *Saccharomyces cerevisiae* and *Pichia pastoris*, present new opportunities in cyanobacterial biotechnology.

This study aimed to develop fast-growing cyanobacteria as a platform for whole-cell catalysis. Two biocatalytic approaches were explored using the fast-growing strains *Synechococcus sp.* UTEX2973 and *Synechococcus sp.* PCC11901.

The first approach focused on expressing a carboxylic acid reductase (CAR) in *Synechococcus sp.* UTEX2973. CARs convert carboxylic acid moieties into their corresponding aldehyde, a chemically challenging reaction. The enzyme requires one molecule of ATP and NADPH each per reaction, posing a burden on the host's metabolism. The efficient photosynthetic machinery of *S. sp.* UTEX2973 is well suited to supply these cofactors. Additionally, Flux Balance Analysis (FBA) was investigated as a tool to identify gene knockouts that could enhance the flux of reducing equivalents

toward the desired reaction. However, the project faced technical challenges related to cloning CAR into a suitable vector for *S. sp.* UTEX2973.

The second approach focused on *Synechococcus sp.* PCC11901 and a two-step enzymatic cascade. *S. sp.* PCC11901 has shown the ability to accumulate higher cell densities than other cyanobacterial strains, making it a promising candidate for industrial applications. The enzymes used in this system were phenolic acid decarboxylase (PAD) and aromatic dioxygenase (ADO), which together convert ferulic acid, a lignin-derived aromatic compound, into the high-value compound vanillin. The first step, catalyzed by PAD, produces 4-vinyl guaiacol and releases CO₂, while the second step, catalyzed by ADO, requires oxygen. By leveraging photosynthesis, the reaction becomes self-fueling, addressing the issue of CO₂ depletion in closed systems.

After the integration of PAD into the genome of *Synechococcus sp.* PCC11901, the toxicity of 4-vinyl guaiacol was determined as the main inhibitor. The hydrophobicity of 4-vinyl guaiacol compared to ferulic acid allowed an *in situ* product removal with an organic solvent. The use of *in situ* product removal with hydrophobic solvents such as diisononyl phthalate (DINP) improved yields. Due to environmental concerns, alternative solvents were evaluated and isopropyl myristate showed similar results to DINP while being considered a 'green solvent'. The process was scaled up to gram-scale production, achieving a yield of 80 mM 4-vinyl guaiacol, the highest reported yield for whole-cell catalysis in cyanobacteria.

Attempts to integrate ADO into *S. sp.* PCC11901 were unsuccessful, and the ADO enzyme itself displayed limited yields and activity. Genome mining identified a more promising ADO variant from *Moesziomyces aphidis* (termed *mapADO*), though its expression in cyanobacteria was also unsuccessful. Subsequently, a mixed-species approach using *E. coli* expressing *mapADO* alongside *S. sp.* PCC11901 was tested to perform the two-step conversion from ferulic acid to vanillin and successfully increased vanillin production.

KURZZUSAMMENFASSUNG

Klimawandel stellt die bedeutendste Herausforderung dar, der die Menschheit je gegenüberstand, und wird hauptsächlich durch anthropogene Treibhausgasemissionen und Umweltzerstörung vorangetrieben. Eine rasche Dekarbonisierung und die Minimierung industrieller Abfallströme sind entscheidend, um die Auswirkungen abzumildern. Cyanobakterien bieten einen vielversprechenden Weg, um die Biotechnologie in eine kohlenstoffneutrale oder sogar kohlenstoffnegative Industrie zu verwandeln.

Cyanobakterien sind urzeitliche Prokaryoten, die zur oxygenen Photosynthese fähig sind. Ihr photoautotropher Stoffwechsel ermöglicht es ihnen, Licht als Energiequelle und atmosphärisches CO₂ als Kohlenstoffquelle zu nutzen, wobei sie lediglich Wasser und Salze benötigen. Diese Eigenschaften machen sie besonders geeignet für biotechnologische Anwendungen, da sie CO₂ in wertvolle Produkte umwandeln können, wie durch mehrere Machbarkeitsstudien und begrenzte industrielle Anwendungen, etwa in der Produktion von Nahrungsergänzungsmitteln und Pigmenten, gezeigt werden konnte. Darüber hinaus verfügen Cyanobakterien über vorteilhafte Eigenschaften für die Ganzzellkatalyse.

Die Ganzzellkatalyse ist ein Teilbereich der Biokatalyse, bei dem statt eines isolierten Enzyms die gesamte Zelle als Reaktionsgefäß genutzt wird, um die Reaktion durchzuführen. Dadurch wird das Enzym stabilisiert, der pH-Wert und der osmotische Druck reguliert und es können sogar Co-Faktoren wie ATP oder NADPH recycelt werden. Traditionelle Ganzzellsysteme erfordern jedoch oft zusätzliche Verbindungen wie Glukose für das Cofaktor-Recycling, was zusätzliche Kosten und Umweltbelastungen mit sich bringt. Cyanobakterien können diese Einschränkung überwinden, indem sie Lichtenergie durch Photosynthese in biologisch verfügbare Energie umwandeln. Zudem kann die *In-situ*-Produktion von Sauerstoff die bei der Ganzzellkatalyse auftretenden Probleme der Sauerstoffübertragung verhindern.

Trotz dieser Vorteile wird die Anwendung von Cyanobakterien in industriellen Prozessen durch ihr langsames Wachstum und die geringe Biomasseproduktion im Vergleich zu herkömmlichen Bakterien wie *E. coli* behindert, was sie wirtschaftlich unrentabel macht. Allerdings bieten jüngste Entdeckungen schnell wachsender Cyanobakterienstämme, wie *Synechococcus* sp. UTEX2973 und *Synechococcus* sp. PCC11901, mit Verdopplungszeiten, die mit Hefearten wie *Saccharomyces cerevisiae* und *Pichia pastoris* vergleichbar sind, neue Möglichkeiten in der Cyanobakterien-Biotechnologie.

Diese Studie zielte darauf ab, schnell wachsende Cyanobakterien als Plattform für die Ganzzellkatalyse zu entwickeln. Zwei biokatalytische Ansätze wurden mit den schnell wachsenden Stämmen *Synechococcus* sp. UTEX2973 und *Synechococcus* sp. PCC11901 untersucht.

Der erste Ansatz konzentrierte sich auf die Expression einer Carbonsäurereduktase (CAR) in *Synechococcus* sp. UTEX2973. CARs wandeln Carbonsäuregruppen in ihre entsprechenden Aldehyde um, eine chemisch anspruchsvolle Reaktion. Das Enzym benötigt jeweils ein Molekül ATP und NADPH pro Reaktion, was eine Belastung für den Stoffwechsel des Wirts darstellt. Der effiziente photosynthetische Mechanismus von *S. sp.* UTEX2973 eignet sich gut zur Bereitstellung dieser Cofaktoren. Darüber hinaus wurde die Flux Balance Analyse (FBA) als Werkzeug zur Identifizierung von Gen-Knockouts untersucht, die den Fluss reduzierender Äquivalente in Richtung der gewünschten Reaktion steigern könnten. Das Projekt stieß jedoch auf technische Schwierigkeiten beim Klonieren von CAR in einen geeigneten Vektor für *S. sp.* UTEX2973.

Der zweite Ansatz konzentrierte sich auf *Synechococcus* sp. PCC11901 und eine zweistufige enzymatische Kaskade. *S. sp.* PCC11901 hat sich als fähig erwiesen, höhere Zelldichten als andere Cyanobakterienstämme zu erreichen, was ihn zu einem vielversprechenden Kandidaten für industrielle Anwendungen macht. Die in diesem System verwendeten Enzyme waren ein Phenolsäuredecarboxylase (PAD) und ein aromatische Dioxygenase (ADO), die zusammen Ferulasäure, eine aus Lignin gewonnene aromatische Verbindung, in die wertvolle Verbindung Vanillin umwandeln. Der erste Schritt, katalysiert durch PAD, produziert 4-Vinylguaiaicol und setzt CO₂ frei, während der zweite Schritt, katalysiert durch ADO, Sauerstoff benötigt. Durch die Nutzung der Photosynthese wird die Reaktion selbsttragend, was das Problem der CO₂-Erschöpfung in geschlossenen Systemen löst.

Nach der Integration von PAD in das Genom von *Synechococcus* sp. PCC11901 wurde die Toxizität von 4-Vinylguaiaicol als Hauptinhibitor ermittelt. Die Hydrophobizität von 4-Vinylguaiaicol im Vergleich zu Ferulasäure ermöglichte eine *In-situ*-Produktentfernung mit einem organischen Lösungsmittel. Der Einsatz von hydrophoben Lösungsmitteln wie Diisononylphthalat (DINP) verbesserte die Ausbeuten. Aufgrund von Umweltbedenken wurden alternative Lösungsmittel evaluiert, und Isopropylmyristat zeigte ähnliche Ergebnisse wie DINP, während es als „grünes Lösungsmittel“ gilt. Der Prozess wurde auf ein Gram hochskaliert, wobei eine Ausbeute von 80 mM 4-Vinylguaiaicol erzielt wurde, die höchste berichtete Ausbeute für Ganzzellkatalyse in Cyanobakterien.

Versuche, ADO in *S. sp.* PCC11901 zu integrieren, waren erfolglos, und das ADO-Enzym selbst zeigte begrenzte Ausbeuten und Aktivität. Durch Genom-Mining wurde eine vielversprechendere ADO-Variante aus *Moesziomyces aphidis* (genannt *mapADO*) identifiziert, deren Expression in Cyanobakterien jedoch ebenfalls erfolglos war. Anschließend wurde ein gemischter Artenansatz mit *E. coli*, welche *mapADO* exprimierte, neben *S. sp.* PCC11901 getestet, um die zweistufige Umwandlung von Ferulasäure zu Vanillin durchzuführen, was die Vanillinproduktion erfolgreich erhöhte.

1 INTRODUCTION

1.1 CYANOBACTERIA – MAKING THE WORLD GO AROUND

1.1.1 In general

Cyanobacteria are ancient prokaryotes, with the earliest forms of oxygenic photosynthesis probably dating back 3 billion years.¹ They are distinct from other photoautotrophs by utilizing water (H₂O) as an electron donor. The advent of two reaction centers for light harvesting, a prerequisite for oxygenic photosynthesis, caused a massive accumulation of oxygen in the atmosphere, known as the great oxidation event. This event shaped the atmosphere of today's world and paved the way for later lifeforms.² Until today, they are the most important primary producers, playing a non-replaceable role in oxygen production and carbon cycling and often pioneering the formation of biocrusts.³ Cyanobacteria are commonly accepted as sharing the same progenitors with chloroplasts in plants and algae, most likely acquired via endosymbiosis, sharing some of their DNA and structural features. These features, combined with their simpler genetic build-up and accessibility for genetic engineering ensured the interest of researchers searching to understand photosynthesis and established them as a platform to understand the connections between genes and photosynthesis. This led to the decision to make the cyanobacterium *Synechocystis* sp. PCC6803 the first photoautotrophic organism to be fully genome sequenced in 1996.⁴ The number of fully sequenced cyanobacterial genomes surpasses 950 today,¹ a rich resource for research.

Cyanobacteria, the only prokaryotes capable of oxygenic photosynthesis, show unique characteristics, distinguishing them from other algae, plants, and any other prokaryotes. These features include the thylakoid, their two-tiered photosynthesis apparatus, their unique set of light-harvesting pigments, and the carboxysome.

1.1.1.1 Light harvesting

The Thylakoid consists of the thylakoid membrane surrounding the Lumen, a unique structure in prokaryotes, resembling a primitive organelle. Among cyanobacteria, the structure differs from species to species, thought to be the result of several convergent evolutionary steps.⁵ The lipid composition resembles those of chloroplasts in plants and harbors the necessary parts of the light reaction of photosynthesis and the respiratory electron transport, a highly dynamic system, allowing fast regulation of light harvesting, photosynthetic electron flow, and respiration, keeping the redox state in the cell balanced.⁶ The biogenesis of the thylakoid membrane and whether it is attached to the plasma membrane or not is still under debate.⁷

Inside the thylakoid, especially in the thylakoid membrane, sits the photosynthesis apparatus of cyanobacteria (with a few exceptions, such as the *Gloeobacter* species).⁸ The structure deviates in plants and algae but relies on the same mechanisms.

In plants, most light is harvested by either Chlorophyll *a* (Chl *a*) or Chlorophyll *b*, while cyanobacteria have developed a wider range of pigments, thereby increasing the spectrum of utilizable light as an energy source. Along the water column, the quality of light changes, which would quickly prevent autotrophic growth in a plant, while cyanobacteria developed a sophisticated and wide range of pigments, dramatically increasing their capability of utilizing light. Next to Chl *a* and *b*, also other variants were described, such as *c*, *d*⁹ and *f*, with Chl *f* even absorbing light in the near-infrared range.¹⁰ Another group of pigments are carotenoids, a highly diverse group of molecules, roughly divided into carotenes and Xanthophylls. While both consist of unsaturated hydrocarbon chains, xanthophylls possess additional oxygen molecules. These pigments have absorption maxima from 400 – 520 nm, but are not all devoted to light harvesting, but also serve as photoprotectors and antioxidants.¹¹ The third group of light-harvesting pigments to be mentioned here are phycobiliproteins. This group of water-soluble proteins are bound covalently to their chromophores via a cysteine. The main phycobiliproteins of cyanobacteria are allophycocyanin (600–660 nm peak), phycocyanin (580–630 nm peak), and phycoerythrin (540–575 nm), which absorb in the so-called ‘green window’, where chlorophylls and carotenoids show only minimal efficiency (see Figure 1).

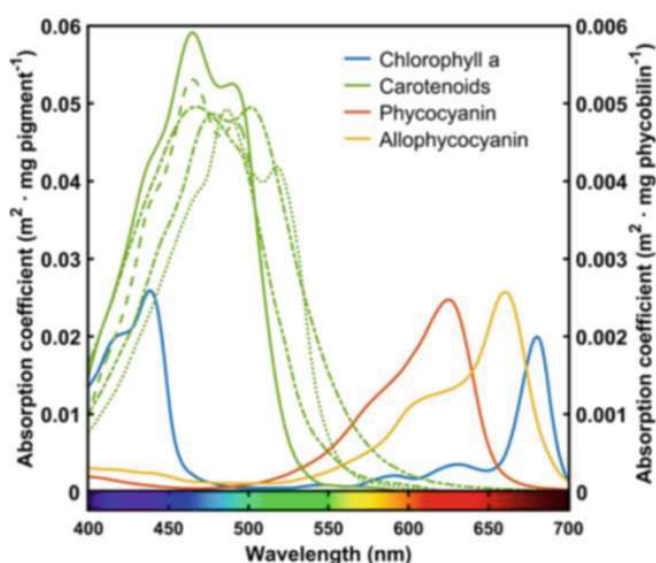


Figure 1 Exemplary absorption spectra of light-harvesting pigments in *Synechocystis* PCC6803. Adapted from Fuentes et al., 2020¹²

They form the Phycobillisome and direct the energy further to Photosystem II. A typical structure of the Phycobillisome in *Synechococcus* is depicted in Figure 2. It is believed that the widening of the available light spectrum for energy harvest developed to mitigate ‘self-shading’, where growing cells are bereft of light by other cells, closer to the light source/sun. Phycobiliproteins also allow cyanobacteria to grow further down the water column in deeper waters, where algae cannot grow anymore.¹³

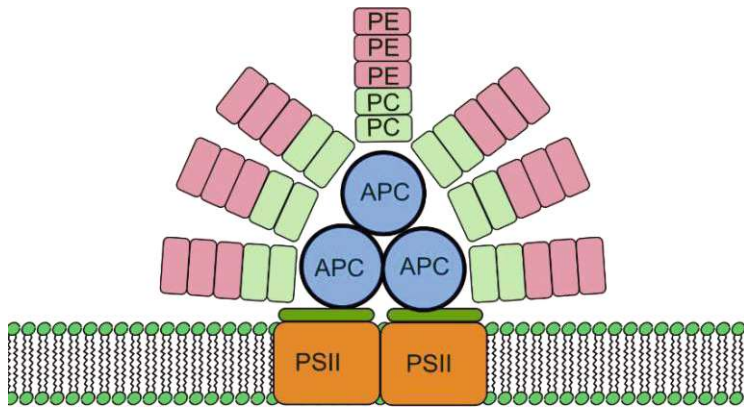


Figure 2 Structure of the Phycobilisome in *Synechococcus*. The Phycobilisome sits on a Photosystem II dimer across the thylakoid membrane. The core is made of allophycocyanin (APC), surrounded by phycocyanin (PC) and phycoerythrin (PE). Adapted from ¹⁴.

1.1.1.2 Energy transformation

The absorbed energy from inciting light must now be converted into bio-available energy. In cyanobacteria, the harvesting of energy by light can be divided into linear electron transport and cyclic electron transport. In linear electron transport, Phycobilisomes act as light-harvesting complexes, absorbing and funneling light energy to the core Chl *a* (P680) within the PSII reaction center. Here, light energy is transformed into chemical energy as the excited Chl *a* (P680) undergoes oxidation by the first electron acceptor, pheophytin. Electrons then travel along a reduction gradient through the electron transport chain, passing from plastoquinone, cytochrome *b*6*f*, and plastocyanin to Photosystem I (PSI). During this journey, protons (H^+) are pumped from the cytosol to the thylakoid lumen, creating a proton gradient. Similar to PSII, Chl *a* (P700) is excited by light energy in PSI. The excited electron facilitates redox reactions within PSI, reducing the water-soluble proteins ferredoxin or flavodoxin. Ferredoxin, crucial in photoautotrophic metabolism, transfers electrons to various metabolic pathways, notably to Ferredoxin-NADP⁺ Reductase (FNR), the final electron acceptor in photosynthetic electron transfer. FNR catalyzes the reduction of NADP⁺ to NADPH, requiring two sequential electrons. The oxidized P680 in PSII is reduced to its ground state by an external electron donor, H_2O , which donates electrons through a Mn_4CaO_5 cluster. This water oxidation results in the production of molecular oxygen and the release of protons into the thylakoid lumen.^{15–18} A simplified version of linear electron transport is depicted in Figure 3.

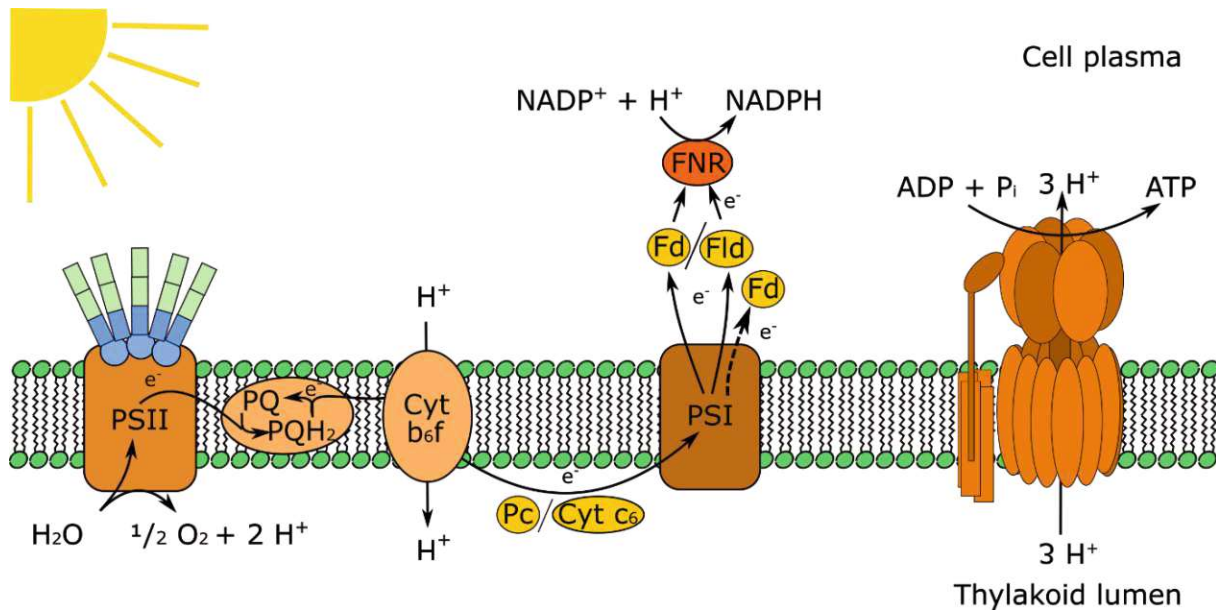


Figure 3 Photosynthesis and electron transfer along the thylakoid membrane in Cyanobacteria. According to Jodlbauer et al., 2022¹⁹

This linear electron transport is a rigid system, but during fluctuating light conditions, cycling electron transport can help to keep the balance of reducing equivalents. During this, the reduced ferredoxin or flavodoxin can pass through the thylakoid membrane and bind the NADPH dehydrogenation-like complex. Together they bind to the thylakoid membrane from the cytosolic site and transfer electrons to plastoquinone. The electrons are transferred through several stations to a terminal cytochrome-c oxidase complex (COX).²⁰

The electrochemical gradient of H^+ ions, generated by H_2O cleavage and H^+ pumping by Cyt b_6f , is utilized by ATP synthase to produce ATP. The products of photosynthesis, ATP and NADPH, are essential for cellular metabolism, and O_2 is formed as a by-product of water oxidation.^{21,22}

In their natural environment, cyanobacteria are exposed to constantly changing light conditions. This could cause a rapid alteration in electron flux, over-reduction of the electron transport chain, and uncontrolled donation of electrons to oxygen, resulting the built-up of radical oxygen species (ROS)²³. Cyanobacteria evolved mechanisms to withstand ROS formation, but their capabilities are limited and the prevention of ROS accumulation is superior.²⁴ Another way to regulate the redox state of the cell is to increase carbon assimilation, converting CO_2 into biomass. The production of one molecule of glucose requires 6 CO_2 , 12 NADPH, and 18 ATP molecules and under carbon-saturated conditions, $NADP^+$ regeneration acts as the main electron sink.²⁵

1.1.1.3 RubisCO and the carbon concentrating mechanism (CCM)

Assimilation of CO_2 and turning it into biomass via light energy is often described as a two-part system, consisting of light absorption and carbon metabolism. The light reaction

has been investigated above, so a closer look at cyanobacterial carbon metabolism is next.

CO₂ in cyanobacteria is incorporated into biomass via the Calvin-Benson-Bassham cycle (CCB). It was first described in 1954 and has since then been widely accepted as correct.^{26,27} In brief, 3 five-carbon molecules (pentoses) are converted into 6 three-carbon compounds (trioses), namely 3-phosphoglycerate (3PG), via carboxylation by ribulose-1,5-bisphosphate carboxylase/oxygenase (RubisCO). One molecule of 3PG leaves the cycle, while the remaining 5 molecules are recycled back into 3 pentoses, which include aldolases, transketolases, isomerases, and biphosphatase.^{26,27} The reaction cycle is demonstrated on the left side of Figure 4.

The enzyme RubisCO stands at the helm of carbon metabolism in cyanobacteria. As the name implies, it is not solely responsible for carboxylation but has also oxidation activity, caused by the competition for the active site by CO₂ and O₂. With oxygen present, 3PG is produced as well as 2-phosphoglycolate, which in turn gets converted into glycolate and is released through the cell wall, so losing 2 C-atoms (right side of Figure 4).^{13,28,29}

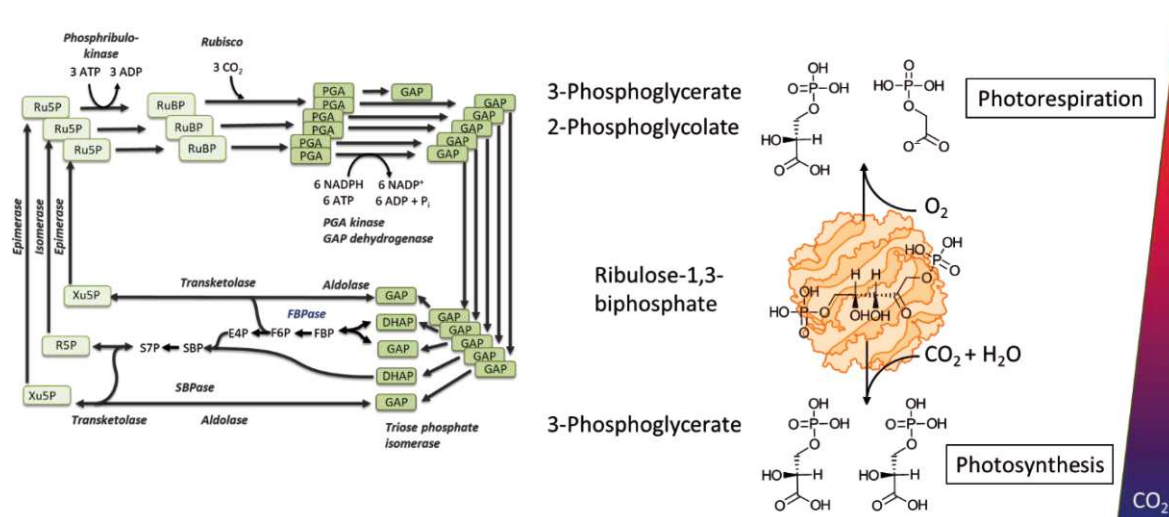


Figure 4 Left: The Calvin-Benson cycle reactions shown in two steps, conversion of pentose to triose (top) and triose to pentose (bottom). The carboxylation reaction results in three five-carbon molecules becoming six three-carbon molecules. One of these can leave the cycle but the other five must be converted back into five-carbon molecules. The conversion of triose phosphates to pentose phosphates is simply two rounds of aldolase, bisphosphatase, transketolase. DHAP = dihydroxyacetone phosphate, E4P = erythrose 4-phosphate, F6(B)P = fructose 6(bis)-phosphate, G6P = glucose 6-phosphate, GAP = glyceraldehyde 3-phosphate, R5P = ribose 5-phosphate, Ru5P = ribulose 5-phosphate, S7(B)P = sedoheptulose 7(bis)-phosphate, Xu5P = xylulose 5-phosphate. Adapted from Sharkey, 2018²⁷. **Right:** A simplified visualization of CO₂ dependency in RubisCO, the lower the concentration of CO₂ in the surrounding of this enzyme, the higher rate of photorespiration and so the concentration of 2-Phosphoglycolate compared to photosynthesis.

This became a problem during the so-called great oxidation event or the oxygen catastrophe. The increase in atmospheric oxygen and depletion of carbon dioxide by the onset of oxygenic photosynthesis changed the world irreversibly,^{1,30} thus demanding a mechanism to increase the inorganic carbon (C_i) concentration around RubisCO, the Carbon Contracting Mechanism (CCM).

At the center of CCM is the carboxysome, a specialized microcompartment, resembling a polyhedral protein shell, encapsulating key enzymes of carbon fixation, mainly ribulose-

1,5-bisphosphate carboxylase/oxygenase (RubisCO) and carbonic anhydrases.^{29,31} Carbonic anhydrases are crucial, as active transporters inside the cell wall and membranes increase the amount of carbonic acid inside the cytosol, diffusing inside the carboxysome that can be converted by carbonic anhydrases into CO₂, creating a CO₂-rich and probably O₂ reduced environment for optimal functionality of RubisCO.¹⁸ The CCM also shows promising results, when adapted into plants, to increase crop yields.³² Figure 5 shows an illustration of CO₂ uptake by different transporters and the concentration in the carboxysome in cyanobacteria.

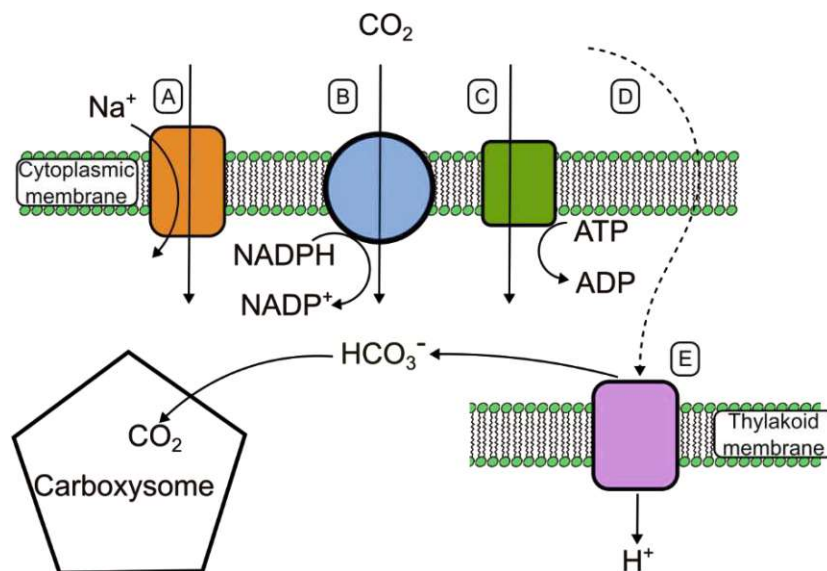


Figure 5 Schematic of the carbon concentrating mechanism and CO₂ transport into a cyanobacterium. **A** A sodium-dependent symporter. **B** and **C** are co-factor-dependent transporters utilizing NADPH and ATP, respectively. All three transporters convert the gaseous CO₂ into carbonate. CO₂ can also enter the cell via diffusion (**D**) and then be converted into carbonate on the thylakoid membrane (**E**). The intracellular carbonate is then taken up by the carboxysome and converted back into CO₂, to be accepted by RubisCO. The figure is adapted from Burnap et al. 2013³³.

The highly sophisticated photosynthesis apparatus of cyanobacteria allows them to utilize the visible light spectrum more efficiently than land plants. Apart from their use as a model to study photosynthesis, cyanobacteria have gained the interest of a more applied field of science: Biotechnology.

1.2 CYANOBACTERIA IN BIOTECHNOLOGY

The ancient and thereby highly advanced metabolism of cyanobacteria, relying on CO₂, light, water, and salts, could be used to mitigate climate change and environmental pollution, the greatest threat to humankind today.³⁴ This could be done by tackling two problems at once.

- i) The cultivation of cyanobacteria and production of their biomass does not require any carbohydrates, but CO₂ as a carbon source, circumventing the competition for arable land (feed vs. fuel)³⁵. Additionally, they can be cultivated

in brackish-, salt- or wastewater, saving precious drinking water in a time of rising need.^{36,37}

- ii) If the products are directly derived from atmospheric CO₂, the process can be directly part of a circular economy and the price of such a product would be lower, than that of carbohydrate-based products (being it sugars for heterotrophic organisms or fossil fuel-based).³⁸

The following chapter will take a closer look at biotechnology employing cyanobacteria, with proof of concepts, market-ready products, failed attempts, and the current limits and problems.

1.2.1 Potential Compounds for cyanobacterial-based Manufacturing

1.2.1.1 Natural products

Naturally occurring products extracted from cyanobacteria currently have the largest market share, especially in the European market due to regulations on genetically modified organisms (GMO). Among these ‘natural’ products are pigments, including the above-mentioned phycocyanin and carotenoids, which are sold as food colorants, with phycocyanin currently being the only natural blue food dye.³⁹ Some cyanobacterial strains are also labeled as ‘food grade’ and are widely sold as nutraceuticals and supplements, due to their high amount of protein and antioxidants.⁴⁰ Studies have shown positive effects on the overall health of using cyanobacteria as a food supplement, e.g. Park et al., 2008.⁴¹ Algae and cyanobacterial biomass are also interesting as feedstock in aquaculture as well as for livestock, especially as an alternative to fish meal, due to the favorable amounts of polyunsaturated fatty acids and high protein content.⁴² Among other natural products, poly-hydroxy butyrate (PHB) is highly promising, due to its possible application as biobased-plastic with promising characteristics. Some cyanobacteria synthesize this polymer naturally as carbon-storage material, especially under nitrogen limitation, and can accumulate up to 85% of their dry biomass as PHB.⁴³ While this is a significant amount, the strains, where these numbers are measured are suboptimal for large-scale production, so endeavors have begun to genetically alter more promising and established strains, such as *Synechocystis sp.* PCC6803, and improve their production.

1.2.1.2 Genetically engineered products

Establishing the connection between a gene and its function frequently necessitates genetic manipulation, either through deletion or over-expression of the gene of interest (GOI). Manipulating eukaryotes, including plants, is often more complex due to their cellular structures, such as the nucleus, and their highly redundant systems.⁴⁴ Therefore, the availability of prokaryotic models for studying gene function in photosynthesis has been particularly valuable. An expanding array of genetic tools has been developed to manipulate genomes and express recombinant proteins, facilitating various biotechnological applications.^{45–49} Some of these tools will be further explored later.

Genetic engineering in cyanobacteria can either be used to optimize and so increase the product titer of a compound they already produce, or new protein(s) can be introduced to either siphon metabolites away from the endogenous metabolism into the desired product, or catalyze a reaction independent of the metabolism, exploiting the host cell as a reaction vessel.

Carotenoids, for example, have been shown to increase their titer not just by optimizing process parameters, but also by genetically introducing alternative enzymes into the metabolic pathway.^{50,51}

Several strategies have been employed to genetically alter cyanobacterial metabolism to increase PHB production, while a deletion of *phaEC*, an essential gene in the PHB pathway, allows to rerouting of carbon flux into other interesting compounds and products.⁵²

Alternatively, genes can be introduced expanding existing pathways with recombinant proteins, resulting in new-to-host compounds, for example, commodity chemicals, such as ethanol,⁵³ butanol,^{54,55} glycerol,⁵⁶ lactic acid⁵⁷ and various more.⁵⁸ These products might one day replace petroleum-based production of fuels or starting material for more complex materials, such as bioplastics, as of today, their production costs cannot compete with cheap and subsidized fossil-based raw materials.

The current approach is, therefore, to aim for high-value compounds, products with a high or increasing demand, but expensive in production, especially with an increase in customers looking for 'natural' materials.³⁸ A large group of chemicals of interest are terpenoids. A highly diverse group of compounds mainly produced in plants, where they act as signal molecules or precursors for phytohormones or pigments. They also gained interest due to their health-promoting properties and are potential anticancer drugs. The two main building blocks are isopentenyl diphosphate and dimethylallyl diphosphate.⁵⁹ Due to their close relation (especially within the plastids) of plants in cyanobacteria, cyanobacteria seem a promising host to produce this group of compounds,^{60,61} with examples including isoprene,⁶² squalene⁶³ or limonene.⁶⁴

The food-grade cyanobacterium *Arthrospira platensis* (or trivial *Spirulina*) has been suggested as production-platform for pharmaceutical proteins for direct oral delivery, such as vaccines⁶⁵ and success have been reported to increase stability⁶⁶ and protein concentration with the production currently on the pilot-plant scale.⁶⁷

Most recently, cyanobacteria have also been used to catalyze reactions independent of their metabolism by expressing enzymes, mainly oxygenases. This class of enzymes is preferably employed in cyanobacteria, as the photosynthetic light reaction supplies reducing equivalents and produces oxygen, both required in the reaction. Examples of this class are Cytochrome P450 and Baeyer-Villiger monooxygenases (BVMO), which have already been successfully expressed in cyanobacteria.^{19,68,69} This aspect will be further explored later.

With such promising ideas, why have cyanobacteria not overtaken the biotechnological economy and processes? The reasons shall now be examined in the next chapter.

1.2.2 Limits and disadvantages of cyanobacteria in biotechnology

The onset of modern biotechnology is said to be in the 1970s and 80s, with the development of recombinant DNA in 1972 and, shortly after, the first genetically modified organism in 1973, and the economic starting signal with the first patented genetically modified organism.^{70,71} The microbial organisms employed consist mostly of heterotrophs. One of the most common bacteria is *Escherichia coli* (*E. coli*), due to its fast growth and ease of genetic manipulation. Since then, most efforts to improve productivity have been directed toward these forms of organisms⁷². Cyanobacteria, photoautotrophs, have highly distinct requirements for growth and biomass accumulation and so these developments can hardly be applied to photosynthetic organisms. The natural habitat of *E. coli* is the intestine of mammals, an environment with highly stable conditions regarding light, temperature, and pH, so a good survival strategy is to metabolize as many different carbohydrates as possible faster than your competitors, while cyanobacteria are open to constantly changing environmental conditions and receive their energy and carbon from two different sources instead of only carbohydrates, namely CO₂ and light. Large-scale application for cyanobacteria therefore necessitates the reinvention of cultivation and production.

In a survey published by Schmelling and Broos,⁷³ scientists with various degrees of experience in cyanobacterial research were asked about the most pressing obstructions in the widespread application of cyanobacteria, three main points were mentioned:

- 1) Lack of standardization. Even when 'standard' conditions are applied, they vary from publication to publication, also databases are often not maintained properly, due to lack of funding and even genome annotations are not standardized, leading to confusion
- 2) Genetic engineering. In most publications on the genetic engineering of cyanobacteria, the lack of tools is mentioned, but it has been commented that the problem is more on the side of reproducibility. Additionally, high-throughput systems are often not applicable for cyanobacteria
- 3) Cultivation. Compared to other established heterotrophic microbes, cyanobacteria grow slower, and every step of up-scaling increases the risk of contamination.

In the next sections, these three points shall be examined more closely.

1.2.2.1 Genetic engineering in cyanobacteria

A prerequisite for metabolic engineering and optimization is tools for genetic engineering, such as knock-outs of native genes or expression systems for recombinant proteins, which are strong, reliable and tunable, to diverge carbon and energy to the desired product.

One of the earliest publications dates to the year 1970, describing the natural transformation of *Anacystis nidulans*, today known as *Synechococcus* PCC7942.⁷⁴ Natural transformation is the process of DNA uptake from the environment and integration into the genome via homologous recombination. A process that greatly facilitated genetic engineering in cyanobacteria. In all gram-negative bacteria, DNA uptake is facilitated by a type-IV-like pilus. These genes involved in the structure and construction of the pilus closely resemble those of the motility pilus. All cyanobacteria that are known to be naturally transformable share a full set of these genes.⁷⁵

Genomic integration comes with a cost: cyanobacteria possess several copies of their genome within a single cell, depending on species and environmental conditions, which increases the time to receive a fully segregated mutant.⁷⁵ Additionally, although genes are typically inserted into 'neutral sites' the position in the genome has a significant effect on expression level and overall gene stability.⁷⁶

Later, hybrid-plasmids allowed the modification and multiplication of plasmids in *E. coli*, that could be directly transferred to cyanobacteria.⁷⁷

Plasmids are an effective alternative to homologous recombination. Many cyanobacteria species harbor native plasmids, but for these to be manipulated and reintroduced into the host, the WT strain must first be cured from the original plasmid.⁷⁸ The next step was to construct hybrid plasmids, which could be expressed in *E. coli* and *Synechococcus*,⁷⁷ and later also applied to other marine cyanobacterial species.⁷⁹ Modern vectors with a broad host spectrum are mostly based on the RSF101 origin.^{80–82} If necessity commands two plasmids to be inserted into a single cyanobacterium, other vectors have been developed.^{83,84}

After the successful transmission of the GOI into the cyanobacterium of choice is possible with an array of tools available, the next hurdle is the expression system. Genetic regulation of expression is a complex machinery, an interplay of promoters, ribosome binding sites (RBS), terminators, RNA-induced silencing and enhancing, and terminators.⁸¹

Native promoter systems, such as *Pcpc* and *Ppsba2*, have been characterized in cyanobacteria.⁸⁵ While these promoters effectively drive strong gene expression, their activity is induced by strong light and is not readily controllable, posing challenges when precise control over expression levels is required.⁸⁵ Systematic approaches, like those implemented by the consortium CyanoFactory, have identified a diverse range of promoter expression profiles, both constitutive and inducible.⁸⁶

Early inducible promoters in cyanobacteria were regulated by metals (e.g., cobalt or nickel) or micronutrients. However, these systems complicate cultivation as they can either limit growth if the inducer is absent or become toxic at higher concentrations. Alternatives such as tetracycline and Isopropyl β -D-1-thiogalactopyranoside (IPTG)-inducible promoters initially performed poorly in cyanobacteria, but subsequent improvements have enhanced their reliability.⁸²

Efforts to identify better inducer compounds have focused on overcoming limitations such as tetracycline degradation under high light intensity and preventing promoter leakiness (unintended protein accumulation without the inducer). Promising compounds identified include rhamnose and vanillic acid, which offer improved control over gene expression in cyanobacteria.⁴⁶

Despite the variety of promoters available, their predictability remains a challenge. The genetic context, including the ribosome binding site (RBS) and the coding sequence of the gene of interest (GOI), significantly influences expression levels. The RBS is the first initiation location for the complex of the 30S ribosomal subunit and the mRNA and thus strongly influences the translation rate.^{87,88} Current prediction tools for cyanobacteria are less reliable compared to those for other organisms, as demonstrated by experimental data.⁸⁹ Genetic constructs such as the ribozyme RiboJ and the bicistronic device (BCD2) can mitigate the effects of genetic context during translation and transcription. RiboJ, a nucleotide sequence derived from the tobacco ringspot virus, is inserted between the promoter and the coding sequence. After transcription, the ribozyme cleaves itself, removing promoter-associated RNA leaders and preventing interference.⁹⁰ BCD2 is a 16-amino acid leader sequence containing a separate Shine-Dalgarno sequence, along with start and stop codons. It couples its translation with that of the GOI, thereby reducing the influence of the surrounding genetic context.⁹¹ In Figure 6, the effect of RiboJ and BCD2 are illustrated.

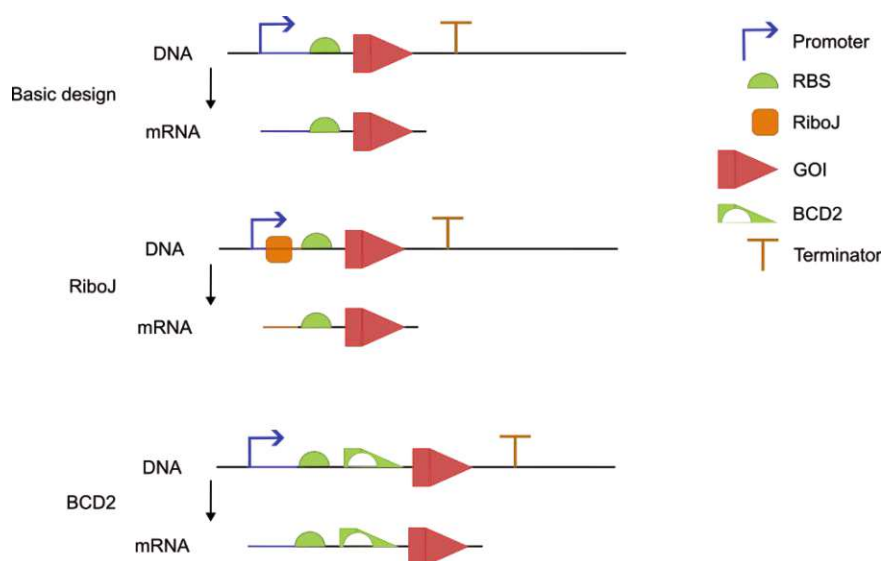


Figure 6 RiboJ and BCD2 can insulate the mRNA from the genetic context of the DNA. RiboJ is a self-cleaving ribozyme, which removes the promoter sequence from the mRNA. BCD2 is inserted between the RBS and the GOI and inserts its own RBS. Both elements minimize the influence of the promoter sequence of the mRNA on the translation initiation. Abbreviations: RBS – Ribosome binding site; GOI – Gene of interest; BCD2- Bicistronic device. Adapted from Jodlbauer et al., 2024.⁹²

The genetic parts mentioned above are pillars of synthetic biology, where genetic circuits are built to better understand biology on a systematic level or improve productivity for biotechnology. A tenet of synthetic biology is the “design, build, test, and learn” cycle,⁹³ which requires reliable and predictable protein expression, as well as rapid cloning and

assembly methods. The CyanoGate Kit provides a system that can achieve these guidelines.⁸⁴ It is based on the MoClo grammar for modular cloning, based on Golden Gate cloning.⁹⁴ Golden gate cloning utilizes type IIS restriction enzymes, which recognize and attach to sequence-specific double-stranded DNA, but cut upstream of the recognition sequence, producing “sticky-ends”. These overhangs can, therefore, be adjusted to the needed adjacent DNA fragment to be inserted.⁹⁵ The CyanoGate Kit applied this cloning technique for cyanobacterial-specific genetic parts. The fast assembly system allowed a high throughput system to test a large array of different promoters in two distinct cyanobacterial species, namely *Synechocystis sp.* PCC6803 and *Synechococcus sp.* UTEX2973. This was necessary, as genetic parts behave differently in cyanobacteria than in *E. coli*.⁹⁶

The CyanoGate Kit allows rapid development of libraries to be tested in cyanobacteria. One shortcoming of the modular system is the coupling of the RBS and the promoter. RBSs can have a strong impact on protein expression but are also dependent on the genetic context, such as the coding sequence or the promoter.^{89,97} A recent publication re-designed the module and allowed the easy exchange of the RBS and showed also the benefits of such a system. This could also be used to improve the predictability of *in silico* tools for protein expression.⁹²

1.2.2.2 Genetic instability

Genetic instability is a recurring problem among cyanobacteria, which can become even more problematic when employed in large-scale production, where suddenly yield is dropping. Instability occurs often, yet is seldomly investigated, so it has been termed the ‘elephant in the room’, obvious, yet ignored.⁷⁶ Cyanobacteria have developed strong DNA repair mechanisms, which is sensible, as their lifestyle is packed with mutagens, such as UV-light and radical oxygen species (ROS). Especially under laboratory conditions, such as constant and high light, high CO₂, and high nutrient availability, mutations can occur rapidly and accumulate. This has been observed and described when the original isolate of *Synechocystis sp.* PCC6803 was re-sequenced, after several years in different laboratories. The strains differed in their sensitivity to glucose, mobility, and phage resistance⁹⁸. The repair mechanisms in cyanobacteria complicate gene-based studies and endeavors to eliminate these systems seldom create stable phenotypes. The phenotype of $\Delta recA$ for example, only grows at low light, while high light cultivation is lethal.^{99,100}

Additionally, due to genetic instability and ‘microevolution’, the experimental results between different laboratories can vary greatly, even in experienced hands. In a study published in 2023, a typical strain (*Synechocystis sp.* PCC6803), expressing the fluorescent protein YFP under 3 different promoters, showed, that although the strains were genetically identical and the cultivation conditions reported were the same, growth rates and expression levels varied between labs, with a potential 36% reduction of growth rates and 32% variance in YFP expression level under the Rhamnose inducible promoter

P_{RhaBAD} . The study shows, that enhanced method documentation and carefulness are necessary in interpreting cyanobacterial data.¹⁰¹

1.2.2.3 Photobioreactor designs

Next to the difficulties in the genetic engineering of cyanobacteria, the design of the photobioreactor is an ongoing process. Large-scale cultivation of cyanobacteria requires the balancing of i) light intensity between Photoinhibition and counteracting self-shadowing and ii) CO₂ dispersion and O₂-degassing.¹⁰² Photoinhibition describes the situation, where cyanobacteria are compromised by degradation of the manganese cluster of Photosystem II, which impedes their growth.¹⁰³ The maximum light intensity cyanobacteria can handle depends on species, cell density, culture tank depth, and wavelength distribution of supplied light.^{103,104} Compared to heterotrophic hosts, current cultivation systems still lag, but become more and more efficient, mainly due to optimized illumination, which differs fundamentally from any component or device used for heterotrophic cultivation. In terms of reactor design, there are two main systems for cyanobacterial cultivation: open raceway ponds (ORP) and closed photobioreactors (PBR).

ORPs were the first and are still most frequently used in cyanobacterial cultivation. They consist of a closed-loop flow channel with a paddlewheel for constant mixing and circulation and are often equipped with microporous gas diffusers for CO₂ supply. Construction and maintenance costs are comparably low, as they can be built on compacted earth or concrete lined with plastic foil.¹⁰² Although they can be placed inside greenhouses, which increases construction costs, their disadvantages include contamination with predators, viruses, or competing algae as well as evaporation, variable culture conditions caused by seasonal and diurnal conditions, and low yields.^{105,106} Improvements in ORP can be made by combining them with direct-air-capture systems. Recently, a system has been described using moisture-swing-sorption of CO₂ to a polymer, which absorbs atmospheric CO₂ and releases it, when in contact with water.¹⁰⁷ Additionally, engineered cyanobacteria can assimilate phosphorus as phosphite, which in turn drastically removes the risk of contamination in an open system.¹⁰⁸

Photobioreactors circumvent some of these drawbacks. These closed systems do not experience evaporation or contamination while allowing the control of most environmental conditions.¹⁰² PBRs can be either tubular, flatbed, airlift, or bubble column reactors, each with its advantages and disadvantages (reviewed by Johnson et al., 2018,¹⁰⁴ see Figure 7), but all in common, is that they contain liquid cultures with maximized surface-to-volume ratio, increasing the light penetration, and providing CO₂ as gas or carbonate. Despite their high costs for construction and maintenance, their higher yield makes them attractive for industrial production, e.g. for biofuels such as ethanol.¹⁰⁹ Improved light distribution can also be obtained by internal illumination by floating LEDs inside the reactor, which are powered via induction from outside the reactor.¹¹⁰ A promising development in PBRs are membrane-based systems. The

company CellDEG (Berlin, Germany) provides cultivation systems with a hydrophobic, gas-permeable membrane at the bottom of the cultivation vessel, allowing a continuous supply of CO₂, either from a gas bottle or from a carbonate buffer, while cultivating under high light intensities. With this, they reached cell densities of 30 g/L on laboratory scale.¹¹¹ Large-scale systems, such as porous substrate membrane reactors, can even reach higher cell densities, comparable to those reached by heterotrophic hosts.¹¹² Constant progress in the design of PBRs shows promising results.

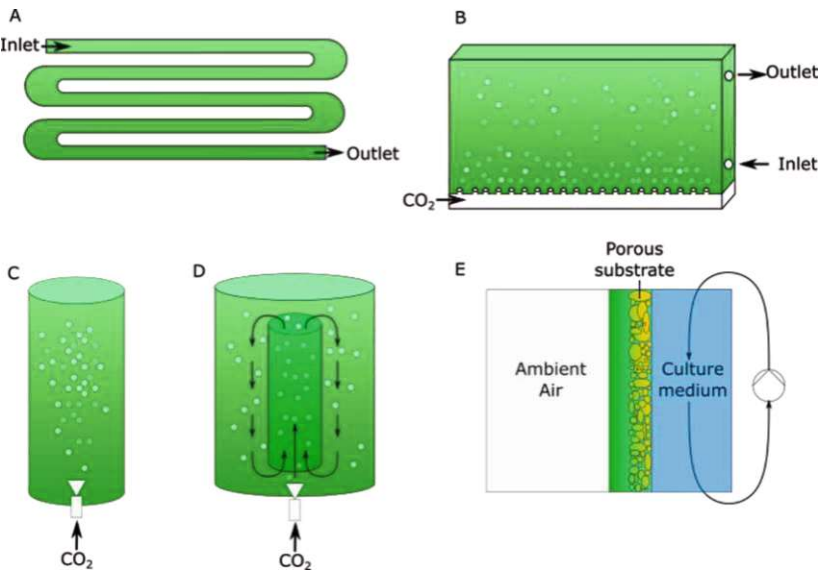


Figure 7 The most common designs for closed photobioreactors for the cultivation of Cyanobacteria are **A** Tubular, **B** Flat-bed, **C** Airlift, and **D** Bubble column. A new design with promising results is the Porous Substrate Reactor (**E**). Adapted from Jodlbauer et al.2021¹⁹.

1.2.3 Cyanobacterial stains used in biotechnology

Cyanobacteria may grow faster and have higher efficiency in terms of quantum yield compared to other photoautotrophic organisms,¹¹³ but are outcompeted by commonly used heterotrophic hosts.¹¹⁴ Table 1 Shows doubling times, maximal cell density, and examples of compounds produced by typically employed and new, promising cyanobacterial strains. Heterotrophic organisms used in biotechnology, such as *E. coli* or *Pichia pastoris*, can easily reach >100 g_{DCW} / L,^{115,116} outranking cyanobacteria by far, yet the constant discovery of new strains renders cyanobacteria more and more compatible.

Table 1 Commonly used cyanobacterial strains, their doubling time, and exemplary products

Strain	Maximal doubling time	Maximal cell	Compounds produced (exemplary)

		density [g _{DCW} /L]	
<i>Synechocystis</i> sp. PCC6803	6.6 ± 0.2 h ¹¹⁷	6.9 ¹¹⁸	Fatty acids ¹¹⁹ , Isoprene ⁶² , squalene ⁶³
<i>Synechococcus</i> sp. PCC7942	4.9 ± 0.7 h ¹¹⁷	6.3 ¹²⁰	2,3-butanediol ¹²¹ , 1-butanol ¹²² , sucrose ¹²³ , ethanol ¹²⁴
<i>Synechococcus</i> sp. PCC7002	4.1 ± 0.4 h ¹¹⁷	19.2 ¹¹⁸	Hydrogen ¹²⁵ , bisabolene, limonene ⁶⁴
<i>Synechococcus</i> sp. UTEX2973	2.1 ± 0.2 h ¹¹⁷	6.5 ¹¹⁸	Sucrose ¹²⁶ , Limonene ¹²⁷ , l-lysine, cadaverine, glutarate ¹²⁸
<i>Synechococcus</i> sp. PCC11801	2.3 h ^{129a}	n.a. ^b	Ethylene, Succinate ¹³⁰
<i>Synechococcus</i> sp. PCC11802	2.8 h ¹³¹	2 ¹³¹	Mannitol ¹³²
<i>Synechococcus</i> sp. PCC11901	<2 h ¹¹⁸	32.6 ¹¹⁸	glucosylglycerol ¹³³ , free fatty acids ¹¹⁸

^a Highest reported growth rate under ambient CO₂

^bn.a. = not available

1.2.3.1 Characteristics of fast-growing cyanobacterial strains

In a typical batch culture, such as a shake flask in a lab incubator, cyanobacterial growth is normally divided into three phases: an exponential, a linear, and a stationary phase. The reason for this deviation of typical heterotrophic bacterium growth phases is the main source of energy: light. With increasing cell density, cells shade each other, underlying bacteria receive less light than the one closer to the light source. In well-mixed batch culture, it can be assumed that the time a cell remains in the area with enough light and without light is evenly distributed among all cells in the batch, thus the average light a cell receives is reduced over time.¹³⁴ In the early exponential phase, light is abundant, and growth is only prohibited by light inhibition. During the short exponential phase, growth is the fastest, but the quantum yield is the lowest, implying that a certain amount of photodamage is correlated with fast growth. Approaching optimal cell density, quantum yield increases.¹³⁵ The cell density increases linearly afterward, as light becomes limiting proportionate to cell density. The linear growth continues until the energy input is equal

to the energy required for the minimal maintenance to keep a cell alive, which is thought to be around 900 $\mu\text{mol photons/g}_{\text{DCW}}/\text{h}$.¹³⁶

Apart from the growth conditions and quantum yield, other factors can influence growth behavior. It is hypothesized, that genome size correlates negatively with growth rate due to the additional burden of niche proteins and reduced space in the crowded cell for ribosomes, as ribosome count affects growth rate.¹³⁷ Although the correlation between genome size and growth rate in cyanobacteria is not ubiquitous¹³⁸, the deletion of parts of its genome ('streamlining') has increased the growth rate in *Synechococcus sp.* UTEX2973.¹³⁹

Cyanobacterial strains, which are considered 'fast-growing', are typically non-filamentous, non-diazotrophic, have a smaller cell size, and grow at moderate to high light intensities.¹⁴⁰

It is also hypothesized that a high growth rate does not necessarily increase product formation. Cells, that are optimized for fast growth, have little capacity to reallocate resources for an additional product, and with increasing cell density, less light can be harvested.¹⁴¹ This hypothesis has not been experimentally tested yet, despite this, strategies have been developed to decouple the production phase from the growth phase.¹⁴²

The limits of cyanobacterial growth are largely underrepresented in current research. The growth rate of the fastest-growing cyanobacterium, *Synechococcus sp.* UTEX2973 has been analyzed via *in silico* models,¹²⁸ isotopic labeling of metabolic fluxes,¹⁴³ comparison of genomic features,^{3,144} and more.¹⁴⁵ These publications characterize well the short period of the high growth rate of *S. sp.* UTEX2973 and add knowledge to the overall picture, but they neglect that the total biomass accumulation rarely outperforms that of the much slower-growing *Synechocystis sp.* PCC6803.

1.2.3.2 *Synechococcus sp.* UTEX2973

First described in 2015, *Synechococcus sp.* UTEX2973 (UTEX2973) has been utilized as proof of concept for the benefits of employing fast-growing cyanobacteria versus slower-growing cyanobacteria and has been equipped with an ever-enlarging toolbox.

UTEX2973 has now been proven in several studies to be a promising platform for photosynthesis-based bioproduction and has outcompeted any other cyanobacterium in the production of α -farnesene,¹⁴⁶ isoprene,¹⁴⁷ polyhydroxy butyrate,¹⁴⁸ Limonene,¹²⁷ glycogen¹²⁶ and sucrose¹⁴⁹.

The closest relative to UTEX2973 is *Synechococcus sp.* PCC7942. They are genetically almost identical and only differ in 55 single nucleotide polymorphisms (SNP) and inversion/deletions, including a 188.6kb inversion and 6 open reading frames are not present in the UTEX2973 genome.¹¹⁷

The fast growth of UTEX2973 compared to *Synechococcus sp.* PCC7942, despite their highly similar genomes, was further investigated by building a genome-scale model

(GSM), applying Flux balance analysis (FBA), and comparing the metabolic fluxes between these two strains.¹⁴⁵ Under non-limiting conditions, the most pronounced difference in the biomass composition between the two strains was the glycogen content, with UTEX973 accumulating less glycogen. At the same time, UTEX2973 has a higher content of amino acids. Additionally, under photon-limiting conditions, where the minimal number of photons is set as a limit to the model, the flux through the amino acid biosynthesis pathways is higher in UTEX2973. In company with several SNPs in the 23S ribosomal subunit, which might code for higher rates, this is in accordance with the observation in other species, that growth rates correlate positively with ribosome content.¹³⁷ Later studies on the metabolic fluxes of UTEX2973 also revealed higher carbon assimilation compared to *Synechococcus sp.* PCC7942, where 96% of CO₂, which is taken up by UTEX2973, is incorporated into biomass (as compared to 86% in *Synechocystis sp.* PCC6803)¹⁴³ and a highly carbon-efficient metabolism, streamlined for fast growth by increased photosynthetic and key central pathway fluxes. Especially of interest is the higher concentration of NADPH and ATP during high growth rates in UTEX2973, compared to other cyanobacterial stains.¹⁵⁰

Recent publications also indicate that the fast growth of UTEX2973 is not the maximal growth rate for cyanobacteria. It has been shown, that cyanobacteria, specifically *Synechocystis sp.* PCC6803, sacrifice some of their potential for optimal growth for 'preparedness' in anticipation of changing conditions.¹⁵¹ Because of this, it is possible that UTEX2973 could grow even faster. The truncation of the antenna of the light-harvesting complex (LHC) in UTEX2973 led to an increase in growth and quantum yield.¹⁵² Another study showed, that the 'streamlining' of the genome, meaning deleting of non-essential parts, increases growth rate and productivity by 23%.¹³⁹ The biomass accumulation and productivity were also increased by optimizing semi-fed batch culture under the supervision of a machine-learning algorithm.¹⁵³

1.2.3.3 *Synechococcus sp.* PCC11801 and 11802

Another strain of interest is *Synechococcus sp.* PCC11801, with doubling times of 2.3 h⁻¹ under ambient CO₂ concentrations, making it the fastest-growing cyanobacterium under these conditions.¹²⁹ *Synechococcus sp.* PCC11801 has been used to produce succinic acid and mannitol, both with unprecedented yield compared to other cyanobacteria.^{132,154} The mannitol study also tested *Synechococcus sp.* PCC11802, a close relative of *S. sp.* PCC11801, sharing 97% of its genome¹³¹. *S. sp.* PCC11802 shows also a high growth rate at 1% CO₂ and might be more suitable for products derived from metabolites of the CBB cycle, as the genes involved in the CBB are not repressed at higher CO₂, in contrast to *Synechococcus sp.* PCC11801. This hypothesis has yet to be proven experimentally.¹³¹

1.2.3.4 *Synechococcus sp.* PCC11901

The cyanobacterial strain *Synechococcus sp.* PCC11901 (from here on PCC11901), was isolated in 2020 from the Johor Strait estuary in Singapore. After enriching the marine water sample with cobalamin (Vitamin B12), and several rounds of re-streaking on a saltwater medium agar plate, an axenic culture of PCC11901 was obtained. This strain

showed a high growth rate and was therefore further investigated. The optimization of the medium, with increased N, P, Fe, and cobalamin allowed unprecedented biomass accumulation of 32.6 g_{DCW}/L, which has not been reported before¹¹⁸ (see Figure 8). On top of the high cell density, PCC11901 also showed other characteristics, rendering it interesting for research.

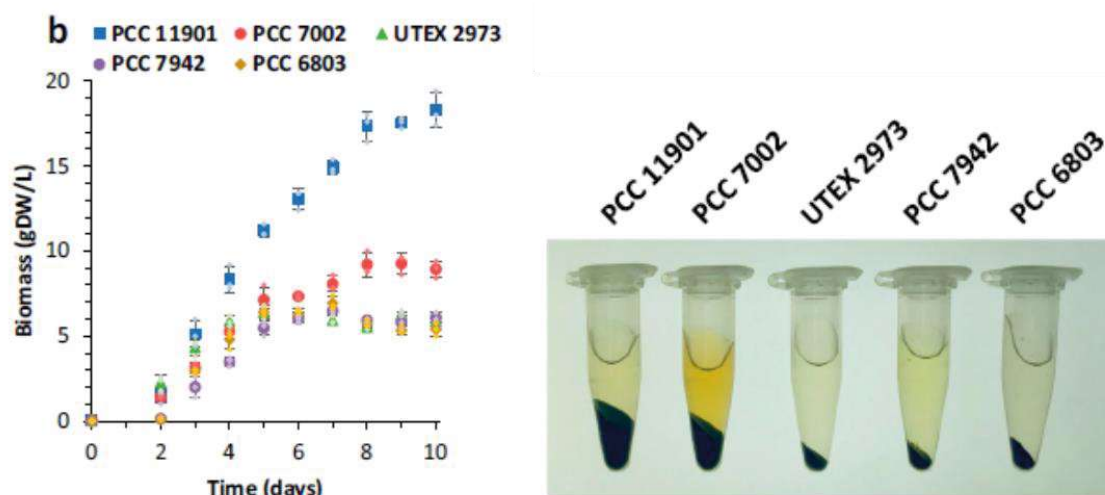


Figure 8 Growth of *Synechococcus* PCC11901 compared to other cyanobacterial model strains (left) and accumulated biomass comparison after centrifugation (right). According to Włodarczyk et al., 2020¹¹⁸.

PCC11901 grows unicellular but occasionally forms filaments of 4-6 cells. The strain can grow on glycerol as the sole carbon source without light and in the presence of a photosynthesis-inhibiting agent. It cannot grow in glucose, probably due to a dysfunctional *glcP* gene, which codes for a glucose transporter.¹⁵⁵

The *metE* gene, which is encoded on a plasmid of PCC11901 should prevent a cobalamin auxotrophy, yet in a medium without cobalamin, PCC11901 has a prolonged lag-phase. The auxotrophy can be abrogated either by rational design, such as expressing a functional *metE* gene, or by directed laboratory evolution, which has been shown by two independent laboratories.^{133,155}

Other genetic differences from the most common cyanobacterium *Synechocystis* sp. PCC6803 includes the lack of a PHB-producing pathway and a missing *glyK* gene, which encodes for the last enzyme in photorespiration. These genetic features are shared with the closest related strain *Synechococcus* sp. PCC7002 (97%), a well-established lab strain, which can be engineered to produce limonene and bisabolene.^{64,155}

Although they share 97% of their genomes, PCC11901 has a higher growth rate and can accumulate more biomass than *Synechococcus* sp. PCC7002. Both strains possess only one CpcC linker protein, which connects the allophycocyanin-hexamers to the Phycobilisome core, thus they probably have only 2 stacked disc-shaped hexamers instead of 3¹⁵⁵. A truncated antenna can increase growth and efficiency in *Synechocystis*

sp. PCC6803¹⁵⁶ and UTEX2973¹⁵² and might be an important factor for the high biomass accumulation property. The truncated antennae possibly reduce self-shading in a batch culture.

The reasons for the superior growth characteristics are not well understood. In comparison to UTEX9273, *Synechocystis sp.* PCC6803, and *Synechococcus sp.* PCC7942, PCC11901 shows less photoinhibition at high light intensities, an increased oxygen evolution rate at the same light conditions, and the highest respiration rate under dark conditions.

PCC11901 is naturally competent, facilitating a simple approach to genetic manipulation. The strain is amenable to triparental mating (or conjugation) by *E. coli*, allowing the transfer of RSF1010-based plasmids into the cytosol of PCC11901.¹⁵⁷ Other genetic tools include an inducible promoter based on the *phlF* system. The promoter shows tight regulation and high dynamic range and is inducible by 2,4-diacetyl phloroglucinol (DAPG). The tight expression regulation was a prerequisite for the construction of a CRISPR-cas12a strain, which allows efficient and markerless insertion of foreign genes and the construction of a CRSPRi system for accurate gene silencing.¹⁵⁷ Despite several attempts, the development of a negative marker system, which facilitates the re-use of antibiotic resistances has not been developed.

1.2.3.5 *Synechococcus sp.* UTEX3222

The recent discovery of *Synechococcus sp.* UTEX3222 brings another fast-growing strain, with a reported doubling time of 2.35h and a high biomass density of up to 31 g_{DCW}/L. Another remarkable characteristic is fast sedimentation, which could decrease the cost of downstream processing. The strain is not mentioned in the table, as it has not been employed for any biotechnological processes yet and the publication is still under review. The strain holds promises for future applications.¹⁵⁸

1.2.3.6 What is limiting cyanobacterial growth?

Fast growth is an important feature when considering the economic feasibility of biotechnological applications, but only focusing on this parameter is not sufficient to assess the productivity of a cyanobacterium. Additionally, the growth rate is the product of several factors, such as the rate of light absorption, photosynthetic effectivity, and maximal biomass production from a certain amount of light.¹⁴¹ Cyanobacteria enter the stationary growth phase when the incident light energy is equal to the amount of energy needed for cell maintenance. The more cells there are, the less light can penetrate through the culture, so-called self-shading (see Figure 9). Self-shading is mostly mentioned when talking about the limits of biomass accumulation in cyanobacteria.¹³⁸ In recent years, the image has changed. Shotgun-proteomics has shown, that the growth in *Synechocystis sp.* PCC6803 is constrained by the abundance of light and CO₂ harvesting proteins, thus allowing the strain to be prepared for changing environmental conditions, but with the penalty of less biomass accumulation and slower growth,¹⁵¹ indicating a trade-off between growth and preparedness.¹⁵⁹ The unprecedented biomass accumulation of *S. sp.* PCC11901 gives rise to the possibility of experimental determination on the limits of growth in cyanobacteria.

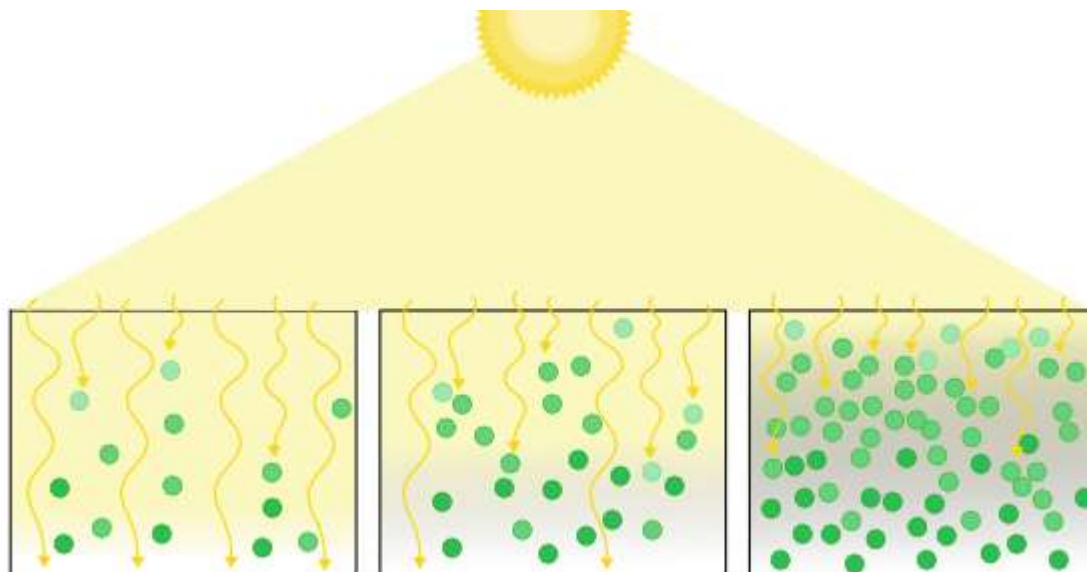


Figure 9 Schematic of self-shading in cyanobacterial fed-batch culture. The more cells in a suspension, the more light they absorb, and the shorter the path, light can penetrate the cultivation vessel.

Cyanobacteria are fascinating and promising prokaryotes for biotechnology. This work will focus on a special subdivision of biotechnology, which will now be further explained.

1.3 BIOCATALYSIS

Biotechnology is a wide term for a variety of processes. This shall be further narrowed down in the next sections. The last few decades have seen several leaps forward from gene sequencing and synthesis to process optimization, pathways design with increasing complexity, and many more, sometimes even referred to as the ‘golden age of biocatalysis’.¹⁶⁰ Biocatalysis, as one part, focuses on turning a substrate into a value-added product with the help of enzymes, either isolated or within a host. But let us be a tad more specific:

1.3.1 Biotransformation and fermentation

As mentioned above, biocatalysis requires enzymes to convert one compound into the next (and maybe further) into a compound with a higher value. These reactions can be catalyzed by a single enzyme, either *in vivo* or *ex vivo*, independent of the host metabolism, or in the form of fermentation, where the substrate is also the carbon source for the host. Additionally, synthetic metabolic pathways can be implemented into a microbial host, thus allowing new-to-nature products or exploiting the beneficial characteristics of the microbe, increasing the yield compared to the natural carrier of this pathway. These pathways can either be independent or dependent on the metabolism, extracting co-factors or metabolites from the central metabolism. Metabolism-independent reactions are often termed biotransformation, as opposed to fermentations, where the substrate and carbon source are identical, but the boundaries of biotransformation and fermentation, with their subcategories, are not solid but rather exist on a continuous spectrum¹⁶¹ (see Figure 10).

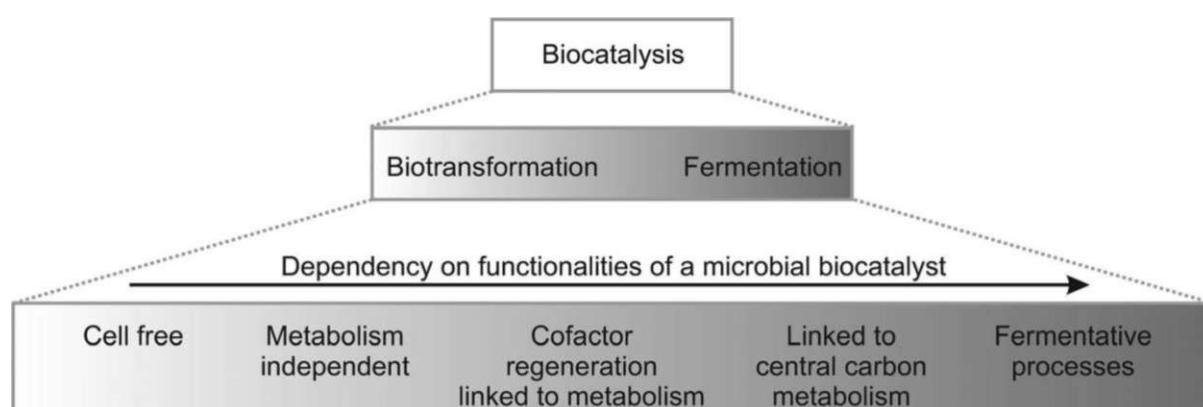


Figure 10 Continuous spectrum of biocatalysis, adapted from Schrewe et al., 2013¹⁶¹.

In fermentation, cells are fed with carbohydrates, such as glucose, glycerol, or organic acids. The cells take the energy-rich compounds as carbon and energy sources to grow and accumulate biomass and convert them into the desired product. The production phase can either be temporally separated from the growth phase or happen simultaneously. The product is so directly derived from the same source as carbon and energy. Early forms of this have been done to preserve food or increase its flavor or

textures and produce alcohol, e.g. cheese, yogurt, beer and wine, sauerkraut, and more.¹⁶² With the onset of recombinant gene expression systems and a deeper understanding of cellular processes, the product palette possesses now a wide spectrum, from pharmaceutical products (insulin,¹⁶³ antibiotics¹⁶⁴) to bulk chemicals (citric acid,¹⁶⁵ acetic acid¹⁶⁶).

Biotransformation has a different role in biocatalysis, as cell growth and product formation are separated, not just by space and time, but also by substrate. The substrate is added to the reaction in addition to the feed. This reaction can be done either by extracting and isolating the enzyme(s) of interest or within the cells in different metabolic stadia, from deceased to resting or actively growing.

An example of a cell-free system is styrene oxidase, which employs monooxygenases to oxidize styrene into the corresponding epoxide. The electrons needed for this reaction are supplied via FADH₂ from NADH by the reductase subunit of the enzyme. The recycling of NAD⁺ to NADH is accomplished by an additional enzyme, a formate dehydrogenase, which converts formate into CO₂ while reducing NAD⁺ to NADH.¹⁶⁷

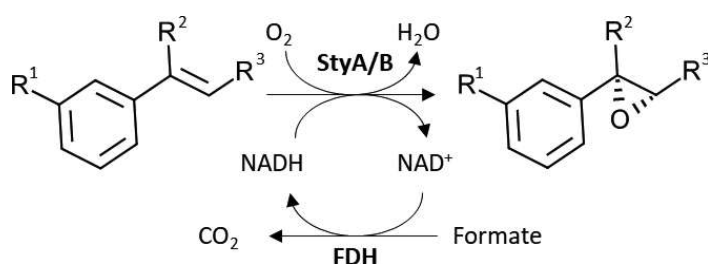


Figure 11 Cell-free, asymmetric epoxidation with NADH regeneration. Styrene monooxygenase (StyA), an NADH-dependent enzyme from *Pseudomonas* sp. VLB120 in collaboration with a formate dehydrogenase (FDH) from *Pseudomonas* sp., allows the NADH recycling with formate as a sacrificial substrate. R¹=H, Cl; R²=R³=H, CH₃. Adapted from.¹⁶⁷

A biotransformation within a cell is termed whole-cell catalysis. The optimization of this process is at the interface of biology, chemistry, and biochemical engineering, and interest in this type of process has grown in academia and industry.

1.3.2 Whole-cell catalysis

Whole-cell catalysis brings advantages for biotransformation reactions. The cell can act as a miniature bioreactor, stabilizing the reaction in terms of pH, osmolarity, increased catalyst stability, and supply of reducing agents or co-substrates.

A large number of factors influence the outcome of a biotransformation, some specific to whole-cell catalysis. These factors include, but are not limited to, the reaction, the way the reaction is interconnected with the host, the metabolic status of the cell, and of course the type of the host cell, which acts as a platform for the reaction. In the next sections, some examples will be described to give a more comprehensive picture of how

these factors influence the overall outcome. Afterward, the focus lies on how cyanobacteria can be utilized beneficially in whole-cell catalysis.

Reactions in whole-cell catalysis type are categorized either as metabolism-independent or dependent.

Exemplary for metabolism-independent biotransformation are alcohol dehydrogenases, which reduce ketones into optically active alcohols. This reaction requires NAD(P)H as a co-factor. Overall yield is increased by making the co-factor recycling metabolism independent. This is achieved by expressing an additional glucose dehydrogenase, which oxidizes glucose into gluconolactone while reducing NAD(P)⁺ into NAD(P)H.¹⁶⁸

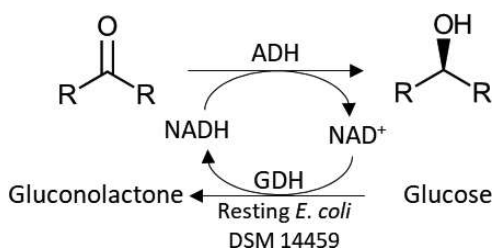


Figure 12 Biocatalytic reduction of ketones to optically pure alcohols. The reaction is catalyzed by an alcohol dehydrogenase (ADH) from *Rhodococcus erythropolis*, and coupled to a NADH-replenishing system, with a glucose dehydrogenase (GDH), converting glucose to gluconolactone. Adapted from.¹⁶⁸

In contrast, metabolism-dependent biotransformation can drain co-factors from the metabolism of the host. Ideally, the cells are in a resting state, so the co-substrate is not used for biomass accumulation. An example is the continuous process of transforming (2,5)-hexanedione into enantioselective pure (2*R*,5*R*)-hexanediol with *Lactobacillus kefir*. The reaction is catalyzed by the endogenous alcohol dehydrogenase of *L. kefir* and fueled with NADPH from the glucose metabolism.¹⁶⁹

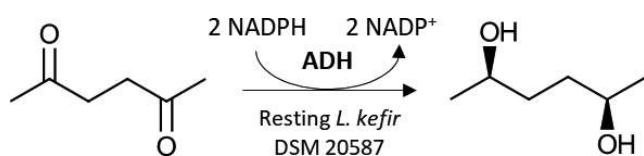


Figure 13 Microbial reduction of (2,5)-hexanedione to enantiopure (2*R*-5*R*)-hexanediol with the endogenous alcohol dehydrogenase (ADH) from *Lactobacillus kefir* DSM20587. The intact, resting cells were used for co-factor recycling by feeding glucose and leeching the required co-factors (2 NADPH molecules per reaction) from the central metabolism. Adapted from.¹⁶⁹

Whether dependent or independent, whole-cell catalysis can also consist of several enzymatic steps, which react in a cascade to the final product. The design and optimization of cascades often require several cycles of design, test, and learn.¹⁷⁰

An example of cascades in whole-cell catalysis, which is strongly connected to the metabolism is the production of heme. Heme, an iron complex with applications in pharmaceutical and food processing, is synthesized from 5-aminolevulinic acid, which can be synthesized from succinyl-CoA or glycine. Heme production requires upregulation and downregulation of several proteins in the native pathways and has been shown in *E.*

coli, *Saccharomyces cerevisiae*, and *Pichia pastoris*.¹⁷¹ In *E. coli*, the knock-down of three competing pathway enzymes, the rational overexpression of certain enzymes in the heme-synthesis pathway, and the expression of a transporter increased strongly the production of heme and facilitated easier downstream processing.¹⁷²

A whole-cell cascade that is only dependent on co-factors, such as NADPH from the host cell, and is divided between two species, is the valorization of limonene to carvolactone. This cascade consists of 4 enzymes and requires 3 molecules of NADPH per reaction, while also restoring one molecule of NADP⁺ into NADPH. The cascade is separated into two host systems, *Pseudomonas putida* and *E. coli*, and can be deployed directly with orange peel waste, without the need for limonene extraction.¹⁷³

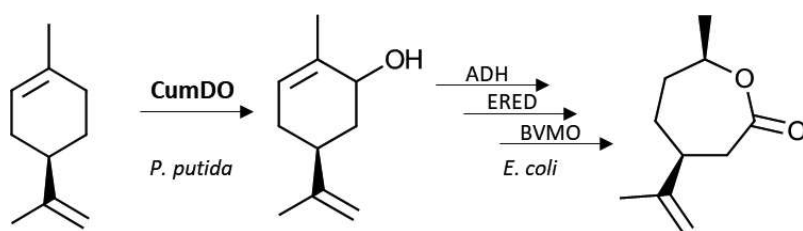


Figure 14 Mixed-species enzyme cascade from limonene to carvolactone. The cascade is composed of cumene dioxygenase (CumDO), expressed in *Pseudomonas putida*, and an alcohol dehydrogenase (ADH), an enoate reductase (ERED), and a Baeyer–Villiger monooxygenase (BVMO), expressed in *E. coli*. Adapted from.¹⁷³

Co-factor recycling is crucial for the feasible production of compounds via whole-cell catalysis, as co-factors, such as ATP or NAD(P)H often exceed the cost of the desired product.

The following two examples of whole-cell catalysis play a crucial role in this work and will thus be examined more closely.

1.3.2.1 Carboxylic Acid Reductases

Another example of whole-cell catalysis is the expression and use of carboxylic acid reductase (CAR).

The reduction of carboxylic acids (CA) into the corresponding aldehyde is industrially interesting but chemically challenging. This reaction can be achieved with a strong reducing agent, such as lithium aluminum hydride, but requires stoichiometric amounts and usually causes over-reduction to the corresponding alcohol¹⁷⁴. Next to transition metals, which require extreme conditions and lead to side-products, a selective reaction can be achieved by employing diisobutyl aluminum hydride. Beforehand, the CA must be activated by an ester, thioester, or acid halide and the reaction is only halted at the aldehyde stage at -78°C.¹⁷⁵

Enzymatic reduction of CA to aldehydes has thus become of great interest. The first described carboxylic acid reductases (CARs) came from *Neurospora crassa* and later

also from other *Nocardia* species. They also require posttranslational modification by phosphopantetheinyl-transferase (PPTase) for proper functionality.¹⁷⁶

The structure of bacterial CARs has been described as modular and follows mostly a 3 domain structure. The N-terminal domain is the adenylation domain, followed by the thiolation domain and a C-terminal reduction domain.¹⁷⁷ The structure is, following basic enzymology, the basis for the mechanism. The proposed catalytic cycle for CARs consists of five steps. First (I) the carboxylic acid moiety is activated by ATP, releasing PPi at the adenylation site. Then (II) the AMP-moiety undergoes a nucleophilic attack from the phosphopantetheine arm, attached to the thiolation domain and is thereby released. The acyl-thioester that is formed is then transferred to the reduction domain (III). At the reductive site, NADPH induces reductive cleavage and releases the formed aldehyde (IV). In the last step (V), the thioester arm swings back and is ready for the next catalytic cycle.¹⁷⁸

In conclusion, CARs require one molecule of ATP and one molecule of NADPH for one reaction, rendering an efficient co-factor recycling system mandatory.

1.3.2.2 Vanillin: applications and production

Vanillin represents one of the most sought-after aromatic compounds globally, with demand significantly outstripping the supply from natural vanilla sources. While chemical synthesis of vanillin is possible, its use in human applications faces substantial regulatory restrictions. Consequently, there is considerable interest in developing enzymatic routes for vanillin production. This section will elucidate the factors driving this demand and the potential advantages of biocatalytic vanillin synthesis.

The extract of the pods of the vanilla orchid contains around 200 different compounds, all contributing to the well-recognizable vanilla aroma. The most pronounced aromatic compound is vanillin, which contains 1-2% (w/w) of the cured vanilla pod, and the extraction of 1 kg of vanillin requires 500 kg of vanilla pods, which corresponds to 40000 vanilla orchid flowers.^{179,180}

Vanillin (IUPAC: 4-hydroxy-3-methoxybenzaldehyde) is one of the most requested flavor ingredients. While the demand for natural vanillin aroma is increasing, production can only cover a fraction of the total vanillin demand worldwide, depending on weather conditions, which heavily influence vanilla harvest. The high demand and low supply for natural vanillin cause a difference in price for chemically synthesized and naturally produced vanillin, with a factor of >10 on the Merck website,¹⁸¹ while other sources mention differences of 3 orders of magnitude.^{182,183}

What makes vanillin so interesting? Apart from its distinct flavor, this compound has also been used for other applications. It can be a precursor for bio-based polymers, such as epoxides, phenolic resins, or polyester.¹⁸⁴ In pharmaceuticals, it not only enhances the flavor of the medications¹⁸⁵ but has also been shown to reduce mutagenesis rate in *E. coli* and *Salmonella*,¹⁸⁶ halts colorectal cancer cells in their cell cycle,¹⁸⁷ acts as a potent

oxygen radical scavenger,¹⁸⁸ and has anti-inflammatory activity in mice.¹⁸⁹ The wide variety of applications asks for more efficient processes for vanillin production.

The first extraction of vanillin from a different source than the vanilla orchid, spent sulfide waste streams of lignin pulping, was described and patented in 1936.¹⁹⁰ This strategy was later changed and optimized, mainly due to environmental concerns.¹⁹¹ Since the 1970s, most chemically synthesized vanillin has been produced from guaiacol.¹⁸³ This reaction is started via an electrophilic aromatic substitution by glyoxylic acid to produce 3-methoxy-4-hydroxy mandelic acid, which further undergoes oxidative decarboxylation to produce vanillin.¹⁹² This is illustrated in Figure 15.

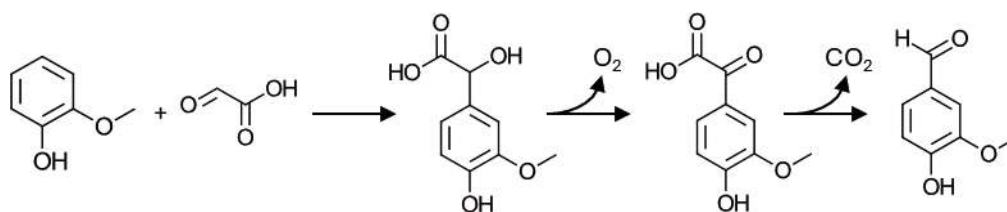


Figure 15 Chemical synthesis of vanillin from guaiacol with glyoxylic acid. Adapted from Xu et al., 2024.¹⁸³

The production of natural vanilla flavor requires natural source material. Genetic engineering of the plant *Capsicum frutescens* allowed the production of vanillin in the cell culture of the plant, but the meager yield prevented commercial exploitation of this technique.¹⁹³

Microbial cell factories have largely been employed to produce vanillin from renewable sources, mainly (iso)eugenol, ferulic acid, and glucose.¹⁹⁴ Here, we focus on ferulic acid (FA) as a resource.

Ferulic acid is one of the main constituents of lignin and promotes rigidity for the cell wall. In plants, it is mainly produced via the shikimate pathway from phenylalanine and tyrosine. It can be free within the cell wall, but also covalently attached. Due to its high occurrence in lignin, several waste streams can be used as a source to extract ferulic acid.¹⁹⁵ Several techniques have been developed to extract ferulic acid and other phenols from this source, such as pressurized aqueous ethanol solutions to extract valuable compounds from wheat bran,¹⁹⁶ or mild alkaline extraction, already tested on a pilot scale from corn fibers.¹⁹⁷ Enzymatic processes are also gaining traction, such as feruloyl esterase can release ferulic acid and other phenols from wheat bran,¹⁹⁸ or from spent brewer's yeast with enzymes.¹⁹⁹ Other sources of FA can be pine apple peels, orange peels, or pomegranate peels.²⁰⁰

1.3.2.2.1 Bacterial conversion of ferulic acid to vanillin

One of the first conversions of ferulic acid to vanillin at rates, that were economically feasible was discovered from *Pseudomonas putida* and *Streptomyces setonii*.²⁰¹ While *Streptomyces setonii* first accumulated vanillic acid and subsequently vanillin, *P. putida* accumulated vanillin directly. Afterward, a variety of wild-type microbes were discovered

to transform ferulic acid into vanillin, without genetic engineering, including bacteria and fungi. Most of these strains use a feruloyl-CoA synthase and an enoyl-CoA hydratase. This reaction requires one molecule of ATP, as well as co-enzyme A. The thermophilic actinomycete *Amycolatopsis thermoflava* expresses thermostable variants of these two enzymes, and when expressed in *E. coli*, these enzymes can convert ferulic acid into vanillin at elevated temperatures, thus preventing vanillic acid formation by endogenous enzymes, due to denaturing.²⁰² Several pathways on ferulic acid conversion to vanillin have been described and some hosts, such as *Pseudomonas fluorescens*, possess several at once.²⁰³

A highly promising route, which requires only two enzymes and is ATP and CoA-independent has been described. The enzymatic decarboxylation of ferulic acid into 4-vinyl guaiacol (4VG) followed by oxidation and the release of formaldehyde²⁰⁴ (see Figure 16).

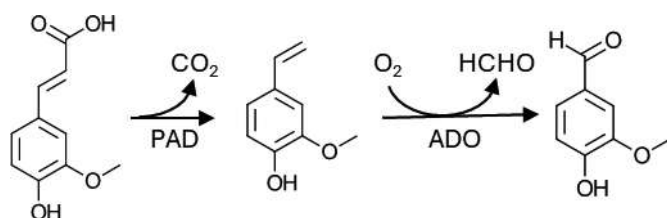


Figure 16 Enzymatic conversion of ferulic acid into vanillin. A phenolic acid decarboxylase (PAD) converts ferulic acid into 4-vinyl guaiacol by removing CO₂ and is further reacted with oxygen to vanillin and formaldehyde. Adapted from Ni et al., 2018.²⁰⁴

In biocatalysis, engineers have gone to great lengths to improve co-factor availability, either funneled from the host's metabolism or via an additional recycling system, which requires sacrificial compounds. Photosynthesis receives the energy to fuel its metabolic reactions from light. The harvest and exploitation of this complex could be greatly beneficial.

1.4 WHOLE-CELL CATALYSIS IN CYANOBACTERIA

Oxygenic photosynthesis holds promising features for whole-cell catalysis and could greatly reduce the cost of reactions, that require co-factors and could prevent oxygen limitations. As mentioned above, cyanobacteria hold great promises in this area of biotechnology, as they are more efficient in terms of quantum yields and grow faster than land plants and the simpler genetic setup compared to eukaryotes renders them more accessible to genetic engineering.^{19,68,69}

The next chapters focus on the advantages and points of attack for whole cell catalysis in cyanobacteria, followed by examples.

1.4.1 *In situ* oxygen production in cyanobacteria

Oxygen, a major byproduct of photosynthesis plays a crucial role as an oxidant in oxidative catalysis, which is essential for the industrial production of value-added chemicals.²⁰⁵ Efficient gas-liquid mass transfer of oxygen has been a significant challenge, particularly in large-scale cultivations, which have considerably limited production yields. Additionally, in heterotrophic hosts, oxygen availability is compromised due to the high demand for cellular respiration, which competes with the target reactions.^{161,206} The effectiveness of oxygen supply via photosynthetic water splitting has been demonstrated by expressing the alkane monooxygenase AlkBGT in *Synechocystis* sp. PCC6803, which successfully converted nonanoic acid methyl esters into ω -hydroxy nonanoic acid methyl esters without the need for aeration.²⁰⁷ Other reaction examples even showed aeration-independent gram-scale conversion with oxygenases, such as the hydroxylation of cyclohexane to cyclohexanone by cytochrome P450 monooxygenase or the production of 6-hydroxyhexanoic acid from cyclohexanone, thereby increasing biomass-specific product yields by a factor of 2.5.^{208,209}

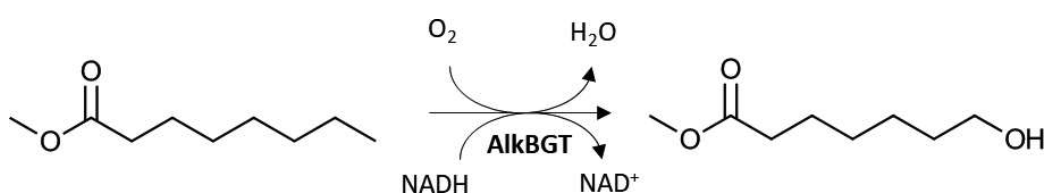


Figure 17 Aeration-independent conversion of nonanoic acid into ω -hydroxy acid methyl esters. The required NADH is supplied by photosynthesis from *Synechocystis* sp. PCC6803²⁰⁷.

1.4.2 Draining reduction equivalents from photosynthesis

As mentioned above, co-factors can be another bottleneck when considering biocatalysis, because they are too expensive to add in equimolar amounts and enzymatic recycling systems reduce the cost but require sacrificial compounds, such as glucose or formate. A light-based recycling system could make other reactions economically feasible.

Under photoautotrophic conditions in cyanobacteria, ATP is produced via an H^+ gradient across the thylakoid membrane. This gradient fuels the ATP-synthase, which converts $ADP + P_i$ into ATP.

Another co-factor of interest is NADPH. In cyanobacteria, the NADPH/NADH ratio is 6.5 times greater than in *E. coli*, as it is the main receiver of electrons from the water-soluble ferredoxin-NADP⁺ reductase.²¹⁰ This reductase receives its electron from ferredoxin, which can transfer its electrons to various electron acceptors/transporters. This is a great point of attack to drain electrons towards the enzymatic reaction of interest.

Electron transport can be further facilitated. The NADPH-dependent conversion of 2-methyl maleimide to 2-methyl succinimide by the recombinant expression of *YqjM* in *Synechocystis sp.* PCC6803 was increased by deleting the genes for flavodiiron proteins 1 and 3. This dimer of flavodiiron proteins acts as an alternative electron sink in a water-water cycle when the generation for NADPH is higher than the demand. The deletion of these two genes frees electrons, which would otherwise be 'wasted'.²¹¹

The deletion of the *hoxYH* genes in *Synechocystis sp.* PCC6803, another alternative electron sink to balance the redox state during photosynthesis has been proven to increase the conversion of the reaction mentioned above with *YqjM*²¹² and the conversion of α -keto acid to the corresponding (*R*)- α -hydroxy acid with *D-HicDH* from *Lactobacillus paracasei*.²¹³

1.4.3 CO₂ limitations in Whole-cell Catalysis and its role in cyanobacterial metabolism

Whole-cell catalysis in cyanobacteria is a promising process to eliminate the need for sacrificial compounds for co-factor recycling and elevating oxygen limitation.^{19,68,69} Several studies tend to overlook a critical aspect when considering reactions in a closed vessel: *Ci* depletion. Optimal yields and high conversion rates are mostly observed under high CO₂ concentration or in a flow-reactor with a constant supply of fresh. Carbonate-containing medium.²¹⁴⁻²¹⁶

The carbon concentrating mechanism (CMM) allows cyanobacteria to grow even under *Ci*-limiting conditions and efficiently feed the CBB-cycle while preventing photorespiration (see above). CO₂ uptake is coupled to NADPH by the transporters and NDH-1 complex, increasing the intracellular HCO₃⁻ concentration for CCM²¹⁷ and *Ci* limitation induces the expression of high-affinity transporters and carbonate hydratases, thus redirecting energy away from the metabolism.²¹⁸ The regulation of the expression of these CCM proteins is regulated by the redox state of the cell rather than directly by the *Ci* concentration.²⁵ Inhibiting the major electron sink, the CBB-cycle, causes electrons to accumulate in the electron transport chain and causes flavodiiron proteins to dissipate electrons.²¹⁹

The CBB-cycle is the main electron sink in cyanobacteria. Under *Ci*-limited conditions, other electron sinks are utilized, but ROS can accumulate when their capacity is

exhausted, ultimately causing the cell's death. An artificial carbon sink can circumvent this problem by redirecting electrons away from futile cycles and into the production of a desired compound.^{220–222}

This problem for whole-cell catalysis in cyanobacteria for lack of reducing equivalents has been shown by expressing an alcohol dehydrogenase from *Lactobacillus kefir* (LkADH) in *Synechococcus* sp. PCC7942. This NADPH-dependent reaction strongly improved under higher CO₂ concentrations.²¹⁵

Ci-depletion could in principle be avoided by gassing with CO₂-enriched air or by adding carbonate to the medium, but this would not circumvent the low mass transfer of gaseous CO₂ into a liquid medium or increase the pH to unphysiological conditions, respectively.

1.4.4 Examples

An overview of the current status of cyanobacteria employed in whole-cell catalysis can be found in the tables underneath, where Table 2 shows biotransformation by native cyanobacterial strains, such as the reduction of cinnamaldehyde to cinnamyl alcohol by *Synechocystis* sp. PCC6803 or the conversion of (S)-(-)-limonene to *cis*- and *trans*-carveol by *Synechococcus* sp. PCC7942.

An additional example is the conversion of cinnamyl aldehyde into cinnamyl alcohol or 3-phenylpropan-ol by *Synechocystis* sp. PCC6803 or *Synechococcus* sp. PCC7942, respectively. The enzymatic reduction of aldehydes commonly requires reduction equivalents, such as NAD(P)H, but both strains almost fully converted the substrate to the respective product (98% and 99% conversion), under light and without the need for a co-factor recycling system.²²³ This highlights both the photosynthesis-powered regeneration of reducing equivalents and the rich diversity of cyanobacteria. The study also points out the low yield of cyanobacterial whole-cell catalysis, the product titer was less than 0.05 g/l, which is several orders of magnitude less than the requirement for a biotechnological viable reaction.¹⁶¹

The expression of recombinant proteins can increase yield, efficiency, and selectivity. A list of proofs-of-concept for whole-cell catalysis in cyanobacteria using recombinant enzymes can be found in Table 3. The enzymes in question are mostly NADPH-dependent, which utilizes the high ratio of NADPH/NADH of photoautotrophic organisms. These enzymes include alkane monooxygenases, Cytochrome P450 monooxygenases, enoate reductases, imine reductases, alcohol dehydrogenases, and Baeyer-Villiger-monooxygenases (BVMOs).

Closely examining individual reactions and their effect on the photosynthetic energy balance can significantly improve the yield. This is exemplified by the conversion of cyclohexanone to 6-hydroxyhexanoic acid, catalyzed by two enzymes. In a previous study, the toxicity of ϵ -caprolactone was determined as the main inhibitor.²¹⁶ The product titer was further improved by the addition of a second enzyme to remove the toxic

intermediate. A high specific rate was also achieved but caused an imbalance in the ATP:NADPH ratio, and reducing the substrate-feeding rate increased the stability of the biotransformation for 48 h and reached a final product concentration of $> 23\text{mM}$.²⁰⁸

The abovementioned optimization approach indicates that a holistic approach to understanding photosynthesis is a prerequisite to fully exploiting its biocatalysis capabilities. In the following sections, some examples are listed, where photosynthesis has been utilized to improve the efficiency in whole-cell catalysis.

Table 2 List of biotransformations performed with native cyanobacteria. Updated version from Jodlbauer et al.¹⁹

Entry	Host	Substrate	Product	Rate/Yield	Source
1 ^a	<i>Nodularia sphaerocarpa</i>	diethyl 2-oxo-2-phenylethyl-phosphonate	(s)-2-hydroxy-2-phenylethylphosphonate	99%, 92% ee	224
2 ^b	<i>Synechocystis</i> sp. PCC 6803	cinnamaldehyde	cinnamyl alcohol	≥98%	223
	<i>Synechococcus</i> sp. PCC 7942	cinnamaldehyde	3-phenylpropanal(3) + 3-phenylpropan-1-ol (4)	≥99%	
3	<i>Nostoc muscorum</i>	hydrocortisone	11 β-hydroxyandrost-4-en-3,17-dione	n.s. ^c	225
			11 β, 17 β -dihydroxyandrost-4-en-3-one	n.s.	
			11 β, 17 α, 20 β, 21-tetrahydroxypregn-4-en-3-one	n.s.	
4 ^d	<i>Synechococcus</i> sp. PCC 7942	2',3',4',5',6'-pentafluoroacetophenone	(S)-pentafluoro(phenyl-)ethanol	2.59 mmol g _{CDW} ⁻¹ ; ≥99.8% ee	226
		ethyl 4-chloroacetoacetate	ethyl (S)-4-chloro-3-hydroxybutanoate	2.49 mmol g _{CDW} ⁻¹ ; 91.8% ee	
		ethylbenzoylacetate	(+)-ethyl (S)-3-hydroxy-3-phenylpropionate	1.59 mmol g _{CDW} ⁻¹ ; 97.5% ee	
	<i>Nostoc muscorum</i>	4-chloroacetophenone	(S)-1-(4-chlorophenyl)ethanol	0.64 mmol g _{CDW} ⁻¹ ; 93.6% ee	
5 ^e	<i>Synechococcus</i> sp. PCC 7942	(S)-(-)-limonene	cis- and trans-carveol	30% and 8%	227
6	<i>Synechococcus</i> sp. PCC 7942	α,α-difluoroacetophenone	(R)-1-phenyl-2,2-difluor ethanol	>99%; 70 % ee	228
7 ^f	<i>Synechococcus</i> sp. PCC 7942	2',3',4',5',6'-pentafluoroacetophenone	corresponding (S)-alcohol	>90%; >99% ee	229
8 ^g	<i>Synechococcus</i> sp. PCC 7942	3-acetylisoxazole derivatives	corresponding (S)-alcohols	20-50%; 91-99% ee	230
	<i>Synechocystis</i> sp. PCC 6803				
9 ^h	<i>Synechococcus</i> sp. PCC 7942	2-methyl-2-cyclopenten-1-one	(S)-2-methylcyclopentanone	99%; 98% ee	231
10 ⁱ	<i>Synechocystis</i> sp. PCC 6803	Aromatic ketones	Aromatic chiral alcohols	Up to 95%, 99% ee	232
11	<i>Anabaena</i> sp.	2",5'-dimethoxy-2'-hydroxychalcone	2",5'-dimethoxy-2'-hydroxydihydrochalcone	70%	233

^a best results shown; *Nodularia sphaerocarpa*, *Arthrospira maxima* and *Nostoc cf-muscorum* converted to diethyl 2-oxo-propylphosphonate, diethyl 2-oxo-2-phenylethyl-phosphonate & Diethyl 2-oxobutylphosphonate

^b best results shown; *Synechocystis* sp. PCC 6803, *Synechococcus* sp. PCC 7942, *Synechocystis* sp. PCC 6714, *Fischerella muscicola* UTEX 1301, *Anabaena cylindrica* IAM M1, *Plectonema boryanum* IAM M101 and *Anabaena* sp. PCC 7120 were tested towards the conversion of cinnamaldehyde

^c n.s. not stated

^d best results shown for each substrate tested; *Synechococcus* sp. PCC 7942, *Nostoc muscorum* and *Anabaena variabilis* were compared for their ability towards all substrates mentioned in the Table.

^e best result shown; *Synechococcus* sp. PCC 7942 showed no conversion of (R)-(-)-limonene or (-)-limonene oxide (mixture), and only poor activity towards (+)-limonene oxide (mixture)

^f best result shown; fifteen acetophenone derivatives were tested and converted by *Synechococcus* sp. PCC 7942 (2-84%; 96-100% ee).

^g seven 3-acetylisoxazole derivatives were tested and converted by *Synechococcus* sp. PCC 7942 and *Synechocystis* sp. PCC 6803.

^h best result shown; sixteen enones and ten ketones were tested

ⁱ after addition of Na₂S₂O₃

Table 3 List of recombinant biotransformation in Cyanobacteria. Updated version from Jodlbauer et al.¹⁹

	Cyanobacterial host system						Heterotrophic host system	
Entry	Host	Enzyme	Substrate	Product	Rate/Yield	Optimizations (+) / Limitations (-)	Rate/Yield	Source
1	<i>Synechocystis</i> . sp. PCC 6803	AlkBGT (alkane monooxygenase)	nonanoic acid methyl ester	ω -hydroxy nonanoic acid methyl ester	0.086 mmol L ⁻¹ h ⁻¹ (5.6 U g _{CDW} ⁻¹ , (3L, 26.2 h)	+two liquid phase approach -substrate toxicity -mass transfer -expression	103 U g _{CDW} ⁻¹ (128 U g _{CDW} ⁻¹ when optimized by recombinant expression of transporter AlkL)	207, 234,235
2 ^a	<i>Synechocystis</i> . sp. PCC 6803	CHX100 (cytochrome P450 monooxygenase)	cyclohexane	cyclohexanol	0.04 g L ⁻¹ h ⁻¹ (39.2 U g _{CDW} ⁻¹ , 3L, for 52h)	+two liquid phase approach +anaerobic cultivation prevents substrate volatility -substrate toxicity -mass transfer -expression	0.4 g L ⁻¹ h ⁻¹ (20 U/gCDW; for 17 days)	236
3	<i>Synechocystis</i> . sp. PCC 6803 & <i>P. taiwanensis</i> VLB120	CHX100 (cytochrome P450 monooxygenase)	cyclohexane	cyclohexanol	0.2 g L ⁻¹ h ⁻¹ (for over a month)	+mixed species biofilm allows stable and high cell density (51.8 gBDW L ⁻¹) -substrate toxicity -expression	0.4 g L ⁻¹ h ⁻¹ (20 U/gCDW; for 17 days)	214
4 ^a	<i>Synechocystis</i> . sp. PCC 6803	YqjM (enoate reductase)	cyclic enones	cyclic ketones	up to 0.5 g L ⁻¹ h ⁻¹	-substrate toxicity	/	237
			cyclic maleimides	cyclic succinimides	up to 1.1 g L ⁻¹ h ⁻¹		/	
5 ^b	<i>Synechocystis</i> . sp. PCC 6803	IREDs (imine reductases)	cyclic imines	cyclic amines	up to 6.3 mM h ⁻¹ (22 U g _{CDW} ⁻¹ , full conv. after 3h)	+optimized promoter -transport of bulkier substrates -substrate toxicity -expression	0.4 mmol g ⁻¹ h ⁻¹	238, 239
6	<i>Synechococcus</i> sp. PCC 7942	LkADH (alcohol dehydrogenase)	acetophenone	chiral 1- pheylethanol	3.1 mM h ⁻¹ (20 mM, full conv. in 6h)	+co-factor recycling through CO ₂ modulation -substrate toxicity	66% conv. (10 mM; optimized by co-factor recycling system)	215, 240
7 ^c	<i>Synechocystis</i> . sp. PCC 6803	BMVO _{xeno} (Baeyer- Villiger monoogygenase)	cyclic ketones	lactones	20 U g _{CDW} ⁻¹ (3.7 mM h ⁻¹)	-substrates toxicity -formation of byproducts by endogenous alcohol dehydrogenases	3.56 U g _{CDW} ⁻¹ (20 g L ⁻¹ from 200 mM; 200 ml; cyclohexanol; 100% conv. after 48h)	241,242,
8	<i>Synechocystis</i> <i>PCC6803</i>	CHX100 (cytochrome P450 monooxygenase) and lactonase	Cyclohexanone	6-hydroxy hexanoic acid	63.1±1.0 U/g _{CDW} 23.5± 0.84 mM in 48h	+ Remove toxic intermediate enzymatically + Improved energy balance + improved sink capabilities of electron surplus from photosynthesis	44.8± 0.2 U/gCDW (5 mM in 3h)	208,243

^a Four cyclic enones and 4 cyclic maleimides were tested and converted by *Synechocystis* sp. PCC 6803 harboring ene-reductase YqjM.

^b Three recombinant imine reductases (IREDs) were tested towards eight cyclic imine substrates in *Synechocystis* sp. PCC 6803. For IRED-A (from *Streptomyces* sp. GF 3587), all eight substrates could be converted to rates ranging from 0.5-6.3 mM h⁻¹.

1.5 AIM OF THIS WORK

Cyanobacteria, ancient prokaryotes, and the only bacteria capable of oxygenic photosynthesis, are the ideal platform for whole-cell catalysis. They supply a light-powered co-factor recycling system, circumventing the need for a sacrificial compound, while simultaneously excreting oxygen as a waste product during this process, potentially preventing oxygen-limitation.

Upon closer examination and scratching the surface, the obstacles are unearthed. These obstacles include genetic instability, insufficient toolboxes and prediction tools for genetic engineering, and a highly advanced and complex system of metabolic balancing and regulation. A major obstruction is the comparable slow growth and low biomass accumulation in comparison to established microbial hosts, such as *E. coli*, while at the same time competing with processes for biomass production and biocatalysis which have been optimized for decades. Taken together, this explains the reluctance to invest in cyanobacterial biotechnology.

The underlying hypothesis of this work was that new, fast-growing cyanobacterial strains can overcome some of these objections. Since 2015, more and more strains have been described with doubling times comparable to heterotrophic yeasts.

The first part sought to prove this hypothesis by expressing a carboxylic acid reductase (CAR) in the fast-growing strain *Synechococcus sp.* UTEX2973. CAR reduces carboxylic acids into their corresponding aldehyde, requiring one molecule of ATP and NADPH per each reaction. Optimistically, putative gene deletions were determined by flux balance analysis, which might redirect fluxes of ATP and NADPH, both co-factors required for the CAR reaction, toward the desired product.

An alternative approach is pursued in the second part. On one side, *Synechocystis sp.* UTEX2973 has a short doubling time under optimal conditions, but this growth phase is short-lived, and the stationary phase is reached quickly, resulting in low biomass accumulation.

Therefore, a different cyanobacterial strain was selected: *Synechococcus sp.* PCC11901. This species has been described with a doubling time competitive to *Synechococcus sp.* UTEX2973, but with an elongated linear growth phase, resulting in unprecedented biomass accumulation. The toolbox for genetic engineering in this strain is limited, due to its novelty, but its natural competence allows simple genomic integration, circumventing the need for hard-to-work with RSF1010-based plasmids.

As an alternative to CAR, two enzymes were chosen as substitutes, namely a phenolic acid decarboxylase (PAD) and an aromatic dioxygenase (ADO). These enzymes have been shown to convert ferulic acid into 4-vinyl guaiacol and finally into vanillin, a biotechnologically interesting route, as it converts an inexpensive aromatic acid, derived from lignin into a high-demand, high-value product. The first reaction, catalyzed by PAD, releases CO₂, while the second requires O₂, in tandem with cyanobacterial photosynthesis, this could be a self-sustaining, light-fueled reaction.

2 RESULTS

2.1 GROWTH AND PHYSIOLOGY

This work focused on two cyanobacterial strains, *S. sp.* UTEX2973 and *S. sp.* PC11901. The primary objective was to establish stable growth conditions and evaluate their behavior in our laboratory.

2.1.1 *Synechococcus sp.* UTEX9273

S. sp. UTEX2973 (from here on UTEX2973) has been described as the fastest-growing cyanobacterium known with doubling times of < 2 h. This high doubling rate can only be achieved under conditions of high light intensity, high CO₂ concentration, and high temperatures, with the best culture conditions described being 500 μmol photons/m²/s, 3% CO₂, and 41°C, while under ambient CO₂ concentrations, growth of UTEX2973 is comparable to *Synechocystis sp.* PCC6803.²⁴⁴

Our laboratory facilities at that time lacked a suitable incubator for such conditions, so an affordable alternative was searched for. The cultivation system by the company CellDEG (CellDEG GmbH, Berlin, Germany) provided such an alternative: A two-tier vessel, separated by a hydrophobic, but gas-permeable membrane, which allows CO₂ supplementation by a carbonate buffer. This buffer steadily releases CO₂, enriching the headspace, and passing through the membrane into the culture medium.¹¹¹ The growth of UTEX2973 was greatly improved in this system (see Figure 18) and it was possible to reproduce the fast growth, with an optimal doubling time of 1.9h.

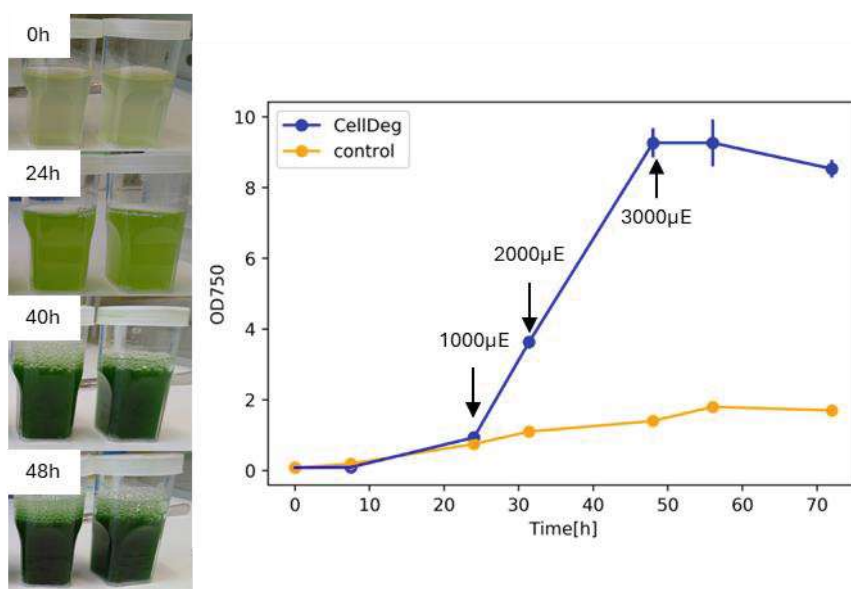


Figure 18 Growth comparison of UTEX2973 in the CellDEG system compared to atmospheric conditions. Left: Photos of culture vessels. Right: Growth measured by optical density at 750nm (OD750), with increasing light intensity. Atmospheric CO₂ (control) and CellDEG cultivation (CellDeg) were compared.

2.1.2 *Synechococcus* sp. PCC11901

The CellDEG system provides a low-cost alternative to CO₂ incubators. As shown above, this system works well for *S. sp.* UTEX2973 (see Figure 18). The next strain, *S. sp.* PCC11901 (from here on PCC11910), has been described with a similar or even higher growth rate compared to *S. sp.* UTEX2973, and additionally with a prolonged linear growth phase, increasing biomass accumulation.^{118,133,155} This was reproducible in the CellDEG system when growing both strains in a nutrient-rich medium (MAD2 for *S. sp.* PCC11901¹¹⁸ and CD-medium for *S. sp.* UTEX2973²⁴⁵, see Table 8 for the medium compositions), as seen in Figure 19. For the first 148 h in the CellDEG system (at 500 μmol photons /s /m² and 39°C), growth for both strains was highly similar, afterwards, *S. sp.* PCC11901 continued to grow, while *S. sp.* UTEX2973 remained in the stationary phase, even after replenishing the carbonate buffer. The increased biomass was detectable after 14 days of incubation and subsequent centrifugation of the biomass (see Figure 19, right).

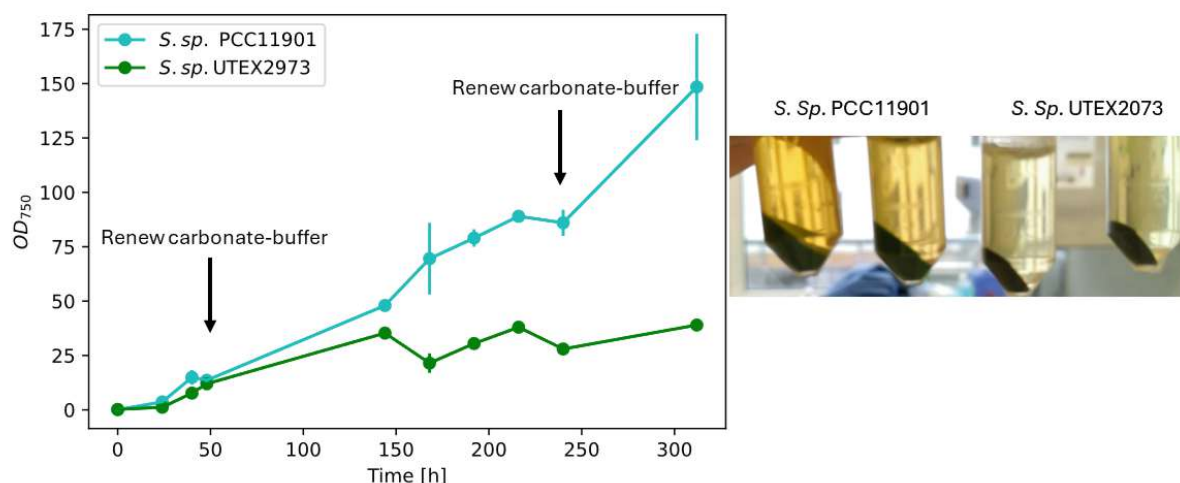


Figure 19 Growth comparison of *S. sp.* UTEX2973 and *S. sp.* PCC11901. Left: Growth in CellDEG system, with 10 mL MAD2 medium (for *S. sp.* PCC11901) and CD medium (for *S. sp.* UTEX2973). The carbonate buffer was replaced twice. Right: Centrifuged cell culture after 14 days of incubation.

The growth pattern of *S. sp.* PCC11901 could also be reproduced in a CO₂ incubator at 500 μmol photons /s/m² and 1% CO₂. The concentration of Chlorophyll a and carotenoids follow the growth trend for 4 and 8 days, respectively. The chlorophyll a concentration increased rapidly after 4 days, while the carotenoid concentration stagnated after 8 days (see Figure 20 left side).

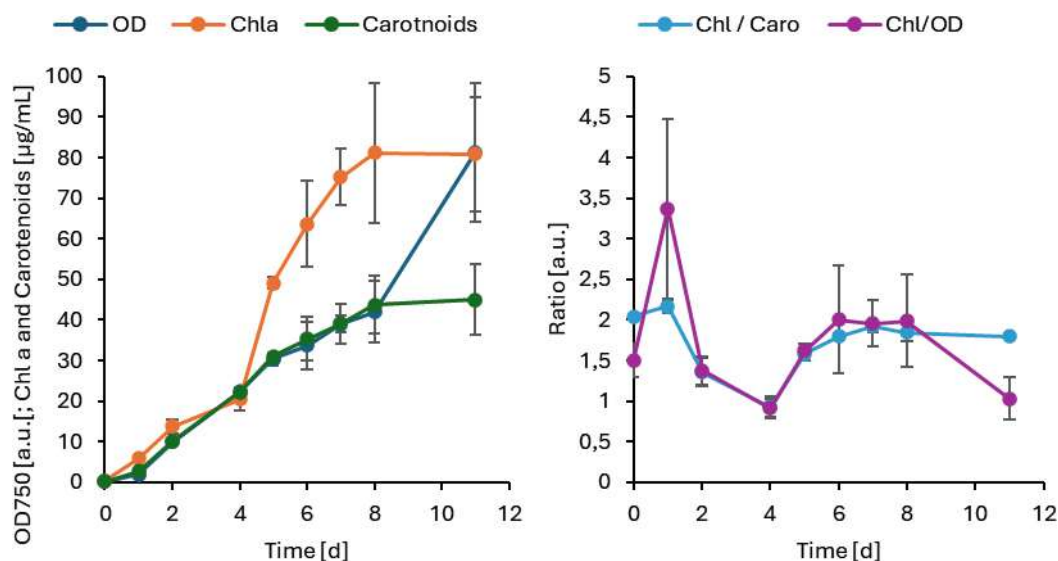


Figure 20 Growth of *S. sp. PCC11901* in CO₂-incubator, including Chlorophyll a (Chl) and Carotenoid (Caro) content. Cells were grown in MAD2 medium, at 39°C, 150rpm, 500 µmol photons/s/m² and 1%CO₂.

2.1.2.1 Oxygen production under carbon limitation

The problem with carbon limitation and thereby suppressed oxygen production via photosynthesis has been described by several publications. The utilization of cyanobacteria for whole-cell catalysis to prevent oxygen limitation thus requires a carbon source, which was tested by measuring the concentration of dissolved oxygen (dO₂) in a closed vessel containing cyanobacteria and close-to-no gas exchange with the environment. The concentration of dO₂ was determined using the OXROB10 probe connected to a FireSting-O2 (PyroScience GmbH, Aachen, Germany), utilizing near-infrared radiation. The set-up in flat-bottom flasks is photographed in Figure 21.

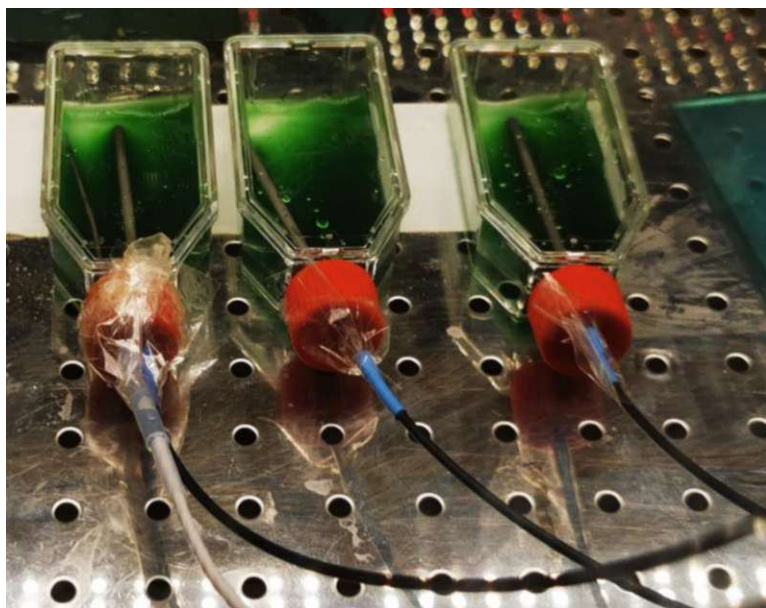


Figure 21 Set-up of measuring dO_2 evolution in a closed vessel by *Synechococcus* sp. PCC11901 via near-infrared radiation. 10 mL of cell suspension was transferred into a 30 mL flat bottom flask and shaken at 55rpm.

The concentration of dO_2 increased upon the addition of a carbonate solution and further increased with higher light intensities. When dO_2 concentrations fell to normal conditions again, further light intensity increases could not increase dO_2 but were elevated after adding more carbonate, as a C_i source, visualizing the dependency of oxygen production on light intensity and C_i -availability (see Figure 22).

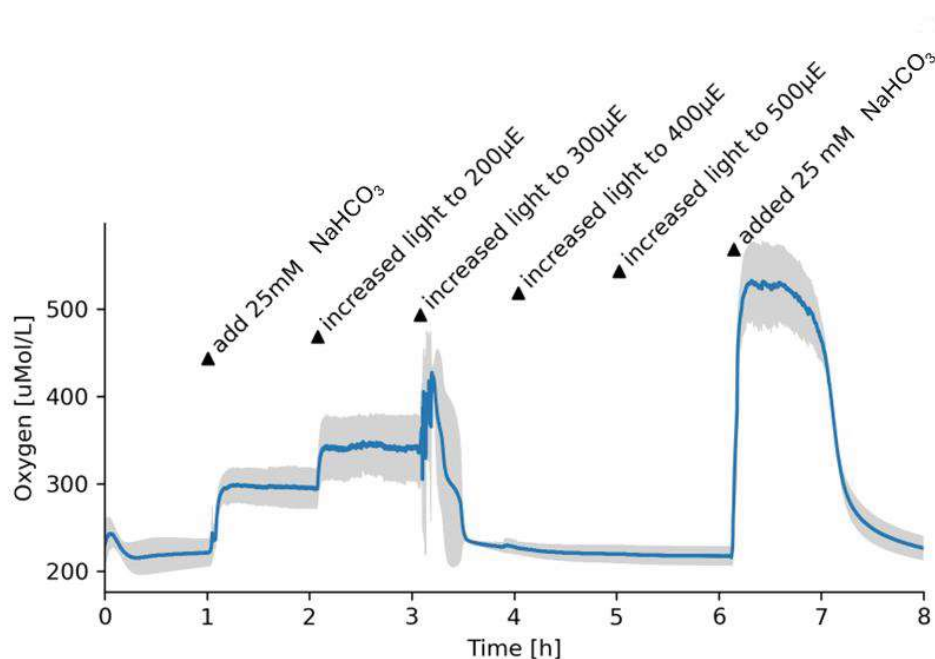


Figure 22 Oxygen production by *S. sp.* PCC11901 depends on light and C_i -availability. Cyanobacteria were incubated at 39°C, 55rpm in a flat bottom flask under various light conditions. Flasks were closed to prevent gas exchange.

The correlation between elevated oxygen levels in PCC11901 and carbonate concentration was further elucidated by examining the duration of increased oxygen levels, depending on the carbonate dosage. The high dO_2 concentration lasted 70 and 74 minutes with 25mM carbonate added (Figure 23 **A** and **B**), while 50mM carbonate elongated the period to 110 min (Figure 23 **C**).

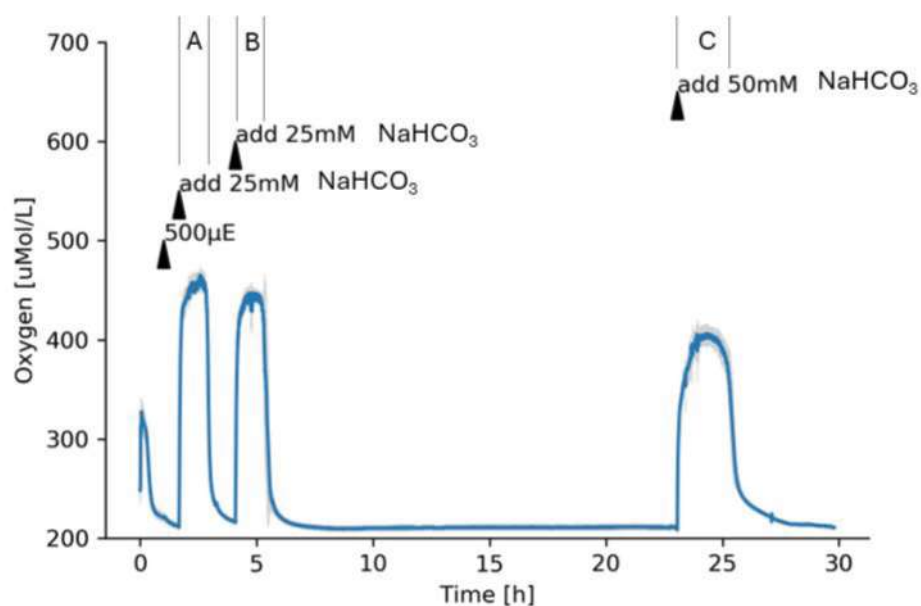


Figure 23 Oxygen production depends on the amount of carbonate at high buffer capacity. Cells were incubated in closed, flat-bottom flasks. The amount of carbon added changes the duration of the high oxygen concentration. A = 70min, B = 74min, C = 110min.

The two cyanobacterial strains of interest showed reliable and stable growth in our laboratories and their growth kinetics were following the literature.

The next part focuses on *S. sp.* UTEX2973 and the expression of a carboxylic acid reductase. This strain was chosen, because we assumed a plasmid-based expression system would allow fast results, in contrast to genomic integration in *S. sp.* PCC11901.

2.2 CARBOXYLIC ACID REDUCTASE IN *SYNECHOCOCCUS. SP. UTEX2973*

Carboxylic acid reductases (CARs) provide an elegant solution for the conversion of carboxylic acids to aldehydes compared to chemical means, but the demand for NADPH and ATP renders them challenging. Cyanobacteria are a promising alternative, as they provide a light-fueled co-factor recycling system. As mentioned above, *Synechococcus sp. UTEX 2973* (UTEX2973) is the fastest-growing cyanobacterium known to date and has a higher concentration of ATP and NADPH compared to other cyanobacterial strains.¹⁴³ This strain was therefore chosen as the platform for this biotransformation. The project is illustrated in Figure 24.

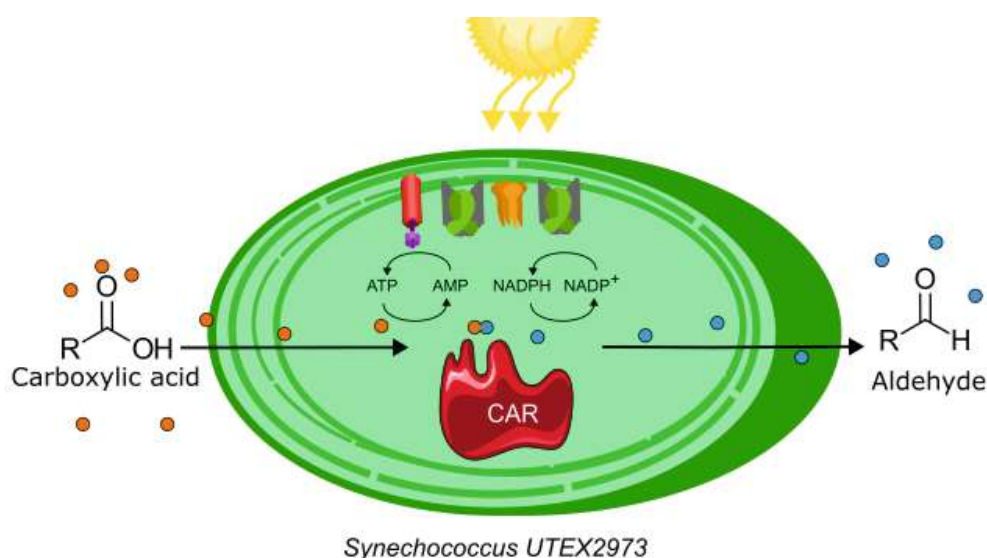


Figure 24 Schematic of a Carboxylic acid reductase (CAR) in the cyanobacterium *Synechococcus sp. UTEX2973*. The enzymatic reduction of carboxylic acids into aldehydes requires ATP and NADPH, which putatively can be regenerated via photosynthesis.

The higher concentration of ATP and NADPH of UTEX2973 was elucidated by flux balance analysis (FBA). A similar approach was to be applied in this study, to detect potential gene deletions, which increase the flux of co-factors towards the reaction of interest.

2.2.1 Genome-scale Models and Flux Balance Analysis

The basis for FBA is a genome-scale model (GSM), represented by a numerical matrix, with every row representing a metabolite and every column representing a reaction. The basis is the gene-protein-reaction association, where a gene produces a protein that catalyzes a reaction.²⁴⁶

The steps involved in building a GSM first start with sequencing and annotating the genome, followed by connecting each annotated gene with a biochemical reaction from a database.²⁴⁷ This results in a draft network, which must then be manually curated by

filling gaps, correcting directional reactions, and detecting futile cycles and dead-end metabolites.²⁴⁸ This cumbersome process is more and more automated by algorithms.²⁴⁹ FBA requires the GSM, in the form of a matrix, to be constrained.

The matrix is constrained to the mass balance in the system by the stoichiometric values for every reaction and metabolite. Together with the additional set of upper and lower boundaries, which can be set on individual reactions, they form the possible solution space for the allowable flux distribution within the system.^{250,251}

The next step is to define a biological objective, which represents the phenotype one is interested in, so for predicting growth rate, the biological objective is biomass accumulation. The objective is added to the matrix as an additional reaction, which consumes biomass precursors, such as amino acids, lipids, or nucleotides. This is the only part of the matrix that requires experimental data, specifically the composition of the biomass of the organism.²⁵²

Finally, exchange reactions are added to the matrix, equal to the uptake rate of metabolites from the environment, such as glucose or oxygen. This can be used to simulate the environment or the culture conditions, such as limited nutrients.

A necessary assumption for FBA is that the cell acts at a steady state. This allows to set the equation to 0 and can thus be solved via linear algebra:

$$S \times v = 0$$

Where S is the matrix and v represents the fluxes through all the reactions in the system.²⁵¹ Together, they form a set of linear equations. typically, this matrix has more reactions than metabolites, leading to more variables than equations, and thus has several solutions. By maximizing or minimizing a function within the solution space, the optimum for a certain reaction can be solved by algorithms. A composition of solving algorithms is compiled in the toolbox named COBRA, which was developed for Matlab.²⁵³ This suite of tools has been optimized to be used with the programming language Python, which is available free of charge.²⁵⁴

The advantage of FBA is, that it does not require actual kinetic measurements, apart from simple growth experiments for validation and the composition of the biomass.²⁵⁵

Once the GSM is implemented and validated, FBA can be used to predict growth rates under varying conditions,²⁵² predict the essentiality of genes,²⁵⁶ and allow a more directional and rational approach to metabolic engineering.²⁵⁷ With an increasing number of sequenced genomes, GSM and FBA can even be used to predict the behavior of communities of different organisms.²⁴⁹

2.2.1.1 Flux balance analysis

The fast-growing cyanobacterium UTEX2973 is a promising host for whole-cell catalysis, especially for CARs, as the photoautotrophic metabolism could be exploited as a recycling system for the co-factors ATP and NADPH. The cyanobacterial metabolism is highly regulated and might not have the capacity to funnel these reducing equivalents to the reaction of interest. Therefore, FBA was employed to identify potential knock-out targets, which could re-route co-factors towards CAR. Molecular cloning is a time-consuming process and to utilize the time in between the GSM of UTEX2973 *imSyu593* was investigated to identify potential knock-out targets to increase co-factor availability.

FBA was done using the COBRApy package in Python.^{254,258} The full script was run in Spyder (<https://anaconda.org/anaconda/spyder>) and can be found in the appendix. The GSM used is derived from a model based on *Synechocystis* sp. PCC6803 and encompasses 593 reactions in total.

After expanding the model by two metabolites, namely aromatic carboxylic acid ('cpd00539_c') and aromatic aldehyde ('cpd00193_c'), the reaction for CAR ('rxn01490') was added which fulfills the following table:

Table 4 List of compounds added to the GSM *imSyu593* and the stoichiometric value to the reaction 'rxn01490', corresponding to the CAR-catalyzed reaction.

Compound	Stoichiometric value
Cpd_00539 (aromatic carboxylic acid)	-1
Cpd_00005 (NADPH)	-1
Cpd_00080 (H ⁺)	-1
Cpd_00002 (ATP)	-1
Cpd_00193 (Aromatic aldehyde)	1
Cpd_00006 (NADP)	1
Cpd_00020 (AMP)	1
Cpd_00013 (PPi)	1

Next, the model objective was assigned for 'rxn01490' and not biomass, as the initial goal was to determine the possible solution space with the maximal rate for the CAR reaction. The solution space is illustrated in the trade-off plot in Figure 25.

The solution space predicts a flux of < 0.05 mM/g_{DCW}/L for the CAR-reaction at maximum growth rate. A reduced growth rate might increase the flux to 0.2 mM/g_{DCW}/L while permitting a reduced growth rate.

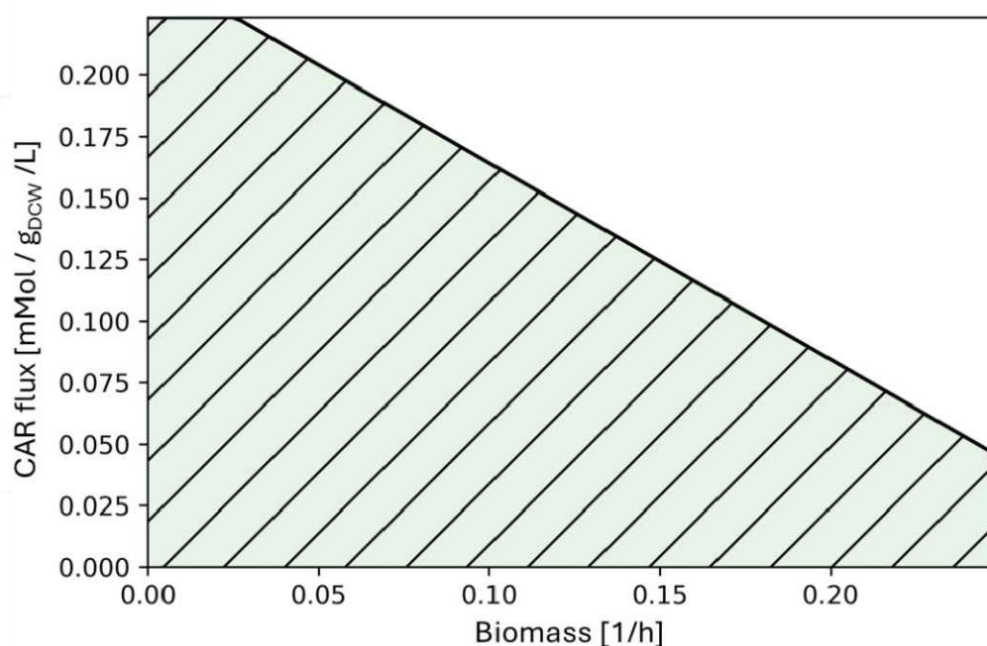


Figure 25 Trade-off plot for Carboxylic acid reductase (CAR) vs biomass accumulation in the GSM imSyu593. The solution space is highlighted in green and represents the possible solution for flux distribution in a steady state in *S. sp. UTEX2973*.

The next step involved the *in silico* knock-out of all endogenous reactions that require ATP and/or NADPH²⁵⁹. Surprisingly, every reaction that consumes or produces NADPH is either essential for survival or indispensable for the CAR reaction to occur. The ATP-related reactions show a different picture, thus indicating, that ATP is more freely available compared to NADPH.

Further investigation in this direction was afterward halted until further progression in the molecular cloning part.

2.2.2 Inducible Protein Expression

Inducible protein expression is a prerequisite for synthetic biology and allows for separated production and growth phases in biotechnological applications. Inducible systems have been described in cyanobacteria, while the availability in UTEX2973 is still limited. The described IPTG-inducible promoters in UTEX2973 either suffer from high 'leakage', meaning protein expression in the absence of inducer, or from weak expression,²⁶⁰ while cobalt-inducible promoters suffer from the toxicity of the inducer molecule. A new suite of inducible promoters was described by Behle et al., utilizing rhamnose, vanillate, and anhydrous Tetracycline (aTc), with good dynamic range and minimal leakage.⁴⁶

The cyanobacterium UTEX2973 is not naturally competent, exacerbating genomic integration of the gene of interest (GOI).²⁶¹ Self-replicating plasmids on the other hand can be transformed via conjugation, also known as tri-parental mating.⁴⁸ During

conjugation, three bacterial strains are involved, the donor strain carries the plasmid of interest, the helper strain contains *mob* genes for nicking the plasmid, preparing it for single-stranded transfer and methylation, which prevents degradation by the third strain, the acceptor strain, in this case UTEX2973.²⁶² Donor and helper strains were *E. coli* purchased from Addgene.com (pRK24 www.addgene.org/51950 and pRL528 www.addgene.org/58495).

It was possible to transform UTEX2973 via conjugation and colony PCR showed positive results for pSHDY_P_{Rha}_eYFP, pSHDY_P_{VanCC}_eYFP, and pSHDY_P_{Lo3}_eYFP. The conjugated cells were then tested for eYFP expression via fluorescence measurement (normalized to optical density (OD) at 750nm). This ratio was compared to cells carrying the plasmids that were induced to non-induced and the WT with and without the inducer (see Figure 26). The concentrations of inducers were 100 mM rhamnose, 2 mM Vanillate, and 1 μ M aTc, respectively.

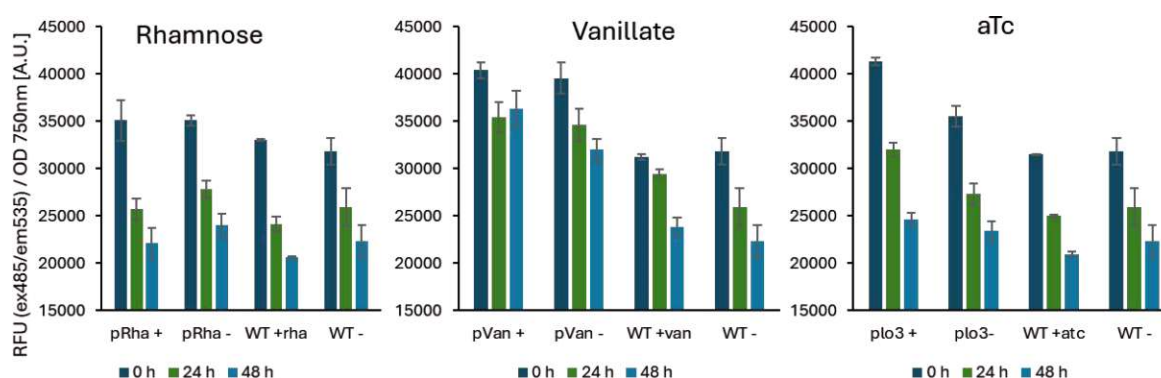


Figure 26 The ratio of fluorescence (ex. 485nm/ em. 535nm) to cell density while testing inducible promoters in UTEX2973. Left: The rhamnose (*rha*) inducible promoter *P_{rha}* induced with 100mM rhamnose (+) or without inducer (-) compared to WT. Middle: Vanillate (*van*) inducible promoter *P_{van}*. I was induced with 2 mM Vanillate. Right: Anhydrotetracycline (aTc) inducible promoter *P_{lo3}* induced with 1 μ M aTc. Error bars indicate the standard error of the mean from at least 3 biological and technical replicates.

The ratio of fluorescence to OD₇₅₀ showed some significant differences after 48h, for example, the difference in the *P_{vanCC}*-controlled expression was significant when comparing the induced to the non-induced cells, but the difference was too low to say confidently, that the expression was happening, especially, as the difference between the three time-points is always higher, then the difference between the induced and non-induced strains.

2.2.3 Cloning

One of the most effective CARs has been described from *Nocardia iowensis* (*niCAR*).²⁶³ The coding sequence is 3600bp long and the enzyme requires a PPTase for posttranslational modification, and the PPTase of *E. coli* has been shown to function properly (*ecPPTase*)¹⁷⁶. Together, they are a comparably large sequence for molecular cloning.

The expression of *niCAR* was supposed to be inducible and not constitutive, to reduce the metabolic burden during growth. The rhamnose inducible promoter P_{Rha} was already established in *Synechocystis* sp. PCC6803 and showed great dynamic range and strong regulation⁴⁶. The vector of choice was thereby set, as pSHDY has been constructed to harbor the regulator and promoter with improved stability and accessibility due to improved supercoiling-inducing mutation.^{80,81} The map in Figure 27 shows the targeted plasmid.

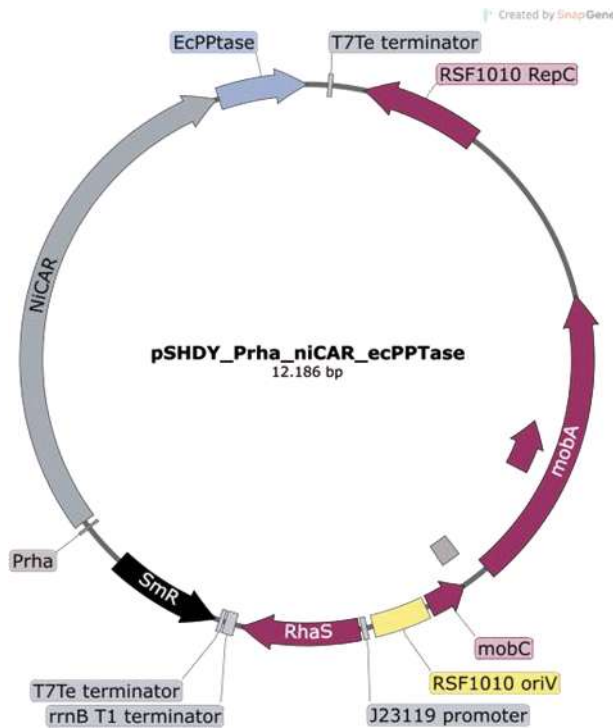


Figure 27 Plasmid map of pSHDY_Prha_niCAR_ecPPTase. The genes of interest, *niCAR*, and *ecPPTase*, were to be cloned down-stream of the rhamnose inducible promoter *Prha*. The plasmid also carries a streptomycin/spectinomycin resistance cassette (*SmR*), the regulator *RhaS*, an origin of replication for multi-species uses (*RSF1010*), and the necessary genes for conjugation (*mobA*).

The cloning strategy of choice was Golden Gate cloning,^{95,264} which takes advantage of Type IIS restriction enzymes. These enzymes cut upstream of their recognition sequence, producing ‘sticky ends’. In combination with a ligase, compatible sticky ends can be used to insert the GOI into the vector and remove the recognition sequence for the restriction enzyme. Several rounds of restriction and ligation, facilitated by temperature changes, increase insertion success.

The recognition sequences can be attached to the GOI by primer design and PCR amplification, which was successful (see Figure 28). The amplification of the backbone required the addition of a ‘GC enhancer’ (New England Biolabs, Ipswich, USA), which can help with the amplification of large and/or GC-rich amplicons. The exact recipe for the GC enhancer is a corporate secret but probably contains DMSO and/or betaine, which has been shown to improve PCR results for complex amplicons.²⁶⁵

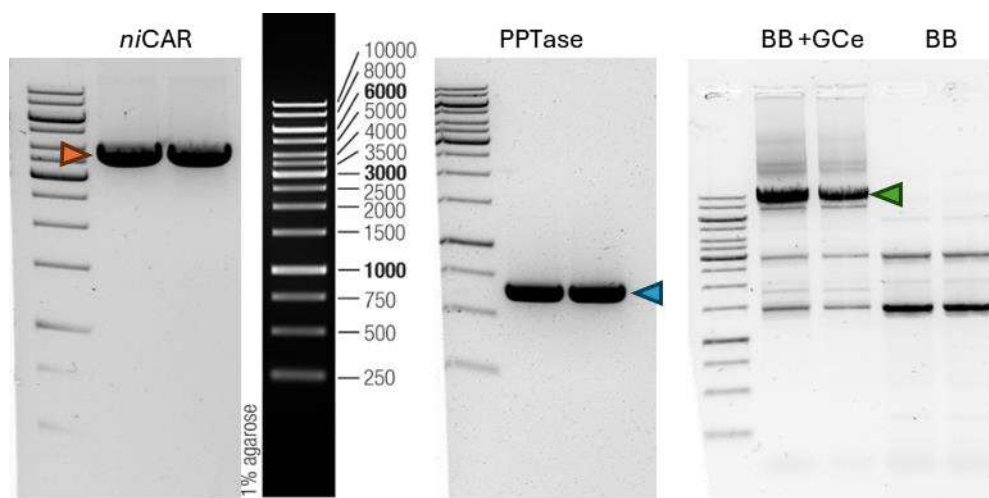


Figure 28 Gel electrophoresis of amplification and attachment of *Bsa*I recognition sequence on *niCAR* (orange arrow, expected size of 3650bp) and *PPTase* (turquoise arrow, expected size of 650bp) and the *pSHDY* as vector backbone (*BB*, green arrow, expected size of 7890bp), from left to right. Reliable amplification of *BB* required the addition of *NEB* GC enhancer (*New England Biolabs*, *Ipswich*, *USA*).

Subsequent ligations and restrictions were not successful. Despite several attempts, the only construct obtained was a *pSHDY* vector with *ecPPTase* under the P_{rha} control, which was supposed to function as a negative control.

The *CyanoGate* Kit presented an alternative approach. This kit also uses *Golden-gate* cloning and combines it with several modules, specifically designed for cyanobacteria.⁸⁴ The level-T vector was beforehand optimized by integrating the mutation *mobAY25F*, which increases supercoiling and thereby restriction.⁸⁰ The strategy for employing the *CyanoGate* Kit is outlined in Figure 29.

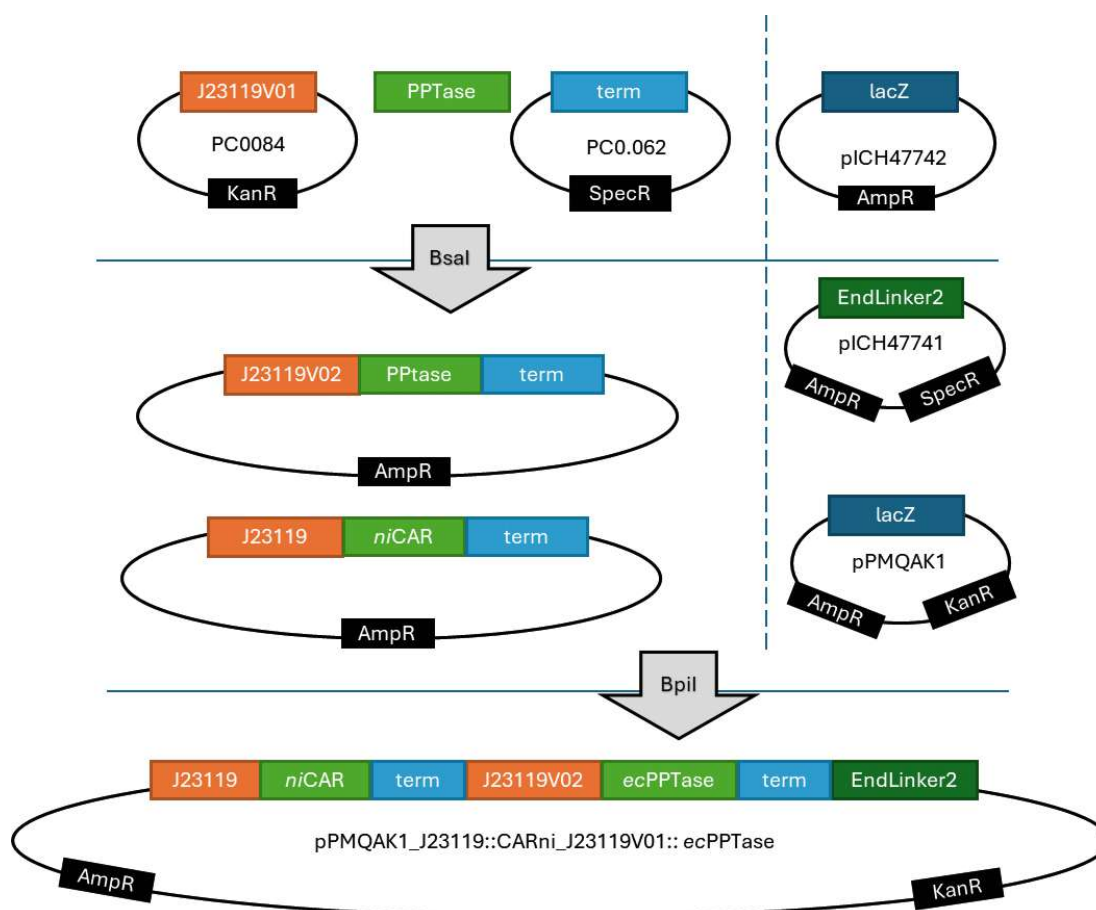


Figure 29 Schematic of cloning strategy for introducing *niCAR* and *ecPPTase* into the CyanoGate T-vector *pPMQAK-1*. The part number from the CyanoGate or MoClo Kit is written inside the 'plasmids'. *J23119* and *J23119V02* are strong promoters of the CyanoGate Kit. Antibiotic resistances are mentioned in the black boxes (AmpR: Ampicillin resistance, KanR: Kanamycin resistance, SpecR: Spectinomycin/Streptomycin resistance). The *lacZ* gene encodes the functional piece for a β -galactosidase, allowing to distinguish successful cloning by blue-white-screening. The vectors used are separated on the right side. Arrows indicate the restriction enzyme used.

The amplification of *niCAR* and *ecPPTase* was successful (Figure 30 left side), but the subsequent cloning was not. We hypothesized that the length of the coding sequence for *niCAR* might cause difficulties during integration and therefore fragmented it into a 2700bp and 1000bp fragment (Figure 30 right side), but this did not yield the plasmid of interest.

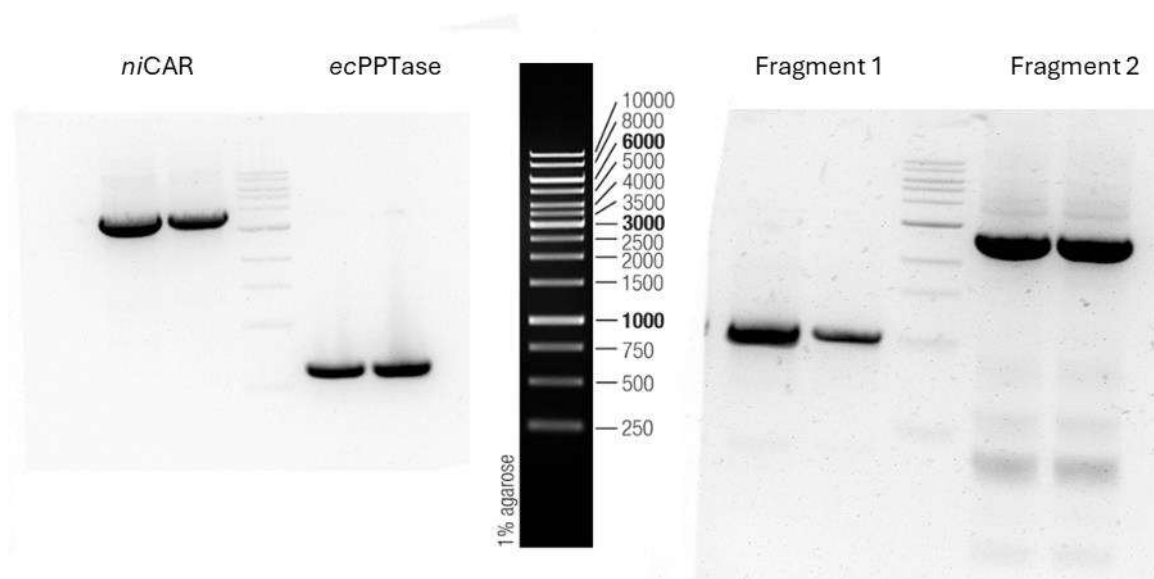


Figure 30 Gel electrophoresis to introduce *niCAR* into pPMQAK-1. Left: insert amplification by PCR. Right: fragmentation of *niCAR* into two fragments, 1000bp and 2700 bp long, resp.

Golden-gate cloning seemed not to be the optimal cloning technique for the assembly of *niCAR*-containing plasmids for cyanobacteria. An alternative cloning technique, which has been used for hard-to-clone constructs and enables the assembly of several DNA fragments simultaneously is Gibson assembly. This is an isothermal reaction, which requires the construction of overlapping DNA fragments and involves three enzymes: a 5'-exonuclease, a polymerase, and a ligase.^{266,267}

Moreover, besides switching the cloning technique, three more CAR variants were tested for integration into pSHDY and pPMQAK_robAY25F. These variants were *Dichomitus squalens* (Ds)²⁶⁸ *Mycobacterium marinum* (Mm),^{269,270} and *Trametes versicolor* (Tv).^{268,271} Amplification of each CAR sequence was successful (see Figure 31), but cloning was still not successful.

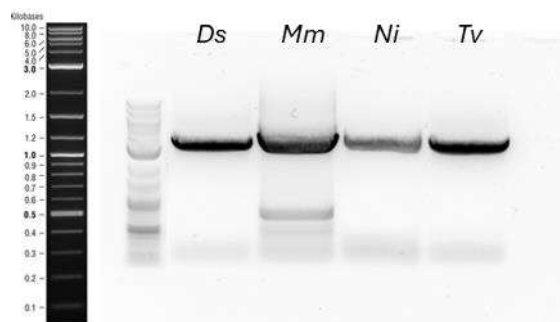


Figure 31 Amplification of inserts of CAR variants from different origins. Amplicons are expected in size between 3500 and 3900 bp. Ds: *Dichomitus squalens*; Mm: *Mycobacterium marinum*; Ni: *Nocardia iowensis*; Tv: *Trametes versicolor*.

The lack of success in cloning led to the halt of further efforts in the direction of expressing a carboxylic acid reductase in UTEX2973.

2.3 SYNECHOCOCCUS SP. PCC11901 AND THE ENZYMATIC CONVERSION OF FERULIC ACID INTO VANILLIN

This project aimed to tackle two problems: The insufficient biomass accumulation of cyanobacteria and carbon depletion in a closed reactor during whole-cell catalysis.

The first obstacle, the inadequate cell density of commonly employed cyanobacteria, was approached by utilizing the newly discovered cyanobacterium *Synechococcus sp.* PCC11901. This strain has demonstrated unprecedented biomass density in comparison to any other cyanobacterium.¹¹⁸ The natural competence supposedly makes this strain tractable for genetic manipulation, and constant progress enlarges the toolbox for this strain.^{133,155,157} However, biotechnological applications have been sparsely explored.

The depletion of *Ci* during whole-cell catalysis with cyanobacteria might be a limiting factor, demonstrated by high yields when a high carbon influx is present.^{214,216} The two-step enzymatic cascade envisioned here is thus self-fueling, as the first step releases CO₂, while the second step utilizes oxygen, preventing the accumulation of radical oxygen species (ROS). This biocatalysis uses ferulic acid, a cheap constituent of lignin, and turns it into the high-value aromatic vanillin. The enzymatic reaction is visualized in Figure 32.

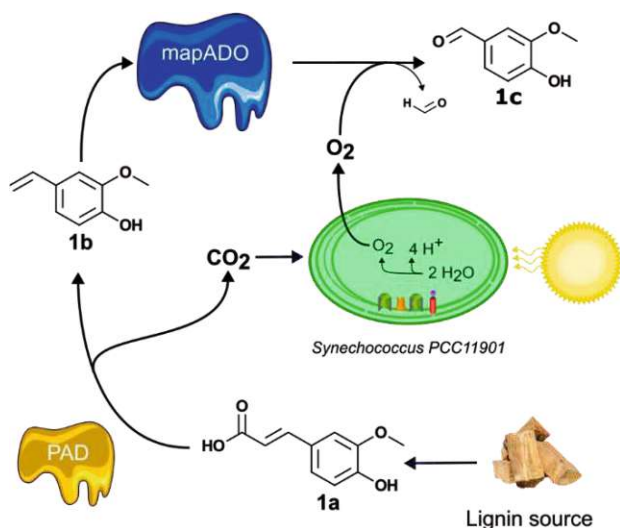


Figure 32 Two-step enzymatic cascade for the conversion of ferulic acid (1a) to 4-vinyl guaiacol (1b) and finally to vanillin (1c). Supported by the cyanobacterium *Synechococcus sp.* PCC11901.

2.3.1 The two-step cascade in *E. coli* BL21

Preliminary experiments with the two-step enzymatic cascade resulted in lower yields compared to the original publication. The co-enzyme and co-factor independent ADO, described by Ni et al., 2018, did not perform satisfactorily and underperformed in our lab compared to the data mentioned in the publication.²⁰⁴ This prompted the search for an alternative and more appropriate enzyme. The search for an alternative enzyme and the subsequent characterization of the most promising candidate was performed by Astrid Schiefer (TU Wien) and Lukas Schober (TU Graz).

2.3.1.1 An alternative Aromatic dioxygenase

11 homologs to ADO were retrieved via genomic mining and tested against 3 substrates: isoeugenol, 4-vinyl guaiacol, and hydroxyanethole. The putative enzymes were expressed in *E. coli* BL21 and tested with 10 mM substrate. The enzyme from *Moesziomyces aphidis* (from here on *mapADO*) showed outstanding conversions and was thus chosen as an appropriate ADO alternative. The comparison of all enzymes is shown in Figure 33, and a list of all tested enzyme variants is in Table 5.

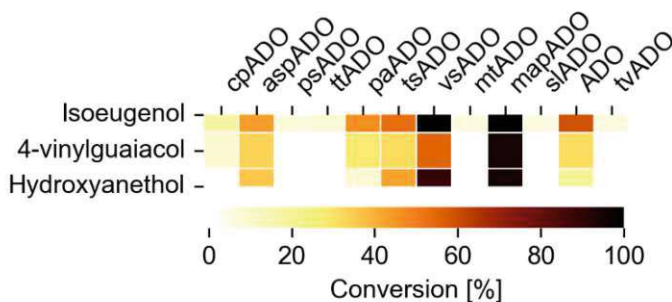


Figure 33 An aromatic dioxygenase from *Moesziomyces aphidis*. 11 variants of aromatic dioxygenases tested on 3 substrates (isoeugenol, 4-vinyl guaiacol, and hydroxyanthole), were expressed in *E. coli* BL21, 10 mM each, the darker the tone, the higher the conversion.

Table 5 Putative aromatic dioxygenase.

Name	Organism of origin	Accession No
pET-21-ADO	<i>Thermothelomyces thermophilus</i>	XP_003665585.1
pET-28-MaeADO	<i>Microcystis aeruginosa</i>	GBD54215.1
pET-28-PsADO	<i>Picea sitchensis</i>	ABR17001.1
pET-28-TvADO	<i>Talaromyces verruculosus</i>	KUL88876.1
pET-28-TsADO	<i>Talaromyces stipitatus</i>	XP_002483504.1

pET-28-MapADO	<i>Moesziomyces aphidis</i>	ETS60306.1
pET-28-AtADO	<i>Alternaria tenuissima</i>	RYN92505.1
pET-28-AspADO	<i>Altererythrobacter</i> sp.	OJU58670.1
pET-28-PaADO	<i>Podospira anserina</i>	XP_001905181.1
pET-28-MtADO	<i>Minwuia thermotolerans</i>	WP_109794489.1
pET-28-TtADO	<i>Thermocatellispora tengchongensis</i>	WP_185048654.1
pET-28-SlADO	<i>Staphylotrichum longicolle</i>	KAG7284374.1
pET-28-VsADO	<i>Valsa sordida</i>	ROV90719.1
pET-28-CpADO	<i>Coniochaeta pulveracea</i>	RKU43285.1
pET-28-MapADO	<i>Moesziomyces aphidis</i>	ETS60306.1
pET-28-StrepII-MapADO	<i>Moesziomyces aphidis</i>	ETS60306.1
pET-28-MapADO-StrepII	<i>Moesziomyces aphidis</i>	ETS60306.1

The pH optimum for *mapADO* was 7.4, but the enzyme showed high activity from pH 6 to 9.5, with less than 10% loss in activity. The highest rate for *mapADO* was determined in the first 20 minutes at 40°C, but higher product yields were achieved at lower temperatures. This is in accordance with the determination of the melting point of *mapADO* by Nano Differential Scanning Fluorimetry (NanoDSF, measured in a Prometheus device, NanoTemper Technologies GmbH, Munich, Germany). The melting point was measured to be at 38.2°C, and an onset of denaturation at 32.9°C was observed (see Figure 34).

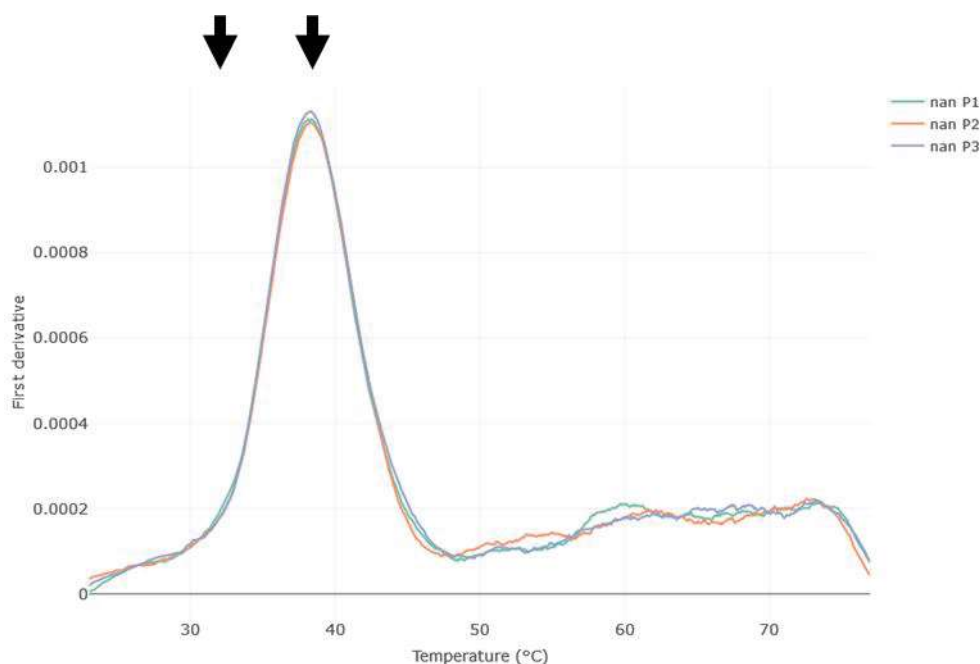


Figure 34 Denaturing curve depending on temperature of mapADO with Nano Differential Scanning Fluorimetry. The graph shows the first derivative of the ratio of the fluorescence at 330nm and 350nm. The left arrow indicates the onset of protein denaturation, and the second arrow indicates the melting point (50% denaturation). mapADO was expressed in *E. coli* BL21 and isolated via immobilized metal affinity chromatography. 1 mg/mL Protein was dissolved in PBS (pH 7.4). Temperature increased 0.1°C / min from 20 to 80°C. The Y-axis shows the derivative of the ratio of fluorescence at 330 and 350 nm. Three replicates are shown in three different colors (green, red, and blue).

The kinetic characterization for mapADO showed a v_{\max} of 0.635 ± 0.002 mM/min and a K_M of 0.58 ± 0.10 mM for isoeugenol.

The enzyme *mapADO* can convert 4-vinyl guaiacol as well as isoeugenol, but the conversion per cell is higher with isoeugenol. An OD_{590} of at least 60, corresponding to a DCW of 12 g/L in *E. coli*, is required to convert >95% of 50 mM of 4-vinyl guaiacol, while for isoeugenol the cell density can be as low as 2 g_{DCW}/L (or OD_{590} 10). This was tested by expressing *mapADO* in *E. coli* BL21, centrifuging, and resuspending cells to the corresponding OD_{590} value in PBS (pH 7.4). The suspension was then incubated with 50 mM substrate for 24 h. The results can be found in Figure 35.

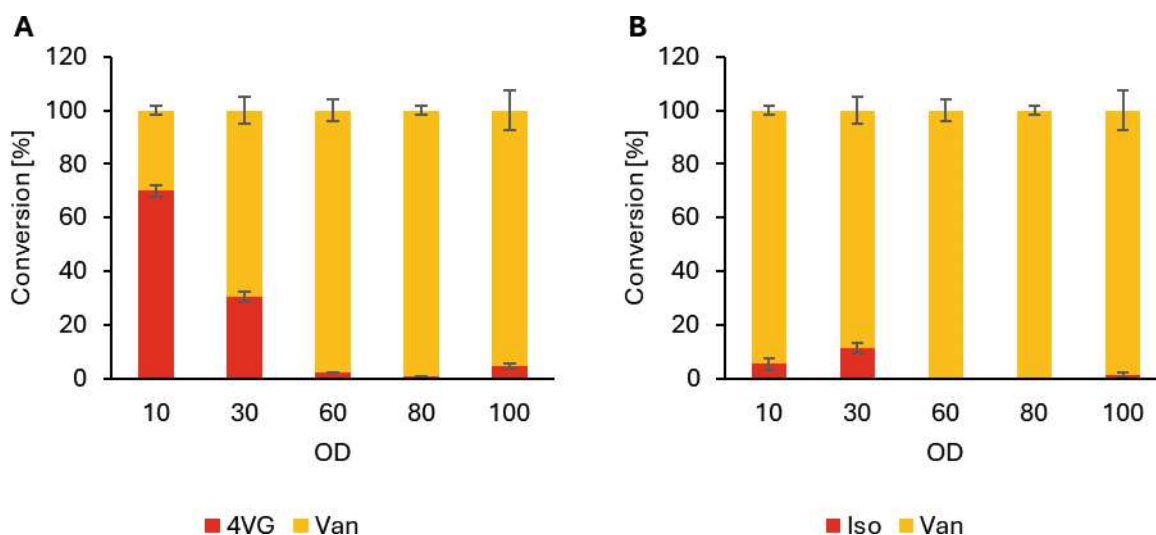


Figure 35 Conversion of 50 mM 4-vinyl guaiacol (**left**) and isoeugenol (**right**) by mapADO expressed in *E. coli* BL21. The reaction was done in closed vials at 30°C and 180rpm with increasing cell concentration, measured as optical density at 590 nm (OD). Concentration is shown as percent, the error bars indicate the standard error of the mean from 3 replicates.

A similar experimental setup showed the stability of mapADO. The enzyme was active for at least 8 h, when incubated in *E. coli* at 30°C, but showed less conversion when incubated for 24 h (see Figure 36). The samples were taken after 60 min.

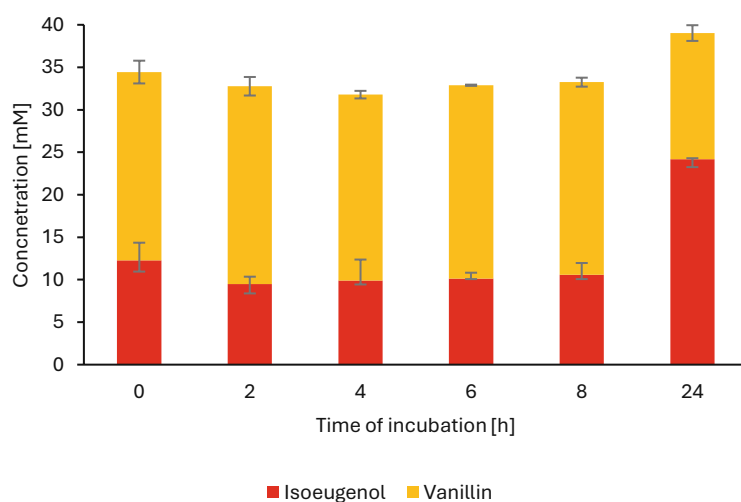


Figure 36 Stability of mapADO at 30°C. *E. coli* BL21 cells, expressing mapADO, were incubated at 30°C to a cell density of ~6 g_{DCW}/L. After 0, 2, 4, 6, 8, and 24h, 40mM isoeugenol was added and 60min later, the concentration of isoeugenol and Vanillin was measured.

2.3.1.2 Limits of mapADO

As mentioned in the introduction, oxygen can be a limiting factor for oxygenation reaction in whole-cell catalysis.¹⁶¹ After establishing isoeugenol as the preferred substrate by *mapADO*, we also tested whether oxygen is the limiting factor there.

E. coli BL21 cells expressing *mapADO* were washed and resuspended in PBS (pH 7.4) and transferred into closed glass vials with oxygen probes (firesting, Pyroscience GmbH, Aachen, Germany) measuring dissolved oxygen (dO_2) through a rubber septum. The substrate (100 mM isoeugenol) was added, and vanillin production was monitored in different glass vials in parallel, to prevent distortion of the dO_2 measurements. Two different rotation speeds (55 and 180 rpm) and cell densities (OD_{590} 10 and 60, corresponding to 2 and 12 g_{DCW}/L , respectively) were compared. The results are shown in Figure 37.

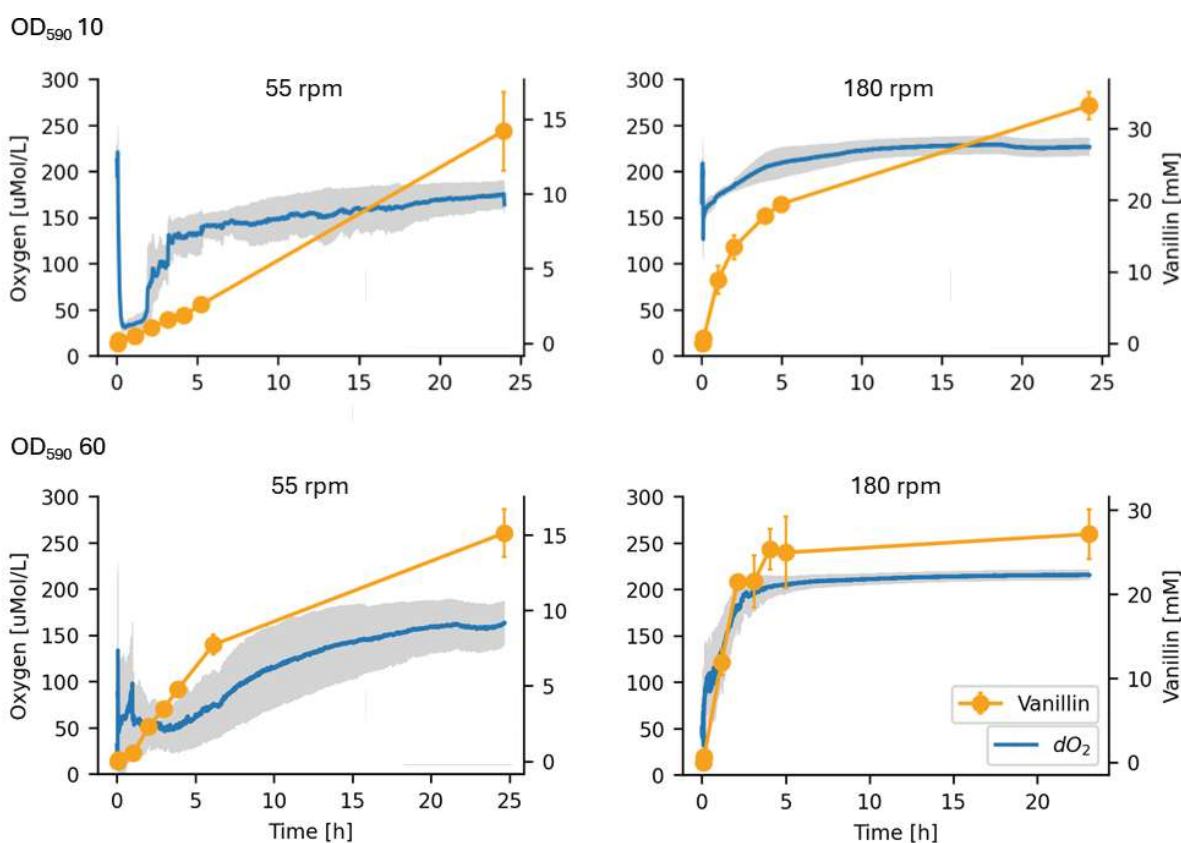


Figure 37 A suspension of *E. coli* BL21 expressing *mapADO* with low or high cell density (2 or 12 g_{DCW}/L) was tested for oxygen-limitation with high substrate loading (100 mM isoeugenol). Dissolved oxygen concentration was measured, as well as product formation. Oxygen concentration is shown in blue and vanillin concentration in orange. The grey area and error bars are the standard error of the mean from 3 replicates.

The total vanillin yield was more influenced by rotation speed than cell density, with 15 mM vanillin produced at 55 rpm and ~ 30 mM vanillin at 180 rpm. The product formation also resembles linearity at low rotation, while at high rotation the formation approaches a typical Monod-kinetic. The dO_2 -concentration approximated 0 at high cell densities, hinting at oxygen limitation, but recovered rapidly afterward.

The possibility of substrate inhibition as a major impediment for conversion in *mapADO* was tested by repeating the whole-cell catalysis with 50 mM substrate (isoeugenol) and increasing amounts of product present at the onset of the reaction, from 15 to 50 mM vanillin (see Figure 38).

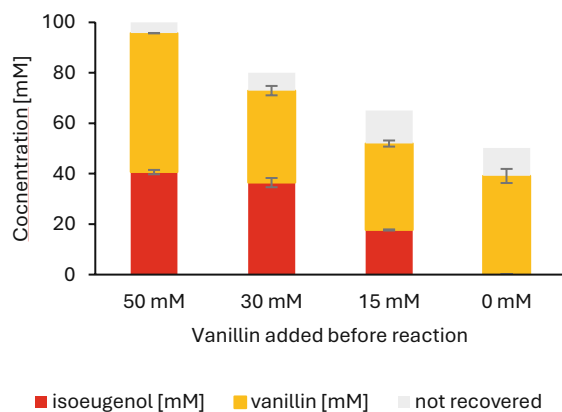


Figure 38 Different amounts of vanillin (50, 30, 15, and 0 mM) and 50 mM isoeugenol were added to a cell suspension of *E. coli* BL21, expressing *mapADO*. After 24h, product formation was measured. Error bars indicate the standard error of the mean from 3 replicates, grey area shows the theoretical yield.

When no vanillin is present, the substrate is fully converted, while, when incubated with 50mM Vanillin present, more than 40 mM isoeugenol remains, and the conversion seems to depend on the amount of vanillin added.

2.3.1.3 PAD and *mapADO* in a cascade

Next, we established whether PAD and *mapADO* can convert ferulic acid into vanillin as a two-step cascade, as described above. Both enzymes were expressed on one plasmid (pET28_ *mapADO*_PAD). The enzymes fully converted 10 and 20 mM ferulic acid into vanillin, while 30 mM yielded only 94% conversion, with 6% remaining as the intermediate 4-vinyl guaiacol. Higher amounts of ferulic acid, 40 or 50 mM, were only converted into 4-vinyl guaiacol and vanillin was only detected in trace amounts (see Figure 39).

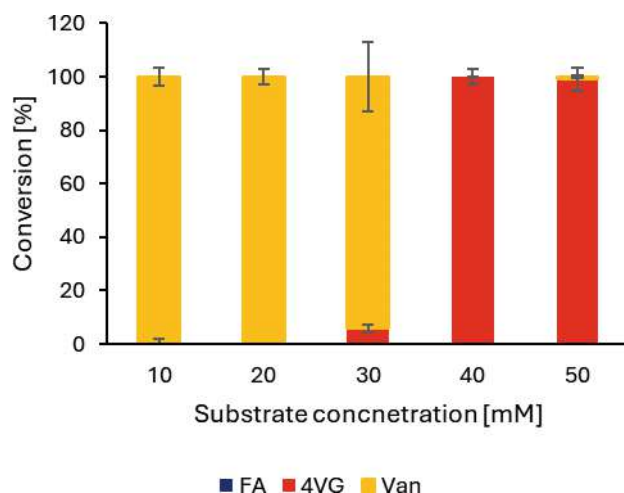


Figure 39 *E. coli* BL21 expressing PAD and mapADO were incubated with different amounts of ferulic acid (10-50 mM). Incubated at 30°C, 180rpm for 24h. The cell density was set to 12 g_{DCW}/L and in PBS (pH7.4). Conversion is calculated as the percentage of the sum of ferulic acid, 4-vinyl guaiacol, and vanillin detected after 24h. Error bars indicate the standard error of the mean of 3 replicates.

After establishing the functionality two-step enzymatic cascade for PAD and mapADO *E. coli* BL21, the next step was to integrate both enzymes into the genome of *S. sp.* PCC11901.

2.3.2 Genomic integration and protein expression in *S. sp.* PCC11901

2.3.2.1 Acrylic acid as a selection marker

The insertion of GOI into the *acsA* locus allows the use of acrylic acid as a selection marker in *S. sp.* PCC11901.¹¹⁸ Preliminary experiments with genomic integration of YFP into *acsA* (the corresponding plasmid was purchased from Addgene.com, catalog number # 140034), showed growth of the WT strain, despite the presence of 150 μ M acrylic acid in the medium (see Figure 40). Consequentially, acrylic acid was not considered for further experiments, and Kanamycin was established as the selection marker.

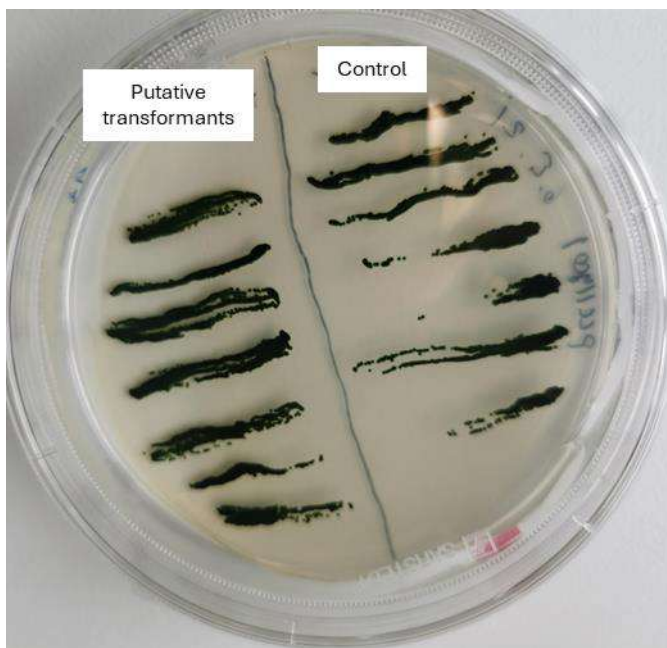


Figure 40 Acrylic acid containing agar-plate with putative transformants of *S. sp.* PCC11901 (left) versus the control growth (right).

2.3.2.2 Integration of Phenolic Acid Decarboxylase

The coding sequence for PAD from *Bacillus coagulans* DMS11²⁰⁴ was codon optimized for *Synechococcus* (Gensmart codon optimizer, Version 28.01.21) and cloned into the PSZT025 plasmid from Addgene.com (catalog number #140033) via Gibson assembly. This plasmid contains two flanking regions for genomic integration into the *fadA* gene, a Kanamycin resistance cassette (Km^R), a *LacI* coding sequence, and a YFP under the control of an IPTG-inducible promoter, which was exchanged for the PAD coding sequence. The Plasmid map is visualized in Figure 41.

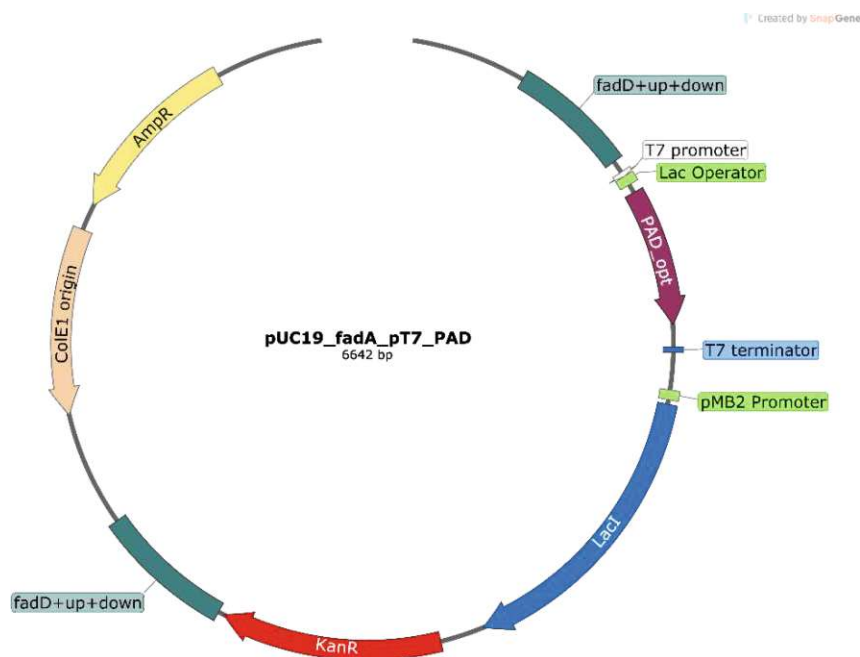


Figure 41 Plasmid map of pUC19_fadA::pad for the integration of PAD coding sequence, flanked by fadA. The plasmid also contains a Kanamycin and Ampicillin resistance cassette (KanR and AmpR), the repressor LacI, and an origin of replication for *E. coli* (ColE1).

The transformation was performed according to the protocol described in Włodarczyk et al., 2020 and verified by colony-PCR (Figure 42) and subsequent DNA sequencing of the amplicon (Microsynth AG, Balgach, Switzerland).

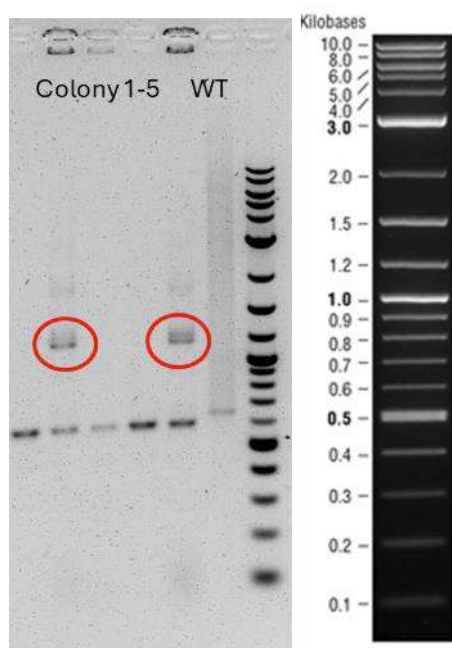


Figure 42 Colony PCR for fadA in putative transformants of fadA::pad mutant and WT as control. The amplicon size for the WT is ~650bp and the successful insert is expected to be around 1250 bp, highlighted by the red circles..

The expression of PAD was detected via SDS polyacrylamide gel electrophoresis (SDS-PAGE). The expression of PAD was less pronounced as in *E. coli* under the T7 promoter, but distinct from the WT (see Figure 43).

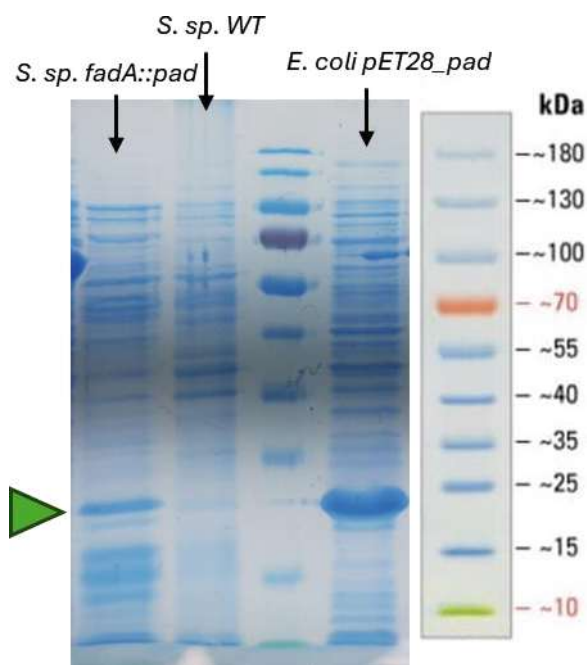


Figure 43 Protein gel electrophoresis (SDS-PAGE) for determination of *pad* expression. The protein has a calculated mass of 41 kDa (indicated by the green arrow). **Left:** *S. sp. PCC11901 fadA::pad* 24h after induction with 1 mM IPTG, **second to left:** *S. sp. PCC11901 WT*. **Right:** *E. coli pet28_PAD* 24h after induction with 1 mM IPTG.

Following the integration and expression of PAD by *S. sp. PCC11901*, the aromatic dioxygenase was next.

2.3.2.3 Attempts at genomic integration of (*map*)ADO into *S. sp. PCC11901*

The genomic integration of an aromatic dioxygenase, whether described by Ni et al., 2018²⁰⁴ or the newly described *map*ADO was achieved. Here, we present the conditions explored for the integration of the gene of interest.

The initial attempt employed standard parameters described in Włodarczyk et al., 2020.¹¹⁸ In brief, the target gene was cloned into the vector pSW039 (plasmid obtained from Peter Nixon, Addgene plasmid #140035), using a ~740 bp upstream and downstream flanking region as the insertion site within the *psbA2* gene. The insert comprised the gene of interest (a codon-optimized version of *ado* from Ni et al., 2018²⁰⁴), *lacI*, and a spectinomycin/streptomycin resistance cassette. PCC11901 wild-type (WT) cultures were grown at 250 $\mu\text{mol photons/s/m}^2$, 39°C, under atmospheric CO₂ in AD7 minimal medium. At an OD₇₅₀ of 0.5-1, 1 mL of the culture was transferred to a 50 mL centrifugation tube, combined with 1 μg of DNA (the insert was amplified by PCR), sealed with parafilm, and incubated at the same conditions. After 24 hours, cells were plated

onto AD7-agar plates containing streptomycin (100 mg/L). This produced no colonies, prompting tests with lower streptomycin concentrations (50 and 20 mg/L), which yielded similar growth to the negative control (no DNA added). This was a surprising observation, as even 1 mg/L had been inhibitory in other cyanobacterial species.⁸⁰ PCC11901 showed stable growth in low-salt YBG-11 medium, and further trials employed YBG-11 agar plates to mitigate salt crystal formation observed on AD7-agar plates during prolonged incubation. Despite these efforts, no stable recombinant strain was achieved, even after consultation and troubleshooting with the authors of the initial study on PCC11901.

New potential integration sites were identified, including the alternative respiratory terminal oxidase (ARTO) and cytochrome-c oxidase complex (COX) loci.¹⁵⁵ Consequentially, new plasmids were constructed, with *mapADO* and ADO inside these flanking regions. Additionally, constructs without the *lacI* gene were tested as well, as shorter inserts increase integration efficiency⁷⁵ and the *lacI* gene would be present in the genome in PCC11901 *fadA::pad*. Yet, none of these constructs yielded recombinant strains.

As previously demonstrated for *Synechococcus* sp. PCC 7942, the circadian rhythm significantly influences natural competence in cyanobacteria.²⁷² We investigated the effect of circadian cycles on *S. sp.* PCC11901 transformation efficiency. The highest efficiency in *S. sp.* PCC7942 was observed during a 16h:8h light cycle, specifically 2 hours before the onset of the dark phase, following 24 hours of darkness. A 25 mL culture of *S. sp.* PCC11901 in AD7 medium was grown under 250 $\mu\text{mol photons/s/m}^2$ at 39°C in a 16h 8h light:dark cycle. After 48 hours, the culture was incubated in darkness for 18 hours before transformation, as previously described. Cells were then incubated for an additional 24 hours in darkness, plated on YBG11 agar plates with 100 mg/L spectinomycin, and maintained under 250 $\mu\text{mol photons/s/m}^2$ and 1% CO₂. None of the attempts yielded stable integration of ADO or *mapADO* into the genome of PCC11901.

Confronted with this problem, alternative solutions were investigated.

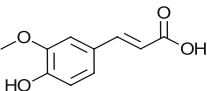
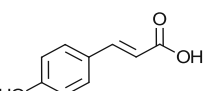
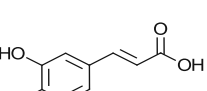
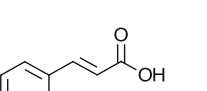
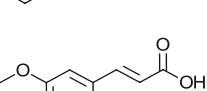
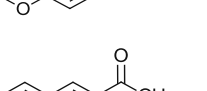
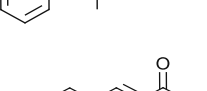
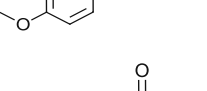
2.3.3 Optimizing 4-vinyl guaiacol production from ferulic acid by *S. sp.* PCC11901 *fadA::pad*

We focused on optimizing the yield of PAD in *S. sp.* PCC11901, by first comparing the results from both hosts.

2.3.3.1 Substrate scope

The substrate scope of PAD, when expressed in *E. coli*, is limited to cinnamic acid derivatives with a hydroxy-group in *para*-position. This is identical when expressed in PCC11901, as PCC11901 *fadA::pad* converted ferulic acid, *p*-coumaric acid, and caffeic acid, but no other cinnamic acid derivatives with methyl- or methoxy-groups in *para*-position. The full set of substrates tested is listed in Table 6.

Table 6 The substrates scope of *S. sp.* PCC11901 *fadA::PAD*. Cells were incubated with 10mM substrate and cultivated for 24h at 39°C, 150 rpm at 500 $\mu\text{mol photons /s /m}^2$. n.c. = no conversion; [a] Based on Substrate consumption; [b] Product could not be detected, probably due to polymerization.

#	Compound	Substrate	Conversion [%] ^[a]
1	Ferulic acid		81 \pm 8
2	<i>p</i> -Coumaric acid		93 \pm 8
3	Caffeic acid		100 ^[b]
4	Cinnamic acid		n.c.
5	3,4-dimethoxy cinnamic acid		n.c.
6	α -methyl cinnamic acid		n.c.
7	4-methoxy cinnamic acid		n.c.
8	4-methyl cinnamic acid		n.c.

The product of decarboxylated caffeic acid, 4-vinyl phenol, could not be detected by HPLC, but a brown discoloration was observed (Figure 44 **A**). When the product alone was incubated under the same conditions (same medium, 500 $\mu\text{mol photons/s/m}^2$, 39°C), the same discoloration was observed (Figure 44**C**). This indicates a strong polymerization of 4-vinyl phenol and could explain the missing detection of the monomer via HPLC.

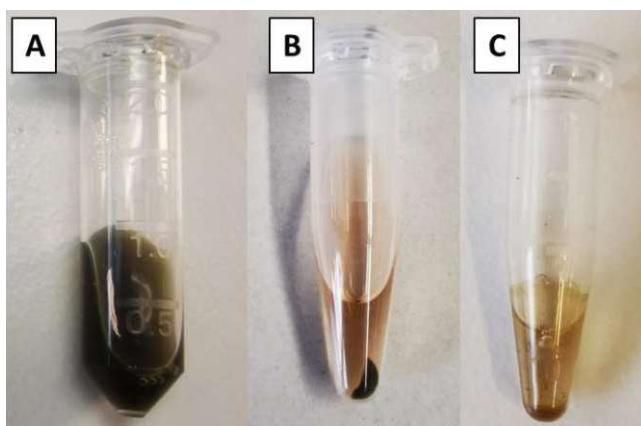


Figure 44 *S. sp. PCC11901 fad::PAD* was incubated with 10mM caffeic acid at 500 $\mu\text{mol photons/s/m}^2$. **A** shows cells after 24h, **B** the same tube, after centrifugation. **C** shows 10mM 3,4-dimethoxystyrene after 24h incubation in the same buffer and light conditions, without cells.

The PCC11901 WT did not convert ferulic acid over 24h and the comparison of PCC11901 *fadA::pad* induced with 1 mM IPTG and without IPTG showed, that the induced strains can fully convert 1 mM ferulic acid within 24h, while the non-induced cells produced < 0.4 mM 4-vinyl guaiacol from 1 mM ferulic acid within 24h.

The conversion of ferulic acid to 4-vinyl guaiacol by PAD was lower in PCC11901 than described in the literature. Also, when expressed in *E. coli* BL21, the enzyme converted 10 mM ferulic acid into 4-vinyl guaiacol in less than 3 h. Additionally, the bright green color of the cell suspension changed into a yellowish-brown during the reaction (see Figure 45), indicating the toxicity of the substrate or the product.



Figure 45 *S. sp. PCC11901 fadA::PAD* before (LEFT) and after (RIGHT) adding 10mM ferulic acid. Cells were incubated with 10 mM ferulic acid and converted into 4-vinyl guaiacol by the expressed enzyme PAD. The mixture was incubated for 24h at 39°C, 500 $\mu\text{mol photons/s/m}^2$ in a closed glass vial.

2.3.3.2 Toxicity assay via oxygen measurement

The quantification of the observed discoloration showed that the concentration of Chlorophyll *a* in PCC11901 after incubation with 10 mM 4-vinyl guaiacol for 24h, was below the limit of detection while incubating the cells with 10 mM Ferulic acid did not affect Chlorophyll *a* content ($100 \pm 5\%$).

We further investigated the effect of 4-vinyl guaiacol on the photoautotrophic metabolism of PCC11901, especially under conditions similar to large-scale production, so we measured the oxygen levels in a closed vessel and the effect of substrate and product on oxygen evolution. The cells were incubated for 48h under the standard conditions, described above. Then 10 mL of the cell suspension was transferred into flat bottom flasks, and the oxygen probe was submerged. The light intensity was set to 500 $\mu\text{mol photons/s/m}^2$ and carbonate was added to verify healthy cells and normal oxygen production. When oxygen levels reached baseline again, 10 mM ferulic acid or 4-vinyl guaiacol was added, followed by another boost with carbonate. While ferulic acid had no significant effect on the oxygen concentration (Figure 46 **A**), 4-vinyl guaiacol inhibited oxygen production immediately (Figure 46 **C**). When ferulic acid was added to PCC11901 *fadA::pad*, after inducing the expression of PAD, an increase in oxygen was observed, as would be expected, due to the release of CO_2 , but declined after a few minutes back to baseline (Figure 46 **B**).

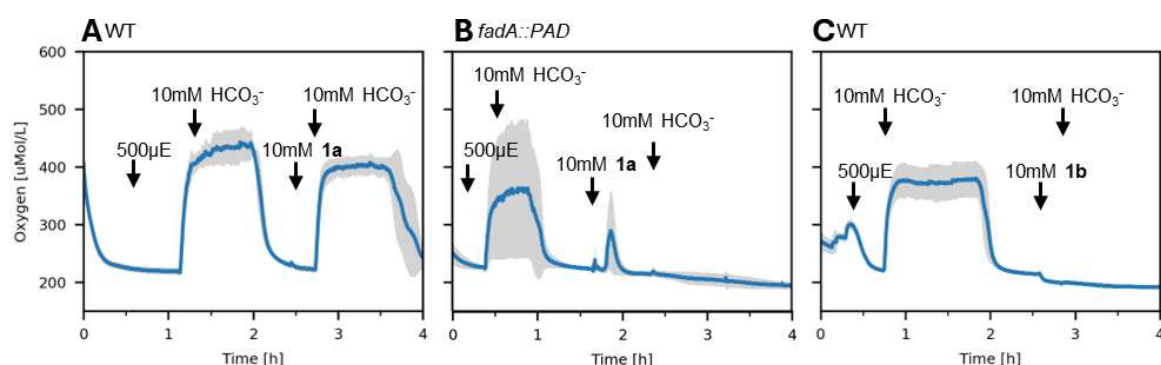


Figure 46 Oxygen measurement of *S. sp.* PCC11901 in the presence of Ferulic acid (**1a**) and 4-vinyl guaiacol (**1b**). Measurement was taken in a closed vessel, prohibiting CO_2 from entering the suspension. Light intensity was increased to 500 $\mu\text{mol photons/s/m}^2$ (μE) until O_2 stagnated, and then 10mM of a carbonate solution was added, causing a spike in O_2 concentration. Then, 10mM of either ferulic acid (**A**, **C**) or 4-vinyl guaiacol (**B**) was added, followed by another addition of carbonate and the oxygen levels were compared. **A** WT strain with 10mM ferulic acid **B** *fadA::PAD* strain with 10mM Ferulic acid and **C** WT with 10mM 4-vinyl guaiacol. The grey area indicates the standard error of the mean from 3 replicates.

In conclusion, the comparable low yield of the enzyme compared to the literature,^{204,273} the decrease of Chl *a* and the suppressed oxygen production are strong indicators, that 4-vinyl guaiacol inhibits photosynthesis in PCC11901. Other causes, such as the solvent used for the substrates (DMSO or ethanol) can be excluded.

2.3.3.3 *In situ* product removal by an organic phase overlay

Ferulic acid is more hydrophilic than 4-vinyl guaiacol, which qualified this reaction for an *in situ* product removal employing an organic phase overlay. Three organic solvents are non-toxic for cyanobacteria and are effective in the removal of toxic, hydrophilic compounds: diisononyl phthalate (DINP), ethyl oleate,²³⁶ and dodecane.^{61,64} DINP was the only one of these three, that dissolves 4-vinyl guaiacol in high enough quantities. Other, more environmentally benign alternatives were also examined. The solvents were incubated with the cells in a 1:1 ratio for 24h at 500 $\mu\text{mol photons /s/m}^2$ and the change in Chlorophyll a and carotenoids was measured. The result, shown in Figure 47, indicated, that DINP and isopropyl myristate (IPM) had the least effect on pigment content within the cells by decreasing the concentration of Chl a and carotenoids by $\sim 13\%$ and $< 2\%$, respectively. The other tested solvents, cyclopentyl methyl ester (CPME), ethyl acetate, limonene, *p*-cymene, methyl tert-butyl ether (MTBE), farnesene, and farnesol decreased the Chl a content by at least 82%, and carotenoids were reduced by at least 59% so DINP and IPM were chosen as an organic phase overlay.

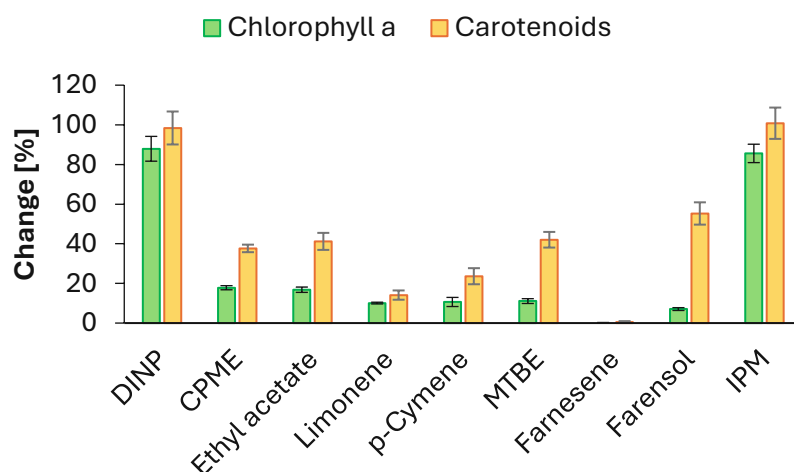


Figure 47 Evaluation of eventual organic layer compounds. Cells were incubated for 24h at high light with different solvents and their chlorophyll a and carotenoid content were compared to a control without any solvent under the same conditions. The solvents tested were diisononyl phthalate (DINP), cyclopentyl methyl ester (CPME), ethyl acetate, limonene, methyl tert-butyl ether (MTBE), farnesene, farnesol, and isopropyl myristate (IPM), Error bars show standard error of the mean of three replicates.

Following the limited toxicity of DINP and IPM, the two solvents were tested for *in situ* product removal during whole-cell catalysis with PCC11901 *fadA::pad*. A cell suspension was combined with the same amount of solvent in a closed glass vial and emulsified with a magnetic stirrer under standard conditions.

The organic phase successfully alleviated the toxicity of 4-vinyl guaiacol, thus allowing full conversion of up to 40 mM ferulic acid into 4-vinyl guaiacol. Higher amounts of ferulic acid remained in the aqueous phase and were not converted (Figure 48). No difference between DINP and IPM was observed, and light did not affect total conversion.

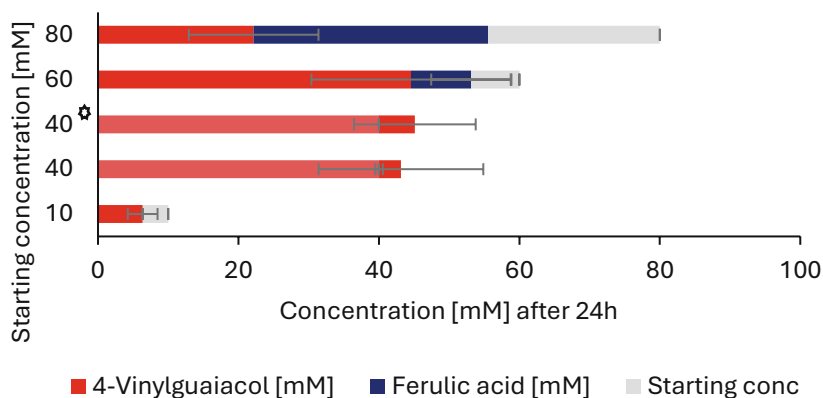


Figure 48 DINP was chosen as the test solvent for *in situ* product removal and cells to *fadA::PAD* with different concentrations of ferulic acid. 40* was done without light. The reactions were performed in closed glass vials with a cell suspension of PCC11901 *fadA::pad* and DINP or IPM in a 1:1 ratio at 39°C, 500 $\mu\text{mol photons/s/m}^2$. The aqueous phase was analyzed via HPLC and the organic phase by gas chromatography. Error bars indicate the standard error of the mean of 3 replicates.

The enzyme remained active for at least 30 hours. A second addition of 40 mM ferulic acid after 24h was fully converted, increasing the yield to ~80 mM, which is not achievable, when the ferulic acid is added all at once (Figure 49 left). The product, 4-vinyl guaiacol remained largely in the organic phase, and only traces could be found in the cell suspension (Figure 49 right), with less than 4 mM of 4-vinyl guaiacol in the aqueous phase and 76 mM in the organic phase after 48h.

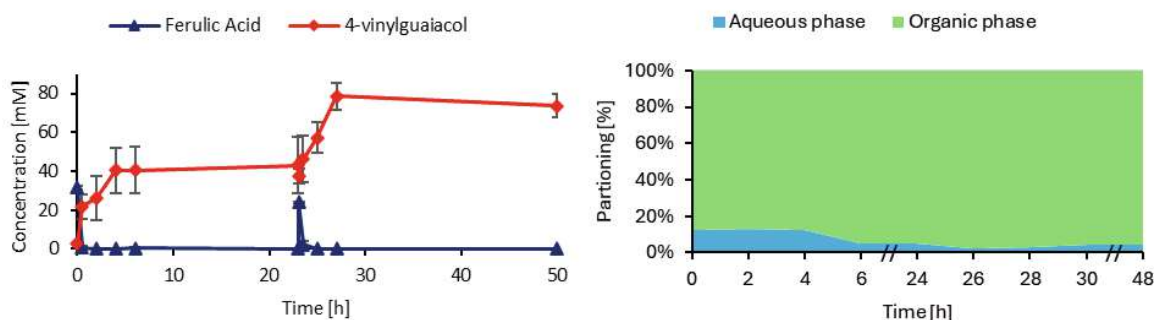


Figure 49 Optimization of biocatalysis in *S. sp. PCC11901 fadA::pad*. The enzymes remained active after 24h, converting 2 x 40mM ferulic acid, when added 24h apart. **LEFT:** The reactions were performed in closed glass vials with a cell suspension of PCC11901 *fadA::pad* and DINP or IPM in a 1:1 ratio at 39°C, 500 $\mu\text{mol photons/s/m}^2$. **RIGHT:** Partitioning of 4-vinyl guaiacol between the aqueous phase and the organic phase in %. The aqueous phase was analyzed via HPLC and the organic phase by gas-chromatography. Error bars indicate the standard error of the mean of 3 replicates

The *in situ* product removal is only effective at high mixing rates, so magnetic stirring was employed here at 300 rpm. According to the manufacturer and verified by tests in our laboratories, the oxygen probes used were unsuitable for organic solvents, thereby preventing a reliable dO_2 measurement in the emulsion.²⁷⁴

2.3.3.4 Gram-scale production of 4-vinyl guaiacol

Biotechnological utilization of cyanobacteria is often hindered by difficulties in up-scaling.^{19,68,69} The gram-scale production of 4-vinyl guaiacol from ferulic acid is thus an important step to test the applicability of PCC11901 *fadA::pad* as a whole-cell catalyst. Simple equipment, instead of an expensive CO₂-incubator was employed to further elucidate this. The bacteria were cultivated in a CellDEG system (HD100 cultivator, CellDEG, Berlin Germany) with a carbonate buffer as a *Ci* source, separated from the culture vessel by a hydrophobic and gas-permeable membrane. After 96h of incubation, at a cell density of ~ 3.9 – 5.2 g_{DCW}/L, cells were harvested and washed twice by centrifugation at 4000 x g for 10 min and resuspended in 100 mL YBG-11 with 100mM HEPES, pH 7.4. The reaction took place in a 500 mL glass bottle (SCHOTT, Germany) with 100 mL DINP or IPM and a magnetic stirrer, at 37°C, 300 rpm, 500 µmol photons/s/m². A schematic of the experimental setup is depicted in Figure 50.

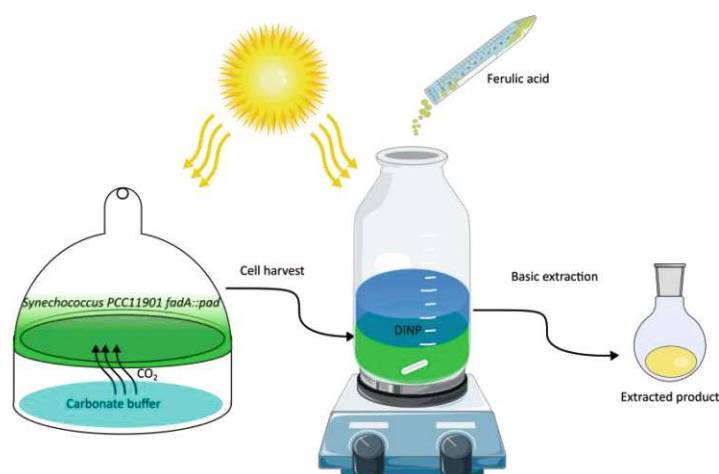


Figure 50 Schematic of gram-scale production of 4-vinyl guaiacol by PCC11901 *fadA::pad*. The cells were incubated in a two-tier vessel with a carbonate buffer releasing CO₂ through a membrane into the culture medium. Cells were harvested by centrifugation and resuspension in a salt-free medium and transferred into a 500 mL glass bottle. An organic solvent (DINP or IMP) was added. The two liquids were emulsified with a magnetic stirrer and the substrate, ferulic acid, was added directly. After the reaction, the product was purified by basic extraction.

Ferulic acid was added in two parts at each 0.78g, 4h apart. After 8h, the reaction was quenched by the removal of the organic phase. Any product, that remained in the aqueous phase was extracted by adding 100 mL ethyl acetate and shaking vigorously. Both solvents, DINP and IPM, reached full conversion and the purification of 4-vinyl guaiacol was possible by basic extraction. The extraction from DINP yielded 1.19 g of 4-vinyl guaiacol, 97% of the theoretical yield. The product was confirmed to be pure by GC and NMR, while NMR showed no signs of polymerization (Figure 51).

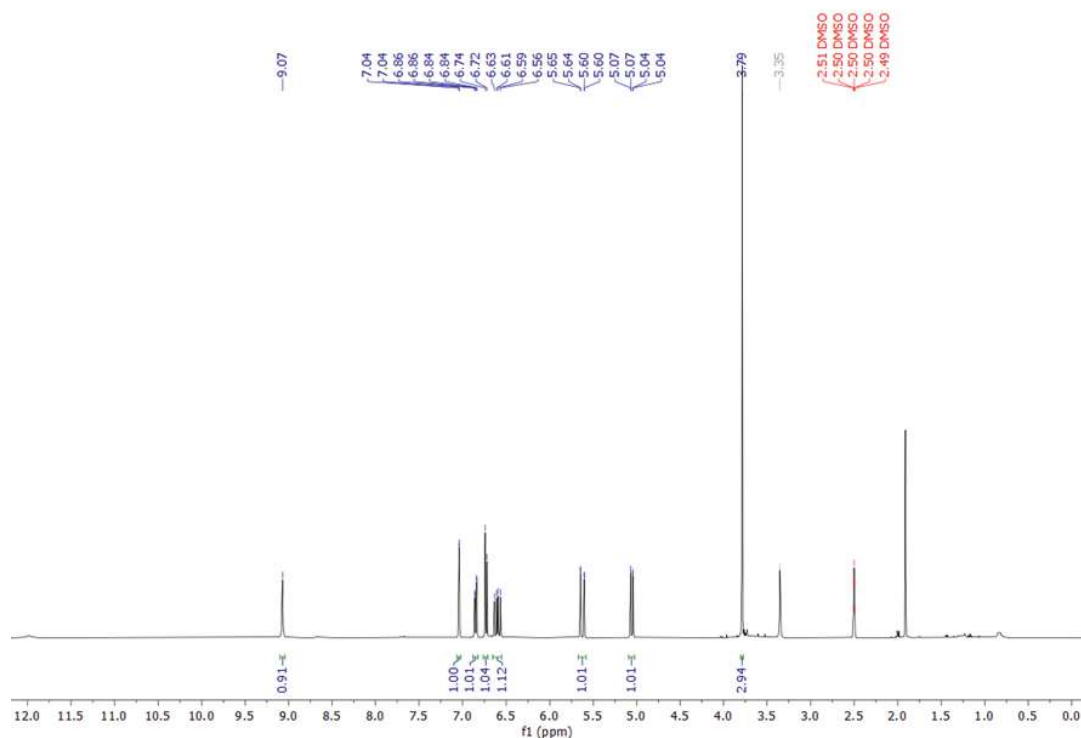


Figure 51 NMR spectrum of 4-vinyl guaiacol, converted from ferulic acid by PCC11901 fadA::PAD and extracted the organic phase of DINP by basic extraction. NMR code: ^1H NMR (400 MHz, DMSO) δ 9.07 (s, 1H), 7.04 (d, J = 2.0 Hz, 1H), 6.85 (dd, J = 8.2, 2.0 Hz, 1H),

Removing IPM from the product via basic extraction yielded 1.10g of 4-vinyl guaiacol with 9% IPM impurity. The remaining IPM was successfully removed via column chromatography.

2.3.4 Mixed species whole-cell catalysis

Despite the set-back, that ADO cannot be integrated into the genome of PCC11901, we hypothesized, that the photosynthetic production of oxygen by a cyanobacterium can still improve the yield of the two-step enzymatic cascade in a mixed-species approach and expressing the enzyme(s) in *E. coli* BL21.

From the previous experiment, it was observed, that substrate concentrations above 30 mM ferulic acid, yield decreased dramatically (see Figure 39), consequently, 40 mM was determined as the benchmark for a mixed-species approach. The cells were cultivated separately and only combined for the reaction. The reaction took place with 12 g_{DCW}/L of *E. coli* in PBS and ~4.5 g_{DCW}/L of PCC11901 (48h of growth) in YBG-11, in a closed vial at 30°C, 500 μ mol photons/s/m² and 180 rpm. The substrate was either added in a single batch or fed as 10 mM batches every 2 h, four times. The results are summarized in Figure 52.

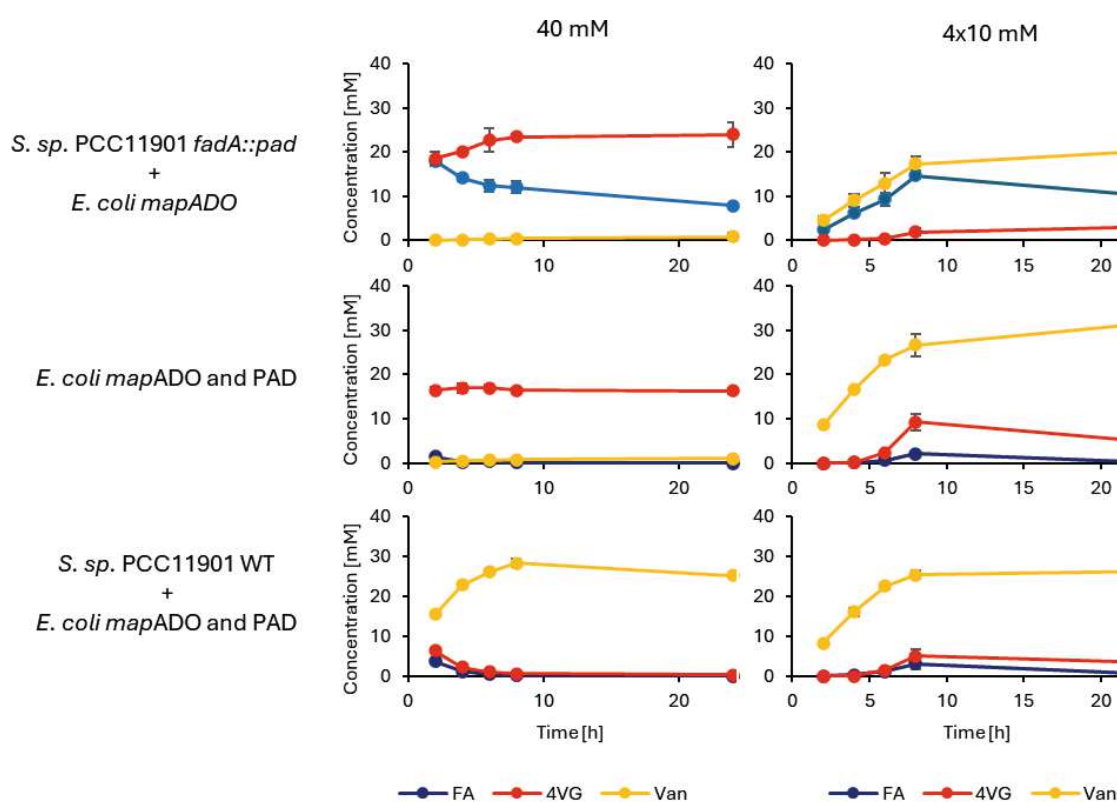


Figure 52 Whole-cell two-step enzymatic cascade to form Vanillin (Van) from 40mM ferulic acid (FA) via 4-vinyl guaiacol (4VG), with PAD and mapADO. Reaction occurred at 30°C, 180 rpm, and 500 μ mol photons/m²/s. The biomass of *E. coli* was 12 g_{DCW}/L and of *S. sp. PCC11901* ~4.5 g_{DCW}/L. In the left column, 40 mM ferulic acid was added directly, in the right column, ferulic acid was added every 2 h á 10 mM, 4 times. The first row shows *S. sp. PCC11901 fadA::pad* mixed with *E. coli* expressing mapADO, the second row shows only *E. coli* expressing mapADO and PAD, the third row shows *S. sp. PCC11901* together with *E. coli* expressing mapADO and PAD. The reactions were done in triplicates and error bars indicate the standard error of the mean, if not visible, the deviation is smaller than the graph points.

When the burden of protein expression was distributed between the two species, the cyanobacterium expressing PAD and *E. coli* BL21 expressing *mapADO*, the batch reaction yielded only trace amounts of vanillin, the majority was converted into 4-vinyl guaiacol while the rest remained as ferulic acid. The fed-batch approach improved yield to 20 ± 2 mM vanillin. The reaction was almost completed after 8 h, although the amount of ferulic acid kept decreasing during 8 and 24h, without the adequate amount of 4-vinyl guaiacol increasing.

Vanillin yield was enhanced in *E. coli* BL21 expressing both enzymes through the implementation of a gradual substrate-feeding strategy over an extended time frame, as compared to a batch approach. The final concentration after 24h of vanillin was then 32 ± 2 mM, with no ferulic acid left.

A synergistic effect was observed when both enzymes were expressed in *E. coli* BL21 and *S. sp.* PCC11901 WT was added to the reaction. In total, 25 ± 1 mM vanillin was measured after 24h, with no ferulic acid or 4-vinyl guaiacol detectable. The conversion was similar to the fed-batch approach (26 ± 2 mM vanillin) but with < 5 mM of substrate and intermediate remaining.

3 DISCUSSION

3.1 CARBOXYLIC ACID REDUCTASE IN *S. SP. UTEX2973*

Cyanobacteria are promising platform organisms for whole-cell catalysis. The autophototrophic metabolism can be exploited as a recycling system for co-factors, relevant for the enzymatic reaction of interest and the *in situ* oxygen production, a waste product of photosynthesis, could alleviate oxygen-limitation in oxygenation reactions. Additionally, the ratio of NADPH to NADH is higher in cyanobacteria compared to heterotrophs, which might circumvent enzyme engineering to switch preferences from NADPH to NADH. In theory, cyanobacteria appear as the best choice for whole-cell catalysis but have not yet replaced heterotrophic bacteria in large-scale production.^{19,68,69}

One obstacle to the widespread application of cyanobacteria is their slow growth. The heterotrophic organisms, typically employed in biocatalysis, such as *E. coli*, *Pichia pastoris*, or *Saccharomyces cerevisiae*, double their biomass in less than 2 hours under optimal conditions, while the most employed cyanobacterium, *Synechocystis sp. PCC6803* doubles in more than 6 hours under optimal conditions.^{118,145,150,244} The re-discovery of *Synechococcus sp. UTEX2973* was auspicious to overcome this obstacle and has since then been proven to have unprecedented capabilities.^{147,148,148,149} This strain was therefore chosen to be tested for its applicability for whole-cell catalysis. The enzymatic reaction, the strain was supposed to be tested with, is the reduction of carboxylic acids to aldehydes by a carboxylic acid reductase (CAR). The enzyme requires one molecule of ATP and NADHP each, for every reaction and is thus costly to be implemented and promising to be powered by photosynthesis.^{178,269–271}

The high growth rate of *S. sp. UTEX2973* could be reproduced but required high light intensities and high CO₂ supply. In the set-up here, the CellDEG system (CellDEG GmbH, Berlin, Germany) provided the optimal atmosphere and is a cheap alternative to a CO₂-controlled incubator. The doubling time of 1.9h is in accordance with the literature, and our experiments also showed the resilience of *S. sp. UTEX2973* against light intensity of up to 2000 $\mu\text{mol photons} / \text{m}^2 / \text{s}^{117}$ (see Figure 18).

The application of flux balance analysis to a genome-scale model allows the prediction of essential genes, growth rates under varying conditions, and the change in fluxes after deleting genes.^{251,252} Here, it was explored, how deleting single genes could redirect co-factors, ATP and NADPH, towards the reaction of interest, the reduction of carboxylic acid to aldehydes.

The trade-off plot of FBA in the GSM *imSyu593*, with CAR as the objective function showed, that a maximum flux of $\sim 0.2 \text{ mmol} / \text{g}_{\text{DCW}} / \text{h}$ through the CAR-catalyzed reaction is possible while maintaining a minimum flux through the biomass reaction. Optimized systems, with co-factor recycling, for example, have been described with a space-time-yield (STY) of 2 mmol/L/h for *niCAR*²⁷¹ and 3.5 mmol/L/h for *tvCAR*.²⁶⁸ A cell density of $>10 \text{ g}_{\text{DCW}} / \text{L}$ would be necessary for *S. sp. UTEX2973* to reach STY similar to this, which is higher than any cell density currently described in the literature for UTEX2973 (see Table 1). The validity of the knock-out predictions for ATP and NADPH-dependent reactions must be

seen critically. The plots indicate that every knock-out involving an NADPH reaction would be detrimental to *S. sp.* UTEX2973, but deletions, for example for flavodiiron proteins, have been done in *Synechocystis sp.* PCC6803 to elucidate the redundancy in the photosynthesis regulation system.²⁷⁵ None of the simulated knock-outs showed increased flux through the CAR reaction, which might be different *in vivo*, as a strong electron sink can out-compete the endogenous electron sinks in cyanobacteria, which was proven for the ene-reductase YqjM in *Synechocystis sp.* PCC6803.

One of the basics for synthetic biology and metabolic engineering is a tight, external regulation of gene expression.^{44,57} The ‘gold standard’ in *E. coli*, the IPTG-inducible, lac-operon-inspired promoter, shows a high leakage and low dynamic range in cyanobacteria.²⁷⁶ In cyanobacteria, cobalt-induced promoter are often used, but the toxicity of the inducing compound limits their application.²⁷⁷ For this reason, the 3 newly employed promoter systems P_{rha} , P_{vanCC} , and P_{LO3} were tested for their applicability in *S. sp.* UTEX2973, as these three showed promising regulation and dynamic ranges in *Synechocystis sp.* PCC6803.⁴⁶ Surprisingly, after induction of the expression of the fluorescence protein eYFP with Rhamnose, vanillate, and aTc, respectively, fluorescence was barely detectable (see Figure 26). There are differences between the plasmid carrying *S. sp.* UTEX2973 strains and the WT that are statistically significant ($p < 0.05$), especially between the WT and the strain carrying the eYFP gene under the control of P_{VanCC} , but fluorescence was in all strains higher at day 0, directly after induction, even if no plasmid was present. This indicates that any changes in fluorescence measured are probably artifacts or measuring errors within the plate reader used for this experiment. The reason for this is unknown. It might be that mutations in the plasmids have prevented functional gene expression, especially as plasmid presence has only been confirmed by growth on the respective antibiotic and colony-PCR and not by DNA sequencing, which would detect mutations, which is common in cyanobacteria, especially under high light intensities.⁷⁶ Alternatively, the promoters used here are unsuitable for expression in *S. sp.* UTEX2973 and are downregulated either on the transcriptional or translational levels. Expression levels can differ from one cyanobacterial strain to another.⁸⁶ Further investigation in this direction might shed light on this.

The unsuccessful attempts to clone the CAR coding sequence into a suitable vector for *S. sp.* UTEX2973 caused the closure of this project. RSF1010-based plasmids are known to be ‘difficult to work with’, with low yields after manipulation, incomplete restriction digests, and low yields in DNA purification.⁸⁰ The vectors pSHDY and pPMQAK are both RSF1010-based plasmids and so suffer the same disadvantages, although the mutation *mobAY25F* in pSHDY and the introduction of it into pPMQAK can improve the effectiveness of molecular cloning attempts, they still pose a major obstacle in self-replicating plasmid construction for cyanobacteria. The natural transformability of *S. sp.* UTEX2973 can be restored, which allows genetic integration as an alternative approach, but this remains time-consuming, due to the plurality of the cyanobacterial genome within every cell.²⁶⁰

3.2 *S. sp.* PCC11901 AND THE ENZYMATIC CONVERSION OF FERULIC ACID INTO VANILLIN

The cyanobacterium *S. sp.* PCC11901 was described as having the highest biomass accumulation of any cyanobacterium and a growth rate similar to yeasts, such as *Saccharomyces cerevisiae* and *Pichia pastoris*.¹¹⁸ In this work, this characteristic could be reproduced. The strain grew as fast as *S. sp.* UTEX2973, the fastest-growing cyanobacterial strain known,²⁴⁴ but continued the linear growth phase, when *S. sp.* UTEX2973 entered the stationary growth phase in the CellDEG system (Figure 19). In a CO₂-incubator, the fast-growing phenotype was equally present but allowed a more detailed observation of pigment concentrations at different growth phases, without interference from varying carbon availability (Figure 20). In the early growth phase, the ratio of Chl a to OD₇₅₀ was the highest, likely corresponding to the short exponential growth phase. This is followed by a linear growth phase and a linear increase in Chl a and carotenoids. With increasing cell density, the need for light-harvesting molecules increases in phototrophic microbes, thus explaining the stable ratio of Chl a and carotenoids to OD₇₅₀ in the linear growth phase.¹³⁸ The continued growth but abrupt stagnation of pigment concentration from day 8 to day 12 contradicted the dogma of increased cell density requiring increased light-harvesting pigments. *S. sp.* PCC11901 has been described as changing its cell structure by enlarging at late-stage growth,¹¹⁸ thus the increase in OD₇₅₀ might be caused by an increase in cell size and not cell count. This phenomenon in cyanobacteria has been described before and has sparked a debate about the reliability of optical density as an indicator for biomass.^{101,278,279} The direct measurement of dry cell weight and/or cell count is preferable, but more time-consuming and not available for every lab. Additionally, the concentration of phycocyanin was omitted in this study, so it cannot be excluded, a shift from chlorophyll a to phycocyanin allowed *S. sp.* PCC11901 to continue to grow. As mentioned above, phycocyanin, and other pigments, enable cyanobacteria to grow at greater depth in the water column than algae by closing the ‘green gap’.

We were able to show, that oxygen production in *S. sp.* PCC11901 is not only dependent on the light intensity but also on the availability of carbon (Figure 22 and Figure 23). Carbon assimilation is a major aspect of the photoautotrophic metabolism of cyanobacteria. Under *Ci*-limitation, photorespiration is increased, causing the accumulation of toxic metabolites, and a vital energy and electron sink is incapacitated, leading to the build-up of ROS and ultimately cell death.^{28,29,215,280} The availability of an inorganic carbon source must therefore be closely watched when exploiting cyanobacteria for biotechnological applications.

3.2.1 The highly efficient aromatic dioxygenase *mapADO*

The newly described *mapADO*, an aromatic dioxygenase from *Moesziomyces aphidis*, showed high yields, as well as exceptional conversion rates when expressed in *E. coli* BL21 and proved its applicability in the two-step cascade with PAD to convert ferulic acid to vanillin. The rotation speed during the reaction affected overall yield and product inhibition was observed, but oxygen-limitation could not be proven unequivocally. Product inhibition is an effective mechanism for regulation and thus common,²⁸¹ but the strong, bacteriostatic effect of vanillin might play a role here as well. The minimal inhibitory concentration of vanillin in *E. coli* is 15 mM and is mainly caused by membrane instability,²⁸² therefore, it is impractical to quantify, which of these two mechanisms interfere the most. At high substrate loading and high cell densities, oxygen concentration approaches 0 at the onset of the reaction, thus likely interfering with the conversion rate (see Figure 37). The newly described *mapADO* was also able to convert ferulic acid into vanillin in tandem with PAD, up to a substrate loading of 30 mM. Higher concentrations resulted in the accumulation of 4-vinyl guaiacol.

3.2.2 Unprecedented yields for whole-cell catalysis in cyanobacteria with a phenolic acid decarboxylase in *S. sp.* PCC11901

S. sp. PCC11901 did not only grow well in our lab, but it was also possible to integrate an enzyme into its genome and perform whole-cell catalysis. The phenolic acid decarboxylase from *Bacillus coagulans* DSM11 was expressed under the control of an IPTG-inducible promoter. Without the addition of the inducer compound, conversion was weaker but still measurable. The ‘leakiness’ of IPTG-inducible promoter systems in cyanobacteria is well-known,⁴⁶ but because the expression did not affect growth, it was deemed irrelevant here. The substrate scope of PAD did not differ when expressed in *S. sp.* PCC11901 as compared to *E. coli* and consisted of cinnamic acid derivatives with a hydroxy-group in *para*-position (Table 6).

We encountered strong product inhibition during the conversion of ferulic acid into 4-vinyl guaiacol, the first step of the planned two-step enzymatic cascade to produce vanillin. 4-vinyl guaiacol inhibited conversion and photosynthetic oxygen production in *S. sp.* PCC11901 *fadA::pad*. We further identified two organic solvents, which appeared to be non-toxic for this cyanobacterium, and utilized them for *in situ* product removal, alleviating product inhibition. PAD remained active in *S. sp.* PCC11901 *fadA::pad* for at least 30 hours when the cell suspension was emulsified in the organic solvents, DINP, or IPM. It converted 80 mM ferulic acid into 4-vinyl guaiacol within 8 h on a gram scale (~12 g/L).

In short, we were able to show the applicability of *S. sp.* PCC11901 as a platform for whole-cell catalysis, showed the up-scaling capabilities to gram-scale with inexpensive equipment, and achieved unprecedented yields compared to any other known whole-cell catalysis performed by cyanobacteria. Finally, we also introduced an environmentally benign alternative solvent for *in situ* product removal in cyanobacteria.

Despite these successes, the reaction still underscores the shortcomings of cyanobacteria in biotechnology: compared to established, heterotrophic hosts, higher titers with phenolic acid decarboxylases can be achieved. PADs from *Bacillus licheniformis* and *Bacillus atrophaeus*, reached 129.9 g/L and 295.8 g/L of 4-vinyl guaiacol, respectively as whole-cell catalysis or purified and immobilized enzymes.^{283,284} Presumably, with further optimization, higher yields are possible with *S. sp.* PCC11901 *fadA::pad*, such as immobilization in alginate beads²⁸⁵ or optimizing the ratio of aqueous and organic phases.

The comparison with other gram-scale production utilizing cyanobacteria in a whole-cell catalysis approach also seems arbitrary, as the two known examples use NADPH-dependent enzymes, an alkane monooxygenase,²⁰⁹ and a cascade of a BVMO and a lactonase²⁰⁸, which are more challenging to work with than a decarboxylase. Nevertheless, this work shows another promising example of *S. sp.* PCC11901 for cyanobacteria-based biotechnology.

3.2.3 The hardships of genomic integration in cyanobacteria

Despite numerous attempts, the genomic integration of an aromatic dioxygenase into *S. sp.* PCC11901 was not achieved. The reason for the failure is currently unknown. Two different enzymes have been tried (ADO and *mapADO*), and one coding sequence was codon-optimized for *Synechococcus*. If *S. sp.* PCC11901 contains restriction enzymes or DNA repair-mechanisms, that target these two sequences, it seems unlikely that both genes share the same sequence leading to this. The advanced genetic repair mechanisms in cyanobacteria are a prerequisite for photoautotrophic growth, due to the strong mutagenic effect of light, but they also cause instability in genetically engineered cyanobacteria.⁷⁶ The enzyme itself might be a problem if it is not the DNA sequence. The full substrate scope of ADO and *mapADO* have not been discussed here, but an oxidative cleavage of a C=C double bond might target a vital metabolite or produce a toxic substance from a metabolite. Examples could be carotenoids, C=C double bonds containing, vital components in cyanobacteria.²⁸⁶ Additionally, if an aromatic dioxygenase burdens the cyanobacterium, it increases the selection pressure to remove the sequence from its genome. A loss of natural competence in the strain used here can also not be excluded, as cyanobacteria tend to undergo involuntary ‘microevolution’ when cultivated continuously,⁹⁸ and even in the very recently described *S. sp.* PCC11901, differences in the phenotype have been described between a strain cultivated in a laboratory and a strain obtained from the Pasteur Culture Collection of Cyanobacteria, Paris, France.¹⁵⁵

3.2.4 A mixed-species approach to increased enzymatic vanillin production

The expression of PAD and *mapADO* in *E. coli* allowed the conversion of 30 mM ferulic acid to vanillin, but at higher substrate concentrations, an accumulation of the intermediate, 4-vinyl guaiacol, was observed. The two-species concept circumvented 4-vinyl guaiacol accumulation at a substrate loading of 40 mM ferulic acid. The expression of PAD in *S. sp.* PCC11901 and of *mapADO* in *E. coli* BL21 did not improve conversion. Here, the susceptibility of *S. sp.* PCC11901 to 4-vinyl guaiacol came into play again. PAD showed high conversion rates, thus the accumulation of the intermediate compound, and hindered export out of the cell by the cell wall and membranes, might prevented further conversion to the less toxic vanillin. Substrate inhibition of *mapADO* could explain the increased yield in a fed-batch approach, which increased vanillin yield comparable to the mixed-species approach. It has been shown before, that at high substrate loading, oxygen limitation might reduce the reaction rate in *mapADO*, thus the fed-batch artificially slowing down the reaction time prevented an accumulation of 4-vinyl guaiacol, which induces substrate inhibition. Similarly in the mixed species approach, where the photosynthetic oxygen production prevented oxygen limitation. Further experiments are advised to elucidate the underlying mechanism.

Artificial communities of heterotrophs and cyanobacteria can lead to highly robust cultures and the design of those has been termed a ‘new era of synthetic biology’.^{287,288} There are several proof-of-concept studies, that highlight the advantage of sharing the burden with several species to increase productivity, such as combining *S. sp.* UTEX2973 with the super-fast-growing *Vibrio natriengens*,²⁸⁹ but also to funnel light energy to fuel biotransformation. A cyanobacterial collaboration with heterotrophic bacteria showed synergistic effects for whole-cell catalysis, such as the prevention of oxygen accumulation in a capillary reactor and simultaneously fueling a BVMO-catalyzed reaction by *Pseudomonas sp.*²¹⁴ Alternatively, cyanobacteria can be spatially separated from the reaction in alginate beads and excrete sucrose to drive biotransformation by *E. coli* or *Pseudomonas sp.*^{290,291} All three examples highlight the advantage of cyanobacteria in co-cultivation and mixed-species approaches, and they are now extended by this work.

4 CONCLUSION AND OUTLOOK

Identifying and characterizing cyanobacterial strains exhibiting rapid growth kinetics and enhanced photosynthetic efficiency provide a crucial foundation for developing carbon-neutral or potentially carbon-negative biotechnological processes. These strains could significantly improve the feasibility and scalability of cyanobacteria-based bioproduction systems, potentially revolutionizing industrial biotechnology's environmental impact.¹⁴¹

Implementing novel cyanobacterial strains necessitates re-optimizing established protocols, which, while effective for model organisms, require validation in the context of these new genetic backgrounds. The persistent challenge of reproducibility in cyanobacterial research, an issue that remains unresolved,¹⁰¹ is further exacerbated when extrapolating existing methodologies and knowledge to newly isolated strains. Whole-cell catalysis in cyanobacteria is auspicious, but the implementation in the group of ‘fast-growing’ cyanobacteria remains unexplored territory. The results from this work might be an indicator of why that is.

The fastest-growing strain, *Synechococcus* sp. UTEX2973 evaded our efforts to express a carboxylic acid reductase, caused by adversity of molecular cloning. Furthermore, the genomic integration of an aromatic dioxygenase into the cyanobacterium with the highest cell density, *Synechococcus* sp. PCC11901 also remained futile. Standardly used cyanobacteria, such as *Synechocystis* sp. PCC6803 or *Synechococcus* sp. PCC7942 can be engineered to express up to 6 recombinant proteins,^{54,292,293} while fast-growing strains are commonly limited to one or two enzymes. The aversion and lack of incentive to publish negative results might hinder the proceeding in elucidating the obstacles for genetic engineering in non-model organisms.^{76,294}

High predictability and established protocols are fundamentals for success in genetic engineering and synthetic biology. Currently, the toolboxes and methods available for cyanobacteria are not sufficient in this prospect and not only for fast-growing strains. This has been highlighted by a comparative study of several laboratories with the same cyanobacterial strains and under identical conditions.¹⁰¹

Improvements in genetic engineering in cyanobacteria are published constantly, such as new vector systems, easily manageable compared to RSF1010-based vectors, such as pMJc01,²⁹⁵ or pSOMA.²⁹⁶ Additionally, a standardized system can help facilitate cloning techniques via a modular system, such as the tried CyanoGate system⁸⁴ or the continuously improving SEVA platform.²⁹⁷

While *S. sp.* UTEX2973 remains cited as the cyanobacterium with the highest reported growth rate, its optimal performance is contingent upon specific environmental conditions, namely high light intensity and elevated CO₂ concentrations, necessitating specialized cultivation equipment. Moreover, the rapid doubling times observed in *S. sp.* UTEX2973 are confined to a brief exponential growth phase.^{118,141}

Alternative strains have demonstrated comparable growth kinetics under more amenable conditions. For instance, *Synechococcus* sp. PCC 11802 exhibits rapid growth

rates at ambient CO₂ levels, with sustained high growth rates over extended periods.¹³¹ Other strains, such as *Synechococcus* sp. PCC 7002, while displaying lower growth rates, achieves higher final cell densities, potentially rendering it more suitable for biotechnological applications.^{99,118}

Of particular interest is *Synechococcus* sp. PCC 11901, which combines rapid growth kinetics with high biomass accumulation, one of the highest described today.¹¹⁸ This dual characteristic renders *Synechococcus* sp. PCC 11901 a promising candidate for biotechnological applications, potentially offering advantages in terms of productivity and process economics.

Despite the above-mentioned failure, there is success: a whole-cell catalysis in the fast-growing strain *S. sp.* PCC11901 was achieved and outperformed, to the best of our knowledge, any other whole-cell catalysis described in cyanobacteria in terms of yield. After the identification of the main inhibitor, the decarboxylation of ferulic acid into 4-vinyl guaiacol could be up-scaled to gram-scale with inexpensive and easy-to-use equipment. The key was to prevent the toxic effect of 4-vinyl guaiacol by *in situ* product removal with organic solvents. Diisononyl phthalate and the environmentally benign isopropyl myristate accumulated 4-vinyl guaiacol and prevented toxic effects in the cell suspension. The cultivation in the CellDEG system required 96h of growth for enough biomass of *S. sp.* PCC11901, but in a more controlled environment, such as in a CO₂-incubator, the time from inoculation to reaction-ready cells took 48h. In our protocols, this is a similar time frame for *E. coli* to produce biomass and expression of recombinant enzymes. Other cyanobacteria, such as *Synechocystis* sp. PCC6803, require up to 10 days to accumulate enough biomass and protein to be used and sometimes even requires centrifugation and resuspension to smaller volumes, to achieve a high enough cell density.^{92,209}

This work is the first step in the direction of fast-growing cyanobacteria for whole-cell catalysis and highlights the impediment when working with non-model organisms, especially in genetic engineering. Yet, future undertakings will require improvements in certain research areas.

Strong and inducible promoters with limited leakage are also restricted to a few examples in *S. sp.* PCC11901 and their reliability and predictability have not been examined yet. A recent publication from our laboratory showed, that the genetic context as well as genetic regulatory elements, such as promoters or ribosome binding sites, are interconnected and more data is required to make reliable predictions on expression strength.⁹² Websites and databases such as bio-protocol.org, jove.com, or proctols.io, which store peer-reviewed research methods in a citable and easy-to-follow manner, are a great advancement compared to the ‘method and materials’ part of typical journals with references, which often do not lead to the original publication.^{298,299}

A recently published genome-scale model for *S. sp.* PCC11901 can help to progress in understanding the properties of this strain and explain the ability to accumulate more biomass than other cyanobacteria,³⁰⁰ a field of cyanobacterial research that has not received enough attention. High growth rates in a cyanobacterial strain do not ensure

high productivity and other characteristics are required for a profound understanding and the decision, of whether a certain strain is ideal for a reaction or product. Other important factors include the rate of light absorption or maximal biomass per mol photons.¹⁴¹ The identification of their potential and limitations applies to established cyanobacterial strains and is currently ongoing,^{134,301,302} but the constant discovery of new, promising strains can also benefit from this development, such as the high-biomass accumulating, fast-growing *Synechococcus* sp. UTEX3222.¹⁵⁸ This also necessitates a stringent declaration of the methods used, for example, the light quality, light source, and light spectrum.

Contamination from fungi, yeasts, or heterotrophic prokaryotes presents a common challenge for cultivating cyanobacteria and microalgae.^{108,303} Interestingly, this susceptibility to contamination may be related to the evolutionary adaptation of cyanobacteria to thrive in communities. Artificial consortia improve the productivity, robustness, and efficiency of cyanobacteria.²⁸⁷ The synergistic effect of cyanobacteria in collaboration with heterotrophic bacteria, could also be shown here. In a mixed-species approach, *E. coli* BL21 harbored PAD and *mapADO*, both enzymes required for the cascade to convert ferulic acid into vanillin, while *S. sp.* PCC11901 supplied oxygen and removed CO₂ via photosynthesis. Together, this co-biotransformation was able to convert 40 mM ferulic acid into vanillin, which is not achieved by *E. coli* in solitary. In nature, no organism thrives in isolation and each species is part of a larger ecosystem, consequentially, all species have adapted to be in a relationship with their surroundings, either in symbiotic, parasitic, competitive, or any other form. The idea of artificial consortia of organisms to share the metabolic burden and improve production has gained track in the field of biotechnology and synthetic biology and has been termed a 'new era'.^{288,304} Especially consortia with phototrophic organisms were already successfully conceptualized and established to produce ethanol,³⁰⁵ lactic acid,²⁸⁹ or 3-hydroxypropionic acid.³⁰⁶ An excess of light can cause an overflow in the photosynthetic metabolism mitigated by energy sinks, such as glycogen accumulation,³⁰⁷ or in a recombinant strain, by excreting sucrose.³⁰⁸ Metabolic models show the optimized flux in consortia and can also predict ideal partners.³⁰⁹ Artificial consortia or mixed-species approaches might also play a crucial role in sustainable biotransformations, as evidenced by several studies.^{214,290,291} Communities with fast-growing cyanobacterial strains have also been reported with promising results, by combining a sucrose-exporting *S. sp.* UTEX2973 with *Vibrio natriengens*.²⁸⁹ Consortia with *S. sp.* PCC11901 have not been reported yet, but hold great potential.

5 METHODS AND MATERIALS

5.1 CULTIVATION AND STRAIN HANDLING

5.1.1 Cyanobacteria

5.1.1.1 *Synechococcus* sp. UTEX2973

Synechococcus sp. UTEX2973 was cultivated in a shaking cultivator at 39°C, 150 rpm under ambient air in baffled flasks, filled to a maximal 1/5 of the maximal volume at 500 $\mu\text{mol photons/s/m}^2$ in YBG-11 medium (Table 8). Culture density was measured as absorbance at 750nm (OD_{750}) in a NanoDrop One (Thermo Fisher Scientific Inc., Waltham, USA). The strain was acquired as a gift from the Spadiut lab (TU Wien, Austria).

5.1.1.2 Tri-parental mating

S. sp. UTEX2973 cells were grown as described above to an $\text{OD}_{750} \sim 0.5$ -1. Simultaneously, *E. coli* strains, carrying the plasmids pRK24, pRK528, and the plasmid to be conjugated were incubated in LB medium at 37°C, 180 rpm overnight with their respective antibiotic. The cultures were then centrifuged (4000 x g, 5 min) and resuspended in fresh medium, without antibiotics 3 times, to remove residual antibiotics and finally resuspended in half the original volume. The same was done with the cyanobacteria in YBG-11 medium. The cell suspensions were combined and pipetted up and down for mixing (not vortexed) and rested for 2h at room temperature. After the 2 h, the mixtures were centrifuged again and resuspended in $\sim 250 \mu\text{L}$ of the supernatant. The suspension was then transferred onto a nitrocellulose filter (Whatman) on an agar plate with YBG-11 medium and 5% LB-medium. The plates were incubated at 39°C, 150 $\mu\text{mol photons /s/m}^2$. After 24h the membranes were transferred onto YBG-11 plates with the respective antibiotics.⁴⁸

5.1.1.3 eYFP Expression by inducible promoters

S. sp. UTEX2973 were incubated as described above to an OD_{750} of ~ 1 and then induced with the corresponding inducer molecule (Rhamnose, anhydrate tetracycline, or vanillic acid). Fluorescence and optical density (OD_{750}) measurements were conducted at 0 (pre-induction), 24, and 48 hours post-induction unless otherwise specified. Analyses were performed using 96-well microtiter plates in conjunction with a plate reader (Tecan Spark, Tecan, Switzerland).

Enhanced yellow fluorescent protein (eYFP) fluorescence was measured at excitation and emission wavelengths of 485 nm and 535 nm, respectively. To ensure measurements remained within the linear range of the plate reader, cell suspensions were diluted to an OD_{750} of 0.6-0.8. Fluorescence values were normalized to cell density (OD_{750}). Each sample was analyzed in 3 to 5 replicates.

5.1.1.4 *Synechococcus* sp. PCC11901

Synechococcus sp. PCC11901 was acquired via the Pasteur Culture Collection of Cyanobacteria (Institut Pasteur, Paris, France). The strain was commonly cultivated at 39°C, 150 rpm, 1% CO₂, and 500 μmol photons/m²/s (light source: Samsung quantum boards LM301B full spec, 3500K) in a high cell density medium MAD2 (Table 8). Cryocultures were prepared by centrifuging a culture in the linear growth phase and resuspending in AD7 medium supplemented with 1% DMSO and stored at -80°C. Culture density was measured as absorbance at 750nm (OD₇₅₀) in a NanoDrop One (Thermo Fisher Scientific Inc., Waltham, USA) with a factor of 0,24 g_{DCW}/L/OD. Cell dry weight was determined by measuring OD₇₅₀ of a 25 mL culture, centrifuging the whole culture, resuspending in deionized water three times, and transferring the remaining culture into a 30 mL glass vial and letting it dry at 75°C for 48h.

5.1.1.5 Natural transformation of *S. sp.* PCC11901

The plasmids used in this work were constructed using the NEBuilder HiFi DNA Assembly system (New England Biolabs, Ipswich, USA). In short, gene sequences for the genes of interest were codon optimized for *Synechococcus* (Gensmart codon optimizer, Version 28.01.21), inserted into pSZT025 (containing the *fadA* flanking region) or pSW039 (containing the *psbA2* flanking region), purchased via Addgene (Watertown, USA). The strain *Synechococcus* sp. PCC11901 *fadA::pad* was constructed via natural transformation. A culture of 25 mL in a 200 mL baffled flask was incubated with AD7 medium (Table 8) at 30°C, 150 rpm, ambient air, 100 μmol photons/s/m² to OD₇₅₀ ~1. Subsequently, 1 mL of culture was transferred into a 50 mL centrifugation tube, mixed with 1 μg DNA (containing the gene of interest and the flanking region, amplified via PCR), and incubated for 24 h at 100 μmol photons/s/m² at 39°C. Cells were then transferred to an agar plate containing AD7 agar and further incubated at 250 μmol photons/s/m² at 1% CO₂. Successful integration and complete segregation were verified via colony PCR.

5.1.1.6 Colony-PCR

Colony PCR was used to verify positive transformants. First, the respective strain was cultured on AD7 agar to obtain sufficient biomass. For cPCR analysis, cellular material was harvested from the plate and resuspended in 50 μL of nuclease-free water to achieve a visibly green suspension. The cell suspension underwent thermal lysis at 95°C for 10 minutes, followed by a 5-minute incubation on ice. Subsequently, the samples were centrifuged at maximum speed for 5 minutes. 1 μL of the resulting supernatant served as template DNA for the PCR reaction. The PCR used OneTaq® Quick-Load® DNA Polymerase (New England Biolabs, Ipswich, MA). Reaction conditions were optimized according to the manufacturer's recommended protocol.

5.1.1.7 Cultivation in CellDEG

The CellDEG system cultivations were performed in the HD10 or HD100 container with 10 and 100 mL medium, respectively. *S. sp.* UTEX2973 was cultivated in CD-medium, *S. sp.* PCC11901 in MAD2-medium (Table 8) and inoculated from a cryo-culture (in YBG-11 or AD7 with 5% DMSO) and a carbonate buffer, resulting in a partial pressure of CO₂ of 92 mbar according to the manual. Incubation was done at 500 μmol photons/s/m², if not

stated otherwise. 100mL cultivations were shaken at 100 rpm, and 10 mL cultivations at 180 rpm. The procedure was adapted from *S. sp.* PCC6803 and protocols.io.³¹⁰

5.1.1.8 Protein expression in *S. sp.* PCC11901

If not cultivated in the CellDEG system, *S. sp.* PCC11901 was incubated in 50 mL MAD2 medium in 250 mL baffled Erlenmeyer flasks. After inoculation with either 500µL from a cryo-culture or a liquid culture, the flasks were shaken at 150 rpm at 39°C, 1%CO₂, and illuminated at 500 µmol photons/s/m². After 24h, 1 mM of IPTG was added and then incubated for another 24h under the same conditions. After this, cells were harvested by centrifugation at 4000 x g, for 10 min and resuspended in YBG-11 medium with 100 mM HEPES buffer. This was repeated 3 times to remove access salt.

5.1.1.9 Light source

The light sources used for cultivating the fast-growing cyanobacterial strains were based on the Samsung quantum boards LM301B, full spec, 3500K. The light spectrum can be found in Figure 53.

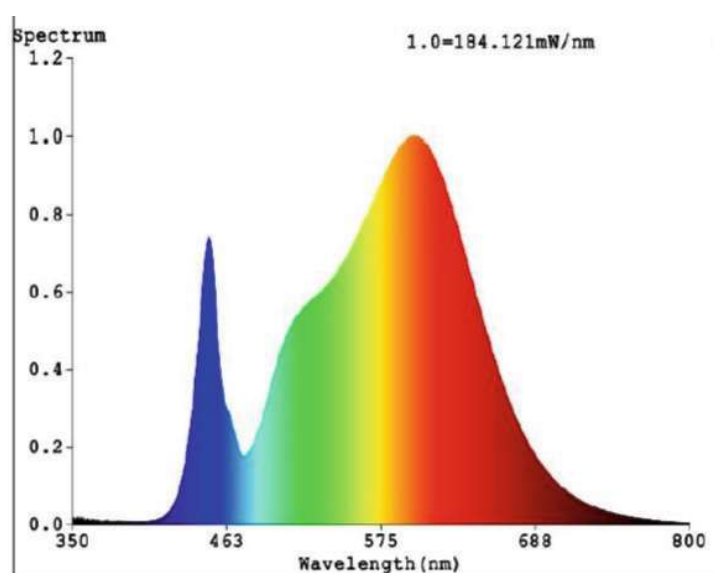


Figure 53 Light spectrum of Samsung quantum board LM301B, 3500K.

5.1.2 *E. coli*

5.1.2.1 Preparation of chemo-competent cells

Chemically competent *E. coli* cells were prepared using the following protocol, with all procedures conducted on ice under aseptic conditions. A single colony of the desired *E. coli* strain was used to inoculate 5 mL of LB medium. The culture was incubated overnight at 37°C with agitation at 200 rpm. Subsequently, 100 mL of LB medium was inoculated with 1% (v/v) of the overnight culture and incubated at 37°C, 180 rpm until reaching an OD₅₉₀ of 0.5.

The culture was then harvested by centrifugation in sterile, pre-chilled 50 mL conical tubes at 4000 rpm for 5 minutes at 4°C (Sigma Laboratory Centrifuge 6K15 or 3K30). Following supernatant removal, the cell pellet was gently resuspended in 20 mL of sterile,

ice-cold RF1 buffer (1/5 volume of the main culture. After a 15-minute incubation, cells were re-centrifuged and resuspended in 4 mL of RF2 buffer (1/5 volume of the RF1 suspension). The resulting cell suspension was aliquoted into 100 μ L volumes in pre-chilled microcentrifuge tubes. Finally, the aliquots were flash-frozen in liquid nitrogen and stored at -80°C for future use. The compositions of the buffers can be found in Table 7.

Table 7 Composition of RF1 and RF2 buffer for chemo-competent *E. coli* cells. The pH was adjusted with 0.2M acetic acid or 1 M NaOH. The solutions were filter-sterilized.

RF1 Buffer (100 ml, pH 5.8)	RF2 Buffer (100 ml, pH 6.8)
1.21 g RbCl	0.12 g RbCl
0.99 g $\text{MnCl}_2 \cdot 2 \text{H}_2\text{O}$	0.21 g MOPS
0.294 g KOAc	0.11 g CaCl_2
0.148 g $\text{CaCl}_2 \cdot 2 \text{H}_2\text{O}$	15 g glycerol
15 g glycerol	

5.1.2.2 Transformation of chemo-competent *E. coli* cells

Transformation of chemically competent *E. coli* cells was performed using a heat shock protocol. For standard plasmid transformations, 1 μ L of plasmid DNA (50-100 ng/ μ L) was used. The amount was increased to 5 μ L for difficult transformations.

The procedure was as follows: Competent cells were thawed on ice, and the appropriate volume of DNA was added. The cell-DNA mixture was incubated on ice for 15 minutes. Heat shock was then applied at 42°C for 1 min, followed by a 5-minute incubation on ice. Subsequently, cells were allowed to recover in 950 μ L of pre-warmed SOC medium for 45 minutes at 37°C with agitation at 600 rpm. Post-recovery, the transformed cells were plated on selective LB agar with the respective antibiotic and incubated overnight at 37°C .

5.1.2.3 Protein expression in *E. coli* BL21

E. coli BL21 cells carrying the plasmid of interest were inoculated from a cryo-stock in a 5 mL culture with TB medium + corresponding antibiotic overnight. The fully grown culture was used as inoculum for the main culture, also consisting of TB medium, but without antibiotics. Cells were incubated at 37°C , 180rpm until the cells reached an OD_{590} 0.5-1 (around 1.5h). Then protein expression was induced with 1 mM IPTG. Additionally, 1 mM of Fe(II)Cl_2 was added to the cell suspension in case of (*map*)ADO expression. Incubation continued at 20°C and 200rpm for at least 16h. After this, cells were harvested by centrifugation (4000 x g, 5 min) and resuspended in PBS pH 7.4. If not used directly, cells were stored at -20°C .

5.2 WHOLE-CELL CATALYSIS

5.2.1 Phenolic acid decarboxylase in *S. sp. PCC11901fadA::pad*

Protein expression was performed as described above. The cells were then transferred to closed glass vials, with at least 4 times the volume of headspace than cell suspension. The reaction was started by adding the substrate, dissolved in DMSO. The vials were shaken at 180 rpm at 39°C and 500 $\mu\text{mol photons/s/m}^2$, if not stated otherwise. Samples were diluted 1:7 or 1:40 in acetonitrile and syringe-filtered and analyzed via high-performance liquid chromatography (HPLC).

The two-phased reaction was performed under the same conditions, except for the shaking. The same amount of organic solvent, DINP or IPM, was added to the cell suspension and mixed by a magnetic stirrer at 300rpm. The product formation was monitored by gas chromatography (GC). The samples were diluted 1:20 in ethyl acetate, dried with Na_2SO_4 , and filtered.

5.2.1.1 Gram-scale production of 4-vinyl guaiacol by *S. sp. PCC11901fadA::pad*

The primary culture for whole-cell catalysis at the gram-scale was cultivated in a 100 mL HD-cultivator (CellDEG, Berlin, Germany) containing 100 mL MAD2 medium. The medium was inoculated with 500 μL of a cryopreserved culture (in AD7 medium supplemented with 5% DMSO) and a carbonate buffer, establishing a CO_2 partial pressure of 92 mbar as per the manufacturer's guidelines. Incubation conditions were maintained at 500 $\mu\text{mol photons/m}^2/\text{s}$, 100 rpm, and 37°C. Protein expression was induced with 1 mM IPTG after 72 hours of growth. At 96 hours post-inoculation, cells were harvested via centrifugation at $4000 \times g$ for 10 minutes and washed twice by resuspension in 100 mL YBG-11 medium supplemented with 100 mM HEPES pH 7.4.

The biotransformation was conducted in a 500 mL glass vessel (SCHOTT, Mainz, Germany) containing 100 mL of cell culture and 100 mL of either diisononyl phthalate (DINP) or isopropyl myristate (IMP). Agitation was achieved using a magnetic stirrer. The substrate, ferulic acid, was added in two equal portions of 0.78 g, separated by a 4-hour interval, with 0.5 mL DMSO used to ensure complete transfer.

The product, 4-vinyl guaiacol, was extracted into the organic phase. The reaction mixture was combined with 100 mL ethyl acetate, vigorously agitated, and the organic phase was separated. The ethyl acetate was then removed via rotary evaporation. The remaining DINP was mixed with 100 mL of 2 N NaOH, agitated, and the aqueous phase was separated. This aqueous phase was neutralized with 2 N HCl and extracted twice with 100 mL ethyl acetate. The ethyl acetate fraction was evaporated under a vacuum to isolate the product. Analysis of the product was done by gas chromatography and NMR. Yield was 97% and 1% with DINP and IPM, respectively.

NMR code: ^1H NMR (400 MHz, DMSO) δ 9.07 (s, 1H), 7.04 (d, $J = 2.0$ Hz, 1H), 6.85 (dd, $J = 8.2, 2.0$ Hz, 1H), 6.73 (d, $J = 8.1$ Hz, 1H), 6.60 (dd, $J = 17.6, 10.9$ Hz, 1H), 5.62 (dd, $J = 17.6, 1.1$ Hz, 1H), 5.06 (dd, $J = 10.9, 1.1$ Hz, 1H), 3.79 (s, 3H).

Impurities with IPM required additional purification via column chromatography. 100 mg crude material was evaporated onto celite. A glass column was packed with 10g SiO₂, the eluent was a mixture of light petroleum and ethyl acetate in a ratio of 20:1.

5.2.2 Aromatic dioxygenase in *E. coli* BL21

The aromatic dioxygenases were expressed in *E. coli* BL21 as described above. Cells were resuspended in PBS, pH 7.4, and transferred to a glass vial with at least 8 times the headspace compared to the buffer volume. If not stated otherwise, the reaction occurred at 30°C, 200 rpm. The reaction was monitored via HPLC, and samples were diluted 1:7 or 1:40 in acetonitrile and filtered.

5.2.3 PAD and *mapADO* in mixed species reaction

The two-step cascade was conducted by expressing PAD and *mapADO* in *E. coli* BL21 or expressing *mapADO* in *E. coli* BL21 and PAD in *S. sp.* PCC11901 *fadA::pad*, as described above. The cells were centrifuged and resuspended in half the amount of buffer or medium and then mixed. *S. sp.* PCC11901 WT was grown under the same conditions as *S. sp.* PCC11901 *fadA::pad* for 48 hours, centrifuged (4000 x g, 10 min), and resuspended in YBG-11 medium. 1 mL of the mixtures were then transferred into 8 mL glass vials, with screwcaps. The closed vials were incubated at 30°C, 500 $\mu\text{mol photons/s/m}^2$, and 200 rpm, if not stated otherwise. The reaction was started by adding the substrate and monitored via HPLC.

5.3 ANALYTICS

5.3.1 HPLC

Samples for HPLC were either measured on Nexera, (Shimadzu, Tokyo, Japan), equipped with a C18 column (Xselect CSH C18 2.5 μm), and eluted with a gradient starting at 95% Water + 0.1% formic acid and 5% acetonitrile and increasing to 98% acetonitrile in 2.521 minutes. The flow rate was set at 1.3 mL/min.

Alternatively, samples were also measured on the JASCO HPLC 2000Plus system (JASCO Deutschland GmbH, Pfungstadt, Germany), composed of a PU-2089 quaternary gradient pump, AS-2057 autosampler, CO-2060 column oven, and LC-NetII/ADC support module. The MD-2018 photodiode array detector was used for detection. The column used was the Agilent ZORBAX Eclipse XDB-C18 5 μm (4.6 x 150 mm) column at 25 °C, and a flow rate of 2 mL/min with a solvent gradient from 95% water with 0.1 % formic acid and 5% Acetonitrile to a 1:1 ration within 12 min. The flow rate was set to 2 mL/min.

5.3.2 Gas-Chromatography

The samples for Gas chromatography were measured on a Trace 1300 by Thermo Fisher Scientific (Waltham, USA) The column was a Rxi-5Sil MS, 15m, 0.25 mm ID, 1.0 μm df, 5% diphenyl(95% dimethyl polysiloxane; The temperature program started at 80°C and increased to 310°C with 40°C/min increase and hold time of 5min. The internal standard was 1 mM methyl benzoate.

5.3.3 NMR spectroscopy

The purity and degree of polymerization of 4-vinyl guaiacol were determined by nuclear magnetic resonance spectroscopy (NMR). ^1H -NMR spectra were recorded at ambient temperature in the solvent indicated using a Bruker Avance Neo 400 MHz spectrometer. Processing of the data was performed with standard software and all spectra were calibrated to the solvent residual peak. Chemical shifts (δ) are reported in ppm, coupling constants (J) in hertz (Hz) and multiplicities are assigned as s = singlet, d = doublet, and dd = doublet of doublets.

5.3.4 Absorbance, optical density, and fluorescence

The optical density of cyanobacterial cell suspension was measured at 750nm in a 1 mL cuvette in a NanoDrop One (Thermo Fisher Scientific Inc., Waltham, USA). The suspension was diluted to a value of < 0.5 , if necessary.

Absorbance and fluorescence were measured in a Tecan Spark (Tecan, Switzerland) with 200 μL in a black 96-well plate with a clear bottom (Greiner Bio-One, Austria). For fluorescence measurement, the z-position of the optics was set automatically, and the gain was set to 50.

5.3.5 SDS-PAGE for protein analysis

The analysis of recombinant protein expression was done with SDS-PAGE, adapted from Laemmli, 1970.³¹¹ The samples were denatured by mixing 20 μL of the protein samples with 20 μL ready-to-use SDS-PAGE sample buffer (65 mM Tris, 4% (w/v) glycerol, 2% (w/v) SDS, 0.01% (w/v) bromophenol blue, 5% (v/v) β -mercapto ethanol) and incubating the samples at 95°C for 10 minutes. The denatured samples were loaded onto the polyacrylamide gels. (15 μg for 0.75 mm thick gels; 30 μg for 1.5 mm thick gels). Gels were purchased from Bio-Rad (Bio-Rad Laboratories, Hercules, California, USA). The gels were submersed in 1 x SDS-PAGE running buffer at 200V for approximately 25 min. The PageRuler™ Prestained Protein Ladder 26616 (Thermo Scientific) functioned as a size marker. The staining was done by opening the gel casket, removing the stacking gel, and submerging the resolving gel in dH_2O . The gels were heated in a microwave at 750 W for 1 min. The gel was slightly shaken at room temperature for 2 min, and the water was exchanged for fresh ones. Afterward, gels were incubated at 500 W for 1 min, and shaken at room temperature for 2 min, again. After the removal of the water, the staining solution was added (SimplyBlue™ Safe Stain; LC6065, Novex) and heated again at 350 W for 45 s. After shaking at 5 min at room temperature, the dying solution was discarded. Then, the gel was submersed again in dH_2O until the excessive dye was removed from the gel. Documentation was done by photographing.

5.3.6 Dissolved oxygen

The concentration of dissolved oxygen in a cell suspension or buffer was measured with the Firesting-O2 (PyroScience GmbH, Aachen, Germany). The probes were OXROB10,

measuring near-infrared measurement. The measurements were done in 30 mL flat bottom flasks with 10 mL of medium and a rotation speed of 55 rpm. The probes were stuck through the screwcaps and fixated with tape. The probes were calibrated as described in the manual, in brief, 10 mL of the medium used was added into a 30 mL glass vial and shaken vigorously for 1 min, then the cap was opened to allow gas exchange, closed, and shaken again. The aerated medium or buffer was then used as the calibration source. The values were corrected for temperature, which was measured with a Pt100 temperature probe. The data was extracted in a CSV file and analyzed with Python 3.0 in the Spyder IDE.

5.3.6.1 Toxicity assay for cyanobacteria based on oxygen measurements

The toxicity assays were performed in 30 mL flat bottom flasks with 10 mL of cell culture at 55 rpm and 37°C and oxygen was measured as described above. The light intensity was increased until no further increase in dO_2 was detected. When the oxygen concentration reached a stable level at around 220 to 240 $\mu\text{mol/L}$, 10 mM of a carbonate solution was added (KHCO_3 or NaHCO_3). Upon a strong increase in oxygen concentration, cells were considered fit. After the dO_2 concentration decreased to normal levels again, 10 mL of the tested compound was added, shaken for a few minutes, and 10 mM of a carbonate solution was added again. The duration and intensity of the increased oxygen concentration, if observed, were then compared to the first administration of carbonate. When no oxygen increase was observed, the compound was considered toxic.

5.3.6.2 Chlorophyll a and carotenoids

The concentration of Chlorophyll a and carotenoids was extracted with methanol. 100 μL cells were centrifuged for 7 min at 12000 x g, resuspended in 1 mL cold methanol incubated at 4°C in the dark for 20 min, and again centrifuged. The supernatant was measured for absorbance at 470, 655, and 720 nm in a microwell-plate-reader (Tecan Spark, Tecan, Switzerland). Pure Methanol was used as blank, and concentration was calculated as follows:

$$\text{Chlorophyll a (Chl}_a\text{)} [\mu\text{g/mL}] = 12.9447(A_{665} - A_{720})$$

$$\text{Carotenoids } [\mu\text{g/mL}] = [1,000 (A_{470} - A_{720}) - 2.86 (\text{Chl}_a [\mu\text{g/mL}])] / 221$$

The protocol was adapted from Zavřel et al., 2015.³¹²

5.3.7 Nano Differential Scanning fluorimetry for the determination of the melting point of mapADO

The enzyme was isolated from cryopreserved cells via immobilized metal affinity chromatography and subsequently resuspended in phosphate-buffered saline (PBS). A protein suspension at a concentration of 1 mg/mL was introduced into a capillary for fluorescence analysis using a NanoTemper Prometheus instrument (NanoTemper Technologies, Munich, Germany). Data visualization and analysis were conducted using the MoltenProt software package (<https://spc.embl-hamburg.de/app/moltenprot>).^{313,314}

5.4 MOLECULAR GENETICS

5.4.1 NEBuilder HiFi DNA Assembly

Plasmid assembly incorporating genes of interest was accomplished using the NEBuilder HiFi DNA Assembly system (New England Biolabs, Ipswich, MA). This method enables seamless integration of multiple DNA fragments with variable overlaps (15-30 bp). Fragment design was optimized using the NEBuilder Assembly Tool (<https://nebuilder.neb.com/#/>), with overlaps designed to have a minimum melting temperature (T_m) of 60°C to ensure efficient hybridization. DNA fragments were either directly synthesized by Twist Bioscience (San Francisco, CA) or generated via PCR using primers containing the requisite overlaps. PCR products were analyzed by gel electrophoresis and purified using either the GeneJet gel extraction kit (for gel-excised fragments) or the GeneJet PCR purification kit (for direct PCR product purification). Assembly reactions were performed according to the manufacturer's protocol. The reaction mixture consisted of 100 ng of backbone DNA, at least a threefold molar excess of insert fragments, and 10 μ L of the NEBuilder HiFi DNA assembly Master mix. Nuclease-free water was added to a final volume of 20 μ L. Samples were incubated at 50°C for 1 hour in a Biometra TAdvanced Twin thermal cycler (Analytik Jena GmbH, Jena, Germany). Post-assembly, 2-5 μ L of the reaction mixture was used to transform chemo-competent *E. coli* cells, as described above. Positive transformants were initially verified by colony PCR. Plasmids from putative positive clones were subsequently isolated using the GeneJET Plasmid isolation Kit (Thermo Fisher Scientific) and confirmed by sequencing (Microsynth AG, Balgach, Switzerland).

5.4.2 Golden Gate Cloning

Golden Gate assembly reactions were performed using FastDigest Bpil (Thermo Fisher Scientific) or Bsal-HFv2 f(New England Biolabs, Ipswich, USA) and T4 DNA ligase (New England Biolabs, Ipswich, MA). Reaction mixtures were prepared on ice with insert DNA added at a 3:1 molar ratio relative to the acceptor vector.

After gentle homogenization by pipetting, the reaction mixture was subjected to a cyclic temperature profile in a thermal cycler: 25 cycles of 3 minutes at 37°C and 1.5 minutes at 16°C, followed by 5 minutes at 50°C to facilitate re-digestion and elimination of residual DNA containing restriction sites. The reaction was terminated by a final incubation at 80°C for 10 minutes to inactivate the enzymes.

Subsequently, 2 μ L of the reaction mixture was used to transform electrocompetent *E. coli* NEB Stable cells (New England Biolabs, Ipswich, USA). Transformants were selected on LB agar supplemented with the respective antibiotics. Putative-positive clones were initially screened by colony PCR. Plasmids isolated from positive clones were then verified by DNA sequencing (Microsynth, Balgach, Switzerland).

The CyanoGate Kit provides a framework for modular cloning of various genetic elements, optimized for cyanobacteria and based on the MoClo kit.⁸⁴ The parts, that were used in this study are mentioned above (Figure 29). In brief, the required parts, promoters, terminator, and GOI, were cloned into a Level 1 acceptor vector, using the restriction

enzyme Bsal-HFv2 f(New England Biolabs, Ipswich, USA). The transformed *E. coli* cells were transferred onto an LB-agar plate containing x-gal as a selection marker. Putative positive transformants were verified by colony PCR. In the next step, the assembled expression cassettes were transferred into a level T acceptor, in this case, pPMQAK1-T Y25F, an optimized version of pPMQAK1-T. Putative transformants were again screened first on x-gal agar plates and verified by colony PCR.

5.4.3 Construction of pPMQAK1-T-Y25F

The improvement of the pPMQAK1-T acceptor vector was done by introducing a mutation in the *mobA* gene.⁸⁰ This was done by site-directed mutagenesis. Site-directed mutagenesis was performed using the Q5® Site-Directed Mutagenesis Kit (New England Biolabs, Ipswich, MA) following the manufacturer's protocol. Mutagenic primers were designed using the NEBaseChanger tool provided by the manufacturer. The plasmid of interest was amplified via exponential amplification using Q5 Hot Start High Fidelity 2X Master Mix and the designed mutagenic primers. Subsequently, a kinase-ligase-DpnI (KLD) enzyme mix was employed to circularize the PCR product and digest the template DNA. Before the transformation, the reaction mixture was desalted using the GeneJET Gel Purification Kit (Thermo Fisher Scientific). The DNA was bound to the column by adding an equal volume of Binding buffer to the reaction mixture. Following centrifugation, the column was washed with 700 µL Washing Buffer. After an additional centrifugation step, the DNA was eluted in 35 µL nuclease-free water. 5 µL of the purified DNA was used to transform electrocompetent *Escherichia coli* Top10 or *E. coli* DH5α cells. Putative positive transformants were initially screened by colony PCR or restriction digestion. Plasmids from positive clones were isolated using the GeneJET Plasmid Isolation Kit (Thermo Fisher Scientific).

The presence of the desired mutation was confirmed by DNA sequencing using appropriate upstream or downstream primers.

6 APPENDIX

6.1 MEDIA USED FOR BACTERIAL CULTIVATION

Table 8 Media used in this study and their composition

Compound	LB ³¹⁵	TB ³¹⁶	AD7 ¹¹⁸	MAD2 ¹¹⁸	CD ²⁴⁵	YBG11 ³¹⁷
Peptone	10 g/L					
Yeast extract	5 g/L	24 g/L				
NaCl	5 g/L		18 g/L	18 g/L		
Tryptone		20 g/L				
KH ₂ PO ₄		17 mM	50 mg/L	50 mg/L		
K ₂ HPO ₄		72 mM		0.27605 g/L	4 mM	0.0305 g/L
MgSO ₄ * 7H ₂ O			5 g/L	5 g/L	2 mM	0.074 g/L
KCl			0.6 g/L	0.6 g/L		
NaNO ₃			1 g/L	16 g/L	50 mM	1.49 g/L
CaCl ₂ * 2H ₂ O			0.37 g/L	0.37 g/L	0.5 mM	36 mg/L
Na ₂ EDTA*2H ₂ O			30 mg/L	30 mg/L	150 µM	5.95 mg/L
FeCl * 6H ₂ O			15 µM	30 µM		0.97 mg/L
Fe-ammonium Citrate					0.15 mM	
Vitamin B12			4 µg/L	12 µg/L		
H ₃ BO ₃			2.86 µg/L	2.86 µg/L	25 µM	2.78 mg/L
MnCl ₂ * 4H ₂ O			1.18 µg/L	1.18 µg/L	20 µM	1.13 mg/L
ZnSO ₄ * 7H ₂ O			222 µg/L	222 µg/L	2 µM	0.2 mg/L
Na ₂ MoO ₄ * 2H ₂ O			1.26 mg/L	1.26 mg/L	3 µM	0.39 mg/L
CuSO ₄ *5H ₂ O			79 µg/L	79 µg/L	20 nM	0.07 mg/L
CoCl ₂ * 6H ₂ O			40.3 µg/L	40.3 µg/L	60 nM	0.16 µM
Citric acid * H ₂ O						6.3 mg/L
Na ₂ CO ₃						160 µM
KHCO ₃					2.5 mM	
Tris (pH 8.4)			1.0375 g/L	1.0375 g/L		
HEPES (pH 7.8)						10/100 mM (depends on use)
BactoAgar	18 g/L (for plates)		12 g/L (for plates)			
Na ₂ S ₂ O ₃			1 g/L (for plates)			

6.2 ENZYMES

6.2.1 Carboxylic acid reductases

CAR from *Nocardia iowensis* (niCAR) Acc. No.: Q6RKB1.1

ATGTCGTACTACCATCACCATCACCATCACGATTACGACATCCCAACGACCGAAAAACCTGTATTTTCAGGGCGCCATGGCT
GATATCGGATCCGAATTCATGGCAGTCGACAGCCAGACGAACGCCTGCAAAGACGCATCGCCCAATTGTTTCGACAGAGG
ACGAGCAGGTGAAGGCGGCTCGCCCGCTGGAAGCCGTGAGCGCGGCTGTTTCTGCTCCGGGTATGCGCCTGGCGCAG
ATCGCAGCGACGGTCATGGCCGGCTATGCCGACCGTCTGCAGCCGGTCAACGCGCATTGAGCTGAACACTGATGAC
GCCACCGGTGCGACAGCTTGCGCCTGCTGCCGCGTTTTGAAACCATCACCTATCGTGAGCTGTGGCAACGCGTGGGC
GAGGTGGCGGTGCTGGCATCATGACCCGGAACCCGTTGCGTGCGGGCGATTTCGTGGCACTGCTGGGTTTCACCA
GCATTGATTATGCGACGCTGGACCTGGCCGACATCCATCTGGGTGCTGTGACCGTGCCGCTGCAGGCCAGCGCAGCAGT
GTCCCAACTGATTGCGATCCTGACGGAACCTCCCTCGCTTGCTGGCGTCTACCCCGGAGCACCTGGACGCAGCGGTT
GAATGCTGCTGGCGGGTACCACCCCGAGCGCCTGGTCTGTGTTGATTATCACCCGGAAGATGACGATCAACGCGCAG
CGTTTGAGAGCGCGCGTGGCGTCTGGCTGATGCGGGTAGCCTGTTATCGTTGAAACCCCTGGACGCGGTCCGTGCACG
TGGCCGTGACCTGCCAGCGGCACCGCTGTTGCTCCCGGACACTGACGATGATCCACTGGCGCTGCTGATTACACCAGC
GGCAGCACCGGTACGCCGAAGGGCGCGATGTACACCAATCGCTTGGCGGCGACCATGTGGCAAGGTAACAGCATGCTG
CAAGGTAACCTCCAGCGTGTGGCATCAATTTGAATTACATGCCGATGAGCCATATTGCGGGTCTGTATTAGCCTGTTCCGTG
TGCTGGCTCGTGGCGGTACGGCCTATTTGCGCAGCGAAGTCCGATATGAGCACCCCTGTTTGAAGATATCGGTCTGGTCCGT
CCGACCGAGATCTTCTCGTTCCGCGTGTGTTGATATGGTGTTCAGCGTTATCAGTCGGAAGTGGACCGTCTGAGCGTGC
CAGGTGCGGACCTGGACACGCTGGATCGCGAGGTCAAAGCCGACCTGCGCCAGAATTATCTGGGCGGTGCTTCTCTGG
TCGCCGTGGTGGGCTCCGCTCCGCTGGCAGCGGAGATGAAACCTTTATGGAGAGCGCTTGGATCTGCCGCTGCACGA
TGGCTATGGTAGCACGGAAGCGGGTGCCTCGTCTTGCTGGATAACCAATTACGCGTCCTCCAGTGCTGGACTATAAACT
GGTGATGTGCCGGAAGTGGGCTATTTCTGATCCGATCGCCCGCATCCGCGTGGTGAGCTGCTGCTGAAGGCGGAACT
ACCATCCCGGGTTACTACAAGCGTCCGGAGGTACGGCAGAAATCTTTGATGAAGATGGTTTCTACAAGACGGGTGACATC
GTTGCGGAGCTGGAACACGATCGTTTGGTTTACGTTGACCGTGCACAACGCTGCTGAACTGTCTCAAGGTGAGTTCGTC
ACTGTTGCTCACCTGGAAGCTGTGTTTGAAGCAGCCCGCTGATTCGTCAGATCTTCATCTACGGTAGCTCTGAACGCAGC
TACTTGCTGGCCGTTATCGTTCCGACCGACGACGATTGCGTGCCGCGGACACTGCAACCCTGAAGAGCGCATTGGCCG
AGAGCATCCAAACGTATTGCAAAAGACGCGAACCTGCAACCATACGAGATCCCGCGTGATTTCTGATCGAAACCGAACCG
TTCACCATTGCGAATGGTCTGCTGAGCGGCATTGCAAAGCTGCTGCGTCCGAATCTGAAAGAGCGTTACGGTGCCCAAGT
GGAGCAGATGTACACGGACTTGGCGACGGGTGAGCGGACGAATTGCTGGCGCTGCGTCTGAGGCGGCGACACCTGC
CGGTACTGGAACCGTTAGCCGTGCGGCCAAAGCGATGCTGGGTGTTGCCAGCGCGGATATGCGTCCGGATGCGCACTT
TACCGACTTGGGCGGTGACAGCCTGAGCGCGCTGAGCTTCTCTAATCTGCTGCAGGAAATCTTTGGCGTGGAGGTGCCG
GTTGGCGCTGCTGGTAGCCCTGCAATGAATTGCGTGATCTGGCTAATTACATCGAGGCCGAACGAATAGCGGTGCGAA
ACGTCCGACCTTTACCAGCGTGATGGCGGTGGCTCGGAGATTGCTGCGGCGGATCTGACGCTGGATAAGTTTATTGATG
CTCGTACGCTGGCAGCCGCTGACAGCATTCCGACGACCGGTGCCAGCGCAGACGGTCTGCTGACGGGTGCCAAC
GGTTACCTGGGTGCTTTCTGTGCCTGGAGTGGCTGGAGCGTCTGGACAAAACGGGCGGTACCCTGATCTGTGTTGTGCG
TGGCTCGGATGACAGCAGCCGACGCAACGTTTGGACAGCGCTTCGACTCGGGTGACCCGGGTCTGTTGGAGCATTAT
CAGCAGCTGGCGGCACGACCCCTGGAGGTTCTGGCGGTGATATTGGCGATCCGAATCTGGGCCTGGACGATGCGACC
TGGCAGCGTCTGGCGGAGACTGTGATTTGATTGTCCACCCGGCAGCGTGGTTAACCATGTTCTGCCGTACACCCAAC
GTTCCGGCCGAACGTTGTAGGTACGGCCGAAATTGTCCGTCTGGCAATCACTGCGCGTGCAGACCGGTACGTTACCTG
AGCACCGTTGGCGTGGCCGATCAGGTTGACCCGGCAGAGTATCAAGAGGATTCTGACGTTCTGAGATGAGCGCGGTTT
GCGTTGTCCGTGAGAGCTATGCGAACGGTTACGGCAACAGCAAGTGGGCGGGTGAAGTTTTGCTGCGTGAGGCTCACGAT
TTGTGCGGCTTGCCGGTGCAGTTTTCCGTTCTGACATGATTCTGGCCACAGCCGTTATGCGGGTCAGCTGAATGTTTCA
GATGTGTTACGCGCTGATTCTGAGCTTGGTGGCAGCCGATCGCGCGTACAGCTTCTACCGTACGGACGCCGACG
GTAACCGCCAGCGTGCCCATACGACGCGCTGCCGGCAGACTTCAGCGCTGCGGCGATTACCGCGCTGGGTATTACGAG
CGACGGAAGGCTTTCTGATCCTATGATGTGCTGAACCCGTACGACGACGGTATCAGCCTGGACGAGTTCGTGGATTGGCTG
GTGGAGAGCGGCCACCCGATTACGCGTATTACGGACTATAGCGATTGGTTTACCGCTTCGAAACCGCCATTCTGCGCT
GCCGGAACACAGCGTCAGGCGTCCGTCTGCGCTGCTGGATGCATATCGTAATCCGTGCCAGCAGTCCGCGGTGC
TATTCTGCCTGCCAAAGAGTTTCAAGCGGCGGTGCAACCGCAAAGATTGGCCCGGAGCAAGACATCCCGCACCTGTCT
GCACCGCTGATCGACAAATACGTTAGCGATTGGAACCTGCTGCAACTGCTGTAA

CAR from *Dichomitus squalens* (dsCAR) Acc. No.: XP_007365851.1

GACATCCCAACGACCGAAAAACCTGTATTTTCAGGGCGCCATGAGCTTGAAAAATGCCCTGGGTTCTACAACCCGGCGGT
CCACACGTACCAGGGTGCCTCCTCAAGACCTTCACTCCTCCCGTTTGGACACATCGCTTACCATTCTGAACTTTTGA
ATTCCATGCCAAACATTGGCAGAGCACCCGTGCTTTGTCTACGCTGATGATGACCAGAAGGAACATGTAATTCATTCCGC
GAGGTCTGGCGTGCCATTCTGATAAAGTGCAACCTTATCGAGTGCGCACTATAATCAGCTTGCCAAATATTATGAGGAGGCC
CAGGTTGGTAAATCTGAGGATGATCCGCCAGTCATTGGTATCTTGGCCACGGCCGATTCCATTACATTTACACCCTTAAGG

TAGGTTAATGTATTGGGGCTTACTCCGTTCCCTATCTCGACGCGTAACAGTGCAATTGCCGTGCGACACCTTGTCTCCAA
GACCGGCGTAAAGCAATGTATGTCTGTCTGACCCCGCAATGCAACGCCTTGCTCAGGAGGCTAACGAAATTTGGCTAA
GGATGGGAATGAATTCGAGCCCTTGCCAATGCCAACGTTTCGAGGACCTGTATGGCCCCGGTGGTGACGAAATCTTCTGC
CGATGGGCAAGGTATCACCGACCAAAACATGCGTAATCCTGCACTCGTCGGGGTGCAGTGCCTTCCCTAAGCCCATCAA
GTTTCTGGATAAGAATTTTCGCAATGGGGTACATTCTGTATTTTCGGAGAGTTCGATTTTGTGGAGTTCGCGTTGGAGGCC
AAGCCAATCCTATGTTCCACGTAATGGGGTCGTTGATGATGACATGGTCCATTATGCGGGTGTCAATTGGACCATGTTCAAA
CCCTCTACACCGCCCGTGGTCCCGACCCCGGAATTGTACTTACAATCCGCAATTTCTACTCACACTGAAATGTATACTGTG
TGCCGGCCTTTATTGAGGCATGGGCCCGTGATCCAGAGAATATGCCGCGTATTAAGACTCTGCGCGCCATGATCTACGCC
GGCGCGCTATGAACAAACAGATCGGGGACCGTTTGGCTTCTGAAGATATTGCATTGATTCCATTTTACGGTTCTACGGAAA
TCGGCGCTGTTGTCCGTTTGATCCCCAATCCCAAGACGATGTATAAGACCGATTGGGACTACTTCCAAATTTACCGCATAT
CGACATCCGCCTGATCCCGCAAGAGGAACAGCCGGGATTTTGTAGCCAGTGGCATTGACTCACCTACGTTTACCCCTA
ACGTATTTAATTCGCTCATTGATGGACGCCCCGCTTACAGCACTTCTGACCTTGTACAACAACATCCGACCAACACAATTT
GTTTCGTGTGTTCCGGCGCGCTGACGATCAGTTAATGTTGAGCACTGGCGAGAAAATAACCCCTGCTCCATTGGAAGCCAT
CCTTGTCAGGATCCGCACGTACACGCGTGCCCTGATGTTTGGTCTGGTCTGCTTTCAGAACCGGAATCCTTATTCAGCCGAA
AGATACGTTTCGACCCTAGTGACGAGGCGAAACTGGAAGAGTACCGCAATAAAATCTGGCCGTCCTCGAAAAATGAATG
CCTTCGCGCCATCTCATAGCCGCGTCTTTAAAGAAATGATTATGGTTACTAAACCGGATAAACCCTTGGGAATACACTGCAAA
GGGAACGCCGCGCGCTCAGGTTTGCCTTGGCGCCTACGCGGATGAAATCGATGCTCTGTATAAGCGTGTGGAAGAAAGC
TCACAGATTGATCTTCGCCACCTCGTAACCTGGACACCGCTCCATCCAGCAATTCGTTGGGGATTTGTCAAGAAGGTC
ATGAAAAATGCGTCCATCCCAAGCTGATGACGACTTGTTCGCAAGGATGTGATAGTCTGCAAGCGAACCTGGATTTCGCAACA
CCTTAATTCACGCCCTTCGTTCCAGCTCCTCGGTTAATACCCATGACATCCCCTCAGGGTTTGTGTACGCGCATCCGCTCTAT
CAGTGCGCTTTCGCTTACTTAGCAAGCCTGTTTAGTGAAAAACAGTCGACAAAGACGTAGACCGCGCCGCCGGAATTG
AGCGTATGGTAGCCTTATTAGACAAATACTCGGCCGACTGGAGCGCTGTTTCCAGAGAAAGCTGTTAATGGACATGCCA
ATGGGCATGCTAATGGCCACGCTAACGGAGTTACAGAGTTTGTCTGTAACGGGCACGACTGGCCGCTTGGGGTCTCAC
CTGCTGGCACAACCTGCTGCAGCGCCCCGACGTGGCAGCGCTGTATGCCCTGAACCGTGACCCAAGTGGGTGAGTCGAC
AATTTGAAGAAGCGTTCCCGTGAAGCCTTCAAGCAATGGTCCCTTGACGAGAGCCTTCTTCAAGATGGAAGGTGTCGTTTC
ATGCCGTCGATCTGGCCAAATCGAATTTCCGGCCTTAGCCAAGCGTTGTATGACGAAATGCGTACATCTGTAACACAAATCAT
CCATAATGCTTGGCGTGTAGACTTCAATGTACGTCTGCCAGTTTGAACCACTGATCGCTGGGGCAGCAACTTGCTGGA
TTTAGCACTTAACCTTCTCAACCCGGAGGGCCTCGCACCTTATTGTAAGTTCCATTTATCGTTACGTAACCACACAGGGC
CGGTCCCAGCAGAGAAGACTATTGGAAGTGGTCCCGAGCTGGCTCAGGCTCAGGGTACAGTGAGTCCAAGTGGGTTAC
TGAACAACTTTTCGCTGCTGCTGCCGAACGTACCGGCTTGCCTACCGTCGCTGTTCCGCTGCGCGTCCAGGCTCAGGGAC
CAGCAGAGCGGGGGCTGGAATACCAACGGAATGGGTTGCCGCTTGACACGTGTATCCAAACGCCCTTGGTTGATTCCCTC
GAAGGACGAGTCGATTACTTGGGTGCGAGTAGATGTAGTAGCCGACGCCCTTCAAGAAATGGTGGCTTCCGCTGAGCGTG
CATTGCATGTAGTTAGTCCACATCCCCTGCCCTTGAATACAGTTTTCATCCCATCGCTGAATACTTAGGAGTCCCAGTAGTT
CCGTACGCGGAATGGGTAGCGCGCCTGGAGCAGTCTGCGGCAGCCGCGTCTGCTCGCGCCGGTGTGAGCAGCACGA
CGCCGCACATAATCTGGTAGGATTTTAAATCGGAAGGGATGGGAGGCGCGGAAGTTGCTCTTAGTACGGATAAGGCAGT
TAAAGCTAGTCGTGCTTAGCCCGCTTCCGCCCTATCGACGTGAGGACGCCCTTCGTTATGTGCAATATTGGGAGAAAGT
GGGCCACTTAATGTATA

CAR from *Trametes versicolor* (tvCAR) Acc. No.: XP_008043822.1

CATCACCATCACCATCACGATTACGACATCCCAACGACCGAAAACTGTATTTTCAGGGCGCCATGCCGCTGCAACTGGC
CGACATCCCGAGCCACCTGTCAATGGAATTTATAGCCCGAGCAACGCAATCGAAAAAGGCGCAACCATCCCGGAACTG
TATGATTGGCATGCGAAAGAAAACCCGACTATCCGCTGTTTCGTACCAGATGGCGAAAAATCTGAATATATCACCTACA
GCTCTGCGAATCGCGCCATTGATCGTGTGCCCGCTATGCTCTGTCTGGTCTGGGTCCGGTGGCAAGTACCGCTGAACGC
GGTGGCGGCAAACTGCCGACCGTTGCCATTTTCGCTCGTGGGATACCATCACGTAATTTTGACCGTCTATTGGCGTGTTC
CGCGCGGGTGTACGGCCTTCTGGTGTCTCCGCGTAACGGTGCAGCTGGCGTTGCCGACATGCTGCAGCGTACCGGCA
CGCTGCAGATGTTTGTGTCCCAAGATGCAACCATGCGTGATCTGGCCCAAGATGCACTGTACAGCCTGCCGGAAGGTCAT
GTGACGCTGCGTGATATGCCGTTTTTGAAGACCTGTTCCCGACCGGTAGCCAGGCAGGTAACCCGGCTTTGAAACGGA
AGTGGAACTGCCGAAAAATGCATGATGTTAATGCCGTTGCCGCAATCCTGCACAGTTCGGGTTCAACCTCGTTTCCGAAAAAC
CATTCCGTGGACGCATAAACCGCTTCTGTTCTGGGTGACGAAGCACAGCGTGGCGGTGGCTCTGTTACCGGTACGATTG
GGGCTGCCATGCGACCCCGATGTTTACGCAATGGGCGCTATTATGATCCCGAGTGCCCCGATCTGTGTTATGTGGTTG
CAGCTTTCAAACCGGCAACCCCGGCTTTTCCGACCGCGACATTGTGTGGCGTGGCCTGGTGGCGTCTCGCGTTGA
TTTTGCTTTACCGTGCCGGCGTTCATTGAAGAATGGGGTCTGACCCGGCAAAAGTGAAGTGTGAAACACATGCGTGG
TGTGATCTTTGGTGGCGCCCCGCTGAACCAGGAAAAAGGCGATGCACTGGCGGCCGAAGGTGTTAATCTGTGCAGTGCGT
ATGGCCTGACCGAAGTGGGTAACTGTTAAGCGTAGCAGCCGTGGCAGCGATTGGGCCTACTTCTGCCGACG
CCGAGCCTGGAATCGAATTTCCCGCGACGGTGACAACAAATATGAAGTTATTGTCTACAGCGATCCGAAAAATCCGCTG
CCGGCGGTGAACACCAAAATTAATGGTGTGATGCTATGCAACCAACGACCTGGTGAACCGCACCCGACGAAACCGA
ATCTGTGGCGTGTTCACGGCCGCGCCGATGAACAGATTATGCTGTGCAACGGTGAAAAACCAATCCGCTGCCGATTGAAA
GCACGATCAACGAAGATCCGCATGTGAAAAGCTCTGCGATGTTGGTCTGCGCGCTTCCAGAATGGCATTCTGATCGAAC
CGGCGGAAGAATCCAAGTGGATGCAGTAACGTCAAAGAAGTGAAGCCTTTCGCAATAAAATCTGGCCGACCGTTGAA
CGTGCGAATGCCACCGCCCCGACGACTCCCGCATCTTCAAAGAAATGATCATCGTGACCTCACCGTTTAAACCGTTCCA
GCTGAATGCGAAAGGTGCCCGCGCTGCGCGGTTATCCTGAAACAATACGAAGAAGAAATCGAAGAAGTGTACCGCCAG

ATTGAAGATAGTTCCTCAAAGCGACCTGCCGGCTCCGAGCGTCTGGGATCAGGCCAGTACCCTGTCCTTCGTGCGTGCCG
TCGTGGAACAAACCTGCGTGCACGATTGCAGATGACGATGACATCTTTCGCAACGGTGGCGATAGCCTGCAGGCCAC
CTATATTCGTAATACGCTGATCCGTGCAGTCCGCGATACCGATGTGAAAGCCGCGGCACGCTGCCGGCAAATCTGGTCTT
TCAGGCCCCGACCGTGGCAGGTCTGACCGACGTTGTCTACCGCGTGTGCATGATGCAGACGCTGCGGGTACCTCATC
GCGTACGCCGAGGATCTGTGGAAATATGTGGAAAAATACAGCGCCAATTTCCCGAGCCGCCGGCATCTCTGGTTGATC
GTAGCGCATCTGCTAAAGACGTGGTTCTGATTACCGGCACACGGGTGGCTTTGGTTGCGACGCGCTGGAACATCTGCTG
CGTGATGAAAGCGTGGAACGCGTCTATGCATTCAACCGTGTGGCAGTAATGCGCTGGAACGCCAGCACGCCCAATTCG
TGACGCGGTCTGGATGAAGCTCTGCTGAGCTCTCCGAAATCAAACCTGATTGAAGCGGTTCTGCATGAACCGGGTTTGG
CGTCGATCCGAAACTGCTGGACGAAGTGCCTCAGAGCATTACCCATATCATGCACAACGCTTGAAAGTTAACTTCAATCT
GTCAGTCGCGTCGTTTGAACCGGACATCCAAGGCGCTCGCAATCTGGTGGATCTGGCGATTAGTTCCCGTTACCAAAG
CCCCGACGATTGTGTTCTGTTGGCAGTATCTCCGTTTTTACCGTTATGAAGGTCCGTCTCCGGCACCGGAAGCTAGTCTGG
AAGATCCGACCAAGTGCCTTTGGTTCCGGCTACCCGGAAGGCAAATGGGTACGGAACATGTGCTGCAGAATGTTGCTAAA
GAACGCGGTGTGCACACCGTTGCGATGCGTCTGGGTCAAGTTACGGGCAACCGCGTCTCGTTATTGGAATGAAAAAGAATG
GTTCCCGTCACTGGTGAAATCGGCCAGTTTCAACGCTGTCTGCCGGATATCGAAGGCTCAGTTTCTGGATTCCGGGTTA
CGAAGCCGCAAAGCGTTACCCGAAATGCGTCATAGCCCGCACCCGTTTCTGCATCTGGTGCACCCGAAACCGGTTTCC
TGGCATAACGCTGATTCAGCGATCGCCAAAGAATTTGGCAACGTCCCGCTGGTGCCGATGACGAATGGCTGTCCGCGCT
GCAGGCCAGCGTTTCTGAAGGTGATGCTGCGGAAGTCAAGTATGCGTGCAAACCCGGCTCTGCGTCTGCTGCCGTTTT
TCCAGGCCGATGAATCAACACGCATCACTGGATCGCAACCGCTGGCGCTGTTTACCTGAGCACCGAAAAATCTGCCGC
AGTCAGTGGTGCACTGGCTAATCTGCCGCAACTGGACGCTGAACGTGCCGAAAGGCTGGCTGGCCGCTTGGAAATCCGCC
GGCTTCTGTAACTCGAGTCTGGTAAAGAAACCGCTGCTGCGAAATTTGAACGCCAGCACATGGACTCGTCTACTAGCGCA
GCTT

CAR from *Mycobacterium marinum* (mmCAR) Acc. no.: B2HN69.1

CATCACCATCACCATCACGATTACGACATCCCAACGACCGAAAAACCTGTATTTTCAGGGCGCCATGTCACCGATTACCCG
CGAAGAACGCCTGGAACGCCGCATTCAAGACCTGTACGCCAACGACCCGCAATTCGCCGCCGCAAACCCGGCGACCG
CCATTACGGCAGCAATCGAACGTCCGGGTCTGCCGTGCCGCAAATTATCGAAACCGTGATGACGGGTTATGCAGATCGT
CCGGCACTGGCTCAGCGCTCCGTCAATTTGTGACCGATGCCGGCACGGGTATACACAGCTCGCTGCTGCCGCAC
TTCGAAACCAATTAGTTACGGTGAACCTGTGGACCCGCATCTCAGCGCTGGCCGATGTGCTGACCGAAGACAGACGGTGAA
ACCGGGCGATCGTGTGCTGCTGGGTTTTAACTCGGTTGACTATGCAACCATTGATATGACGCTGGCTCGTCTGGGTGC
AGTCGCTGTGCCGCTGCAAACCTCAGCAGCTATTACGCAGCTGCAACCGATCGTTGCGGAAACCCAGCCGACGATGATC
GCAGCCAGTGTGATGCACTGGCAGACGCAACCGAACTGGCACTGTCCGGCCAAACCGCTACGCGCGTTCTGGTCTTC
GACCATCACCGTCAGGTGGATGCACATCGCGCAGCTGTTGAAAGCGCTCGTGAACGCCTGGCAGGCTCTGCTGTGGTTG
AAACCCTGGCTGAAGCGATTGCCCGTGGTGTGTCGCCGCGCGGTGCAAGCGCTGTTCTGCACCGGGTACCGATGTTAG
TGATGACTCCCTGGCACTGCTGATCTATACCTCAGGTTGACGGGTGCACCGAAAGGTGCAATGTACCCGCGTGCACACG
TGGCAACCTTTTGGCGTAAACGCACGTGGTTTCAAGGCGGTTATGAACCGAGCATTACCCTGAACTTTATGCCGATGTCTC
ATGTTATGGGCCGTCAGATCCTGTATGGTACCCTGTGTAATGGCGGTACGGCATACTTTGTTGCTAAATCAGACCTGTCGAC
CCTGTTGCAAGATCTGGCGCTGGTGCGTCCGACCGAACTGACGTTCTGTTCCGCGCGTCTGGGATATGGTTTTTGACGAAT
CCAATCTGAAGTTGATCGTCGCTGGTGCATGGTGAGAGCTGTGCACTGGAAGCACAGGTGAAAGCCGAAATTCGTA
ATGATGCTGGCGGTCGCTATACCAAGCGCACTGAGGCTAGTGCCAGCTCCGACGAAATGAAAGCTGGGTCGA
AGAAGTCTGGATATGCATCTGGTGGAAGGCTACGGTTCTACCGAAGCAGCATGATTCTGATCGACGGTGCAATTCGTCG
CCCGGCTGTGCTGGATTATAAACTGGTGGATGTTCCGGACCTGGGCTACTTTCTGACCGACCGTCCGCACCCGCGCGGT
GAACTGCTGGTTAAACCGGATAGCCTGTTCCCGGGTTATTACCAGCGTGCGGAAGTGACCGCCGACGTTTTTGATGCAGAC
GGCTTCTATCGCACGGGTGATATCATGGCGGAAGTTGGCCCGGAACAATTTGTCTACCTGGATCGTCGCAACAATGTGCTG
AACTGAGTCAGGGTGAATTTGTCACCGTGTCCAACTGGAAGCGGTCTTCGGCGATTACCGCTGGTGGCTCAAATTTATA
TCTACGGTAACTCGGCGCGTGCATCTGCTGGCCGTTATTGTCCCGACCCAGGAAGCACTGGATGCTGTGCCGGTTGAA
GAACTGAAAGCACGTCTGGGCGATAGCCTGCAGGAAGTTGCGAAAGCGGCCGGTCTGCAATCTTACGAAATCCCGCGCG
ATTTTATTATCGAAACACGCCGTGGACCCCTGGAAGTGGCCTGCTGACGGGTATTCTGTAACCTGGCGCGCCCGCAGCTG
AAAAACATTATGGCGAACTGCTGGAACAGATCTACACCGACCTGGCACACGGCCAAGCTGATGAACTGCGTTCACTGCG
CCAGTCCGGTGACAGTCTCCGGTCTGGTGACCGTTTCCCGTGCAGTGCAGCACTGCTGGGCGGTAGCGCATCTGAT
GTGACGCTGGGACGCCCAATTTACCGATCTGGGCGTGACAGCTGTCCGCGCTGAGCTTTACGAACCTGCTGCACGAAAT
TTTCGATATCGAAGTCCCGGTGGGCGTATTGTCTCTCCGGCCAATGACCTGCAAGCGCTGGCCGATTATGTGGAAGCAG
CTCGTAAACCGGGTAGCTCTCGCCCCGACCTTTGCGAGCGTTTATGGCGCCTCTAACGGTCAGGTGACCGAAGTTACGC
GGGCGATCTGAGCCTGGACAAATTCATTGATGCAGCAACCCCTGGCAGAAGCTCCGCGTCTGCCGGCAGCTAATACCCAG
GTCCGTACGGTGCTGCTGACCGGTGCAACGGGTTTTCTGGGCCGTTATCTGGCTCTGGAATGGCTGGAACGCATGGATCT
GGTGACGGTAAACTGATCTGTCTGGTTCGTGCGAAATCAGACACCGAAGCGCGTGCCCGCCTGGATAAAACGTTTCGATT
CGGGCGACCCGGAAGTCTGGGCCATTATCGCGCACTGGCTGGTGACCACTGGAAGTCTGGCGGGTGATAAAGGCG
AAGCCGACCTGGGCGTGGATCGTCAGACCTGGCAACGCCTGGCGGATACGGTCGACCTGATTGTGGATCCGGCGGCC
TGGTTAACCATGTCCTGCCGTATAGTCAGCTGTTTGGCCCGAATGCGCTGGGTACCGCCGAACTGCTGCGTCTGGCACTG
ACGTCCAAAATCAAACCGTATAGCTACACCTCTACGATTGGCGTGGCGGATCAGATCCCGCCGTGACATTACCCGAAGA
TGCTGACATTCTGTTATCTCAGCGACGCGCGCGCTCGATGACTCGTATGCGAAGGCTACTCAAATTCGAAATGGGCGG
GTGAAGTGTGCTGCGTGAAGCACATGATCTGTGCGGTCTGCCGGTGGCAGTTTTTCGCTGTGACATGATTCTGGCGGATA

CCACGTGGGCCGGTCAGCTGAACGTTCCGGATATGTTTACCCGCATGATTCTGAGTCTGGCAGCTACGGGTATCGCACCG
GGTTCCTTCTATGAACTGGCAGCAGACGGTGCACGTCAGCGTGCTACTACGATGGTCTGCCGGTGGAATTTATTGCGGAA
GCCATCAGTACCCTGGGCGCCAGTCCCAAGATGGTTCCATACGTATCACGTCATGAACCCGTACGATGACGGCATTGG
TCTGGACGAATTTGTGGATTGGCTGAATGAAAGTGGCTGCCCGATTCAACGTATCGCGGATTATGGTGACTGGCTGCAGCG
TTTCGAAACCGCACTGCGCGCTCTGCCGGATCGTCAACGCCATAGTTCCTGCTGCCGCTGCTGCACAATTACCGTCAGC
CGGAACGTCCGGTTCGCGGCAGCATTGCACCGACCGATCGTTTTCCGCGCAGCTGTCCAGGAAGCAAAAATTGGTCCGGA
TAAAGACATCCCGCATGTTGGTGCTCCGATTATTGTCAAATATGTCAGTGATCTGCGTCTGCTGGGTCTGCTGTAACTCGAGT
CTGGTAAAGAAACCGCTGCTGCGAAATTTGAACGCCAGCACATGGACTCGTCTACTAGCGCAGCTT

Phosphopantetheinyl transferase PPTase from *E. coli*

ATGGTCGATATGAAAACCTACGCATACCTCCCTCCCTTTGCCGGACATACGCTGCATTTTGTGAGTTTCGATCCGGCGAATT
TTTGTGAGCAGGATTTACTCTGGCTGCCGCACTACGCACAACCTGCAACACGCTGGACGTAAACGTAAACAGAGCATTAG
CCGGACGGATCGCTGCTGTTTATGCTTTGCCGGAATATGGCTATAAATGTGTGCCCGCAATCGGCGAGCTACGCCAACCT
GTCTGGCCTGCGGAGGTATACGGCAGTATTAGCCACTGTGGGACTACGGCATTAGCCGTGGTATCTCGTCAACCGATTGG
CATTGATATAGAAGAAATTTTCTGTACAAACCGCAAGAGAATTGACAGACAACATTATTACACCAGCGGAACACGAGCGA
CTCGCAGACTGCGGTTTAGCCCTTTTCTGTGGCGTGCACGTGGCATTTCGCCCAAAGAGAGCGCATTAAAGGCAAGTGAG
ATCCAAACTGATGCAGGTTTTCTGGACTATCAGATAATTAGCTGGAATAAACAGCAGGTCATTCATCGTGAGAATGAGAT
GTTTGTGTGCACTGGCAGATAAAAGAAAAGATAGTCATAACGCTGTGCCAACACGATTAA

6.2.2 Aromatic Dioxygenases

ADO from *Thermothelomyces thermophila*, Codon-optimized for *Synechococcus*

TTAAGTATAAGAAGGAGATATACATATGCATCATCACCATCACCATGCTCACATCCACGACCTGGCGCCGGAAGTAAGCAA
CTACTCTTCTGGTCGCCTGACCCCGCCGACCCAGTTAGGTTCCCGCGCACCCAGTGTTGCGATCTATGAACAAACCGT
GCCGCTTCAAGGTGACGTTTTGACCTGGAAGTTTCTGGTGCTATCCCGCCGGACATCGACGGTACCTTCTTCCGCGTTT
AGCCGGACCAACCGCTTCCCGCCGCTGTTGAAGACGACATCCACTTCAACGGTGACGGTCTGTTACCGCTATCCGCAT
CTCTGGTGGTCACGCTGACCTGCGCCAGCGCTACGTTGCGACCGAACGCTACCTGCTGGAACCCGCGCTCGCCGCTC
TCTGTTCCGTCGCTACCGCAACCCGTGGACCGACAACGAATCTGTTGCGGTGTTATCCGCACCGCTTCTAACACCAACG
TTGTTTTCTGGCGCGGTGCTCTGCTGGCTATGAAAGAAGACGGTCCGCCGTTGCTATGGACCCGGTACCCTGGAAACC
CTGGGTGCTACGACTTCAAGGTGAGATCCTGTCTCCGACCTTACCGCTCACCCGAAAATCGACCCGGACACCGGTG
AAATGGTTTGTCTCGTTACGAAGCTGGTGGTGACGGTCTGACTGCTCTGTTGACGTTGCTGTTGGACCGTTGACGCTGA
CGGTAAGAAAGTTGAAGAATGCTGGTACAAAGCTCCGTTGCTGGTATGATCCACGACTGCGGTATCACAAAACTGGGT
TGTTCTGCCGCTGACCCCGATCAAAATGGACCTGGAACGCATGAAACGCGGTGGTAACAAATTGCTTGGGACCCGCTG
AAGACCAAGTGGTACGGTGTGTTCCGCGCCGCGGTGCTAAATCTGACGACATCATCTGGTTCGCGCTGACAACGGCTTC
CACGGTCACGTTGCTGTTGCTACGAACCTGCCGTCTGGTGAATCGTTTTGACCTGACAGTTGCGGACGGCAACGCTTTC
TTCTTCTTCCCGCCGGACGACAACATCACCCCGCCGGCTGACGGTGTGCTAAACGCAACCGCCTGTCTTCTCCGACCG
TTCGCTGGATCTTCGACCCGAAAGCTAAAAATCTGCTATCCGCACCGAAGCTGCTGGTGACGCTGACATCTGGGTTGCTG
ACGAACGCGTTAAACCGGCTCTGACCTGGCCGACCAACGGTGAATTCTCTGCATCGACGACCGCTACGTTACCAAAACC
GTACCGCCACTTCTGGCAGGCTGTTGTTGACCCGACCCGCGCGTACGACTTCGAAAAATGCGGTCCGCGCGCTGGTGGT
CTGTTCAACTGCCTGGGTCACTACACCTGGTCTGACCAGAACTACCACCACGGTCACAACACCGGTGACCCGTCTGGT
ACGGTGCCTCTAACGTTCTGCTGAAGAAGCTACCGCTGGTAAATTCGGCTGCAGGACGTATACTCGCCGGTCCGACC
ATGACCTTCAGGAACCGACCTTCATCCCGCGCCAGGGTGTGCTGTAAGGTGAAGGTACCTGATCGCTCTGCTGAACCA
CCTGGACGAACGCGCAACGACGTTGTTATCTTCAAGCTCGCAACCTGGGTAAAGGTCCGCTGGCTGTTATCCACCTGC
CGCTGAAACTGAACTGGGTCTGCACGGTAACTGGGTGACTCTCGCGAAATCGAAGCTTGGCGCCCGCCGCGCTGA
AAACGGTGACGTTGGTCCGCTGCGCGTTGCTAAAGAACCGCTGCCGTGGCAGAAAAAATTCGCTGCTGCTCAGAACG
GTTCTAACGGTGTTAA

ADO from *Moesziomyces aphidis*

ATGCACCATCATCATCATCAGCTCCTACTGCAACGCAGGAGCCAGTGCCCTGTGCCAGTCACTTCAAAAGCAGCTCCGTC
GCATGGATATGTCCATCCGACTGATATTCTGCCCTCGGGATGGCCACCGCTACTGACTTATCCGGCGGAGCACAGCCA
CGTCGTTTTGAGGGTACGATTTTACGCTGATGACCCGTGGCACAATTCGAAGGAGCTTCACGGAACTTTTACCGTATTAT
GCCTGACTATGCACAGCCACCTACTATTACAAGGGAGGAGAACTGAATGCTCCAATTGATGGAGACGGCACTGTGGCCG
CATTTTCGCTTCAAGGATGGGAAGGTAGACTACCGTCAACGCTTCGTGGAACGGATCGTTTAAAGGTGAGCGTCGCGCA
CGTAAATCTATGTACGGTCTGTACCGCAACCCGTACACGCACCAACCCATGCGTACGCCAAACCGTAGAATCGACTGCCAA
CACCAACGTCGTCATGCACGCAGGCCGTTTTCTTGCCATGAAGGAAAATGGCAACGCATACGAAATGGACCCGCAcACTC
TGAAGACCCCTTGGTTATAACCCGTTCAATTTGCCATCTAAGACTATGACGGCACACCCTAAGCAGTGCTCGGTTACCGGCA
ATTTGGTGGGCTTCGGATACGAGGCGAAGGGGTTGGCAACCAAGACGTGTATTATTTGAGGTGGACCCCTCAGGAAAG
GTAGTGCGCGACTTGTGGTTAGAAGCCCCCTGGTGCGGTTTATTACGATTGCGCTCTTACGCCAACTATCTGGTATTG
ATGTTGTGGCCGTTTCGAGGCTAATCTTGAGCGCATGAAAGCCGGAGGACATCATTGGGCCTACGACTACACGAAACCTAT

CACGTGGATCACGATCCCCGTGGGGCTAAGTCTAAAGATGAAGTAAATACTGGCATTGGAAGAATGGGATGCCCATTCAC
 ACCGCTAGCGGTTTCGAAGACGAGCAAGGGCGCATTATCATTGATTCCCTCCTTAGTGACGGTAATGCCTCCCGTTTTTC
 CCTCCCGACAGTGATGAGCAGAAGAAAAAGCAGGAGGCTGATGGTACGCCTAAAGCGCAATTTGTGCGTTGGACAATCGA
 TCCCGCAAAGATAACAATGAGCAACTTCCGGATCCCGAGGTGATCTTAGATACGCCTTCAGAATCCCGCAAATTGATAAT
 CGTTTTATGGGAGTCGAGTATTCATCGGCATTTATTAACGTTTTCGTCCCTGACCGTTCGGACGGTAATAAGAAGCTCTTTCAA
 GGCCTGAACGGCCTGGCTCACTATAAGCGTAAGGAAGGTACTACTGAGTGGTATTATGCGGGAGATAATTGCTTGATCCAG
 GAACCACTCTTTAGCCCTCGCTCGAAGGATGCGCCGGAAGGTGACGGGTTCTGTGTTAGCTATCGTAGACCGTCTGGACTT
 AAACCGTTCGGAAGTCGTTGTAATCGATACCCGCGACTTCACAAAAGCAGTCGCAGCGGTCCAACTTCCTTTTGCTATTCTG
 TCGGGCATCCACGGGCAATGGATTCTGGAGAGGTCACTCCAGATTTTGAGACGAAGGGACTTGTGATCTGCCGAAAGA
 GGAACATTGGGCGCCATTAAGTCAATCCCCATACGATCCCGACGCTTAA

6.2.3 Phenolic Acid Decarboxylase

Phenolic acid Decarboxylase from *Bacillus coagulans* DSM11 codon-optimized for
Synechococcus

AAAACCTGGAAGAATTTTTGGGAACCCACATGATCTACACCTACGAAAATGGCTGGGAATACGAGTTCTACGTCAAGAATC
 AAAACACTGTTGACTATCGAATTCACCTCTGGCATGGTAGGTGGTTCGCTGGGTTTCGCGGTCAGAAAGCTGATATTGTCAAAT
 TACCGATGGCGTTTTCAAAGTCAGCTGGACGGAGCCGACAGGGACGGATGTCAGTCTAACTTCATGCCTGACGACAAGC
 GGATGCATGGGGTGATTTTTTCCCGAAGTGGGTGCATGAGCATCCCGAGATTACAGTCTGCTATCAGAATGATCACATCGA
 TCTGATGGAAGAGTCGCGCGAAAAATATGAAACCTATCCCAAGTATGTGGTGCCAGAGTTTGCCGATATCACTTACATCAA
 AATGAAGGCATCAACAACGAAAAGGTGATCAGCGAGGCACCCTACGCCACGATGGCGGATGACATTCTGTCAGGCAAAC
 CAAGTTTTCCTAA

6.3 PLASMIDS

Table 9 List of plasmids from this work and which *E. coli* strain carries those. Abbreviation: Amp – Ampicillin; Kan – Kanamycin; Strep: Streptomycin/Spectinomycin.

Strain	Plasmid	Resistance	Description
E. coli	RP4	Amp	Conjugation with <i>Synechocystis</i> PCC6803
DH5α	pSHDY*mobAY25F	Strep	Multi-Species-Vector
DH5α	pSHDY*plo3_mVenus_119rhaS	Strep	anhydrous tetracycline-inducible Promoter for <i>Synechocystis</i> PCC6803
DH5α	pSHDY*pVan_mVenus_119rhaS	Strep	Vanillate-inducible Promoter for <i>Synechocystis</i> PCC6803
DH5α	pSHDY*pRha_mVenus_119rhaS	Strep	Rhamnose-inducible Promoter for <i>Synechocystis</i> PCC6803
DH5α	pSHDY*pRha_ecPPTase	Strep	carrying PPTase from <i>E. coli</i> for CAR
Top10	pET-Duet_CARni_ecPPTase	Amp	
HB101	pRL443	Amp	Conjugation with <i>Synechococcus</i> UTEX2973
HB101	pRL443 + pRL623	Amp + Chlor	Helper for Conjugation with <i>Synechococcus</i> UTEX2973
NEB stable	pSZT025	Amp	Genomic integration in <i>Synechococcus</i> PCC 11901
NEB stable	pSW036	Amp	Genomic integration in <i>Synechococcus</i> PCC 11901
NEB stable	pSW039	Amp	Genomic integration in <i>Synechococcus</i> PCC 11901
BL21	pET21_T7_ADO	Amp	ADO codon optimized <i>E. coli</i>
BL21	pET28_T7_PAD	Kan	PAD codon optimized for <i>Synechococcus</i>
BL21	pET21_T7_ADO pET28_T7_PAD	and Amp+ Kan	
NEB stable	pUC19_fadD_PAD	Amp	Genomic integration of PAD in <i>Synechococcus</i> PCC 11901
NEB stable	pUC19_psbA2_ADO	Amp	Genomic integration of ADO in <i>Synechococcus</i> PCC 11901
DH5α	pSHDY*pRha_PAD	Strep	PAD (<i>Synechococcus</i> codon-optimized)
NEB stable	pPMQAK_ptrc20_Y25F	Amp+Kan	improved version of pPMQAK1
NEB stable	pPMQAK_ptrc20_BCD2_ADO	Amp+Kan	ADO codon optimized for <i>Synechococcus</i>
NEB stable	pUC19_fadD_CHMOs7	Amp	Genomic integration of CHMO S7 in <i>Synechococcus</i> PCC 11901
NEB stable	pUC19_fadD_PPTaseEC	Amp	Genomic integration of PPTase from <i>E. coli</i> in <i>Synechococcus</i> PCC 11901
NEB stable	pICH_arto_ado_lacI	Amp+Strep	Genomic integration of PAD in <i>Synechococcus</i> PCC 11901 at alternative respiratory terminal oxidase (ARTO)
NEB stable	pICH_cox_ado_lacI	Amp+Strep	Genomic integration of PAD in <i>Synechococcus</i> PCC 11901 at aa3-type cytochrome-c oxidase complex (COX)
NEB stable	pICH_arto_ado	Amp+Strep	like 23, without lacI
NEB stable	pUC19_psbA2_ADO	Amp+Strep	like 17 without lacI
NEB stable	pUC19_psbA2_mapADO_lacI	Amp+Strep	like 17 but with mapADO
NEB stable	pICH_cox_mapADO_lacI	Amp+Strep	like 24 but with mapADO

6.4 PRIMER

Table 10 List of primers from this work. Abbreviation: GG - GoldenGate cloning

Name	Sequence	Comment
#1_NiCAR_seq_fwd_1	ATGTCGTAACCATCACCATCAC	For sequencing of EcPPTase and NiCAR
#2_NiCAR_seq_fwd_2	GCAAGGTAACCTCCAGCGT	For sequencing of EcPPTase and NiCAR
#3_NiCAR_seq_fwd_3	GCAAAAGACGCGAACCTGC	For sequencing of EcPPTase and NiCAR
#4_NiCAR_seq_fwd_4	GTTGGTTAACCATGTTCTGCCG	For sequencing of EcPPTase and NiCAR
#5_EcPPTase_seq_fwd_1	CATGGTCGATATGAAAACACGCATAC	For sequencing of EcPPTase
#6_Prha::EcPPTase_GG_fwd	CACTAGGGTCTCGAGATGGTCGATATGAAAACACGC	GG into pSHDY
#7_Prha::EcPPTase_GG_rev	CACTAGGGTCTCGAAAGGCCTGCCGCCAACGAC	GG into pSHDY
#8_Prha::NiCar_GG_fwd	GGTTTCGGTCTCCAGATGTCGTAACCATCAC	GG into pSHDY
#9_Prha::NiCAR_GG_rev	GGTTTCGGTCTCCATCTAGTAACCTCCACTACTCTAGTAttcattacgacc	GG into pSHDY
#10_pSHDY::EcPPTase_GG_fwd	CACTAGGGTCTCGATCTAGTAACCTCCACTACTCTAGTAttcattacgac	GG into pSHDY
#11_pSHDY::EcPPTase_GG_rev	CACTAGGGTCTCGCTTTAATCGTGTGGCACAGC	GG into pSHDY
#12_pSHDY::NiCAR_GG_fwd	GGTTTCGGTCTCCAAAGGCCTGCCGCCAACGAC	GG into pSHDY
#13_pSHDY::NiCAR_GG_rev	GGTTTCGGTCTCCCTTTACAGCAGTTGCAGCAG	GG into pSHDY
#14_pSHDY::EcPPTase_GG_fwd	CACTAGGGTCTCGATCTAGTAACCTCCACTACTCTAGTATTCATTA	GG into pSHDY HANDMADE
#15_Prha::EcPPTase_GG_rev	CACTAGGGTCTCGAAAACGAAAGGCTCAGTCGAAA	GG into pSHDY HANDMADE
#16_Prha::NiCar_GG_fwd	GGTTTCGGTCTCCAGATGTCGTAACCATCA	GG into pSHDY HANDMADE
#17_pSHDY::NiCAR_GG_rev	GGTTTCGGTCTCCCTTTACAGCAGTTGCAG	GG into pSHDY HANDMADE
#18_Prha::NiCAR_GG_rev	GGTTTCGGTCTCCATCTAGTAACCTCCACTACTCTAGTATTCATTA	GG into pSHDY HANDMADE
#19_Backbone_fwd	TACTATGGTCTCTAAAGGCCTGCCGCC	GG into pSHDY pRha optimized
#20_BioBrick_prefix	GAATTCGCGCGCCGCTTctagag	BioBrick forward
#21_BioBrick_suffix	TGCAGCGGCCGCTACTAGTA	BioBrick reverse
#22_CG_CAR_fwd	AGGTCTCTAATGtcgtactaccatcaccatc	CAR into CyanoGate
#23_CG_CAR_rev	AGGTCTCTAAGCtgcgctagtagacgag	CAR into CyanoGate
#24_CG_PPTase_fwd	AGGTCTCTAATGGTCGATATGAAAACACGCATA	PPTase into CyanoGate
#25_CG_PPTase_rev	AGGTCTCTAAGCTTAATCGTGTGGCACAG	PPTase into CyanoGate

#26_J23119_fwd	ttgacagctagctcagtc	For colony PCR and sequencing
#27_J23119v02_fwd	ttgacggctaggctc	For colony PCR and sequencing
#28_BBaTerm_rev	agcgaaataataaaaaagccgg	For colony PCR and sequencing
#29_CG_CAR_fwd_new	atcgaGGTCTCTAATGtcgtactaccatcacc	CAR into CyanoGate new
#30_CG_CAR_rev_new	tgcacGGTCTCTAAGCttacagcagttgca	CAR into CyanoGate new
#31_CG_PPTase_fwd_new	atcgaGGTCTCTAATGGTCGATATGAAAACACTACG	PPTase into CyanoGate new
#32_CG_PPTase_rev_new	tgcacGGTCTCTAAGCTTAATCGTGTGGCA	PPTase into CyanoGate new
#33_pPMQAK_fwd	agctttcgctaaggatgatttc	ColonyPCR for pPMQAK
#34_pPMQAK_rev	acaccttgccctttttgc	ColonyPCR for pPMQAK
#35_CAR_sep_rev	tacacGGTCTCtatggctcatcggca	Separating CAR for better efficiency
#36_CAR_sep_fwd	atcgaGGTCTCTacatattgcgggtcgat	Separating CAR for better efficiency
#37_Gibson1	gagaaagaggagaaataactaatgtcgtactaccatcacca	Gibbson Assemblby CAR
#38_gibson 2	gcttttatattctctaagcttacagcagttgcagcagtt	Gibbson Assemblby CAR
#39_gibson 3	aactgctgcaactgctgtaagcttagagaataaaaaagccaga	Gibbson Assemblby CAR
#40_gibson 4	tggtgatggtagtagacattagtagtttctcctctttctctagtag	Gibbson Assemblby CAR
#41_GA_BB_fwd	TAGTGGAGGTTACTAGATGGTCGATAT	Gibbson Assemblby pSHDY_pRha Backbone
#42_GA_BB_rev	ttcattacgaccagtctaaaaagcg	Gibbson Assemblby pSHDY_pRha Backbone
#43_GA_NiCAR_fwd	tcaggcgcttttagactggcgtaataaTACTAGAGTAGTGGAGGTTACTAGatgctgtactaccatcaccatcaccatcac	Gibbson Assemblby pSHDY_pRha NiCAR
#44_GA_NiCAR_rev	GTCTTTGACTGAGCCTTTTCGTTTTATTTGttacagcagttgcagcagtt	Gibbson Assemblby pSHDY_pRha NiCAR
#45_GA_xxCAR_fwd	tcaggcgcttttagactggcgtaataaTACTAGAGTAGTGGAGGTTACTAGcatcaccatcaccatcacgattac	Gibbson Assemblby pSHDY_pRha Tv/Ds/MmCAR
#46_GA_xxCAR_rev	GTCTTTGACTGAGCCTTTTCGTTTTATTTGttaagctgcgctagtagacga	Gibbson Assemblby pSHDY_pRha Tv/Ds/MmCAR
#47_GA_xxCAR_fwd_2	tcaggcgcttttagactggcgtaataaTACTAGAGTAGTGGAGGTTACTAGATGcatcaccatcaccatcacgattac	Gibson Ass. WITH startcodon
#48_pRha_seq	agactggcgtaataaTAC	For Rha sequencing
#49_J23119fwd	TCCTTAGCTTTTCGCTAAGGATGATTTCTGGTtgacagctagctcagt	constructing
#50_J23119rev	tgatgggtgatgggtgatggtagtagacatttagtatttctcctctttctctag	pPMQAK1_J21339_CARni_ecPPTase
#51_CAR_fwd	cacatactagagaaaggaggagaaataactaaatgtcgtactaccatc	constructing
#52_CAR_rev	tcatatcgaccattagtagtttctcctctttcgttcaaatttcgcagca	pPMQAK1_J21339_CARni_ecPPTase
		constructing
		pPMQAK1_J21339_CARni_ecPPTase

#53_PPTase_fwd	taaagaaaccgctgctgcgaaatttgaacgaaagaggagaaataactaatggctcgatatgaaaactacg	constructing
#54_PPTase_rev	ttaatcgtgttgccacagCCTTCGTTTTATTTGATGCCTGGTACTAG	pMQAK1_J21339_CARni_ecPPTase
#55_PPTase_rev	agCCTTCGTTTTATTTGATGCCTGGTACTAGttaatcgtgttgccac	FALSE!!!
#56_xxCAR_rev	tcatatcgaccattagtatttctcctctttttattgctcagcgggtg	constructing
#57_xxPPTase_fwd	acctaggctgctgccaccgctgagcaataaaaagaggagaaataactaatggctcgatatgaaaactacg	pMQAK1_J21339_CARni_ecPPTase
#58niCAR_fwd	tttttagactggctgtaataaTACTAGAGTAGTGGAGGTTACTAGatgctgtactaccatca	constructing
#59pSHDY_rev	tgatggttagtacacatCTAGTAACCTCCACTACTCTAGTAttcattacgaccagtctaaaaa	pMQAK1_J21339_CARxx_ecPPTase
#60pSHDY_fwd	ctgcaactgctgtaaTAGTGGAGGTTACTAGATGGT	constructing
#61niCAR_rev	ACCATCTAGTAACCTCCACTAttacagcagttgcag	pMQAK1_J21339_CARxx_ecPPTase
#62 Kan_fwd	tttatactcgagagcggccgaagctagtcgaacgaccgag	GibsonAssembly into pSHDY_pRha_PPTase
#63 Kan_rev	tgttcacaatttgctgaattgtggctctagtaacgacctgccc	GibsonAssembly into pSHDY_pRha_PPTase
#64 psbA2_rev	tggcaggcgagacaac	GibsonAssembly into pSHDY_pRha_PPTase
#65 psbA2_fwd	aattagtgtaggagatcaccgttga	GibsonAssembly into pSHDY_pRha_PPTase
#66 fadD_fwd	tcaggtcaatgacattgccac	GA Kanamycin into pSHDY_pRha
#67 FadD_rev	accagattatcgcccactttc	GA Kanamycin into pSHDY_pRha
#68 pclac_fwd	ccaactcataaagtcaagtaggag	Check Insertion in PCC11901
#69 term_rev	cttcctttcgggctttgtta	Check Insertion in PCC11901
#70 ADO in psbA2_fwd	gccatatcgaaggtcgtcatATGGCTCACATCCACGATCT	Check Insertion in PCC11901
#71 ADO in psbA_rev	ctgccaagcaccgcccctcgTTAAACACCGTTGGAACCGTTTTGG	for sequencing in PCC11901
#72 psbA for ADO_fwd	ACGGTTCCAACGGTGTTAACgagggcgggtgctttg	for sequencing in PCC11901
#73 psbA for ADO_rev	AGATCGTGGATGTGAGCCATatgacgaccttcgatatggcc	ADO for insertion into psbA2
#74 PAD into fadD_fwd	tcaagtaggagattaattccATGAAAACCCTGGAAGAATTTTTGGG	ADO for insertion into psbA2
#75 PAD into fadD_rev	gtttgtacaagaaatctagaTTAGGAAAACCTTGAGTTTGCCTGAACG	Backbone for ADO insertion
#76 fadD for PAD_fwd	GCAAACCTCAAGTTTTCCTAAtctagatttctgtacaaactcggcc	Backbone for ADO insertion
#77 fadD for PAD_rev	AATTCTCCAGGGTTTTCATggaattaatctcctacttgactttatgagt	PAD insertion into fadD
#78 M13/pUC Forward	CCCAGTCACGACGTTGTAAAACG	PAD insertion into fadD
#79 M13/pUC Reverse	AGCGGATAACAATTTACACAGG	Backbone for PAD insertion
#80 PPTase in fadA_fwd	tcaagtaggagattaattccatggctcgatatgaaaactacgcatacctcc	Backbone for PAD insertion
		For genome insert
		For genome insert
		PPTase in fadA in PCC11901

#81 PPTase in fadA_rev	gtttgtacaagaaatctagattaatcgtgttgccacagcgt
#82 fadA_PPTase_fwd	cgctgtgccaaacacgattaatctagatttctgtacaaactcggcc
#83 fadA_PPTase_rev	gtagtttcatatcgaccatggaattaatctcctacttgactttatgag
#84 CAR in psbA_fwd	gccatatacgaaggctgctcatatgtcgtactaccatcaccatcacc
#85 CAR in psbA_rev	ctgccaaagcaccgccctcgttacagcagttgcagcagttcc
#86 psbA_Car_fwd	aactgctgcaactgctgtaacgagggcggtgctt
#87 psbA_Car_rev	tggtgatggtagtagacatatgacgaccttcgatatggcc
#88 ADO_for_psbA_fwd2	tcaagtaggagattaattccATGGCTCACATCCACGATCT
#89_psbA_forADO_rev2	AGATCGTGGATGTGAGCCATggaattaatctcctacttgactttatgagttgg
#90_plcac_to_p7_fwd	taatacgactcactataggtgtgtggaattgtgagcgga
#91 pcalc_to_p7_rev	cctatagtgagtcgtattagaattccgaattgtgagcgctC
#92 PAD_in_pet28_fwd	TGATGATGATGGCTGCTGCCTTAGGAAAACCTTGAGTTTGCCTGAACG
#93 PAD_in_pET28_rev	CTTTAAGAAGGAGATATACCATGAAAACCCTGGAAGAATTTTGGG
#94 acsA_fwd	gcaatgctgagatgacctc
#95 acsA_rev	agtaaatcagagacagaaacctc
#96 CG_PAD_fwd	gaaacctgctGAAGACATAATGAAAACCCTGGAAGAATTTTGG
#97 CG_PAD_rev	attacgtctcGAAGACATCGAATAGGAAAACCTTGAGTTTGCCTGAAC
#98 CG_ADO_fwd	gaaacctgctGAAGACATAATGGCTCACATCCACGATC
#99 CG_ADO_rev	attacgtctcGAAGACATCGAATTAAACACCGTTGGAACCGTTTT
#100_FKO_PADL1_fwd	atcgaGGTCTCAATGAAAACCCTGGAAGAATTT
#101_FKO_PADL1_rev	atcgaGGTCTCAAGCTTAGGAAAACCTTGAGTTTGC
#102_FKO_ADOL1_fwd	atcgaGGTCTCaATGGATGGCTCACATC
#103_FKO_ADOL1_rev	atcgaGGTCTCAAGCTTAAACACCGTTGGAAC
#104_ADO_fwd	catgctaaggaggttttctAATGGCTCACATCCACG
#105_ADO_rev	gcttttatattctctaagcTAAACACCGTTGGAACCG
#106_ADO_BB_fwd	ACGGTTCCAACGGTGTTTAAgcttagagaataaaaaagccagattat
#107_ADO_BB_rev	GATCGTGGATGTGAGCCATTaagaaaacctccttagcatgatta
#108_PAD_fwd	catgctaaggaggttttctAATGAAAACCCTGGAAGAATTTTG
#109_PAD_rev	gcttttatattctctaagcTTAGGAAAACCTTGAGTTTGCCT
#110_PAD_BB_fwd	GCAAACCTCAAGTTTTCTAAgcttagagaataaaaaagccagattattaatcc

PPTase in fadA in PCC11901
PPTase in fadA in PCC11901
PPTase in fadA in PCC11901
CAR in psbA PCC11901
CAR in psbA PCC11901
CAR in psbA PCC11901
CAR in psbA PCC11901
ADO for insertion into psbA2 no His_Tag
Backbone for ADO insertion no His_Tag
switch Pclac promoter to p7 (from syn to ecoli
switch Pclac promoter to p7 (from syn to ecoli
insert PAD (syn_opt) in PET28a+
insert PAD (syn_opt) in PET28a+
for colony PCR of delta_acsA
for colony PCR of delta_acsA
CyanoGate for PAD
CyanoGate for PAD
CyanoGate for ADO
CyanoGate for ADO
CyanoGate for PAD LVL1
CyanoGate for PAD LVL1
CyanoGate for ADO LVL1
CyanoGate for ADO LVL1
Gibson Assembly ADO into pPMQAK
Gibson Assembly ADO into pPMQAK
Gibson Assembly ADO into pPMQAK
Gibson Assembly PAD into pPMQAK
Gibson Assembly PAD into pPMQAK
Gibson Assembly PAD into pPMQAK

#111_PAD_BB_rev	AATTCTTCCAGGGTTTTTCATTaaaaacctccttagcatgat
#112_ADOintoPAD_insert_fwd	tgggctgcttcctaatgcagctctggacatctccaaaC
#113_ADOintoPAD_insert_rev	cgctctcccttatgc
#114_ADOintoPAD_BB_rev	ctgcattaggaagcagccca
#115_ADOintoPAD_BB_fwd	gagtcgcataagggaga
#116_CHMOinfad_fwd	tcaagtaggagattaattccAatgagccagaagatggactttg
#117_CHMOinfad_rev	gtttgtacaagaaatctagacgcgttcgcccgttg
#118_faddforCHMO_rev	agtcctatcttctggctcatTggaattaatctcctacttgacttt
#119_fadforCHMO_fwd	ttaaacaaccggcgaacgcgtctagatttctgtacaaactcg
#120_ADOforFADD_fwd	tcaagtaggagattaattccATGGCTCACATC
#121_ADOforFADD_rev	gtttgtacaagaaatctagaTTAAACACCGTTGGAACCGTTTT
#122_FADDforAD0_fwd	ACGGTCCAACGGTGTTTAAtctagatttctgtacaaactcgccc
#123_FADDforAD0_rev	AGATCGTGGATGTGAGCCATggaattaatctcctacttgactttatgagt
#124_ADOintoNS2_fwd	agacgcctgcgccttcttcttctggacatctccaaac
#125_ADOintoNS2_rev	aaattcgctttgcagaaactttgaaaaactcatcgagc
#126_NS2forADO_fwd	tgctcgatgagttttctaaagtttctgcaaagcg
#127_NS2forADO_rev	ttcgtttggagatgtccagaagaagaaggcgag
#128_ARTO_LF	ATCGAGGTCTCAGGAGCGGAAACCAACCAGAGAAATT
#129_ARTO_LR	AGCTCGGTCTCTTCATGTAATCGCTCACAAACCATGACC
#130_ARTO_RF	TGCACGGTCTCAATAACATTGGTCACTAAAGCCTCTTG
#131_ARTO_RR	GCTCAGGTCTCTAGCGTGTATGTCCACGGCACTTTG
#132_COX_LF	ATCGAGGTCTCAGGAGCCTTTAGTGGTTGACGTGAA
#133_COX_LR	AGCTCGGTCTCTTCATTGCAAGTTCTGTGCGGACA
#134_COX_RF	TGCACGGTCTCAATAAGATGAACCGCCGCATTGCC
#135_COX_RR	GCTCAGGTCTCTAGCGATCAGTGCCGTAATCCCGAA
#136_COXfor	AGGCAATGTTCCCCTAGAGA
#137_COXrev	ACCCCGTCAGCACATAGAAA
#138_ARTOfor	CGAAGAGTAACATCACCGCC
#139_ARTOrev	ATACGATGATTGGCACGGC

Gibson Assembly PAD into pPMQAK

Add ADO into fadD:PAD with ONETAQ pol

Add ADO into fadD:PAD with ONETAQ pol

Add ADO into fadD:PAD with ONETAQ pol

Add ADO into fadD:PAD with ONETAQ pol

CHMO into fadD with OneTaq

CHMO into fadD with OneTaq

CHMO into fadD with OneTaq

CHMO into fadD with OneTaq

Add ADO into fadD

Add ADO into fadD

Add ADO into fadD

Add ADO into NS2 from 7002

Add ADO into NS2 from 7002

Add ADO into NS2 from 7002

Add ADO into NS2 from 7002

integrating ARTO into CyanoGate

integrating ARTO into CyanoGate

integrating ARTO into CyanoGate

integrating ARTO into CyanoGate

integrating COX into CyanoGate

integrating COX into CyanoGate

integrating COX into CyanoGate

integrating COX into CyanoGate

Check for integration

Check for integration

Check for integration

Check for integration

#140 CG_ado_fwd	AGCTCGGTCTCTATGAgactccccctctggacatctc	adding ado between ARTO/COX into CyanoGate Kit
#141 CG_ado_rev	AGCTCGGTCTCATTATacattaattgcgttgcgctc	adding ado between ARTO/COX into CyanoGate Kit
#142 CG_ado_rev	AGCTCGGTCTCATTATAAACGGATGAAGGCACGAAC	adding ado between ARTO/COX into CyanoGate Kit
#143 lacI deletion	TTATTGCCGACTACCTTG	deleting lacI from psbA::ado (rev. Primer: #113)
#144 mapADO_fwd	tcaagtaggagattaattccATGCACCATCATCATCACGCT	
#145 mapADO_rev	ctgccaaagcaccgccctcgTTAAGCGTCGGGATCGTATGGGGA	
#146 BB_mapADO_fwd	CATACGATCCCCGACGCTTAACgagggcggtgctttg	
#147 BB_mapADO_rev	TGATGATGATGATGGTGCATggaattaatctcctacttgactttatgagttg	
#148 niCAR ARTO fwd	tcaagtaggagattaattccatgctgtactaccatcacca	
#149 niCAR ARTO rev	cattaattgcgttgcgctcattacagcagttgcagcag	
#150 BB_ARTO niCAR fwd	aactgctgcaactgctgtaatgagcgcaacgcaa	
#151 BB_ARTO niCAR rev	tggtgatggtagtacgacatggaattaatctcctacttgact	
#152 YqjM ARTO fwd	tcaagtaggagattaattccatggccagaaaattttacacctattac	
#153 YqjM ARTO rev	ctgccaaagcaccgccctcgccagcctcttctgtattgaac	
#154 BB_ARTO YqjM fwd	ttcaatacgaaagaggctggcgagggcggtgc	
#155 BB_ARTO YqjM rev	gtaaataattttctggccatggaattaatctcctacttg	
#156 YqjMinFadA_fwd	tcaagtaggagattaattccatggccagaaaattttacacctattac	
#157 YqjMinFadA_rev	cttcctttcgggctttgttaccagcctcttctgtattgaac	
#158 fadAfor YqjM_fwd	ttcaatacgaaagaggctgtaacaaagcccgaaggaag	
#159 fadAforYqjm_rev	gtaaataattttctggccatggaattaatctcctacttgactttatgag	
#160 mapADOforfadA_fwd	tcaagtaggagattaattccATGCACCATCATCATCAC	YqjM into fadA
#161 mapADOforfadA_rev	cttcctttcgggctttgttaTTAAGCGTCGGGATCGTAT	YqjM into fadA
#162 fadAformapADO_fwd	CATACGATCCCCGACGCTTAAtacaaagcccgaaggaag	fadA for YqjM
#163 fadAformapADO_rev	TGATGATGATGATGGTGCATggaattaatctcctacttgactttatgagttg	fadA for YqjM
#164 mapADOforQAK_fwd	catgctaaggaggttttctAATGCACCATCATCATCAC	mapADO for fadA
#165 mapADOforQAK_rev	gctttttatattctctaagcTTAAGCGTCGGGATCGTATG	mapADO for fadA
		fadA for mapADO
		fadA for mapADO
		mapdADO for pPMQAK
		mapdADO for pPMQAK

#166 QAKformapADO_fwd	CATACGATCCCGACGCTTA	Agcttagagaatataaaaagccagattattaatcc	mapdADO for pPMQAK
#167 QAKformapADO_rev	TGATGATGATGATGGTGCATT	agaaaacctccttagcatgattaagatg	mapdADO for pPMQAK
#168 pad for pet28mADO_fwd	CCTCGACCCCCAAAAA	CTTGATTAGGGTGATAATACGACTCACTATAGGGGAATTGTGAG	
#169 pad for pet28mADO_rev	AAAGAACGTGGACTCCAAC	GTCAAAGGGCGCAAAAACCCCTCAAGACCCG	
#170 pet28mADOfor pad_fwd	GCCTCTAAACGGGTCTTG	AGGGGTTTTTTCGCCCTTTGACGTTGGAGTCC	
#171 pet28mADO for pad_rev	CTCACAATTCCCCTATAGT	GAGTCGTATTATCACCCCTAATCAAGTTTTTGGGGT	

6.5 PYTHON SCRIPT FOR FLUX BALANCE ANALYSIS

The script was written in Python 3.0 and executed in the Spyder IDE Version 5.^{258,318}

```

# -*- coding: utf-8 -*-

"""

Created on Mon Jan 27 15:39:34 2020

@author: trohr

"""

from __future__ import print_function

import csv

import matplotlib.pyplot as plt

import cobra

import cobra.test

from pandas import Series, DataFrame

import cameo

import os

#set working directory

#For Home

#os.chdir("C:/Users/tom/Dropbox/phd/")

#for work

os.chdir("C:/Users/trohr/Dropbox/phd/")

# add function from https://gist.github.com/Midnighter/6ac96204f433c0ab8d99a91ff5721fd1

# lists all fluxes of one metabolites


def metabolite_flux_balance(metabolite, solution):

    """

    Return a vector of reaction fluxes scaled by the stoichiometric coefficient.

    Parameters
    -----

    metabolite : cobra.Metabolite

        The metabolite whose fluxes are to be investigated.

    solution : cobra.Solution

        Solution with flux values.

    Returns
    -----

    pandas.Series
    
```

A vector with fluxes of reactions that consume or produce the given metabolite scaled by the corresponding stoichiometric coefficients. The reaction identifiers are given by the index.

```
"""
```

```
rxn_ids = list()
```

```
adj_flux = list()
```

```
for rxn in metabolite.reactions:
```

```
    coef = rxn.get_coefficient(metabolite)
```

```
    rxn_ids.append(rxn.id)
```

```
    adj_flux.append(coef * solution.fluxes[rxn.id])
```

```
return Series(data=adj_flux, index=rxn_ids, dtype=float, name="reaction")
```

```
# Import Model and check
```

```
model_syn = cobra.io.read_sbml_model("GSM Syn2973/srep41569-s3.xml")
```

```
print(len(model_syn.reactions))
```

```
print(len(model_syn.metabolites))
```

```
print(len(model_syn.genes))
```

```
print(model_syn.compartments)
```

```
print(model_syn.metabolites.cpd00004_c.summary()) #check NADPH
```

```
print(model_syn.metabolites.cpd00002_c.summary()) #check ATP
```

```
# adding new metabolites
```

```
# adding aromatic carboxylic acid
```

```
cpd00539_c = cobra.Metabolite(
```

```
    "cpd00539_c",
```

```
    formula = "C7H6O2",
```

```
    name = "aromatic acid",
```

```
    compartment = "c") #adding new metabolites
```

```
model_syn.add_metabolites([cpd00539_c])
```

```
model_syn.metabolites.get_by_id("cpd00539_c") #Check
```

```
# adding carboxylic acid as external
```

```
cpd00539_e = cobra.Metabolite(
    "cpd00539_e",
    formula = "C7H6O2",
    name = "aromatic acid",
    compartment = "e") #adding new metabolites
```

```
model_syn.add_metabolites([cpd00539_e])
model_syn.metabolites.get_by_id("cpd00539_e") # Check
```

```
# Adding CAR reaction to model
```

```
CAR = cobra.Reaction("rxn01490")
CAR.name = "carboxylate reductase"
CAR.lowerbound = 1000
CAR.lowerbound = -1000
CAR.gene_reaction_rule = '( NiCAR )'
CAR.add_metabolites({
    model_syn.metabolites.get_by_id("cpd00539_c"): -1,
    model_syn.metabolites.get_by_id("cpd00005_c"): -1,
    model_syn.metabolites.get_by_id("cpd00080_c"): -1,
    model_syn.metabolites.get_by_id("cpd00002_c"): -1,
    model_syn.metabolites.get_by_id("cpd00193_c"): 1,
    model_syn.metabolites.get_by_id("cpd00006_c"): 1,
    model_syn.metabolites.get_by_id("cpd00020_c"): 1,
    model_syn.metabolites.get_by_id("cpd00013_c"): 1})
```

```
model_syn.add_reactions([CAR])
print(model_syn.reactions.get_by_id("rxn01490"))
print(model_syn.genes.get_by_id("NiCAR"))
```

```
# adding carboxylate uptake to model
```

```

print(model_syn.summary())

CA_in = cobra.Reaction("rxn9999")
CA_in.name = "carboxylate intake"
CA_in.lowerbound = 1000
CA_in.lowerbound = -1000
CA_in.gene_reaction_rule = '(carboxylate intake)'
CA_in.add_metabolites({
    model_syn.metabolites.get_by_id("cpd00539_c"): 1,
    model_syn.metabolites.get_by_id("cpd00539_e"): -1})

model_syn.add_reactions([CA_in])
print(model_syn.reactions.get_by_id("rxn9999"))

model_syn.add_boundary(model_syn.metabolites.cpd00539_e, type = "exchange", lb = -1000, ub = 1000)

model_syn.objective = "rxn01490"
model_syn.optimize()
model_syn.optimize().objective_value

print(model_syn.summary()) # How does the reaction influence growth rate and flux
model_syn.objective = "Biomass_Auto_2973"
model_syn.optimize()
model_syn.optimize().objective_value

###listing and printing all reactions of NADPH

nadph_c = model_syn.metabolites.get_by_id("cpd00004_c")
nadph_c_reactions = open("GSM models/nadph_c.txt", "r+")
for x in nadph_c.reactions:
    nadph_c_reactions.write(str("%s : %s" % (x.id, x.reaction)))
    nadph_c_reactions.write("\n")
nadph_c_reactions.close
    
```



```
# listing and printing all reactions with ATP

atp_c = model_syn.metabolites.get_by_id("cpd00002_c")
atp_c_reactions = open("GSM models/list of atp.txt", "r+")
for x in atp_c.reactions:
    atp_c_reactions.write(str("%s : %s" % (x.id, x.reaction)))
    atp_c_reactions.write("\n")
atp_c_reactions.close
```

```
### TRADE-OFF plot by AnnaGermann ####
```

```
model_syn.objective = "Biomass_Auto_2973"
model_syn.optimize()
```

```
maxi = model_syn.optimize().objective_value
print(maxi)

maxi
maxlist = []

x = 0
```

```
while x <= maxi:
    maxlist.append(x)
    x+=0.0999*maxi
print(maxlist)
```

```
model_syn.objective = "rxn01490"
```

```
xwerte = []
y01490 = []
```

```
model_syn.reactions.rxn01490
```

```
for x in maxlist:
```

```

model_syn.reactions.Biomass_Auto_2973.lower_bound = x

model_syn.optimize()

xwerte.append(x)

y01490.append(model_syn.reactions.rxn01490.x)


print(xwerte)
print(y01490)


ax = plt.subplot(111)
ax.plot(xwerte,y01490, color = "black")
#ax.scatter(xwerte,y01490)
plt.ylim(0,max(y01490))
plt.xlim(0,max(xwerte))
plt.xlabel("Biomass [h-1]")
plt.ylabel("CAR Flux [mMol*(gDW*h)-1]")
ax.fill_between(xwerte,y01490, alpha = 0.1, fc = "green")
plt.savefig("Trade-off plot 2", dpi=600, replace = True)


###Knocking out all ATP reactions subsequently and plot###
model_syn.objective = "Biomass_Auto_2973"


atp_c_knock_outs = DataFrame(columns = ["Reaction", "Growth Rate", "CAR flux"])


for i in atp_c.reactions:
    with model_syn:
        flux = ()
        fba_soltuion = ()
        i.knock_out()
        fba_solution = model_syn.optimize()
        flux = (i,fba_solution.objective_value,fba_solution.fluxes["rxn01490"])
        atp_c_knock_outs.loc[len(atp_c_knock_outs)] = flux
    print(i.bounds)
print(atp_c_knock_outs)


ax = plt.subplot(111)

```

```

#ax.plot(xwerte,y01490, color = "black")

ax.scatter(atp_c_knock_outs["Growth Rate"], atp_c_knock_outs["CAR flux"], marker = "x", color = "black")

ax.fill_between(xwerte,y01490, alpha = 0.1, fc = "c")

plt.ylim(-0.01,max(y01490)+0.01)

plt.xlim(-0.01,max(xwerte)+0.01)

plt.xlabel("Biomass [h-1]")

plt.ylabel("CAR Flux [mMol*(gDW*h)-1]")

plt.savefig("ATP KO Trade-off plot", dpi=600, replace = True)

###Knocking out all NADPH subsequently reactions and plot###

```

```

nadph_c_knock_outs = DataFrame(columns = ["Reaction", "Growth Rate", "CAR flux"])

```

```

for i in nadph_c.reactions:

    with model_syn:

        flux = ()

        i.knock_out()

        model_syn.optimize()

        fba_solution = model_syn.optimize()

        flux = (i,fba_solution.objective_value,fba_solution.fluxes["rxn01490"])

        nadph_c_knock_outs.loc[len(nadph_c_knock_outs)] = flux

        print(i.bounds)

    print(i.bounds)

print(nadph_c_knock_outs)

```

```

ax = plt.subplot(111)

#ax.plot(xwerte,y01490, color = "black")

ax.scatter(nadph_c_knock_outs["Growth Rate"], nadph_c_knock_outs["CAR flux"], marker = "x", color = "black")

ax.fill_between(xwerte,y01490, alpha = 0.1, fc = "c")

plt.ylim(-0.01,max(y01490)+0.01)

plt.xlim(-0.01,max(xwerte)+0.01)

plt.xlabel("Biomass [h-1]")

plt.ylabel("CAR Flux [mMol*(gDW*h)-1]")

plt.savefig("NADPH KO Trade-off plot", dpi=600, replace = True)

```

```

### exporting knock out list in csv-file

atp_c_knock_outs.to_csv("GSM models/atp_knocuouts.csv", header = True)

nadph_c_knock_outs.to_csv("GSM models/nadph_knocuouts.csv", header = True)


###Knock out EVERY gene and check growth and flux###
"""

sim_knock_outs = DataFrame(columns = ["Reaction", "Growth Rate", "CAR flux"])

for i in model_syn.reactions:

    #if model_syn.optimize().fluxes[i] < 0:

        with model_syn:

            flux = ()

            i.knock_out()

            model_syn.optimize()

            fba_solution = model_syn.optimize()

            flux = (i,fba_solution.objective_value,fba_solution.fluxes["rxn01490"])

            sim_knock_outs.loc[len(sim_knock_outs)] = flux

            print(i.bounds)

        print(i.bounds)

    print(sim_knock_outs)

"""

###OPTKNOCK###

#setup = cobra.design.design_algorithms.set_up_optknock(model_syn,chemical_objective = "rxn01490",
knokable_reactions = model_syn.reactions, biomass_objective = "Biomass_Auto_2973", copy = True)

```

7 CONTRIBUTIONS TO THIS THESIS

Thomas Rohr and Florian Rudroff were involved in the conception and design of the study.

Thomas Rohr performed the overall experimental work and collected all the data.

Astrid Schiefer (TU Wien) and Lukas Schober (TU Graz) identified the enzyme *mapADO* and performed experiments concerning the substrate scope, kinetics, pH stability, and product inhibition.

Nina Biedermann and Astrid Schiefer did NMR analysis and data interpretation.

Thomas Rohr did the final data analysis and interpretation.

8 PUBLICATIONS RESULTING FROM THIS THESIS

Jodlbauer, J.*; Rohr, T.*; Spadiut, O.; Mihovilovic, M. D.; Rudroff, F.

Biocatalysis in Green and Blue: Cyanobacteria.

Trends Biotechnology, 2021, 39 (9), 875–889.

* with equal contributions

Jodlbauer, J; Schmal, M, Walzl, C; Rohr, T; Mach-Aigner, A, R; Mihovilovic, M,D; Rudroff, F

Unlocking the potential of cyanobacteria: a high-throughput strategy for enhancing biocatalytic performance through genetic optimization

Trends in Biotechnology, 08/2024

8.1 POSTER PRESENTATIONS

Biotrans 2021, Graz, Austria

Biocatalysis in green and blue: Cyanobacteria

Thomas Rohr, Ilka Axmann, Florian Rudroff

Cyano2022 - 7th Early Career Researcher Symposium on Cyanobacteria

September 26-28, 2022; Leipzig, Germany

Biocatalysis in green and blue: Cyanobacteria

Thomas Rohr, Ilka Axmann, Florian Rudroff

14th Workshop on cyanobacteria, CyanoCon

June, 2022, Michigan, USA

BIOCATALYSIS IN GREEN AND BLUE: SYNECHOCOCCUS PCC11901 AS A NEW WORKHORSE

Thomas Rohr, Ilka Axmann, Florian Rudroff

Biotrans2023 - 16th International Symposium on Biocatalysis & Biotransformations

June 25-29, 2023; La Rochelle, France

BIOCATALYSIS IN GREEN AND BLUE: SYNECHOCOCCUS PCC11901 AS A NEW WORKHORSE?

Thomas Rohr, Ilka Axmann, Florian Rudroff

The 6th Multi Enzyme Catalyzed Processes Conference, MECP

April, 2024, Vienna, Austria

BIOCATALYSIS IN GREEN AND BLUE: SYNECHOCOCCUS PCC11901 AS A NEW WORKHORSE?

Thomas Rohr, Florian Rudroff

9 CURRICULUM VITAE



Thomas Rohr

Date of birth: 26/06/1991

Martinstraße 38/8

1180 Vienna, Austria

E-mail: tom.rohr@gmx.net

Study

- Since 09/2019 PhD student at TU Wien, Institut für Bioorganische Synthesechemie, under the supervision of Prof. Dr. Florian Rudroff
- 04/2017 – 05/2019 **Master of Science in Biology**, Major in Systems Biotechnology (grade 1,8), at Heinrich-Heine-University Düsseldorf; Topic of Master-thesis: *CoilHack – Synthetic Modulation of Supercoiling as global Regulator in Escherichia coli W3110Z1*
- 09/2016 – 03/2017 **Master of Science in Bio- and Process-engineering** at Trier University of Applied Sciences (unfinished)
- 09/2011 – 10/2015 **Bachelor of Science in Applied Biology** (Grade 2,3) at the University of Applied Sciences Bonn Rhein-Sieg in Rheinbach; topic of Bachelor-Thesis: *Impact of Glucosinolates and their Breakdown-Products on the Microbiome in Soil* (Grade 1,0),

History

- Since 09/2018 **Working Student at NUMAFERM GmbH**, Merowingerplatz 1a, 40225 Düsseldorf

10/2017 – 02/2018	Intern at Artes Biotechnologies , Elisabeth-Selbert-Straße 9, 40764 Langenfeld
05/2017 – 08/2017	Working Student at RheinCell Therapeutics GmbH , Berghausener Straße 98, 40764 Langenfeld
12/2015 – 01/2016	Assistant in Production at Alpha Laboratories (NZ) Ltd. , Auckland, New Zealand
08/2011 – 09/2015	Groupleader at „Verein zu Förderung der städtischen Kinder und Jugendeinrichtungen“ , Wellenstraße 18, 53757 Sankt Augustin
07/2010 – 07/2011	Community Service at Helios Klinikum Siegburg, Department for Cardiovascular Surgery, Ringstraße 49, 53721 Siegburg

School

06/2010	Abitur at Antoniuskolleg Neunkirchen-Seelscheid, Pfarrer-Schaaf-Straße 1, 53819 Neunkirchen-Seelscheid
---------	---

Stays abroad

11/2015 – 04/2016	Work and Travel in New Zealand
07/2013 – 12/2013	Semester abroad at Høgskolen i Sør-Trøndelag, Trondheim, Norway

Miscellaneous

Since 09/2016	Volunteering at Viva con Agua de Sankt Pauli e.V. , organization of donation campaigns and education on the topic of clean drinking water
01/2012 – 07/2015	Volunteering at CVJM Siegburg , organization of holiday camps for children as educator and cook
01/2007 – 01/2009	Volunteering at Johanniter-Unfall-Hilfe Much as First-Aider

Scientific Skills

Microbiology

Cloning	Restriction and Ligation, Gibson Assembly, Primer Extension PCR, Golden Gate Cloning, AQUA cloning
Cell Culture	Handling and transformation of HEK and CHO

Analytics

Protein	SDS-PAGE, Western Blot, Dot Blot, Bradford/BCA-Assay, Dynamic Light Scattering
Chromatography	GC-MS, Tandem MS (Q-ToF), Size-Exclusion-chromatography, Ion-exchange, IEF
Programming	Basics in R and Python
IT knowledge	Experienced in common MS Office applications , such as Word, Excel and Power Point

Language skills

German	Mother tongue
English	Fluent
Norwegian	Basics
French	Basics

Interests

Climbing, Acroyoga, Pen and Paper games, Jogging, Traveling

10 REFERENCES

1. Sánchez-Baracaldo, P., Bianchini, G., Wilson, J. D. & Knoll, A. H. Cyanobacteria and biogeochemical cycles through Earth history. *Trends Microbiol.* **30**, 143–157 (2022).
2. Lyons, T. W., Reinhard, C. T. & Planavsky, N. J. The rise of oxygen in Earth's early ocean and atmosphere. *Nature* **506**, 307–315 (2014).
3. Chen, M.-Y. *et al.* Comparative genomics reveals insights into cyanobacterial evolution and habitat adaptation. *ISME J.* **15**, 211–227 (2021).
4. Kaneko, T. *et al.* Sequence Analysis of the Genome of the Unicellular Cyanobacterium *Synechocystis* sp. Strain PCC6803. II. Sequence Determination of the Entire Genome and Assignment of Potential Protein-coding Regions. *DNA Res.* **3**, 109–136 (1996).
5. Mareš, J., Strunecký, O., Bučinská, L. & Wiedermannová, J. Evolutionary Patterns of Thylakoid Architecture in Cyanobacteria. *Front. Microbiol.* **10**, 277 (2019).
6. Zedler, J. A. Z. Photosynthetic Proteins in Cyanobacteria: from Translocation to Assembly of Photosynthetic Complexes. in *Endosymbiotic Organelle Acquisition* (eds. Schwartzbach, S. D., Kroth, P. G. & Oborník, M.) 323–348 (Springer International Publishing, Cham, 2024). doi:10.1007/978-3-031-57446-7_11.
7. Baers, L. L. *et al.* Proteome Mapping of a Cyanobacterium Reveals Distinct Compartment Organization and Cell-Dispersed Metabolism. *Plant Physiol.* **181**, 1721–1738 (2019).
8. Guglielmi, G., Cohen-Bazire, G. & Bryant, D. A. The structure of *Gloeobacter violaceus* and its phycobilisomes. *Arch. Microbiol.* **129**, 181–189 (1981).
9. Larkum, A. W. D. & Barrett, J. Light-harvesting Processes in Algae. in *Advances in Botanical Research* vol. 10 1–219 (Elsevier, 1983).
10. Chen, M. *et al.* A Red-Shifted Chlorophyll. *Science* **329**, 1318–1319 (2010).

11. Sandmann, G. Diversity and origin of carotenoid biosynthesis: its history of coevolution towards plant photosynthesis. *New Phytol.* **232**, 479–493 (2021).
12. Fuente, D., Lazar, D., Oliver-Villanueva, J. V. & Urchueguía, J. F. Reconstruction of the absorption spectrum of *Synechocystis* sp. PCC 6803 optical mutants from the in vivo signature of individual pigments. *Photosynth. Res.* **147**, 75–90 (2021).
13. *Photosynthesis in Algae: Biochemical and Physiological Mechanisms*. vol. 45 (Springer International Publishing, Cham, 2020).
14. Wiethaus, J., Busch, A. W. U., Dammeyer, T. & Frankenberg-Dinkel, N. Phycobiliproteins in *Prochlorococcus marinus*: Biosynthesis of pigments and their assembly into proteins. *Eur. J. Cell Biol.* **89**, 1005–1010 (2010).
15. Blankenship, R. E. & Prince, R. C. Excited-state redox potentials and the Z scheme of photosynthesis. *Trends Biochem. Sci.* **10**, 382–383 (1985).
16. Umena, Y., Kawakami, K., Shen, J.-R. & Kamiya, N. Crystal structure of oxygen-evolving photosystem II at a resolution of 1.9 Å. *Nature* **473**, 55–60 (2011).
17. Vinyard, D. J., Ananyev, G. M. & Charles Dismukes, G. Photosystem II: The Reaction Center of Oxygenic Photosynthesis. *Annu. Rev. Biochem.* **82**, 577–606 (2013).
18. *Cyanobacteria Biotechnology*. (Wiley-VCH, Weinheim, 2021).
19. Jodlbauer, J., Rohr, T., Spadiut, O., Mihovilovic, M. D. & Rudroff, F. Biocatalysis in Green and Blue: Cyanobacteria. *Trends Biotechnol.* (2021) doi:10.1016/j.tibtech.2020.12.009.
20. Howitt, C. A. & Vermaas, W. F. J. Quinol and Cytochrome Oxidases in the Cyanobacterium *Synechocystis* sp. PCC 6803. *Biochemistry* **37**, 17944–17951 (1998).

21. Mullineaux, C. W. Co-existence of photosynthetic and respiratory activities in cyanobacterial thylakoid membranes. *Biochim. Biophys. Acta BBA - Bioenerg.* **1837**, 503–511 (2014).
22. Lea-Smith, D. J., Bombelli, P., Vasudevan, R. & Howe, C. J. Photosynthetic, respiratory and extracellular electron transport pathways in cyanobacteria. *Biochim. Biophys. Acta BBA - Bioenerg.* **1857**, 247–255 (2016).
23. Allahverdiyeva, Y., Suorsa, M., Tikkanen, M. & Aro, E.-M. Photoprotection of photosystems in fluctuating light intensities. *J. Exp. Bot.* **66**, 2427–2436 (2015).
24. Latifi, A., Ruiz, M. & Zhang, C.-C. Oxidative stress in cyanobacteria. *FEMS Microbiol. Rev.* **33**, 258–278 (2009).
25. Holland, S. C., Kappell, A. D. & Burnap, R. L. Redox changes accompanying inorganic carbon limitation in *Synechocystis* sp. PCC 6803. *Biochim. Biophys. Acta BBA - Bioenerg.* **1847**, 355–363 (2015).
26. Bassham, J. A. *et al.* The Path of Carbon in Photosynthesis. XXI. The Cyclic Regeneration of Carbon Dioxide Acceptor ¹. *J. Am. Chem. Soc.* **76**, 1760–1770 (1954).
27. Sharkey, T. D. Discovery of the canonical Calvin–Benson cycle. *Photosynth. Res.* **140**, 235–252 (2019).
28. Badger, M. R. & Schreiber, U. Effects of inorganic carbon accumulation on photosynthetic oxygen reduction and cyclic electron flow in the cyanobacterium *Synechococcus* PCC7942. *Photosynth. Res.* **37**, 177–191 (1993).
29. Price, G. D. & Badger, M. R. Evidence for the role of carboxysomes in the cyanobacterial CO₂-concentrating mechanism. *Can. J. Bot.* **69**, 963–973 (1991).

30. Mrnjavac, N., Degli Esposti, M., Mizrahi, I., Martin, W. F. & Allen, J. F. Three enzymes governed the rise of O₂ on Earth. *Biochim. Biophys. Acta BBA - Bioenerg.* **1865**, 149495 (2024).
31. Huffine, C. A., Zhao, R., Tang, Y. J. & Cameron, J. C. Role of carboxysomes in cyanobacterial CO₂ assimilation: CO₂ concentrating mechanisms and metabolon implications. *Environ. Microbiol.* **25**, 219–228 (2023).
32. Rae, B. D. et al. Progress and challenges of engineering a biophysical CO₂-concentrating mechanism into higher plants. *J. Exp. Bot.* **68**, 3717–3737 (2017).
33. Burnap, R. L., Nambudiri, R. & Holland, S. Regulation of the carbon-concentrating mechanism in the cyanobacterium *Synechocystis* sp. PCC6803 in response to changing light intensity and inorganic carbon availability. *Photosynth. Res.* **118**, 115–124 (2013).
34. Calvin, K. et al. *IPCC, 2023: Climate Change 2023: Synthesis Report. Contribution of Working Groups I, II and III to the Sixth Assessment Report of the Intergovernmental Panel on Climate Change [Core Writing Team, H. Lee and J. Romero (Eds.)]. IPCC, Geneva, Switzerland. <https://www.ipcc.ch/report/ar6/syr/> (2023) doi:10.59327/IPCC/AR6-9789291691647.*
35. Al-Haj, L., Lui, Y., Abed, R., Gomaa, M. & Purton, S. Cyanobacteria as Chassis for Industrial Biotechnology: Progress and Prospects. *Life* **6**, 42 (2016).
36. Kriechbaum, R., Kronlachner, L., Limbeck, A., Kopp, J. & Spadiut, O. Towards a circular economy - Repurposing side streams from the potato processing industry by *Chlorella vulgaris*. *J. Environ. Manage.* **366**, 121796 (2024).
37. Demirbas, A. Progress and recent trends in biodiesel fuels. *Energy Convers. Manag.* **50**, 14–34 (2009).

38. Fabris, M. *et al.* Emerging Technologies in Algal Biotechnology: Toward the Establishment of a Sustainable, Algae-Based Bioeconomy. *Front. Plant Sci.* **11**, 279 (2020).
39. Begum, H., Yusoff, F. Md., Banerjee, S., Khatoon, H. & Shariff, M. Availability and Utilization of Pigments from Microalgae. *Crit. Rev. Food Sci. Nutr.* **56**, 2209–2222 (2016).
40. Barone, G. D. *et al.* Recent developments in the production and utilization of photosynthetic microorganisms for food applications. *Heliyon* **9**, e14708 (2023).
41. Park, H. J. *et al.* A Randomized Double-Blind, Placebo-Controlled Study to Establish the Effects of Spirulina in Elderly Koreans. *Ann. Nutr. Metab.* **52**, 322–328 (2008).
42. Kim, S. W. *et al.* Meeting Global Feed Protein Demand: Challenge, Opportunity, and Strategy. *Annu. Rev. Anim. Biosci.* **7**, 221–243 (2019).
43. Samantaray, S. & Mallick, N. Production and characterization of poly- β -hydroxybutyrate (PHB) polymer from *Aulosira fertilissima*. *J. Appl. Phycol.* **24**, 803–814 (2012).
44. Andres, J., Blomeier, T. & Zurbriggen, M. D. Synthetic Switches and Regulatory Circuits in Plants. *Plant Physiol.* **179**, 862–884 (2019).
45. Viola, S., Rühle, T. & Leister, D. A single vector-based strategy for marker-less gene replacement in *Synechocystis* sp. PCC 6803. *Microb. Cell Factories* **13**, 4 (2014).
46. Behle, A., Saake, P., Germann, A. T., Dienst, D. & Axmann, I. M. Comparative Dose-Response Analysis of Inducible Promoters in Cyanobacteria. *ACS Synth. Biol.* **9**, 843–855 (2020).

47. Johnson, T. J., Gibbons, J. L., Gu, L., Zhou, R. & Gibbons, W. R. Molecular genetic improvements of cyanobacteria to enhance the industrial potential of the microbe: A review. *Biotechnol. Prog.* **32**, 1357–1371 (2016).
48. Gale, G. A. R., Schiavon Osorio, A. A., Puzorjov, A., Wang, B. & McCormick, A. J. Genetic modification of cyanobacteria by conjugation using the cyanogate modular cloning toolkit. *J. Vis. Exp.* **2019**, 1–17 (2019).
49. Li, S., Sun, T., Xu, C., Chen, L. & Zhang, W. *Development and Optimization of Genetic Toolboxes for a Fast-Growing Cyanobacterium Synechococcus Elongatus UTEX 2973. Metabolic Engineering* vol. 48 (Elsevier Inc., 2018).
50. Lagarde, D., Beuf, L. & Vermaas, W. Increased Production of Zeaxanthin and Other Pigments by Application of Genetic Engineering Techniques to *Synechocystis* sp. Strain PCC 6803. *Appl. Environ. Microbiol.* **66**, 64–72 (2000).
51. Pagels, F., Vasconcelos, V. & Guedes, A. C. Carotenoids from Cyanobacteria: Biotechnological Potential and Optimization Strategies. *Biomolecules* **11**, 735 (2021).
52. Damrow, R., Maldener, I. & Zilliges, Y. The Multiple Functions of Common Microbial Carbon Polymers, Glycogen and PHB, during Stress Responses in the Non-Diazotrophic Cyanobacterium *Synechocystis* sp. PCC 6803. *Front. Microbiol.* **7**, (2016).
53. Gao, Z., Zhao, H., Li, Z., Tan, X. & Lu, X. Photosynthetic production of ethanol from carbon dioxide in genetically engineered cyanobacteria. *Energy Env. Sci* **5**, 9857–9865 (2012).
54. Lan, E. I., Ro, S. Y. & Liao, J. C. Oxygen-tolerant coenzyme A-acylating aldehyde dehydrogenase facilitates efficient photosynthetic n-butanol biosynthesis in cyanobacteria. *Energy Environ. Sci.* **6**, 2672 (2013).

55. Vikromvarasiri, N., Shirai, T. & Kondo, A. Metabolic engineering design to enhance (R,R)-2,3-butanediol production from glycerol in *Bacillus subtilis* based on flux balance analysis. *Microb. Cell Factories* **20**, 196 (2021).
56. Savakis, P. *et al.* Photosynthetic production of glycerol by a recombinant cyanobacterium. *J. Biotechnol.* **195**, 46–51 (2015).
57. Angermayr, S. A. *et al.* Exploring metabolic engineering design principles for the photosynthetic production of lactic acid by *Synechocystis* sp. PCC6803. *Biotechnol. Biofuels* **7**, 99 (2014).
58. Angermayr, S. A., Gorchs Rovira, A. & Hellingwerf, K. J. Metabolic engineering of cyanobacteria for the synthesis of commodity products. *Trends Biotechnol.* **33**, 352–361 (2015).
59. Pichersky, E. & Raguso, R. A. Why do plants produce so many terpenoid compounds? *New Phytol.* **220**, 692–702 (2018).
60. Lin, P.-C. & Pakrasi, H. B. Engineering cyanobacteria for production of terpenoids. *Planta* **249**, 145–154 (2019).
61. Dienst, D., Wichmann, J., Mantovani, O., Rodrigues, J. S. & Lindberg, P. High density cultivation for efficient sesquiterpenoid biosynthesis in *Synechocystis* sp. PCC 6803. *Sci. Rep.* **10**, (2020).
62. Lindberg, P., Park, S. & Melis, A. Engineering a platform for photosynthetic isoprene production in cyanobacteria, using *Synechocystis* as the model organism. *Metab. Eng.* **12**, 70–79 (2010).
63. Germann, A. T. *et al.* A systematic overexpression approach reveals native targets to increase squalene production in *Synechocystis* sp. PCC 6803. *Front. Plant Sci.* **14**, 1024981 (2023).

64. Davies, F. K., Work, V. H., Beliaev, A. S. & Posewitz, M. C. Engineering Limonene and Bisabolene Production in Wild Type and a Glycogen-Deficient Mutant of *Synechococcus* sp. PCC 7002. *Front. Bioeng. Biotechnol.* **2**, (2014).
65. Barzegari, A., Saeedi, N., Zarredar, H., Barar, J. & Omid, Y. The search for a promising cell factory system for production of edible vaccine: *Spirulina* as a robust alternate to plants. *Hum. Vaccines Immunother.* **10**, 2497–2502 (2014).
66. Dehghani, J. *et al.* Stable transformation of *Spirulina* (*Arthrospira*) *platensis*: a promising microalga for production of edible vaccines. *Appl. Microbiol. Biotechnol.* **102**, 9267–9278 (2018).
67. Jester, B. W. *et al.* Development of spirulina for the manufacture and oral delivery of protein therapeutics. *Nat. Biotechnol.* **40**, 956–964 (2022).
68. Malihan-Yap, L., Grimm, H. C. & Kourist, R. Recent Advances in Cyanobacterial Biotransformations. *Chem. Ing. Tech.* **94**, 1628–1644 (2022).
69. Toepel, J., Karande, R., Klähn, S. & Bühler, B. Cyanobacteria as whole-cell factories: current status and future perspectives. *Curr. Opin. Biotechnol.* **80**, 102892 (2023).
70. Demain, A. L. Small bugs, big business. *Biotechnol. Adv.* **18**, 499–514 (2000).
71. Glick, B. R. & Patten, C. L. *Molecular Biotechnology: Principles and Applications of Recombinant DNA*. (ASM Press, Washington, DC, 2022).
72. *Comprehensive Biotechnology*. (Pergamon, Amsterdam, 2019).
73. Schmelling, N. M. & Bross, M. What is holding back cyanobacterial research and applications? A survey of the cyanobacterial research community. *Nat. Commun.* **15**, 6758 (2024).

74. Shestakov, S. V. & Khyen, N. T. Evidence for genetic transformation in blue-green alga *Anacystis nidulans*. *Mol. Gen. Genet. MGG* **107**, 372–375 (1970).
75. Wendt, K. E. & Pakrasi, H. B. Genomics Approaches to Deciphering Natural Transformation in Cyanobacteria. *Front. Microbiol.* **10**, 1259 (2019).
76. Jones, P. R. Genetic instability in cyanobacteria – an elephant in the room ? **2**, 1–5 (2014).
77. Golden, S. S. & Sherman, L. A. A hybrid plasmid is a stable cloning vector for the cyanobacterium *Anacystis nidulans* R2. *J. Bacteriol.* **155**, 966–972 (1983).
78. Chen, Y. *et al.* Self-replicating shuttle vectors based on pANS, a small endogenous plasmid of the unicellular cyanobacterium *Synechococcus elongatus* PCC 7942. *Microbiology* **162**, 2029–2041 (2016).
79. Brahamsha, B. A genetic manipulation system for oceanic cyanobacteria of the genus *Synechococcus*. *Appl. Environ. Microbiol.* **62**, 1747–1751 (1996).
80. Taton, A. *et al.* Broad-host-range vector system for synthetic biology and biotechnology in cyanobacteria. *Nucleic Acids Res.* **42**, e136–e136 (2014).
81. Behle, A. & Axmann, I. M. pSHDY: A New Tool for Genetic Engineering of Cyanobacteria. in *Plant Synthetic Biology* (ed. Zurbriggen, M. D.) vol. 2379 67–79 (Springer US, New York, NY, 2022).
82. Huang, H.-H., Camsund, D., Lindblad, P. & Heidorn, T. Design and characterization of molecular tools for a Synthetic Biology approach towards developing cyanobacterial biotechnology. *Nucleic Acids Res.* **38**, 2577–2593 (2010).
83. Jin, H., Wang, Y., Idoine, A. & Bhaya, D. Construction of a Shuttle Vector Using an Endogenous Plasmid From the Cyanobacterium *Synechocystis* sp. PCC6803. *Front. Microbiol.* **9**, 1662 (2018).

84. Vasudevan, R. *et al.* Cyanogate: A modular cloning suite for engineering cyanobacteria based on the plant moclo syntax. *Plant Physiol.* **180**, 39–55 (2019).
85. Zhou, J. *et al.* Discovery of a super-strong promoter enables efficient production of heterologous proteins in cyanobacteria. *Sci. Rep.* **4**, 4500 (2014).
86. Lindblad, P. *et al.* CyanoFactory, a European consortium to develop technologies needed to advance cyanobacteria as chassis for production of chemicals and fuels. *Algal Res.* **41**, 101510 (2019).
87. Duval, M., Simonetti, A., Caldelari, I. & Marzi, S. Multiple ways to regulate translation initiation in bacteria: Mechanisms, regulatory circuits, dynamics. *Biochimie* **114**, 18–29 (2015).
88. Watson, J. D. *Molecular Biology of the Gene*. (Pearson/Benjamin Cummings Cold Spring Harbor laboratory press, San Francisco Cold Spring Harbor, N.Y, 2004).
89. Thiel, K. *et al.* Translation efficiency of heterologous proteins is significantly affected by the genetic context of RBS sequences in engineered cyanobacterium *Synechocystis* sp. PCC 6803. *Microb. Cell Factories* **17**, 34 (2018).
90. Clifton, K. P. *et al.* The genetic insulator RiboJ increases expression of insulated genes. *J. Biol. Eng.* **12**, 23 (2018).
91. Mutalik, V. K. *et al.* Precise and reliable gene expression via standard transcription and translation initiation elements. *Nat. Methods* **10**, 354–360 (2013).
92. Jodlbauer, J. *et al.* Unlocking the potential of cyanobacteria: a high-throughput strategy for enhancing biocatalytic performance through genetic optimization. *Trends Biotechnol.* (2024) doi:10.1016/j.tibtech.2024.07.011.
93. Nielsen, J. & Keasling, J. D. Engineering Cellular Metabolism. *Cell* **164**, 1185–1197 (2016).

94. Werner, S., Engler, C., Weber, E., Gruetzner, R. & Marillonnet, S. Fast track assembly of multigene constructs using Golden Gate cloning and the MoClo system. *Bioengineered* **3**, 38–43 (2012).
95. Engler, C., Kandzia, R. & Marillonnet, S. A One Pot, One Step, Precision Cloning Method with High Throughput Capability. *PLoS ONE* **3**, e3647 (2008).
96. Heidorn, T. *et al.* Synthetic Biology in Cyanobacteria. in *Methods in Enzymology* vol. 497 539–579 (Elsevier, 2011).
97. Englund, E., Liang, F. & Lindberg, P. Evaluation of promoters and ribosome binding sites for biotechnological applications in the unicellular cyanobacterium *Synechocystis* sp. PCC 6803. *Sci. Rep.* **6**, 36640 (2016).
98. Trautmann, D., Voss, B., Wilde, A., Al-Babili, S. & Hess, W. R. Microevolution in Cyanobacteria: Re-sequencing a Motile Substrain of *Synechocystis* sp. PCC 6803. *DNA Res.* **19**, 435–448 (2012).
99. Murphy, R. C., Gasparich, G. E., Bryant, D. A. & Porter, R. D. Nucleotide sequence and further characterization of the *Synechococcus* sp. strain PCC 7002 *recA* gene: complementation of a cyanobacterial *recA* mutation by the *Escherichia coli* *recA* gene. *J. Bacteriol.* **172**, 967–976 (1990).
100. Minda, R., Ramchandani, J., Joshi, V. P. & Bhattacharjee, S. K. A homozygous *recA* mutant of *Synechocystis* PCC6803: construction strategy and characteristics eliciting a novel RecA independent UVC resistance in dark. *Mol. Genet. Genomics* **274**, 616–624 (2005).
101. Mager, M. *et al.* Interlaboratory Reproducibility in Growth and Reporter Expression in the Cyanobacterium *Synechocystis* sp. PCC 6803. *ACS Synth. Biol.* **12**, 1823–1835 (2023).

102. Bux, F. & Chisti, Y. Algae biotechnology. Products and processes. *Green Energy Technol.* **344** (2016) doi:10.1007/978-3-319-12334-9.
103. Ogawa, K., Yoshikawa, K., Matsuda, F., Toya, Y. & Shimizu, H. Transcriptome analysis of the cyanobacterium *Synechocystis* sp. PCC 6803 and mechanisms of photoinhibition tolerance under extreme high light conditions. *J. Biosci. Bioeng.* **126**, 596–602 (2018).
104. Johnson, T. J. *et al.* Photobioreactor cultivation strategies for microalgae and cyanobacteria. *Biotechnol. Prog.* **34**, 811–827 (2018).
105. Chisti, Y. *Algae Biotechnology Science*. (2016). doi:10.1007/978-3-319-12334-9.
106. Kamravamanesh, D., Lackner, M. & Herwig, C. Bioprocess engineering aspects of sustainable polyhydroxyalkanoate production in cyanobacteria. *Bioengineering* **5**, 1–18 (2018).
107. Vermaas, W. *Multi-Pronged Approach to Improving Carbon Utilization by Cyanobacterial Cultures*. DOE-ASU--08515, 1877928 <https://www.osti.gov/servlets/purl/1877928/> (2024) doi:10.2172/1877928.
108. González-Morales, S. I. *et al.* Metabolic engineering of phosphite metabolism in *Synechococcus elongatus* PCC 7942 as an effective measure to control biological contaminants in outdoor raceway ponds. *Biotechnol. Biofuels* **13**, 119 (2020).
109. de Farias Silva, C. E. & Bertucco, A. Bioethanol from microalgae and cyanobacteria: A review and technological outlook. *Process Biochem.* **51**, 1833–1842 (2016).
110. Hobisch, M. *et al.* Internal Illumination to Overcome the Cell Density Limitation in the Scale-up of Whole-Cell Photobiocatalysis. *ChemSusChem* **14**, 3219–3225 (2021).

111. Bähr, L., Wüstenberg, A. & Ehwald, R. Two-tier vessel for photoautotrophic high-density cultures. *J. Appl. Phycol.* **28**, 783–793 (2016).
112. Podola, B., Li, T. & Melkonian, M. Porous Substrate Bioreactors: A Paradigm Shift in Microalgal Biotechnology? *Trends Biotechnol.* **35**, 121–132 (2017).
113. Singh, N. K., Sonani, R. R., Prasad Rastogi, R. & Madamwar, D. The phycobilisomes: An early requisite for efficient photosynthesis in cyanobacteria. *EXCLI J.* **14**, 268–289 (2015).
114. Jahn, M. *et al.* Growth of Cyanobacteria Is Constrained by the Abundance of Light and Carbon Assimilation Proteins. *Cell Rep.* **25**, 478–486.e8 (2018).
115. Lee, S. Y. High cell-density culture of Escherichia coli. *Trends Biotechnol.* **14**, 98–105 (1996).
116. Liu, W. C. *et al.* Fed-batch high-cell-density fermentation strategies for Pichia pastoris growth and production. *Crit. Rev. Biotechnol.* **39**, 258–271 (2019).
117. Yu, J. *et al.* Synechococcus elongatus UTEX 2973, a fast growing cyanobacterial chassis for biosynthesis using light and CO₂. *Sci. Rep.*
118. Włodarczyk, A., Selão, T. T., Norling, B. & Nixon, P. J. Unprecedented biomass and fatty acid production by the newly discovered cyanobacterium Synechococcus sp. PCC 11901. *bioRxiv* (2020) doi:<https://doi.org/10.1101/684944>.
119. Liu, X., Sheng, J. & Curtiss Iii, R. Fatty acid production in genetically modified cyanobacteria. *Proc. Natl. Acad. Sci.* **108**, 6899–6904 (2011).
120. Broddrick, J. T. *et al.* Unique attributes of cyanobacterial metabolism revealed by improved genome-scale metabolic modeling and essential gene analysis. *Proc. Natl. Acad. Sci.* **113**, (2016).

121. Oliver, J. W. K., Machado, I. M. P., Yoneda, H. & Atsumi, S. Cyanobacterial conversion of carbon dioxide to 2,3-butanediol. *Proc. Natl. Acad. Sci.* **110**, 1249–1254 (2013).
122. Lan, E. I. & Liao, J. C. Metabolic engineering of cyanobacteria for 1-butanol production from carbon dioxide. *Metab. Eng.* **13**, 353–363 (2011).
123. Abramson, B. W., Lensmire, J., Lin, Y.-T., Jennings, E. & Ducat, D. C. Redirecting carbon to bioproduction via a growth arrest switch in a sucrose-secreting cyanobacterium. *Algal Res.* **33**, 248–255 (2018).
124. Deng, M.-D. & Coleman, J. R. Ethanol Synthesis by Genetic Engineering in Cyanobacteria. *Appl. Environ. Microbiol.* **65**, 523–528 (1999).
125. McNeely, K., Xu, Y., Bennette, N., Bryant, D. A. & Dismukes, G. C. Redirecting Reductant Flux into Hydrogen Production via Metabolic Engineering of Fermentative Carbon Metabolism in a Cyanobacterium. *Appl. Environ. Microbiol.* **76**, 5032–5038 (2010).
126. Song, K., Tan, X., Liang, Y. & Lu, X. The potential of *Synechococcus elongatus* UTEX 2973 for sugar feedstock production. *Appl. Microbiol. Biotechnol.* **100**, 7865–7875 (2016).
127. Lin, P.-C., Zhang, F. & Pakrasi, H. B. Enhanced limonene production in a fast-growing cyanobacterium through combinatorial metabolic engineering. *Metab. Eng. Commun.* **12**, e00164 (2021).
128. Dookeran, Z. A. & Nielsen, D. R. Systematic Engineering of *Synechococcus elongatus* UTEX 2973 for Photosynthetic Production of L -Lysine, Cadaverine, and Glutarate. *ACS Synth. Biol.* **10**, 3561–3575 (2021).

129. Jaiswal, D. *et al.* Genome Features and Biochemical Characteristics of a Robust, Fast Growing and Naturally Transformable Cyanobacterium *Synechococcus elongatus* PCC 11801 Isolated from India. *Sci. Rep.* **8**, (2018).
130. Sengupta, A. *et al.* Photosynthetic Co-production of Succinate and Ethylene in a Fast-Growing Cyanobacterium, *Synechococcus elongatus* PCC 11801. *Metabolites* **10**, 250 (2020).
131. Jaiswal, D. *et al.* A novel cyanobacterium *Synechococcus elongatus* pcc 11802 has Distinct Genomic and Metabolomic Characteristics Compared to its Neighbor PCC 11801. (2020) doi:10.1038/s41598-019-57051-0.
132. Pritam, P., Sarnaik, A. P. & Wangikar, P. P. Metabolic engineering of *Synechococcus elongatus* for photoautotrophic production of mannitol. *Biotechnol. Bioeng.* **120**, 2363–2370 (2023).
133. Zhang, T., Li, S., Chen, L., Sun, T. & Zhang, W. Extended toolboxes enable efficient biosynthesis of valuable chemicals directly from CO₂ in fast-growing *Synechococcus* sp. PCC 11901. Preprint at <https://doi.org/10.1101/2023.08.23.554402> (2023).
134. Zavřel, T. *et al.* Monitoring fitness and productivity in cyanobacteria batch cultures. *Algal Res.* **56**, 102328 (2021).
135. Schuurmans, R. M., Matthijs, J. C. P. & Hellingwerf, K. J. Transition from exponential to linear photoautotrophic growth changes the physiology of *Synechocystis* sp. PCC 6803. *Photosynth. Res.* **132**, 69–82 (2017).
136. Touloupakis, E., Boutopoulos, C., Buonasera, K., Zergioti, I. & Giardi, M. T. A photosynthetic biosensor with enhanced electron transfer generation realized by laser printing technology. *Anal. Bioanal. Chem.* **402**, 3237–3244 (2012).

137. Burnap, R. L. Systems and Photosystems: Cellular Limits of Autotrophic Productivity in Cyanobacteria. *Front. Bioeng. Biotechnol.* **3**, (2015).
138. Srivastava, M., Hudson, E. P. & Wangikar, P. P. Traits of Fast-Growing Cyanobacteria. in *Cyanobacteria Biotechnology* (eds. Nielsen, J., Lee, S., Stephanopoulos, G. & Hudson, P.) 441–476 (Wiley, 2021). doi:10.1002/9783527824908.ch14.
139. Sengupta, A. *et al.* Genome streamlining to improve performance of a fast-growing cyanobacterium *Synechococcus elongatus* UTEX 2973. *mBio* **15**, e03530-23 (2024).
140. Nielsen, S. L. Size-dependent growth rates in eukaryotic and prokaryotic algae exemplified by green algae and cyanobacteria: comparisons between unicells and colonial growth forms. *J. Plankton Res.* **28**, 489–498 (2006).
141. Steuer, R. Fast-growing phototrophic microorganisms and the productivity of phototrophic cultures. *Biotechnol. Bioeng.* **119**, 2261–2267 (2022).
142. Shabestary, K. *et al.* Targeted Repression of Essential Genes To Arrest Growth and Increase Carbon Partitioning and Biofuel Titters in Cyanobacteria. *ACS Synth. Biol.* **7**, 1669–1675 (2018).
143. Hendry, J. I. *et al.* Genome-Scale fluxome of *Synechococcus elongatus* UTEX 2973 using transient ¹³C-labeling data. *Plant Physiol.* **179**, 761–769 (2019).
144. Ungerer, J., Wendt, K. E., Hendry, J. I., Maranas, C. D. & Pakrasi, H. B. Comparative genomics reveals the molecular determinants of rapid growth of the cyanobacterium *Synechococcus elongatus* UTEX 2973. *Proc. Natl. Acad. Sci.* **115**, (2018).
145. Mueller, T. J., Ungerer, J. L., Pakrasi, H. B. & Maranas, C. D. Identifying the Metabolic Differences of a Fast-Growth Phenotype in *Synechococcus* UTEX 2973. *Sci. Rep.* **7**, 3–10 (2017).

146. Rautela, A., Yadav, I., Gangwar, A., Chatterjee, R. & Kumar, S. Photosynthetic production of α -farnesene by engineered *Synechococcus elongatus* UTEX 2973 from carbon dioxide. *Bioresour. Technol.* **396**, 130432 (2024).
147. Yadav, I. *et al.* Enhancement of isoprene production in engineered *Synechococcus elongatus* UTEX 2973 by metabolic pathway inhibition and machine learning-based optimization strategy. *Bioresour. Technol.* **387**, 129677 (2023).
148. Roh, H. *et al.* Improved CO₂-derived polyhydroxybutyrate (PHB) production by engineering fast-growing cyanobacterium *Synechococcus elongatus* UTEX 2973 for potential utilization of flue gas. *Bioresour. Technol.* **327**, 124789 (2021).
149. Lin, P.-C., Zhang, F. & Pakrasi, H. B. Enhanced production of sucrose in the fast-growing cyanobacterium *Synechococcus elongatus* UTEX 2973. *Sci. Rep.* **10**, 390 (2020).
150. Abernathy, M. H. *et al.* Deciphering cyanobacterial phenotypes for fast photoautotrophic growth via isotopically nonstationary metabolic flux analysis. *Biotechnol. Biofuels* **10**, 1–13 (2017).
151. Jahn, M. *et al.* Growth of Cyanobacteria Is Constrained by the Abundance of Light and Carbon Assimilation Proteins. *Cell Rep.* **25**, 478-486.e8 (2018).
152. Sengupta, A., Bandyopadhyay, A., Schubert, M. G., Church, G. M. & Pakrasi, H. B. Antenna Modification in a Fast-Growing Cyanobacterium *Synechococcus elongatus* UTEX 2973 Leads to Improved Efficiency and Carbon-Neutral Productivity. *Microbiol. Spectr.* **11**, e00500-23 (2023).
153. Long, B. *et al.* Machine learning-informed and synthetic biology-enabled semi-continuous algal cultivation to unleash renewable fuel productivity. *Nat. Commun.* **13**, 541 (2022).

154. Sengupta, S. *et al.* Metabolic engineering of a fast-growing cyanobacterium *Synechococcus elongatus* PCC 11801 for photoautotrophic production of succinic acid. *Biotechnol. Biofuels* **13**, 89 (2020).
155. Mills, L. *et al.* Development of a Biotechnology Platform for the Fast-Growing Cyanobacterium *Synechococcus* sp. PCC 11901. *Biomolecules* **12**, 872 (2022).
156. Kirst, H., Formighieri, C. & Melis, A. Maximizing photosynthetic efficiency and culture productivity in cyanobacteria upon minimizing the phycobilisome light-harvesting antenna size. *Biochim. Biophys. Acta BBA - Bioenerg.* **1837**, 1653–1664 (2014).
157. Victoria, A. J., Astbury, M. J. & McCormick, A. J. Engineering highly productive cyanobacteria towards carbon negative emissions technologies. *Curr. Opin. Biotechnol.* **87**, 103141 (2024).
158. Schubert, M. G. *et al.* Cyanobacteria newly isolated from marine volcanic seeps display rapid sinking and robust, high density growth. Preprint at <https://doi.org/10.1101/2023.10.30.564770> (2023).
159. Bruggeman, F. J., Teusink, B. & Steuer, R. Trade-offs between the instantaneous growth rate and long-term fitness: Consequences for microbial physiology and predictive computational models. *BioEssays* **45**, 2300015 (2023).
160. Turner, N. J. & Kumar, R. Editorial overview: Biocatalysis and biotransformation: The golden age of biocatalysis. *Curr. Opin. Chem. Biol.* **43**, A1–A3 (2018).
161. Schrewe, M., Julsing, M. K., Bühler, B. & Schmid, A. Whole-cell biocatalysis for selective and productive C–O functional group introduction and modification. *Chem. Soc. Rev.* **42**, 6346–6377 (2013).

162. Sharma, R., Garg, P., Kumar, P., Bhatia, S. K. & Kulshrestha, S. Microbial Fermentation and Its Role in Quality Improvement of Fermented Foods. *Fermentation* **6**, 106 (2020).
163. Goeddel, D. V. *et al.* Expression in *Escherichia coli* of chemically synthesized genes for human insulin. *Proc. Natl. Acad. Sci.* **76**, 106–110 (1979).
164. Waksman, S. A. & Schatz, A. Streptomycin–Origin, Nature, and Properties*††Journal Series Paper of the Department of Microbiology of the New Jersey Agricultural Experiment Station, Rutgers University. *J. Am. Pharm. Assoc. Sci. Ed* **34**, 273–291 (1945).
165. Shu, P., Funk, A. & Neish, A. C. MECHANISM OF CITRIC ACID FORMATION FROM GLUCOSE BY *ASPERGILLUS NIGER*. *Can. J. Biochem. Physiol.* **32**, 68–80 (1954).
166. Acetic Acid. in *Biotechnology Set* 381–401 (Wiley, 2001). doi:10.1002/9783527620999.ch12f.
167. Hofstetter, K., Lutz, J., Lang, I., Witholt, B. & Schmid, A. Coupling of Biocatalytic Asymmetric Epoxidation with NADH Regeneration in Organic–Aqueous Emulsions. *Angew. Chem. Int. Ed.* **43**, 2163–2166 (2004).
168. Gröger, H. *et al.* Enantioselective Reduction of Ketones with “Designer Cells” at High Substrate Concentrations: Highly Efficient Access to Functionalized Optically Active Alcohols. *Angew. Chem. Int. Ed.* **45**, 5677–5681 (2006).
169. Haberland, J., Hummel, W., Daussmann, T. & Liese, A. New Continuous Production Process for Enantiopure (2 *R*, 5 *R*)-Hexanediol. *Org. Process Res. Dev.* **6**, 458–462 (2002).
170. Muschiol, J. *et al.* Cascade catalysis – strategies and challenges en route to preparative synthetic biology. *Chem. Commun.* **51**, 5798–5811 (2015).

171. Su, H., Chen, X., Chen, S., Guo, M. & Liu, H. Applications of the Whole-Cell System in the Efficient Biosynthesis of Heme. *Int. J. Mol. Sci.* **24**, 8384 (2023).
172. Zhao, X. R., Choi, K. R. & Lee, S. Y. Metabolic engineering of *Escherichia coli* for secretory production of free haem. *Nat. Catal.* **1**, 720–728 (2018).
173. Oberleitner, N. *et al.* From waste to value – direct utilization of limonene from orange peel in a biocatalytic cascade reaction towards chiral carvolactone. *Green Chem.* **19**, 367–371 (2017).
174. Seyden-Penne, J. & Seyden-Penne, J. *Reductions by the Alumino- and Borohydrides in Organic Synthesis*. (Wiley-VCH, New York Weinheim, 1997).
175. Zakharkin, L. I. & Khorlina, I. M. Preparation of aldehydes by reduction of esters of carboxylic acids with diisobutyl aluminum hydride. *Bull. Acad. Sci. USSR Div. Chem. Sci.* **11**, 497–497 (1962).
176. Venkitasubramanian, P., Daniels, L. & Rosazza, J. P. N. Reduction of carboxylic acids by *Nocardia* aldehyde oxidoreductase requires a phosphopantetheinylated enzyme. *J. Biol. Chem.* **282**, 478–485 (2007).
177. Stolterfoht, H., Schwendenwein, D., Sensen, C. W., Rudroff, F. & Winkler, M. Four distinct types of E.C. 1.2.1.30 enzymes can catalyze the reduction of carboxylic acids to aldehydes. *J. Biotechnol.* **257**, 222–232 (2017).
178. Qu, G., Guo, J., Yang, D. & Sun, Z. Biocatalysis of carboxylic acid reductases: Phylogenesis, catalytic mechanism and potential applications. *Green Chem.* **20**, 777–792 (2018).
179. Sinha, A. K., Sharma, U. K. & Sharma, N. A comprehensive review on vanilla flavor: Extraction, isolation and quantification of vanillin and others constituents. *Int. J. Food Sci. Nutr.* **59**, 299–326 (2008).

180. Gallage, N. J. & Møller, B. L. Vanillin–Bioconversion and Bioengineering of the Most Popular Plant Flavor and Its De Novo Biosynthesis in the Vanilla Orchid. *Mol. Plant* **8**, 40–57 (2015).
181. Vanillin natural, ≥97%, FCC, FG | Sigma-Aldrich. <http://www.sigmaaldrich.com/>.
182. Furuya, T., Miura, M. & Kino, K. A Coenzyme-Independent Decarboxylase/Oxygenase Cascade for the Efficient Synthesis of Vanillin. *ChemBioChem* **15**, 2248–2254 (2014).
183. Xu, L. *et al.* Advances in the vanillin synthesis and biotransformation: A review. *Renew. Sustain. Energy Rev.* **189**, 113905 (2024).
184. Fache, M., Boutevin, B. & Caillol, S. Vanillin, a key-intermediate of biobased polymers. *Eur. Polym. J.* **68**, 488–502 (2015).
185. Olatunde, A., Mohammed, A., Ibrahim, M. A., Tajuddeen, N. & Shuaibu, M. N. Vanillin: A food additive with multiple biological activities. *Eur. J. Med. Chem. Rep.* **5**, 100055 (2022).
186. Shaughnessy, D. T., Schaaper, R. M., Umbach, D. M. & DeMarini, D. M. Inhibition of spontaneous mutagenesis by vanillin and cinnamaldehyde in *Escherichia coli*: Dependence on recombinational repair. *Mutat. Res. Mol. Mech. Mutagen.* **602**, 54–64 (2006).
187. Ho, K., Yazan, L. S., Ismail, N. & Ismail, M. Apoptosis and cell cycle arrest of human colorectal cancer cell line HT-29 induced by vanillin. *Cancer Epidemiol.* **33**, 155–160 (2009).
188. Mahal, H. S., Badheka, L. P. & Mukherjee, T. Radical scavenging properties of a flavouring agent–Vanillin. *Res. Chem. Intermed.* **27**, 595–604 (2001).

189. Niazi, J., Sachdeva, R., Bansal, Y., Gupta, V. & Kaur, N. Anti-inflammatory and antinociceptive activity of vanillin. *Drug Dev. Ther.* **5**, 145 (2014).
190. Tomlinson, G. H. & Hibbert, H. Studies on Lignin and Related Compounds. XXIV. The Formation of Vanillin from Waste Sulfite Liquor ¹. *J. Am. Chem. Soc.* **58**, 345–348 (1936).
191. Hocking, M. B. Vanillin: Synthetic Flavoring from Spent Sulfite Liquor. *J. Chem. Educ.* **74**, 1055 (1997).
192. Fatiadi, A. J. & Schaffer, R. An Improved Procedure for Synthesis of DL-4-Hydroxy-3-methoxymandelic Acid (DL-"Vanillyl"-mandelic Acid, VMA). *J. Res. Natl. Bur. Stand. Sect. Phys. Chem.* **78A**, 411–412 (1974).
193. Chee, M. J. Y., Lycett, G. W., Khoo, T.-J. & Chin, C. F. Bioengineering of the Plant Culture of *Capsicum frutescens* with Vanillin Synthase Gene for the Production of Vanillin. *Mol. Biotechnol.* **59**, 1–8 (2017).
194. Paul, V., Rai, D. C., T.S, R. L., Srivastava, S. K. & Tripathi, A. D. A comprehensive review on vanillin: its microbial synthesis, isolation and recovery. *Food Biotechnol.* **35**, 22–49 (2021).
195. Kumar, N. & Pruthi, V. Potential applications of ferulic acid from natural sources. *Biotechnol. Rep. Amst. Neth.* **4**, 86–93 (2014).
196. Pazo-Cepeda, V., Benito-Román, Ó., Navarrete, A. & Alonso, E. Valorization of Wheat Bran: Ferulic Acid Recovery Using Pressurized Aqueous Ethanol Solutions. *Waste Biomass Valorization* **11**, 4701–4710 (2020).
197. Valério, R., Cadima, M., Crespo, J. G. & Brazinha, C. Extracting Ferulic Acid from Corn Fibre Using Mild Alkaline Extraction: A Pilot Scale Study. *Waste Biomass Valorization* **13**, 287–297 (2022).

198. Ferri, M. *et al.* Advances in combined enzymatic extraction of ferulic acid from wheat bran. *New Biotechnol.* **56**, 38–45 (2020).
199. Al-Shwafy, K. W. A., Chadni, M., Hariz Abg Zamari, M. H. & Ioannou, I. Enzymatic extraction of ferulic acid from brewer's spent grain: Effect of physical pretreatments and optimization using design of experiments. *Biocatal. Agric. Biotechnol.* **51**, 102779 (2023).
200. Tilay, A., Bule, M., Kishenkumar, J. & Annapure, U. Preparation of Ferulic Acid from Agricultural Wastes: Its Improved Extraction and Purification. *J. Agric. Food Chem.* **56**, 7644–7648 (2008).
201. Muheim, A. & Lerch, K. Towards a high-yield bioconversion of ferulic acid to vanillin. *Appl. Microbiol. Biotechnol.* **51**, 456–461 (1999).
202. Ni, J., Gao, Y.-Y., Tao, F., Liu, H.-Y. & Xu, P. Temperature-Directed Biocatalysis for the Sustainable Production of Aromatic Aldehydes or Alcohols. *Angew. Chem.* **130**, 1228–1231 (2018).
203. Huang, Z., Dostal, L. & Rosazza, J. P. Purification and characterization of a ferulic acid decarboxylase from *Pseudomonas fluorescens*. *J. Bacteriol.* **176**, 5912–5918 (1994).
204. Ni, J., Wu, Y.-T., Tao, F., Peng, Y. & Xu, P. A Coenzyme-Free Biocatalyst for the Value-Added Utilization of Lignin-Derived Aromatics. *J. Am. Chem. Soc.* **140**, 16001–16005 (2018).
205. Gavriilidis, A. *et al.* Aerobic oxidations in flow: opportunities for the fine chemicals and pharmaceuticals industries. *React. Chem. Eng.* **1**, 595–612 (2016).

206. Duetz, W. A., Van Beilen, J. B. & Witholt, B. Using proteins in their natural environment: potential and limitations of microbial whole-cell hydroxylations in applied biocatalysis. *Curr. Opin. Biotechnol.* **12**, 419–425 (2001).
207. Hoschek, A., Bühler, B. & Schmid, A. Overcoming the Gas–Liquid Mass Transfer of Oxygen by Coupling Photosynthetic Water Oxidation with Biocatalytic Oxyfunctionalization. *Angew. Chem. - Int. Ed.* **56**, 15146–15149 (2017).
208. Tüllinghoff, A., Djaya-Mbissam, H., Toepel, J. & Bühler, B. Light-driven redox biocatalysis on gram-scale in *Synechocystis* sp. PCC 6803 via an *in vivo* cascade. *Plant Biotechnol. J.* pbi.14113 (2023) doi:10.1111/pbi.14113.
209. Hoschek, A. *et al.* Light-Dependent and Aeration-Independent Gram-Scale Hydroxylation of Cyclohexane to Cyclohexanol by CYP450 Harboring *Synechocystis* sp. PCC 6803. *Biotechnol. J.* **14**, 1–10 (2019).
210. Tamoi, M., Miyazaki, T., Fukamizo, T. & Shigeoka, S. The Calvin cycle in cyanobacteria is regulated by CP12 via the NAD(H)/NADP(H) ratio under light/dark conditions. *Plant J.* **42**, 504–513 (2005).
211. Assil-Companioni, L. *et al.* Engineering of NADPH Supply Boosts Photosynthesis-Driven Biotransformations. *ACS Catal.* **10**, 11864–11877 (2020).
212. Spasic, J., Oliveira, P., Pacheco, C., Kourist, R. & Tamagnini, P. Engineering cyanobacterial chassis for improved electron supply toward a heterologous ene-reductase. *J. Biotechnol.* **360**, 152–159 (2022).
213. Jurkaš, V. *et al.* Expression and activity of heterologous hydroxyisocaproate dehydrogenases in *Synechocystis* sp. PCC 6803 Δ hoxYH. *Eng. Microbiol.* **2**, 100008 (2022).

214. Hoschek, A. *et al.* Mixed-species biofilms for high-cell-density application of *Synechocystis* sp. PCC 6803 in capillary reactors for continuous cyclohexane oxidation to cyclohexanol. *Bioresour. Technol.* **282**, 171–178 (2019).
215. Sengupta, A., Sunder, A. V., Sohoni, S. V. & Wangikar, P. P. The effect of CO₂ in enhancing photosynthetic cofactor recycling for alcohol dehydrogenase mediated chiral synthesis in cyanobacteria. *J. Biotechnol.* **289**, 1–6 (2019).
216. Tüllinghoff, A. *et al.* Maximizing Photosynthesis-Driven Baeyer–Villiger Oxidation Efficiency in Recombinant *Synechocystis* sp. PCC6803. *Front. Catal.* **1**, 780474 (2022).
217. Battchikova, N., Eisenhut, M. & Aro, E.-M. Cyanobacterial NDH-1 complexes: Novel insights and remaining puzzles. *Biochim. Biophys. Acta BBA - Bioenerg.* **1807**, 935–944 (2011).
218. Nishimura, T. *et al.* Mechanism of low CO₂ -induced activation of the *cmp* bicarbonate transporter operon by a LysR family protein in the cyanobacterium *Synechococcus elongatus* strain PCC 7942. *Mol. Microbiol.* **68**, 98–109 (2008).
219. Bersanini, L. *et al.* Flavodiiron Protein Flv2/Flv4-Related Photoprotective Mechanism Dissipates Excitation Pressure of PSII in Cooperation with Phycobilisomes in Cyanobacteria. *Plant Physiol.* **164**, 805–818 (2014).
220. Ducat, D. C., Avelar-Rivas, J. A., Way, J. C. & Silver, P. A. Rerouting Carbon Flux To Enhance Photosynthetic Productivity. *Appl. Environ. Microbiol.* **78**, 2660–2668 (2012).
221. Santos-Merino, M. *et al.* Improved photosynthetic capacity and photosystem I oxidation via heterologous metabolism engineering in cyanobacteria. *Proc. Natl. Acad. Sci.* **118**, e2021523118 (2021).

222. Hendry, J. I. *et al.* Rerouting of carbon flux in a glycogen mutant of cyanobacteria assessed via isotopically non-stationary ^{13}C metabolic flux analysis. *Biotechnol. Bioeng.* **114**, 2298–2308 (2017).
223. Yamanaka, R., Nakamura, K., Murakami, M. & Murakami, A. Selective synthesis of cinnamyl alcohol by cyanobacterial photobiocatalysts. *Tetrahedron Lett.* **56**, 1089–1091 (2015).
224. Górak, M. & Zymańczyk-Duda, E. Application of cyanobacteria for chiral phosphonate synthesis. *Green Chem.* **17**, 4570–4578 (2015).
225. Yazdi, M. T. *et al.* Biotransformation of hydrocortisone by a natural isolate of *Nostoc muscorum*. *Phytochemistry* **65**, 2205–2209 (2004).
226. Havel, J. & Weuster-Botz, D. Comparative study of cyanobacteria as biocatalysts for the asymmetric synthesis of chiral building blocks. *Eng. Life Sci.* **6**, 175–179 (2006).
227. Hamada, H. *et al.* Stereoselective Biotransformation of Limonene and Limonene Oxide by Cyanobacterium, *Synechococcus* sp. PCC 7942. *J. Biosci. Bioeng.* **96**, 581–584 (2003).
228. Nakamura, K. & Yamanaka, R. *Light-Mediated Regulation of Asymmetric Reduction of Ketones by a Cyanobacterium*. *TETRAHEDRON: ASYMMETRY* vol. 13 (2002).
229. Nakamura, K., Yamanaka, R., Tohi, K. & Hamada, H. Cyanobacterium-catalyzed asymmetric reduction of ketones. *Tetrahedron Lett.* **41**, 6799–6802 (2000).
230. Itoh, K. I., Sakamaki, H., Nakamura, K. & Horiuchi, C. A. Biocatalytic asymmetric reduction of 3-acetylisoxazoles. *Tetrahedron Asymmetry* **16**, 1403–1408 (2005).

231. Shimoda, K., Kubota, N., Hamada, H., Yamane, S. Y. & Hirata, T. Asymmetric transformation of enones with *Synechococcus* sp. PCC 7942. *Bull. Chem. Soc. Jpn.* **77**, 2269–2272 (2004).
232. Fan, J., Zhang, Y., Wu, P., Zhang, X. & Bai, Y. Enhancing cofactor regeneration of cyanobacteria for the light-powered synthesis of chiral alcohols. *Bioorganic Chem.* **118**, 105477 (2022).
233. Żyszka-Haberecht, B., Poliwoda, A. & Lipok, J. 'Structural constraints in cyanobacteria-mediated whole-cell biotransformation of methoxylated and methylated derivatives of 2'-hydroxychalcone. *J. Biotechnol.* **293**, 36–46 (2019).
234. Schrewe, M., Magnusson, A. O., Willrodt, C., Bühler, B. & Schmid, A. Kinetic analysis of terminal and unactivated C-H bond oxyfunctionalization in fatty acid methyl esters by monooxygenase-based whole-cell biocatalysis. *Adv. Synth. Catal.* **353**, 3485–3495 (2011).
235. Julsing, M. K. *et al.* Outer membrane protein alkL boosts biocatalytic oxyfunctionalization of hydrophobic substrates in *Escherichia coli*. *Appl. Environ. Microbiol.* **78**, 5724–5733 (2012).
236. Hoschek, A. *et al.* Light-Dependent and Aeration-Independent Gram-Scale Hydroxylation of Cyclohexane to Cyclohexanol by CYP450 Harboring *Synechocystis* sp. PCC 6803. *Biotechnol. J.* **14**, (2019).
237. Königer, K. *et al.* Biotechnology Hot Paper Recombinant Cyanobacteria for the Asymmetric Reduction of C = C Bonds Fueled by the Biocatalytic Oxidation of Water Angewandte. *Angew. Chem. - Int. Ed.* **55**, 5582–5585 (2016).

238. Büchsenschütz, H. C. *et al.* Stereoselective Biotransformations of Cyclic Imines in Recombinant Cells of *Synechocystis* sp. PCC 6803. *ChemCatChem* **12**, 726–730 (2020).
239. Velikogne, S., Resch, V., Dertnig, C., Schrittwieser, J. H. & Kroutil, W. Sequence-Based In-silico Discovery, Characterisation, and Biocatalytic Application of a Set of Imine Reductases. *ChemCatChem* **10**, 3236–3246 (2018).
240. Weckbecker, A. & Hummel, W. Improved synthesis of chiral alcohols with *Escherichia coli* cells co-expressing pyridine nucleotide transhydrogenase, NADP+-dependent alcohol dehydrogenase and NAD+-dependent formate dehydrogenase. *Biotechnol. Lett.* **26**, 1739–1744 (2004).
241. Böhmer, S. *et al.* Enzymatic oxyfunctionalization driven by photosynthetic water-splitting in the cyanobacterium *Synechocystis* sp. PCC 6803. *Catalysts* **7**, (2017).
242. Erdem, E. *et al.* Photobiocatalytic Oxyfunctionalization with High Reaction Rate using a Baeyer–Villiger Monooxygenase from *Burkholderia xenovorans* in Metabolically Engineered Cyanobacteria. *ACS Catal.* **12**, 66–72 (2022).
243. Schäfer, L., Bühler, K., Karande, R. & Bühler, B. Rational Engineering of a Multi-Step Biocatalytic Cascade for the Conversion of Cyclohexane to Polycaprolactone Monomers in *Pseudomonas taiwanensis*. *Biotechnol. J.* **15**, 2000091 (2020).
244. Yu, J. *et al.* *Synechococcus elongatus* UTEX 2973, a fast growing cyanobacterial chassis for biosynthesis using light and CO₂. *Sci. Rep.* **5**, 8132 (2015).
245. Mantovani, O. & Dd Dienst, D. CD Media for High Density Cultivation of *Synechocystis* sp. PCC 6803 v1. Preprint at <https://doi.org/10.17504/protocols.io.2bxgapn> (2019).

246. Machado, D., Herrgård, M. J. & Rocha, I. Stoichiometric Representation of Gene–Protein–Reaction Associations Leverages Constraint-Based Analysis from Reaction to Gene-Level Phenotype Prediction. *PLOS Comput. Biol.* **12**, e1005140 (2016).
247. Ashburner, M. *et al.* Gene Ontology: tool for the unification of biology. *Nat. Genet.* **25**, 25–29 (2000).
248. Thiele, I. & Palsson, B. Ø. A protocol for generating a high-quality genome-scale metabolic reconstruction. *Nat. Protoc.* **5**, 93–121 (2010).
249. Machado, D., Andrejev, S., Tramontano, M. & Patil, K. R. Fast automated reconstruction of genome-scale metabolic models for microbial species and communities. *Nucleic Acids Res.* **46**, 7542–7553 (2018).
250. Price, N. D., Reed, J. L. & Palsson, B. Ø. Genome-scale models of microbial cells: evaluating the consequences of constraints. *Nat. Rev. Microbiol.* **2**, 886–897 (2004).
251. Orth, J. D., Thiele, I. & Palsson, B. Ø. What is flux balance analysis? *Nat. Biotechnol.* **28**, 245–248 (2010).
252. Edwards, J. S., Covert, M. & Palsson, B. Metabolic modelling of microbes: the flux-balance approach. *Environ. Microbiol.* **4**, 133–140 (2002).
253. Becker, S. A. *et al.* Quantitative prediction of cellular metabolism with constraint-based models: the COBRA Toolbox. *Nat. Protoc.* **2**, 727–738 (2007).
254. Ebrahim, A., Lerman, J. A., Palsson, B. O. & Hyduke, D. R. COBRApy: COntstraints-Based Reconstruction and Analysis for Python. *BMC Syst. Biol.* **7**, 74 (2013).
255. Covert, M. W. *et al.* Metabolic modeling of microbial strains in silico. *Trends Biochem. Sci.* **26**, 179–186 (2001).

256. Joyce, A. R. & Palsson, B. Ø. Predicting Gene Essentiality Using Genome-Scale in Silico Models. in *Microbial Gene Essentiality: Protocols and Bioinformatics* (eds. Osterman, A. L. & Gerdes, S. Y.) vol. 416 433–457 (Humana Press, Totowa, NJ, 2008).
257. Park, J. M., Kim, T. Y. & Lee, S. Y. Constraints-based genome-scale metabolic simulation for systems metabolic engineering. *Biotechnol. Adv.* **27**, 979–988 (2009).
258. *Python Cookbook*. (O'Reilly, Beijing ; Sebastopol, CA, 2005).
259. AnnaGermann. AnnaGermann/Master-Thesis. (2018).
260. Li, S., Sun, T., Xu, C., Chen, L. & Zhang, W. *Development and Optimization of Genetic Toolboxes for a Fast-Growing Cyanobacterium Synechococcus Elongatus UTEX 2973. Metabolic Engineering* vol. 48 (Elsevier Inc., 2018).
261. Wendt, K. E., Walker, P., Sengupta, A., Ungerer, J. & Pakrasi, H. B. Engineering Natural Competence into the Fast-Growing Cyanobacterium *Synechococcus elongatus* Strain UTEX 2973. *Appl. Environ. Microbiol.* **88**, e01882-21 (2022).
262. Elhai, J. & Wolk, C. P. Conjugal Transfer of DNA to Cyanobacteria. *Methods Enzymol.* **167**, 747–754 (1988).
263. Li, T. & Rosazza, J. P. N. Purification, characterization, and properties of an aryl aldehyde oxidoreductase from *Nocardia* sp. strain NRRL 5646. *J. Bacteriol.* **179**, 3482–3487 (1997).
264. Engler, C., Gruetzner, R., Kandzia, R. & Marillonnet, S. Golden gate shuffling: a one-pot DNA shuffling method based on type IIs restriction enzymes. *PloS One* **4**, e5553 (2009).
265. Frackmann, Susanne. Betaine and DMSO: Enhancing Agents for PCR. *Promega Notes* **65**, 27 (1998).

266. Gibson, D. G. Enzymatic Assembly of Overlapping DNA Fragments. in *Methods in Enzymology* vol. 498 349–361 (Elsevier, 2011).
267. Gibson, D. G. *et al.* Enzymatic assembly of DNA molecules up to several hundred kilobases. *Nat. Methods* **6**, 343–345 (2009).
268. Horvat, M., Fritsche, S., Kourist, R. & Winkler, M. Characterization of Type IV Carboxylate Reductases (CARs) for Whole Cell-Mediated Preparation of 3-Hydroxytyrosol. *ChemCatChem* **11**, 4171–4181 (2019).
269. Akhtar, M. K., Turner, N. J. & Jones, P. R. Carboxylic acid reductase is a versatile enzyme for the conversion of fatty acids into fuels and chemical commodities. *Proc. Natl. Acad. Sci.* **110**, 87–92 (2013).
270. Winkler, M. & Ling, J. G. Biocatalytic Carboxylate Reduction – Recent Advances and New Enzymes. *ChemCatChem* **14**, e202200441 (2022).
271. Horvat, M. & Winkler, M. *In Vivo* Reduction of Medium- to Long-Chain Fatty Acids by Carboxylic Acid Reductase (CAR) Enzymes: Limitations and Solutions. *ChemCatChem* **12**, 5076–5090 (2020).
272. Taton, A. *et al.* The circadian clock and darkness control natural competence in cyanobacteria. *Nat. Commun.* **11**, 1688 (2020).
273. Petermeier, P. *et al.* Integrated preservation of water activity as key to intensified chemoenzymatic synthesis of bio-based styrene derivatives. *Commun. Chem.* **7**, 57 (2024).
274. PyroScience GmbH. <https://www.pyroscience.com>.
275. Allahverdiyeva, Y. Functional redundancy between flavodiiron proteins and NDH-1 in *Synechocystis* sp. PCC 6803. *Biochim. Biophys. Acta BBA - Bioenerg.* **1863**, 148636 (2022).

276. Ferreira, E. A. *et al.* Expanding the toolbox for *Synechocystis* sp. PCC 6803: validation of replicative vectors and characterization of a novel set of promoters. *Synth. Biol.* **3**, ysy014 (2018).
277. Peca, L., Křs, P. B., Mřtř, Z., Farsang, A. & Vass, I. Construction of bioluminescent cyanobacterial reporter strains for detection of nickel, cobalt and zinc. *FEMS Microbiol. Lett.* **289**, 258–264 (2008).
278. Stevenson, K., McVey, A. F., Clark, I. B. N., Swain, P. S. & Pilizota, T. General calibration of microbial growth in microplate readers. *Sci. Rep.* **6**, 38828 (2016).
279. Myers, J. A., Curtis, B. S. & Curtis, W. R. Improving accuracy of cell and chromophore concentration measurements using optical density. *BMC Biophys.* **6**, 4 (2013).
280. Hagemann, M., Song, S. & Brouwer, E. Inorganic Carbon Assimilation in Cyanobacteria: Mechanisms, Regulation, and Engineering. in *Cyanobacteria Biotechnology* (eds. Nielsen, J., Lee, S., Stephanopoulos, G. & Hudson, P.) 1–31 (Wiley, 2021). doi:10.1002/9783527824908.ch1.
281. Reed, M. C., Lieb, A. & Nijhout, H. F. The biological significance of substrate inhibition: A mechanism with diverse functions. *BioEssays* **32**, 422–429 (2010).
282. Fitzgerald, D. J. *et al.* Mode of antimicrobial action of vanillin against *Escherichia coli*, *Lactobacillus plantarum* and *Listeria innocua*. *J. Appl. Microbiol.* **97**, 104–113 (2004).
283. Chen, Y., Li, L., Long, L. & Ding, S. High cell-density cultivation of phenolic acid decarboxylase-expressing *Escherichia coli* and 4-vinylguaiacol bioproduction from ferulic acid by whole-cell catalysis. *J. Chem. Technol. Biotechnol.* **93**, 2415–2421 (2018).

284. Li, L., Long, L. & Ding, S. Direct Affinity-Immobilized Phenolic Acid Decarboxylase by a Linker Peptide on Zeolite for Efficient Bioconversion of Ferulic Acid into 4-Vinylguaiacol. *ACS Sustain. Chem. Eng.* **8**, 14732–14742 (2020).
285. Alfaro-Sayes, D. A. *et al.* Alginate immobilization as a strategy for improving succinate production during autofermentation using cyanobacteria *Synechocystis* sp. PCC 6803. *Biochem. Eng. J.* **188**, 108681 (2022).
286. Graham, J. E. & Bryant, D. A. The Biosynthetic Pathway for Synechoxanthin, an Aromatic Carotenoid Synthesized by the Euryhaline, Unicellular Cyanobacterium *Synechococcus* sp. Strain PCC 7002. *J. Bacteriol.* **190**, 7966–7974 (2008).
287. Hays, S. G., Yan, L. L. W., Silver, P. A. & Ducat, D. C. Synthetic photosynthetic consortia define interactions leading to robustness and photoproduction. *J. Biol. Eng.* **11**, 4 (2017).
288. Matuszyńska, A., Ebenhöf, O., Zurbriggen, M. D., Ducat, D. C. & Axmann, I. M. A new era of synthetic biology—microbial community design. *Synth. Biol.* **9**, ysae011 (2024).
289. Li, C. *et al.* A Highly Compatible Phototrophic Community for Carbon-Negative Biosynthesis. *Angew. Chem. Int. Ed.* **62**, e202215013 (2023).
290. Fedeson, D. T., Saake, P., Calero, P., Nickel, P. I. & Ducat, D. C. Biotransformation of 2,4-dinitrotoluene in a phototrophic co-culture of engineered *Synechococcus elongatus* and *Pseudomonas putida*. *Microb. Biotechnol.* **13**, 997–1011 (2020).
291. Tóth, G. S. *et al.* Photosynthetically produced sucrose by immobilized *Synechocystis* sp. PCC 6803 drives biotransformation in *E. coli*. *Biotechnol. Biofuels Bioprod.* **15**, 146 (2022).

292. Atsumi, S., Higashide, W. & Liao, J. C. Direct photosynthetic recycling of carbon dioxide to isobutyraldehyde. *Nat. Biotechnol.* **27**, 1177–1180 (2009).
293. Cao, K. *et al.* Enhanced Production of High-Value Porphyrin Compound Heme by Metabolic Engineering Modification and Mixotrophic Cultivation of *Synechocystis* sp. PCC6803. *Mar. Drugs* **22**, 378 (2024).
294. Call, S. N. & Andrews, L. B. CRISPR-Based Approaches for Gene Regulation in Non-Model Bacteria. *Front. Genome Ed.* **4**, 892304 (2022).
295. Juteršek, M. & Dolinar, M. A chimeric vector for dual use in cyanobacteria and *Escherichia coli* , tested with cystatin, a nonfluorescent reporter protein. *PeerJ* **9**, e12199 (2021).
296. Opel, F. *et al.* Generation of Synthetic Shuttle Vectors Enabling Modular Genetic Engineering of Cyanobacteria. *ACS Synth. Biol.* **11**, 1758–1771 (2022).
297. Martínez-García, E. *et al.* SEVA 4.0: an update of the Standard European Vector Architecture database for advanced analysis and programming of bacterial phenotypes. *Nucleic Acids Res.* **51**, D1558–D1567 (2023).
298. Baker, M. 1,500 scientists lift the lid on reproducibility. *Nature* **533**, 452–454 (2016).
299. McKiernan, E. C. *et al.* How open science helps researchers succeed. *eLife* **5**, (2016).
300. Ravindran, S. *et al.* Genome-Scale Metabolic Model Reconstruction and Investigation into the Fluxome of the Fast-Growing Cyanobacterium *Synechococcus* sp. PCC 11901. *ACS Synth. Biol.* acssynbio.4c00379 (2024)
doi:10.1021/acssynbio.4c00379.

301. Zavřel, T. *et al.* A Comprehensive Study of Light Quality Acclimation in *Synechocystis* Sp. PCC 6803. *Plant Cell Physiol.* **65**, 1285–1297 (2024).
302. Zavřel, T. *et al.* Quantitative insights into the cyanobacterial cell economy. *eLife* **8**, e42508 (2019).
303. Gupta, S., Pawar, S. B. & Pandey, R. A. Current practices and challenges in using microalgae for treatment of nutrient rich wastewater from agro-based industries. *Sci. Total Environ.* **687**, 1107–1126 (2019).
304. Jiang, L. *et al.* Evidence for a mutualistic relationship between the cyanobacteria *Nostoc* and fungi *Aspergilli* in different environments. *Appl. Microbiol. Biotechnol.* **104**, 6413–6426 (2020).
305. Bader, A. N., Sanchez Rizza, L., Consolo, V. F. & Curatti, L. Efficient saccharification of microalgal biomass by *Trichoderma harzianum* enzymes for the production of ethanol. *Algal Res.* **48**, 101926 (2020).
306. Zhang, L. *et al.* Construction and analysis of an artificial consortium based on the fast-growing cyanobacterium *Synechococcus elongatus* UTEX 2973 to produce the platform chemical 3-hydroxypropionic acid from CO₂. *Biotechnol. Biofuels* **13**, 82 (2020).
307. Cano, M. *et al.* Glycogen Synthesis and Metabolite Overflow Contribute to Energy Balancing in Cyanobacteria. *Cell Rep.* **23**, 667–672 (2018).
308. Abramson, B. W., Kachel, B., Kramer, D. M. & Ducat, D. C. Increased Photochemical Efficiency in Cyanobacteria via an Engineered Sucrose Sink. *Plant Cell Physiol.* **57**, 2451–2460 (2016).
309. Zuñiga, C. *et al.* Synthetic microbial communities of heterotrophs and phototrophs facilitate sustainable growth. *Nat. Commun.* **11**, 3803 (2020).

310. Mantovani, O., Dd Dienst, D. & Lindberg, P. High Density Cultivation of *Synechocystis* sp. PCC 6803 using the HDC 6.10B system (CellDeg) v2. Preprint at <https://doi.org/10.17504/protocols.io.9cgh2tw> (2019).
311. Laemmli, U. K. Cleavage of Structural Proteins during the Assembly of the Head of Bacteriophage T4. *Nature* **227**, 680–685 (1970).
312. Zavrel, T., Sinetova, M. & Cervený, J. Measurement of Chlorophyll a and Carotenoids Concentration in Cyanobacteria. *BIO-Protoc.* **5**, (2015).
313. Kotov, V. *et al.* In-depth interrogation of protein thermal unfolding data with MOLTENPROT. *Protein Sci.* **30**, 201–217 (2021).
314. Burastero, O. *et al.* eSPC: an online data-analysis platform for molecular biophysics. *Acta Crystallogr. Sect. Struct. Biol.* **77**, 1241–1250 (2021).
315. Bertani, G. STUDIES ON LYSOGENESIS I: The Mode of Phage Liberation by Lysogenic *Escherichia coli*. *J. Bacteriol.* **62**, 293–300 (1951).
316. KD, T. Improved media for growing plasmid and cosmid clones. *Bethesda Res Lab Focus* **9**, 12 (1987).
317. Shcolnick, S., Shaked, Y. & Keren, N. A role for mrgA, a DPS family protein, in the internal transport of Fe in the cyanobacterium *Synechocystis* sp. PCC6803. *Biochim. Biophys. Acta BBA - Bioenerg.* **1767**, 814–819 (2007).
318. Raybout, I. Welcome to Spyder's Documentation — Spyder 5 documentation. *Spyder-documentation* <https://docs.spyder-ide.org/current/index.html>.